Title:
A Few Possible Explanations of Physics Beyond the Standard Model

Author:
Stolarski, Daniel Julian

Acceptance Date:
2010

Series:
UC Berkeley Electronic Theses and Dissertations

Degree:
Ph.D., PhysicsUC Berkeley

Advisor(s):
Nomura, Yasunori

Committee:
Hall, Lawrence J., Borcherds, Richard E.

Permalink:
https://escholarship.org/uc/item/0g521082

Abstract:

A Few Possible Explanations of Physics Beyond the Standard Model

by

Daniel Julian Stolarski

A dissertation submitted in partial satisfaction of the

requirements for the degree of

Doctor of Philosophy

in

Physics

in the

Graduate Division

of the

University of California, Berkeley

Committee in charge:

Professor Y. Nomura, Chair

Professor L. J. Hall

Professor R. Borcherds

Spring 2010

A Few Possible Explanations of Physics Beyond the Standard Model

Abstract

A Few Possible Explanations of Physics Beyond the Standard Model

by

Daniel Julian Stolarski

Doctor of Philosophy in Physics

University of California, Berkeley

Professor Y. Nomura, Chair

Weak scale supersymmetry provides elegant solutions to many of the problems of the standard model, but it also generically gives rise to excessive flavor and CP violation. I show that if the mechanism that suppresses the Yukawa couplings also suppresses flavor changing interactions in the supersymmetry breaking parameters, essentially all the low energy flavor and CP constraints can be satisfied. The standard assumption of flavor universality in the supersymmetry breaking sector is not necessary. I also study signatures of this framework at the LHC. The mass splitting among different generations of squarks and sleptons can be much larger than in conventional scenarios, and even the mass ordering can be changed. I find that there is a plausible scenario in which the NLSP is a long-lived right-handed selectron or smuon decaying into the LSP gravitino. This leads to the spectacular signature of monochromatic electrons or muons in a stopper detector, providing strong evidence for the framework.

I also present concrete realizations of this framework in higher dimensions. The Higgs fields and the supersymmetry breaking field are localized in the same place in the extra dimension(s). The Yukawa couplings and operators generating the supersymmetry breaking parameters then receive the same suppression factors from the wavefunction profiles of the matter fields, leading to a specific correlation between these two classes of interactions. I construct both unified and non-unified models in this framework, which can be either strongly or weakly coupled at the cutoff scale. I analyze one version in detail, a strongly coupled unified model, which addresses various issues of supersymmetric grand unification. The models presented here provide an explicit example in which the supersymmetry breaking spectrum can be a direct window into the physics of flavor at a very high energy scale.

I also study, in an operator analysis, the compatibility between low energy flavor and CP constraints and observability of superparticles at the LHC, assuming a generic correlation between the Yukawa couplings and the supersymmetry breaking parameters. I find that the superpotential operators that generate scalar trilinear interactions are generically problematic. I discuss several ways in which this tension is naturally avoided. In particular, I focus on several frameworks in which the dangerous operators are naturally absent. These frameworks can be combined with many theories of flavor, including those with (flat

or warped) extra dimensions, strong dynamics, or flavor symmetries. I show that the resulting theories can avoid all the low energy constraints while keeping the superparticles light. The intergenerational mass splittings among the sfermions can reflect the structure of the underlying flavor theory, and can be large enough to be measurable at the LHC. Detailed observations of the superparticle spectrum may thus provide new handles on the origin of the flavor structure of the standard model.

Independent of supersymmetry, I also study the electron/positron excesses seen by PAMELA and ATIC. One interpretation of these excesses is dark matter annihilation in the galactic halo. Depending on the annihilation channel, the electron/positron signal could be accompanied by a galactic gamma ray or neutrino flux, and the non-detection of such fluxes constrains the couplings and halo properties of dark matter. I study the interplay of electron data with gamma ray and neutrino constraints in the context of cascade annihilation models, where dark matter annihilates into light degrees of freedom which in turn decay into leptons in one or more steps. Electron and muon cascades give a reasonable fit to the PAMELA and ATIC data. Compared to direct annihilation, cascade annihilations can soften gamma ray constraints from final state radiation by an order of magnitude. However, if dark matter annihilates primarily into muons, the neutrino constraints are robust regardless of the number of cascade decay steps. I also examine the electron data and gamma ray/neutrino constraints on the recently proposed "axion portal" scenario.

To all the experimental physicists,

who make our research worthwhile.

Contents

List of Figures

List of Tables

Acknowledgments

I want to thank Professor Nomura for his constant feedback on my research and his tremendous enthusiasm for physics, which I hope I can emulate for the rest of my career. I would also like to thank the rest of the graduate students in the CTP for answering all the dumb questions I came up with and showing me that not all of them were dumb. This work was supported by the Alcatel–Lucent Foundation and by the National Science Foundation.

Chapter 1

Introduction

The Standard Model (SM) of particle physics [1, 2, 3] has been extremely successful in predicting the results of nearly all experiments done in particle physics. Despite its success, there are many reasons to believe that it is incomplete, and that there is physics beyond the standard model. One of the oldest such reasons is called the hierarchy problem. In the SM, the particle which breaks electroweak symmetry down to electromagnetism and the weak force is called the Higgs boson [4]. The potential for the Higgs boson, however, is unstable under radiative corrections, so the physics at the highest energy which couples to the Higgs controls its mass. We know, however, that its mass should be of the same order as the mass of the W and Z bosons, about 100 GeV. Therefore, if we want the Higgs potential to be natural, we need new physics beyond the SM to come in around the weak scale.

Another line of reasoning for physics beyond the SM is that the SM has a large number of free parameters which are not predicted by the theory. Once the parameters are measured, then the theory can make a large number of predictions, but a fundamental theory should have zero or very few parameters and explain a large number of phenomena. Of the 19 parameters, 13 arise in the so-called flavor sector, meaning the couplings of the fermions to one another and their resulting masses. The large number of parameters is made worse by the fact that they are all dimensionless, yet they have a range of five orders of magnitude. Namely, the ratio of the mass of the top quark to that of the electron more than 100,000! It is hard to imagine a fundamental theory which generates such a large range of numbers at random. On the other hand, all the parameters in the flavor sector are dimensionless, so if there is new physics which generates these parameters, there is no reason to expect it to be at an energy scale that will ever be accessible to human experiments.

The first two reasons given to expect physics beyond the SM come from theoretical prejudice. We have a belief for how a theory that explains the universe should look, and because the SM does not conform to that belief, we expect it to be superseded by a better theory. On the other hand, there is no proof that fundamental theories should not be fine-tuned, and no proof that fundamental theories should not have many parameters which vary over large ranges. A third line of reasoning for physics beyond the SM is much more solid. Recent observations of the cosmic microwave background (CMB) have shown that

the particles of the SM, the atoms which make up all the structures we have ever seen, only comprise about 5% of the energy in the universe [5]. Most of the energy in the universe, about 72% comes from dark energy. While dark energy is quite a puzzle, there is not necessarily a particle physics interpretation. The remaining 23% of the energy of the universe, referred to as dark matter (DM), does point to new physics beyond the SM.

The gravitational properties of dark matter have been well studied [6], and it is now known that no particle in the SM has the necessary properties of DM. A DM candidate must be the seed for the gravitational formation of galaxies, so it must not have much self-interactions and it must be non-relativistic. Furthermore, in order to not have been discovered thus far by a wealth of experiments looking for it, its coupling to SM particles, if it has any at all, must be very weak. Thus, an active avenue of research in the particle physics community has been to come up with models of dark matter. These models are often motivated by other types of physics, such as the hierarchy problem, and have definite predictions for experiments.

One rich avenue of research in physics beyond the standard model is supersymmetry (SUSY) [7]. SUSY is an extension of spacetime symmetry to include fermionic generators. It posits a symmetry between fermions and bosons such that all particles are represented by a supermultiplet. Because we have not observed any superpartners, for example, there is no scalar electron, SUSY must be broken if it exists in nature. If SUSY is only softly broken, namely all SUSY breaking parameters have positive mass dimension, then the hierarchy problem is softened down to the scale of SUSY breaking. Furthermore, if SUSY is broken at the TeV scale, then the hierarchy is almost completely solved, and we should expect to discover a host of new SUSY particles when we explore the TeV scale with the now running Large Hardron Collider (LHC).

If SUSY is softly broken at the TeV scale and has all renormalizable operators allowed by the Standard Model gauge symmetries, we lose the baryon number and lepton number conservation which is automatic in the SM. Therefore, the minimal supersymmetric standard model (MSSM) includes a discrete $\mathcal{Z}_2$ symmetry called R-parity which eliminates renormalizable operators which violate baryon and lepton number and thus stabilizes the proton. An immediate consequence of R-parity is that the lightest particle which is R-odd is stable. Since all of the SM particles are R-even, this stable particle will be the lightest supersymmetric particle (LSP). In much of the MSSM parameter space, the LSP is neutral and makes a great dark matter candidate. SUSY not only solves the hierarchy problem, but it has a good chance to explaining the dark matter of the universe.

Despite having many nice properties, SUSY does not explain the strange pattern of masses and mixings of the SM fermions. Furthermore, SUSY introduces new problems associated with flavor because precision experiments require new physics at the TeV scale to have virtually no new flavor structure. Therefore, generic SUSY breaking is completely excluded, and most of the literature considers minimally flavor violating setups such as gauge mediation [8, 9] where there is a mechanism to make all flavor violating parameters zero at tree level, or the cMSSM or mSUGRA [10] which simply assumes that these parameters are zero.

In chapter 2, I show that if the flavor violating parameters of the SUSY breaking sector are the same size as the Yukawa couplings, then there is a large region of parameter space that is not only allowed by low energy experiments, but also can give insights into the standard model flavor puzzle at future collider experiments. In this framework, which I call flavorful supersymmetry, the deviations from minimal flavor violation are small but the phenomenology can be quite distinct. For example, if the gravitino is the LSP and a slepton is the next to lightest SUSY particle (NLSP), then the prediction of minimal flavor violation is that the stau is the NLSP. In flavorful SUSY, however, any of the three sleptons can be the lightest, and the splittings can be much larger than in traditional models. If a long lived slepton NLSP is discovered, various experimental proposals have shown that its decay could be measured. While most SUSY models would predict a 3-body decay of a stau with a broad energy spectrum, we could see a monochromatic spectrum in the 2-body decay of a smuon or selectron.

In chapter 3, I describe extra dimensional models where there is a correlation between the SUSY breaking parameters and the Yukawa couplings. These models localize the physics that generates the Yukawa couplings in the same part of the extra dimension as the physics which breaks SUSY. Some of these models incorporate grand unification and utilize the success of extra dimensional SUSY GUTs. One model is constructed in a warped extra dimension and can viewed as a 4 dimensional model through the AdS/CFT correspondence. In chapter 4, I do an operator analysis of SUSY breaking in the flavor sector and find that one particular class of operators must be suppressed if TeV scale supersymmetry is to be discovered at the LHC. I describe several natural ways in which these operators can be suppressed. I also describe how measurement of the SUSY spectrum at the LHC can give insight into the standard model flavor puzzle, even if the physics which generates the flavor parameters is operative at energies much higher than those which we will be directly probing.

While SUSY provides a good dark matter candidate, dark matter is such an interesting and important problem in physics that it is being explored in many different avenues. One avenue which is independent of SUSY is indirect detection. Dark matter particles are abundant throughout our galaxy, and while they are stable[1], occasionally two dark matter particles could collide and annihilate into standard model particles. In the majority of theories of dark matter, some of the annihilation products are positrons or anti-protons or both. Further, we would expect that these annihilation products are higher energy than many of the particles produced by astrophysical sources. Therefore, indirect detection experiments look for either antimatter, or high energy particles coming from space in excess of what we would expect from astrophysical sources.

In the last two years, there has been a tremendous amount of excitement in the field of indirect detection because several experiments, including PAMELA [11] and ATIC [12], have discovered an excess of high energy electrons and positrons coming from space. While these anomalies could be caused by some poorly understood astrophysics, the possibility

[1]Dark matter may decay, but its lifetime must be at least the age of the universe. If dark matter does decay, its decay products could also be detected in indirect detection experiments

that they are due to dark matter is very tantalizing. Due to the peculiarities of the data, models in which dark matter annihilates to a pair of light bosons which then decay to muons or electrons better explain the data than vanilla models such as the lightest supersymmetric particle.

In chapter 5, I preform an analysis of the PAMELA [13] and ATIC [14] electron and positron data in the framework of "cascade annihilation" where dark matter annihilates into a pair of light scalars. I determine the best fit region in the dark matter mass vs. annihilation cross section plane, and I compare direct to cascade annihilations. The best fit regions turn out to be relatively insensitive to the distribution of dark matter in the galaxy and to the details of particle propagation through the galaxy. Dark matter with a mass of a few TeV and a cross section about one hundred times the thermal relic cross section provides the best fit to the data. Going to cascade annihilation does not change the goodness of fit, but it raises the best fit mass and cross section.

In addition to fitting the electron and positron data, I also placed constraints from null searches for galactic gamma rays and neutrinos. I use the fact that there will be final state radiation of photons in any process involving charged leptons, and that there will be neutrinos in any final state involving muons. Experimental searches for photons have mostly focused on the galactic center where there is considerable uncertainty in the dark matter distribution. I find that while the constraints are significant for direct annihilation, they become substantially weaker for cascade models, strengthening the hypothesis of an intermediate light scalar. I also find that neutrino searches place stringent bounds on annihilation models. Furthermore, these bounds are more robust than the ones from gamma rays because the neutrinos come from a much larger region of the galaxy, so the halo uncertainties are less important. Neutrino bounds do not change much with cascades, suggesting that the annihilation proceeds dominantly to electrons.

While there are many mysteries in particle physics, experiments in the coming years will shed light on many of them, but probably produce more questions than answers. It is important to fully understand what the different questions are in fundamental physics and the possible connections between them. Furthermore, all the answers will be driven by experiment so it is important to understand not only what previous experiments have done, but also what capabilities future experiments such as the LHC have to shed light on these important questions. This work makes modest progress toward trying to answer some of these questions.

Chapter 2

Flavorful Supersymmetry[1]

2.1 Introduction

Despite many new alternatives, weak scale supersymmetry is still regarded as the leading candidate for physics beyond the standard model. It not only stabilizes the electroweak scale against potentially large radiative corrections, but also leads to successful gauge coupling unification at high energies and provides a candidate for dark matter. The fact that supersymmetry must be broken, however, leads to a severe flavor and CP problem. Including generic supersymmetry breaking parameters of order the weak scale causes flavor changing and CP violating processes with rates much greater than current experimental bounds. In fact, the problem has become more severe because of recent experimental progress, especially in B physics.

The most common approach to this problem is to assume that supersymmetry breaking and its mediation to the supersymmetric standard model sector preserve flavor. In other words, the mechanism for generating the Yukawa couplings for the quarks and leptons is separate from that which mediates supersymmetry breaking, so the fundamental supersymmetry breaking parameters do not contain any sources of flavor or CP violation. This is typically achieved in one of two ways. The first is to simply assume flavor universality and CP conservation for the supersymmetry breaking parameters at the scale where the low energy field theory arises [10], and the second is to impose a low energy mechanism which leads to flavor universality [8, 9].

A careful look at the problem, however, shows that the situation does not need to be as described above. We know that the Yukawa couplings for the first two generations of quarks and leptons are suppressed, implying that there is some mechanism responsible for this suppression. Suppose that this mechanism suppresses all non-gauge interactions associated with light generation fields, not just the Yukawa couplings. Then the supersymmetry breaking masses for the light generation squarks and sleptons are also suppressed at the scale where the mechanism is operative, suppressing flavor and CP violation associated with

[1] This chapter was co-written with Yasunori Nomura and Michele Papucci and published in [15].

these masses. This scenario was considered before in Ref. [16] in the context of reducing fine-tuning in electroweak symmetry breaking. The necessary flavor universal contribution to the squark and slepton masses arises automatically at lower energies from the gaugino masses through renormalization group evolution. An additional contribution may also arise from a low energy mechanism leading to flavor universal supersymmetry breaking masses.

In this chapter we study a scenario in which the physics responsible for the quark and lepton masses and mixings is also responsible for the structure of the supersymmetry breaking masses. We call this scenario flavorful supersymmetry in order to emphasize the direct connection between flavor physics and supersymmetry breaking. To preserve the success of gauge coupling unification in the most straightforward way, we assume that this physics lies at or above the unification scale $M_U \approx 10^{16}$ GeV. We find that, in contrast to naive expectations, a large portion of parameter space is not excluded by current experimental data. We study implications of this scenario on the low energy superparticle spectrum, which can be tested at future colliders. In particular, we point out distinct signatures at the LHC, arising in the plausible case where the gravitino is the lightest supersymmetric particle. Throughout the chapter we assume that R parity is conserved, although the framework can be extended straightforwardly to the case of R parity violation.

The organization of the chapter is as follows. In section 2.2 we describe our basic framework, and in section 2.3 we show that it satisfies experimental constraints from low energy flavor and CP violation. In section 2.4 we discuss implications on the weak scale superparticle spectrum, and we analyze signatures at the LHC in section 2.5. Finally, conclusions are given in section 2.6.

2.2 Framework

Suppose that the supersymmetric standard model, or supersymmetric grand unified theory, arises at a scale M_* ($\gtrsim M_U$) as an effective field theory of some more fundamental theory, which may or may not be a field theory. We consider that the physics generating the Yukawa couplings suppresses all non-gauge interactions associated with the quark, lepton and Higgs superfields Q_i, U_i, D_i, L_i, E_i, H_u and H_d (and N_i if we introduce the right-handed neutrinos), where $i = 1, 2, 3$ is the generation index. In particular, it suppresses the operators generating the supersymmetry breaking masses at the scale M_*:

$$\begin{aligned}
\mathcal{L} \;=\; & \left(\sum_{A=1,2,3} \int d^2\theta \, \eta_A \frac{X}{M_*} \mathcal{W}^{A\alpha} \mathcal{W}^A_\alpha + \text{h.c.} \right) \\
& + \int d^4\theta \left[\kappa_{H_u} \frac{X^\dagger X}{M_*^2} H_u^\dagger H_u + \kappa_{H_d} \frac{X^\dagger X}{M_*^2} H_d^\dagger H_d \right. \\
& \left. + \left(\kappa_\mu \frac{X^\dagger}{M_*} H_u H_d + \kappa_b \frac{X^\dagger X}{M_*^2} H_u H_d + \eta_{H_u} \frac{X}{M_*} H_u^\dagger H_u + \eta_{H_d} \frac{X}{M_*} H_d^\dagger H_d + \text{h.c.} \right) \right.
\end{aligned}$$

$$+ (\kappa_\Phi)_{ij} \frac{X^\dagger X}{M_*^2} \Phi_i^\dagger \Phi_j + \left((\eta_\Phi)_{ij} \frac{X}{M_*} \Phi_i^\dagger \Phi_j + \text{h.c.} \right) \Bigg]$$
$$+ \left[\int d^2\theta \left((\zeta_u)_{ij} \frac{X}{M_*} Q_i U_j H_u + (\zeta_d)_{ij} \frac{X}{M_*} Q_i D_j H_d + (\zeta_e)_{ij} \frac{X}{M_*} L_i E_j H_d \right) + \text{h.c.} \right], \quad (2.1)$$

where $X = \theta^2 F_X$ is a chiral superfield whose F-term vacuum expectation value is responsible for supersymmetry breaking, $\mathcal{W}_\alpha^A$ ($A = 1, 2, 3$) are the field-strength superfields for $U(1)_Y$, $SU(2)_L$ and $SU(3)_C$, and $\Phi = Q, U, D, L$ and E. The κ_Φ are 3×3 Hermitian matrices, while η_Φ, ζ_u, ζ_d and ζ_e are general complex 3×3 matrices. (Here, we have omitted the operators involving N_i because in most cases they do not affect our analysis.)

Assuming that suppression factors ϵ_{Φ_i}, ϵ_{H_u} and ϵ_{H_d} appear associated with the fields Φ_i, H_u and H_d, we obtain for the parameters in Eq. (2.1)

$$\kappa_{H_u} \approx \tilde{\kappa}_{H_u} \epsilon_{H_u}^2, \qquad \kappa_{H_d} \approx \tilde{\kappa}_{H_d} \epsilon_{H_d}^2, \quad (2.2)$$

$$\kappa_\mu \approx \tilde{\kappa}_\mu \, \epsilon_{H_u} \epsilon_{H_d}, \qquad \kappa_b \approx \tilde{\kappa}_b \, \epsilon_{H_u} \epsilon_{H_d}, \qquad \eta_{H_u} \approx \tilde{\eta}_{H_u} \epsilon_{H_u}^2, \qquad \eta_{H_d} \approx \tilde{\eta}_{H_d} \epsilon_{H_d}^2, \quad (2.3)$$

$$(\kappa_\Phi)_{ij} \approx \tilde{\kappa}_\Phi \, \epsilon_{\Phi_i} \epsilon_{\Phi_j}, \qquad (\eta_\Phi)_{ij} \approx \tilde{\eta}_\Phi \, \epsilon_{\Phi_i} \epsilon_{\Phi_j}, \quad (2.4)$$

$$(\zeta_u)_{ij} \approx \tilde{\zeta}_u \, \epsilon_{Q_i} \epsilon_{U_j} \epsilon_{H_u}, \qquad (\zeta_d)_{ij} \approx \tilde{\zeta}_d \, \epsilon_{Q_i} \epsilon_{D_j} \epsilon_{H_d}, \qquad (\zeta_e)_{ij} \approx \tilde{\zeta}_e \, \epsilon_{L_i} \epsilon_{E_j} \epsilon_{H_d}, \quad (2.5)$$

and for the Yukawa couplings

$$(y_u)_{ij} \approx \tilde{y}_u \, \epsilon_{Q_i} \epsilon_{U_j} \epsilon_{H_u}, \qquad (y_d)_{ij} \approx \tilde{y}_d \, \epsilon_{Q_i} \epsilon_{D_j} \epsilon_{H_d}, \qquad (y_e)_{ij} \approx \tilde{y}_e \, \epsilon_{L_i} \epsilon_{E_j} \epsilon_{H_d}, \quad (2.6)$$

where tilde parameters represent the "natural" size for the couplings without the suppression factors. For example, if the theory is strongly coupled at M_*, $\tilde{y}_u \sim \tilde{y}_d \sim \tilde{y}_e \sim O(4\pi)$, while if it is weakly coupled, we expect $\tilde{y}_u \sim \tilde{y}_d \sim \tilde{y}_e \sim O(1)$. Note that $O(1)$ coefficients are omitted in the expressions of Eqs. (2.2 – 2.6); for example, $(\kappa_\Phi)_{ij}$ is not proportional to $(\eta_\Phi)_{ij}$ because of an arbitrary $O(1)$ coefficient in each element.

Depending on the setup, some of the coefficients may be vanishing. For example, if the supersymmetry breaking sector does not contain an "elementary" gauge singlet at M_*, then $\eta_A = \tilde{\kappa}_\mu = \tilde{\eta}_{H_u} = \tilde{\eta}_{H_d} = \tilde{\eta}_\Phi = \tilde{\zeta}_u = \tilde{\zeta}_d = \tilde{\zeta}_e = 0$, and the gaugino masses must be generated by some low energy mechanism. (The supersymmetric Higgs mass, the μ term, must also be generated at low energies unless it exists at M_* in the superpotential.) The precise pattern for η_A and the tilde parameters affects low energy phenomenology, but our analysis of flavor and CP violation is independent of the detailed pattern.

In this chapter we consider the case where $\epsilon_{H_u} \sim \epsilon_{H_d} \sim O(1)$, and assume for simplicity that the two Higgs doublets obey the same scaling, $\tilde{\kappa}_{H_u} \sim \tilde{\kappa}_{H_d} \sim \tilde{\kappa}_H$ and $\tilde{\eta}_{H_u} \sim \tilde{\eta}_{H_d} \sim \tilde{\eta}_H$, as do the matter fields, $\tilde{\kappa}_Q \sim \tilde{\kappa}_U \sim \tilde{\kappa}_D \sim \tilde{\kappa}_L \sim \tilde{\kappa}_E \sim \tilde{\kappa}_\Phi$ and $\tilde{\eta}_Q \sim \tilde{\eta}_U \sim \tilde{\eta}_D \sim \tilde{\eta}_L \sim \tilde{\eta}_E \sim \tilde{\eta}_\Phi$, leading to $\tilde{\zeta}_u \sim \tilde{\zeta}_d \sim \tilde{\zeta}_e \sim \tilde{\zeta}$ and $\tilde{y}_u \sim \tilde{y}_d \sim \tilde{y}_e \sim \tilde{y}$. An extension to more general cases is straightforward. The supersymmetry breaking (and μ) parameters are then obtained from Eqs. (2.1 – 2.5) as

$$M_A \approx \eta_A M_{\rm SUSY}, \qquad \mu \approx \tilde{\kappa}_\mu M_{\rm SUSY}^\dagger, \qquad b \approx (\tilde{\kappa}_b + \tilde{\kappa}_\mu \tilde{\eta}_H) |M_{\rm SUSY}|^2, \quad (2.7)$$

$$m_{H_u}^2 \approx m_{H_d}^2 \approx (\tilde{\kappa}_H + |\tilde{\eta}_H|^2)|M_{\rm SUSY}|^2, \qquad (m_\Phi^2)_{ij} \approx \{(\kappa_\Phi)_{ij} + (\eta_\Phi^\dagger \eta_\Phi)_{ij}\}|M_{\rm SUSY}|^2, \tag{2.8}$$

$$(a_u)_{ij} \approx \{(y_u)_{kj}(\eta_Q)_{ki} + (y_u)_{ik}(\eta_U)_{kj} + (y_u)_{ij}\tilde{\eta}_H\} M_{\rm SUSY} + \tilde{\zeta}\, \epsilon_{Q_i}\epsilon_{U_j} M_{\rm SUSY}, \tag{2.9}$$

$$(a_d)_{ij} \approx \{(y_d)_{kj}(\eta_Q)_{ki} + (y_d)_{ik}(\eta_D)_{kj} + (y_d)_{ij}\tilde{\eta}_H\} M_{\rm SUSY} + \tilde{\zeta}\, \epsilon_{Q_i}\epsilon_{D_j} M_{\rm SUSY}, \tag{2.10}$$

$$(a_e)_{ij} \approx \{(y_e)_{kj}(\eta_L)_{ki} + (y_e)_{ik}(\eta_E)_{kj} + (y_e)_{ij}\tilde{\eta}_H\} M_{\rm SUSY} + \tilde{\zeta}\, \epsilon_{L_i}\epsilon_{E_j} M_{\rm SUSY}, \tag{2.11}$$

where $M_{\rm SUSY} \equiv F_X/M_*$, and M_A are the gaugino masses, $m_{H_u}^2$, $m_{H_d}^2$ and m_Φ^2 are non-holomorphic supersymmetry breaking squared masses, b is the holomorphic supersymmetry breaking Higgs mass-squared, and $(a_u)_{ij}$, $(a_d)_{ij}$ and $(a_e)_{ij}$ are holomorphic supersymmetry breaking scalar trilinear interactions. We find that the pattern of the supersymmetry breaking parameters is correlated with that of the Yukawa couplings, which now read

$$(y_u)_{ij} \approx \tilde{y}\, \epsilon_{Q_i}\epsilon_{U_j}, \qquad (y_d)_{ij} \approx \tilde{y}\, \epsilon_{Q_i}\epsilon_{D_j}, \qquad (y_e)_{ij} \approx \tilde{y}\, \epsilon_{L_i}\epsilon_{E_j}. \tag{2.12}$$

In general, the correlation between Eqs. (2.7 – 2.11) and Eq. (2.12) significantly reduces the tension between supersymmetry breaking and flavor physics [16]. We note again that $O(1)$ coefficients are omitted in each term in Eqs. (2.7 – 2.12); for instance, the last terms of Eqs. (2.9 – 2.11) are not proportional to the corresponding Yukawa matrices, Eq. (2.12), because of these $O(1)$ coefficients.

Taking $\epsilon_{\Phi_1} \leq \epsilon_{\Phi_2} \leq \epsilon_{\Phi_3}$ without loss of generality, the Yukawa couplings of Eq. (2.12) lead to the following quark and lepton masses and mixings

$$\begin{array}{lcl} (m_t, m_c, m_u) & \approx & \tilde{y}\,\langle H_u\rangle\,(\epsilon_{Q_3}\epsilon_{U_3},\, \epsilon_{Q_2}\epsilon_{U_2},\, \epsilon_{Q_1}\epsilon_{U_1}), \\ (m_b, m_s, m_d) & \approx & \tilde{y}\,\langle H_d\rangle\,(\epsilon_{Q_3}\epsilon_{D_3},\, \epsilon_{Q_2}\epsilon_{D_2},\, \epsilon_{Q_1}\epsilon_{D_1}), \\ (m_\tau, m_\mu, m_e) & \approx & \tilde{y}\,\langle H_d\rangle\,(\epsilon_{L_3}\epsilon_{E_3},\, \epsilon_{L_2}\epsilon_{E_2},\, \epsilon_{L_1}\epsilon_{E_1}), \\ (m_{\nu_\tau}, m_{\nu_\mu}, m_{\nu_e}) & \approx & \frac{\tilde{y}^2\langle H_u\rangle^2}{M_N}\,(\epsilon_{L_3}^2,\, \epsilon_{L_2}^2,\, \epsilon_{L_1}^2), \end{array} \tag{2.13}$$

and

$$V_{\rm CKM} \approx \begin{pmatrix} 1 & \epsilon_{Q_1}/\epsilon_{Q_2} & \epsilon_{Q_1}/\epsilon_{Q_3} \\ \epsilon_{Q_1}/\epsilon_{Q_2} & 1 & \epsilon_{Q_2}/\epsilon_{Q_3} \\ \epsilon_{Q_1}/\epsilon_{Q_3} & \epsilon_{Q_2}/\epsilon_{Q_3} & 1 \end{pmatrix}, \qquad V_{\rm MNS} \approx \begin{pmatrix} 1 & \epsilon_{L_1}/\epsilon_{L_2} & \epsilon_{L_1}/\epsilon_{L_3} \\ \epsilon_{L_1}/\epsilon_{L_2} & 1 & \epsilon_{L_2}/\epsilon_{L_3} \\ \epsilon_{L_1}/\epsilon_{L_3} & \epsilon_{L_2}/\epsilon_{L_3} & 1 \end{pmatrix}, \tag{2.14}$$

where we have included the neutrino masses through the seesaw mechanism with the right-handed neutrino Majorana masses $W \approx M_N \epsilon_{N_i}\epsilon_{N_j} N_i N_j$, and $V_{\rm CKM}$ and $V_{\rm MNS}$ are the quark and lepton mixing matrices, respectively. The values of the ϵ parameters are then constrained by the observed quark and lepton masses and mixings.

There are a variety of possibilities for the origin of the ϵ factors. They may arise, for example, from distributions of fields in higher dimensional spacetime or from strong conformal dynamics at or above the scale M_*. In a forthcoming chapter we will discuss an explicit example of such models. In general, if the suppressions of the Yukawa couplings arise from wavefunction effects in a broad sense, as in the examples described above, we can obtain the correlation given in Eqs. (2.7 – 2.11) and Eq. (2.12). Another possibility is to

introduce a non-Abelian flavor symmetry connecting all three generations. Flavor violating supersymmetry breaking parameters having a similar correlation to Eqs. (2.7 – 2.12) may then be generated through the breaking of that symmetry.[2] While this allows flavor universal contributions to the supersymmetry breaking parameters in addition to Eqs. (2.7 – 2.11), the essential features of the framework are not affected.

2.3 Constraints from Low Energy Processes

The supersymmetry breaking parameters are subject to a number of constraints from low energy flavor and CP violating processes. Here we study these constraints for the parameters given in Eqs. (2.7 – 2.11). We assume that CP violating effects associated with the Higgs sector are sufficiently suppressed. This is achieved if either $b \ll |\mu|^2$ at M_* or the phases of μ and b are aligned in the basis where the M_A are real.

The values of low energy supersymmetry breaking parameters are obtained from Eqs. (2.7 – 2.11) by evolving them down to the weak scale using renormalization group equations. Contributions from other flavor universal sources, such as gauge mediation, may also be added. To parameterize these effects in a model-independent manner, we simply add universal squark and slepton squared masses, $m_{\tilde{q}}^2 \equiv \lambda_{\tilde{q}}^2 |M_{\rm SUSY}|^2$ and $m_{\tilde{l}}^2 \equiv \lambda_{\tilde{l}}^2 |M_{\rm SUSY}|^2$, to $(m_\Phi^2)_{ij}$:

$$(m_\Phi^2)_{ij} \to \begin{cases} (m_\Phi^2)_{ij} + \lambda_{\tilde{q}}^2 |M_{\rm SUSY}|^2 \delta_{ij} & \text{for } \Phi = Q, U, D \\ (m_\Phi^2)_{ij} + \lambda_{\tilde{l}}^2 |M_{\rm SUSY}|^2 \delta_{ij} & \text{for } \Phi = L, E \end{cases} . \tag{2.15}$$

We neglect the differences of the flavor universal contribution among various squarks and among various sleptons, but it is sufficient for our purposes here. Effects on the gaugino masses and the scalar trilinear interactions are absorbed into the redefinition of η_A and $\tilde{\eta}_H$, respectively. The $m_{H_u}^2$ and $m_{H_d}^2$ are also renormalized, but this effect is incorporated by treating $\tan\beta \equiv \langle H_u \rangle / \langle H_d \rangle$ as a free parameter.

We use the mass insertion method [18] to compare the expected amount of flavor violation in the present scenario to low energy data. In order to do a mass insertion analysis, we need to work in the super-CKM basis where the Yukawa matrices are diagonalized by supersymmetric rotations of Q_i, U_i, D_i, L_i and E_i. The mass insertion parameters, δ_{ij}, are then obtained by dividing the off-diagonal entry of the sfermion mass-squared matrix by the average diagonal entry. Using Eqs. (2.7 – 2.11, 2.15), we obtain

$$(\delta_{ij}^u)_{LL} \approx \frac{1}{\lambda_{\tilde{q}}^2} \Big(\tilde{\kappa}_\Phi + |\tilde{\eta}_\Phi|^2 \epsilon_{Q_3}^2 \Big) \epsilon_{Q_i} \epsilon_{Q_j}, \qquad (\delta_{ij}^u)_{RR} \approx \frac{1}{\lambda_{\tilde{q}}^2} \Big(\tilde{\kappa}_\Phi + |\tilde{\eta}_\Phi|^2 \epsilon_{U_3}^2 \Big) \epsilon_{U_i} \epsilon_{U_j}, \tag{2.16}$$

$$(\delta_{ij}^u)_{LR} = (\delta_{ji}^u)_{RL}^* \approx \frac{1}{\lambda_{\tilde{q}}^2} \Big\{ \tilde{y}\, \tilde{\eta}_\Phi (\epsilon_{Q_j}^2 + \epsilon_{U_i}^2) + \tilde{\zeta} \Big\} \epsilon_{Q_i} \epsilon_{U_j} \frac{v \sin\beta}{M_{\rm SUSY}}, \tag{2.17}$$

[2] For earlier analyses on flavor violation in models with non-Abelian flavor symmetries, see e.g. [17].

for the up-type squarks,

$$(\delta^d_{ij})_{LL} \approx \frac{1}{\lambda^2_{\tilde{q}}}\Big(\tilde{\kappa}_\Phi + |\tilde{\eta}_\Phi|^2\epsilon^2_{Q_3}\Big)\,\epsilon_{Q_i}\epsilon_{Q_j}, \qquad (\delta^d_{ij})_{RR} \approx \frac{1}{\lambda^2_{\tilde{q}}}\Big(\tilde{\kappa}_\Phi + |\tilde{\eta}_\Phi|^2\epsilon^2_{D_3}\Big)\,\epsilon_{D_i}\epsilon_{D_j}, \tag{2.18}$$

$$(\delta^d_{ij})_{LR} = (\delta^d_{ji})^*_{RL} \approx \frac{1}{\lambda^2_{\tilde{q}}}\Big\{\tilde{y}\,\tilde{\eta}_\Phi(\epsilon^2_{Q_j} + \epsilon^2_{D_i}) + \tilde{\zeta}\Big\}\,\epsilon_{Q_i}\epsilon_{D_j}\frac{v\cos\beta}{M_{\rm SUSY}}, \tag{2.19}$$

for the down-type squarks,

$$(\delta^e_{ij})_{LL} \approx \frac{1}{\lambda^2_{\tilde{l}}}\Big(\tilde{\kappa}_\Phi + |\tilde{\eta}_\Phi|^2\epsilon^2_{L_3}\Big)\,\epsilon_{L_i}\epsilon_{L_j}, \qquad (\delta^e_{ij})_{RR} \approx \frac{1}{\lambda^2_{\tilde{l}}}\Big(\tilde{\kappa}_\Phi + |\tilde{\eta}_\Phi|^2\epsilon^2_{E_3}\Big)\,\epsilon_{E_i}\epsilon_{E_j}, \tag{2.20}$$

$$(\delta^e_{ij})_{LR} = (\delta^e_{ji})^*_{RL} \approx \frac{1}{\lambda^2_{\tilde{l}}}\Big\{\tilde{y}\,\tilde{\eta}_\Phi(\epsilon^2_{L_j} + \epsilon^2_{E_i}) + \tilde{\zeta}\Big\}\,\epsilon_{L_i}\epsilon_{E_j}\frac{v\cos\beta}{M_{\rm SUSY}}, \tag{2.21}$$

for the charged sleptons, and

$$(\delta^\nu_{ij})_{LL} \approx \frac{1}{\lambda^2_{\tilde{l}}}\Big(\tilde{\kappa}_\Phi + |\tilde{\eta}_\Phi|^2\epsilon^2_{L_3}\Big)\,\epsilon_{L_i}\epsilon_{L_j}, \tag{2.22}$$

for the sneutrinos. Here, $v \equiv (\langle H_u\rangle^2 + \langle H_d\rangle^2)^{1/2} \simeq 174$ GeV and $\tan\beta = \langle H_u\rangle/\langle H_d\rangle$.

The values of the ϵ parameters are constrained to reproduce the observed quark and lepton masses and mixings through Eqs. (2.13, 2.14). They depend on $\tilde{y}$ as well as the value of $\tan\beta$. For illustrative purpose, we take the pattern

$$\begin{array}{lll}
\epsilon_{Q_1} \approx \tilde{y}^{-\frac{1}{2}}\alpha_q\,\epsilon^2, & \epsilon_{U_1} \approx \tilde{y}^{-\frac{1}{2}}\alpha_q^{-1}\epsilon^2, & \epsilon_{D_1} \approx \tilde{y}^{-\frac{1}{2}}\alpha_q^{-1}\alpha_\beta\,\epsilon, \\
\epsilon_{Q_2} \approx \tilde{y}^{-\frac{1}{2}}\alpha_q\,\epsilon, & \epsilon_{U_2} \approx \tilde{y}^{-\frac{1}{2}}\alpha_q^{-1}\epsilon, & \epsilon_{D_2} \approx \tilde{y}^{-\frac{1}{2}}\alpha_q^{-1}\alpha_\beta\,\epsilon, \\
\epsilon_{Q_3} \approx \tilde{y}^{-\frac{1}{2}}\alpha_q, & \epsilon_{U_3} \approx \tilde{y}^{-\frac{1}{2}}\alpha_q^{-1}, & \epsilon_{D_3} \approx \tilde{y}^{-\frac{1}{2}}\alpha_q^{-1}\alpha_\beta\,\epsilon,
\end{array} \tag{2.23}$$

$$\begin{array}{ll}
\epsilon_{L_1} \approx \tilde{y}^{-\frac{1}{2}}\alpha_l\,\epsilon, & \epsilon_{E_1} \approx \tilde{y}^{-\frac{1}{2}}\alpha_l^{-1}\alpha_\beta\,\epsilon^2, \\
\epsilon_{L_2} \approx \tilde{y}^{-\frac{1}{2}}\alpha_l\,\epsilon, & \epsilon_{E_2} \approx \tilde{y}^{-\frac{1}{2}}\alpha_l^{-1}\alpha_\beta\,\epsilon, \\
\epsilon_{L_3} \approx \tilde{y}^{-\frac{1}{2}}\alpha_l\,\epsilon, & \epsilon_{E_3} \approx \tilde{y}^{-\frac{1}{2}}\alpha_l^{-1}\alpha_\beta,
\end{array} \tag{2.24}$$

with

$$\tan\beta \approx \alpha_\beta\,\epsilon^{-1}, \tag{2.25}$$

where $\epsilon \sim O(0.1)$ and α_q, α_l and α_β are numbers parameterizing the freedoms unfixed by the data of the quark and lepton masses and mixings. Here, we have assumed that $\tan\beta$ is larger than ≈ 2, as suggested by the large top quark mass. The pattern of Eq. (2.23 – 2.25) leads to

$$\begin{array}{lcl}
(m_t, m_c, m_u) & \approx & v\,(1, \epsilon^2, \epsilon^4), \\
(m_b, m_s, m_d) & \approx & v\,(\epsilon^2, \epsilon^3, \epsilon^4), \\
(m_\tau, m_\mu, m_e) & \approx & v\,(\epsilon^2, \epsilon^3, \epsilon^4), \\
(m_{\nu_\tau}, m_{\nu_\mu}, m_{\nu_e}) & \approx & \frac{v^2}{M_N}(1, 1, 1),
\end{array} \tag{2.26}$$

and

$$V_{\rm CKM} \approx \begin{pmatrix} 1 & \epsilon & \epsilon^2 \\ \epsilon & 1 & \epsilon \\ \epsilon^2 & \epsilon & 1 \end{pmatrix}, \qquad V_{\rm MNS} \approx \begin{pmatrix} 1 & 1 & 1 \\ 1 & 1 & 1 \\ 1 & 1 & 1 \end{pmatrix}, \tag{2.27}$$

which successfully reproduces the gross structure of the observed quark and lepton masses and mixings [19]. The mass insertion parameters are obtained by substituting Eqs. (2.23 – 2.25) into Eqs. (2.16 – 2.22).

Here we summarize the constraints from low energy flavor and CP violating processes, compiled from Ref. [20]. In the quark sector, the most stringent experimental constraints come from K-$\bar{K}$, D-$\bar{D}$ and B-$\bar{B}$ mixings, $\sin 2\beta$ and the $b \to s\gamma$ process. The model-independent constraints are obtained by turning on only one (or two) mass insertion parameter(s) and considering the gluino exchange diagrams. They are summarized as

$$\sqrt{|{\rm Re}(\delta^d_{12})^2_{LL/RR}|} \lesssim (10^{-2}\text{–}10^{-1}), \quad \sqrt{|{\rm Re}(\delta^d_{12})^2_{LR/RL}|} \lesssim (10^{-3}\text{–}10^{-2}),$$

$$\sqrt{|{\rm Re}(\delta^d_{12})_{LL}(\delta^d_{12})_{RR}|} \lesssim 10^{-3}, \qquad \sqrt{|{\rm Im}(\delta^d_{12})^2_{LL/RR}|} \lesssim (10^{-3}\text{–}10^{-2}),$$

$$\sqrt{|{\rm Im}(\delta^d_{12})^2_{LR/RL}|} \lesssim (10^{-4}\text{–}10^{-3}), \quad \sqrt{|{\rm Im}(\delta^d_{12})_{LL}(\delta^d_{12})_{RR}|} \lesssim 10^{-4},$$

$$|(\delta^u_{12})_{LL/RR}| \lesssim (10^{-2}\text{–}10^{-1}), \qquad |(\delta^u_{12})_{LR/RL}| \lesssim 10^{-2},$$

$$|(\delta^u_{12})_{LL}| = |(\delta^u_{12})_{RR}| \lesssim (10^{-3}\text{–}10^{-2}), \quad |(\delta^d_{13})_{LL/RR}| \lesssim (0.1\text{–}1),$$

$$|(\delta^d_{13})_{LR/RL}| \lesssim (10^{-2}\text{–}10^{-1}), \qquad |(\delta^d_{13})_{LL}| = |(\delta^d_{13})_{RR}| \lesssim 10^{-2},$$

$$|(\delta^d_{23})_{LR/RL}| \lesssim 10^{-2},$$

where we have taken the gluino and squark masses to be the same order of magnitude and $m_{\tilde{q}} = 500$ GeV. For heavier superparticles, the bounds scale roughly linearly with $m_{\tilde{q}}$, i.e. all the bounds weaken for larger $m_{\tilde{q}}$ by a factor of $m_{\tilde{q}}/500$ GeV. In the lepton sector, the most stringent constraint comes from the $\mu \to e\gamma$ process, and is given by

$$|(\delta^e_{12})_{LL}| \lesssim (10^{-4}\text{–}10^{-3}), \qquad |(\delta^e_{12})_{LR/RL}| \lesssim (10^{-6}\text{–}10^{-5}),$$

where we have taken the weak gaugino and slepton masses to be the same order of magnitude and $m_{\tilde{l}} = 200$ GeV. For heavier superparticles, the bound on $|(\delta^e_{12})_{LL}|$ scales roughly quadratically with $m_{\tilde{l}}$, while that on $|(\delta^e_{12})_{LR/RL}|$ scales roughly linearly with $m_{\tilde{l}}$. Finally, the bounds from the neutron and electron electric dipole moments (EDMs) constrain the flavor conserving entry of the sfermion mass matrices:

$$|{\rm Im}(\delta^u_{11})_{LR}| \lesssim 10^{-6}, \qquad |{\rm Im}(\delta^d_{11})_{LR}| \lesssim 10^{-6}, \qquad |{\rm Im}(\delta^e_{11})_{LR}| \lesssim 10^{-7},$$

where we have again taken $m_{\tilde{q}} = 500$ GeV and $m_{\tilde{l}} = 200$ GeV, and the bounds become weaker linearly with increasing superparticle masses.

We now determine whether flavor and CP violation arising from Eqs. (2.16 – 2.25) is compatible with the experimental bounds given above. We take $\epsilon \approx (0.05 - 0.1)$ to reproduce the gross structure of the quark and lepton masses and mixings, and take $\tilde{\kappa}_\Phi \sim \tilde{\eta}_\Phi \sim O(1)$ for simplicity. For $\tilde{\zeta} \sim O(1)$, we find stringent constraints coming from the electron EDM and $\mu \to e\gamma$, which push the supersymmetry breaking scale up to $M_{\rm SUSY} \gtrsim 5$ TeV for $\tilde{y} \sim 1$ and $M_{\rm SUSY} \gtrsim 1.5$ TeV for $\tilde{y} \sim 4\pi$. Here, we have taken $M_{\rm SUSY} \approx m_{\tilde{q}} \approx (5/2) m_{\tilde{l}}$. This implies that the superpotential couplings in Eq. (2.1), $\tilde{\zeta}$, must somehow be suppressed, unless the superparticles are relatively heavy. This may naturally arise from physics above M_*, since the superpotential has the special property of not being renormalized at all orders in perturbation theory.

For $\tilde{\zeta} \ll 1$, a wide parameter region is open. For $\tilde{y} \sim 1$, we find that the region

$$0.2 \lesssim \alpha_q \lesssim 3, \qquad \frac{\alpha_q}{\alpha_\beta} \gtrsim 0.5, \qquad \alpha_l \lesssim 0.3, \qquad \frac{\alpha_l}{\alpha_\beta} \gtrsim 0.2, \tag{2.28}$$

satisfies all the constraints for $\epsilon = 0.05$, $M_{\rm SUSY} = m_{\tilde{q}} = 500$ GeV and $m_{\tilde{l}} = 200$ GeV. The region is somewhat smaller for $\epsilon = 0.1$. For $\tilde{y} \sim 4\pi$, we find the region

$$0.05 \lesssim \alpha_q \lesssim 10, \qquad \frac{\alpha_q}{\alpha_\beta} \gtrsim 0.1, \qquad \alpha_l \lesssim 1, \qquad \frac{\alpha_l}{\alpha_\beta} \gtrsim 0.04, \tag{2.29}$$

for $\epsilon = 0.05$, $M_{\rm SUSY} = m_{\tilde{q}} = 500$ GeV and $m_{\tilde{l}} = 200$ GeV, and somewhat smaller for $\epsilon = 0.1$.[3] This result agrees with that of Ref. [16], which analyzed the case of $\tilde{y} \sim 1$ without including the constraints from the EDM bounds.

We have used the particular parameterization of Eq. (2.23 – 2.25) in the analysis here, but we can adopt a more refined scheme for the values of the ϵ parameters to better accommodate the observed quark and lepton masses and mixings. For example, we can make ϵ_{L_1} somewhat smaller than Eq. (2.24) to explain the smallness of the $e3$ element of $V_{\rm MNS}$, which is experimentally smaller than about 0.2. A value of $\tan\beta$ somewhat larger than Eq. (2.25) also improves the top to bottom mass ratio. Our basic results above are not affected by these modifications.

We conclude that the current experimental constraints allow the existence of the general supersymmetry breaking parameters of Eq. (2.1) where the couplings are suppressed by the factors suggested by Yukawa couplings, as long as the superparticles are relatively heavy or the superpotential couplings, $\tilde{\zeta}$, are suppressed. For $\tilde{\zeta} \ll 1$, a wide parameter region is open even for light superparticles, $m_{\tilde{q}} \approx 500$ GeV and $m_{\tilde{l}} \approx 200$ GeV. In the next section, we discuss implications of this scenario, which we call flavorful supersymmetry, on the low energy spectrum.

[3] If we require the absence of cancellation among diagrams for $\mu \to e\gamma$, the bound $|(\delta^e_{12})_{RR}| \lesssim (10^{-3}$–$10^{-2})$ arises. This, however, changes the regions of Eqs. (2.28, 2.29) only slightly. The lower bound on α_l/α_β becomes 0.5 in Eq. (2.28), and 0.1 in Eq. (2.29).

2.4 Implications on the Superparticle Spectrum

Phenomenology of supersymmetric theories depends strongly on the spectrum of superparticles. In particular, the order of the superparticle masses controls decay chains, and thus affects collider signatures significantly. In this section we discuss the splitting and ordering of the superparticle masses among different generations and between different superparticle species.

2.4.1 Mass splitting and ordering among generations

Among the various sfermions, the lightest species are most likely the right-handed sleptons: $\tilde{e}_R$, $\tilde{\mu}_R$ and $\tilde{\tau}_R$. This is because the sfermion squared masses receive positive contributions from the gaugino masses through renormalization group evolution at one loop, and these contributions are proportional to the square of the relevant gauge couplings. Since the right-handed sleptons are charged under only $U(1)_Y$, they receive contributions from just the hypercharge gaugino and are expected to be lighter than the other sfermions. A possible low energy gauge mediated contribution will not change the situation because it gives positive contributions to the sfermion squared masses proportional to the fourth power of the relevant gauge couplings (at least in the simplest case). Thus we focus on the right-handed sleptons and analyze the mass splitting among the three generations. A similar analysis, however, can also be performed for the other sfermion species.[4]

We consider the field basis in which the lepton Yukawa couplings, $(y_e)_{ij}$, are real and diagonal. If there is no intrinsic flavor violation in the sfermion masses, the 3×3 mass-squared matrix for the right-handed sleptons, m_E^2, receives a flavor universal contribution, $m_{\tilde{e}}^2\,\mathrm{diag}(1,1,1)$, and flavor dependent contributions through renormalization group evolution. This leads to

$$m_E^2 = \begin{pmatrix} m_{\tilde{e}}^2 - I_e & 0 & 0 \\ 0 & m_{\tilde{e}}^2 - I_\mu & 0 \\ 0 & 0 & m_{\tilde{e}}^2 - I_\tau \end{pmatrix}, \tag{2.30}$$

at the weak scale, where I_e, I_μ and I_τ parameterize the effect of renormalization group evolution from the Yukawa and scalar trilinear couplings, and $I_e : I_\mu : I_\tau \approx (y_e)_{11}^2 : (y_e)_{22}^2 : (y_e)_{33}^2 \approx m_e^2 : m_\mu^2 : m_\tau^2$. (The effects from the neutrino Yukawa couplings that may exist above the scale of right-handed neutrino masses, M_N, are neglected here since they are expected to be small.) The expression of Eq. (2.30) tells us that, in the absence of a flavor violating contribution, (i) the interaction and mass eigenstates of the right-handed sleptons coincide, and (ii) the mass of a slepton corresponding to a heavier lepton is always lighter, since $I_\tau > I_\mu > I_e > 0$ due to the form of the renormalization group equations of the

[4]The mass splitting and ordering for heavier species may also provide important tests for flavorful supersymmetry. Moreover, if there exists a $U(1)_Y$ D-term contribution, i.e. $m_{H_u}^2 - m_{H_d}^2 + \mathrm{Tr}[m_Q^2 - 2m_U^2 + m_D^2 - m_L^2 + m_E^2] \neq 0$, then the left-handed sleptons and sneutrinos may be lighter than the right-handed sleptons. It is also possible to consider the case in which a squark is the lightest sfermion if M_3 is significantly smaller than $M_{1,2}$ at M_*.

supersymmetric standard model when $(m_E^2)_{ii}, (m_L^2)_{ii}, m_{H_d}^2 > 0$. Inclusion of flavor universal left-right mixing does not change these conclusions.

The situation is very different if there exists intrinsic flavor violation in supersymmetry breaking. The supersymmetry breaking parameters at M_* in our scenario are given parametrically by Eqs. (2.7 – 2.11, 2.4) even in the basis where $(y_e)_{ij}$ is diagonal. In particular,

$$m_E^2(M_*) \approx \begin{pmatrix} \epsilon_{E_1}^2 & \epsilon_{E_1}\epsilon_{E_2} & \epsilon_{E_1}\epsilon_{E_3} \\ \epsilon_{E_1}\epsilon_{E_2} & \epsilon_{E_2}^2 & \epsilon_{E_2}\epsilon_{E_3} \\ \epsilon_{E_1}\epsilon_{E_3} & \epsilon_{E_2}\epsilon_{E_3} & \epsilon_{E_3}^2 \end{pmatrix} |M_{\rm SUSY}|^2, \tag{2.31}$$

for $\tilde{\kappa}_\Phi \sim \tilde{\eta}_\Phi \sim O(1)$. In addition, m_E^2 receives universal contributions from the $U(1)_Y$ gaugino mass through renormalization group evolution, as well as possibly from other sources such as low energy gauge mediation. It also receives flavor violating contributions from the Yukawa and scalar trilinear couplings through renormalization group evolution. We find that the evolution effect on the off-diagonal elements is not significant; the changes of the coefficients are at most of order unity. The diagonal elements receive flavor universal contributions, which we denote as $m_{\tilde{e}}^2 \equiv \xi_{\tilde{e}}^2 |M_{\rm SUSY}|^2$, as well as flavor dependent contributions. Defining the flavor dependent part as $\hat{m}_{E_i}^2 \equiv (m_E^2)_{ii} - (m_E^2)_{ii}|_{y_e=a_e=0}$, the renormalization group equation for $\hat{m}_{E_i}^2$ is given by

$$\frac{d}{d\ln\mu_R}\hat{m}_{E_i}^2 = \frac{1}{4\pi^2}\left[(y_e)_{ii}^2\left\{(m_E^2)_{ii} + (m_L^2)_{ii} + m_{H_d}^2\right\} + \sum_k |(a_e)_{ki}|^2\right], \tag{2.32}$$

where i in the right-hand-side is not summed. This leads to m_E^2 at the weak scale of the form

$$m_E^2 \approx \begin{pmatrix} m_{\tilde{e}}^2 - K_e & 0 & 0 \\ 0 & m_{\tilde{e}}^2 - K_\mu & 0 \\ 0 & 0 & m_{\tilde{e}}^2 - K_\tau \end{pmatrix} + \begin{pmatrix} \epsilon_{E_1}^2 & \epsilon_{E_1}\epsilon_{E_2} & \epsilon_{E_1}\epsilon_{E_3} \\ \epsilon_{E_1}\epsilon_{E_2} & \epsilon_{E_2}^2 & \epsilon_{E_2}\epsilon_{E_3} \\ \epsilon_{E_1}\epsilon_{E_3} & \epsilon_{E_2}\epsilon_{E_3} & \epsilon_{E_3}^2 \end{pmatrix} |M_{\rm SUSY}|^2, \tag{2.33}$$

where $O(1)$ coefficients are omitted in each element in the second term, but not in the first term. The quantities K_e, K_μ and K_τ are defined by $K_\tau \equiv \hat{m}_{E_3}^2(M_*) - \hat{m}_{E_3}^2(M_{\rm SUSY})$ and $\{\tau, 3\} \to \{e, 1\}, \{\mu, 2\}$, and are given by solving Eq. (2.32). They are always positive for $(m_E^2)_{ii}, (m_L^2)_{ii}, m_{H_d}^2 > 0$, and $K_e : K_\mu : K_\tau \approx (y_e)_{11}^2 : (y_e)_{22}^2 : (y_e)_{33}^2$ for $(a_e)_{ij} \propto (y_e)_{ij}$.

The contributions K_e, K_μ and K_τ compete in general with the second term in Eq. (2.33). For $\tilde{\kappa}_\Phi \sim \tilde{\eta}_\Phi \sim \tilde{\eta}_H \sim O(1)$ and $\tilde{\zeta} \lesssim \tilde{y}$, for example, Eq. (2.32) scales as

$$\frac{d}{d\ln\mu_R}\hat{m}_{E_i}^2 \approx \frac{1}{4\pi^2}(y_e)_{ii}^2\left(\xi_{\tilde{e}}^2 + 2\xi_{\tilde{l}}^2 + \sum_k \frac{\epsilon_{L_k}^2}{\epsilon_{L_i}^2}\right)|M_{\rm SUSY}|^2, \tag{2.34}$$

where we have set $(m_L^2)_{ii} \approx m_{H_d}^2 \equiv \xi_{\tilde{l}}^2 |M_{\rm SUSY}|^2$. With the choice of Eqs. (2.23 – 2.25), this gives

$$K_\tau \approx \frac{1}{4\pi^2}(y_e)_{33}^2\left(\xi_{\tilde{e}}^2 + 2\xi_{\tilde{l}}^2 + O(1)\right)|M_{\rm SUSY}|^2 \ln\frac{M_*}{M_{\rm SUSY}} \sim \tilde{y}^2\epsilon_{L_3}^2\epsilon_{E_3}^2|M_{\rm SUSY}|^2, \tag{2.35}$$

and $\{\tau, 3\} \to \{e, 1\}, \{\mu, 2\}$, leading to

$$m_E^2 \approx \begin{pmatrix} \xi_{\tilde{e}}^2 - \tilde{y}^2\epsilon_{L_1}^2\epsilon_{E_1}^2 + \epsilon_{E_1}^2 & \epsilon_{E_1}\epsilon_{E_2} & \epsilon_{E_1}\epsilon_{E_3} \\ \epsilon_{E_1}\epsilon_{E_2} & \xi_{\tilde{e}}^2 - \tilde{y}^2\epsilon_{L_2}^2\epsilon_{E_2}^2 + \epsilon_{E_2}^2 & \epsilon_{E_2}\epsilon_{E_3} \\ \epsilon_{E_1}\epsilon_{E_3} & \epsilon_{E_2}\epsilon_{E_3} & \xi_{\tilde{e}}^2 - \tilde{y}^2\epsilon_{L_3}^2\epsilon_{E_3}^2 + \epsilon_{E_3}^2 \end{pmatrix} |M_{\rm SUSY}|^2. \quad (2.36)$$

Note that the signs of the $\tilde{y}^2\epsilon_{L_i}^2\epsilon_{E_i}^2$ terms are all negative, while each $\epsilon_{E_i}\epsilon_{E_j}$ term has an $O(1)$ coefficient whose sign can be either positive or negative.

The expression of Eq. (2.36) shows that in flavorful supersymmetry (i) the interaction and mass eigenstates of the right-handed sleptons do not in general coincide, and (ii) the mass ordering of the sleptons is not necessarily anticorrelated with that of the leptons. In particular, we find that the lightest sfermion can easily be $\tilde{e}_R$ or $\tilde{\mu}_R$ (with slight mixtures from other flavors), in contrast to the usual supersymmetry breaking scenarios in which $\tilde{\tau}_R$ is the lightest because $I_\tau > I_\mu > I_e > 0$ in Eq. (2.30). In our case, $\tilde{\tau}_R$ is heavier than $\tilde{e}_R$ and $\tilde{\mu}_R$ if, for example, $\tilde{y} \sim 1$ and the $\epsilon_{E_3}^2$ term in the 3-3 entry of Eq. (2.36) has a positive coefficient. As we will see in section 2.5, this can lead to distinct signatures at the LHC which provide strong evidence for the present scenario. Note that even when the mass ordering is not flipped, the amount of mass splitting between the generations differs from the conventional scenarios, which may provide a direct test of this scenario at future colliders. In particular, with our choice of Eqs. (2.23 – 2.25), the flavor dependent contribution to the 3-3 entry of Eq. (2.36), $\epsilon_{E_3}^2|M_{\rm SUSY}|^2$, can be of the same order as the flavor universal contributions. This implies that the $\tilde{\tau}_R$ mass may be significantly split from those of $\tilde{e}_R$ and $\tilde{\mu}_R$, giving a window into the effect of intrinsic flavor violation in the supersymmetry breaking sector. The mass splitting between $\tilde{e}_R$ and $\tilde{\mu}_R$ is of order $\epsilon_{E_2}^2|M_{\rm SUSY}|^2$, which can also be much larger than the conventional scenarios and may be measurable.

2.4.2 The lightest and next-to-lightest supersymmetric particles

Phenomenology at colliders depends strongly on the species of the lightest superparticle (LSP) and the next-to-lightest superparticle (NLSP). As we have seen, it is natural to expect that (any) one of the right-handed sleptons is the lightest sfermion. For the gauginos, we expect that the bino, $\tilde{B}$, is naturally the lightest because of the renormalization group property of the gaugino masses, $M_A(\mu_R) = (g_A^2(\mu_R)/g_A^2(M_*))M_A(M_*)$, where g_A $(A = 1, 2, 3)$ are the $U(1)_Y$, $SU(2)_L$ and $SU(3)_C$ gauge couplings. This implies that the LSP and NLSP are determined by the competition between the right-handed sleptons, bino, and gravitino, which may also be lighter than the other superparticles.

The mass ordering between the right-handed sleptons, bino, and gravitino depends on the mechanism generating the gaugino masses and the universal contributions to the sfermion masses. Here we consider three representative cases. The first is the simplest case that all the operators of Eq. (2.1) exist with all η_A and tilde parameters of order unity, except that $\tilde{\zeta}$ is somewhat smaller (to suppress dangerous low energy processes). The second is that the theory does not contain an elementary singlet at M_* $(> M_U)$, so that $\eta_A = \tilde{\kappa}_\mu =$

$\tilde{\eta}_H = \tilde{\eta}_\Phi = \tilde{\zeta} = 0$, and the gaugino and scalar masses are generated by gauge mediation with the messenger scale of order the unification scale, M_U. An interesting aspect of this theory is that the μ term can be generated from the interaction $\mathcal{L} \approx \int d^4\theta \, (H_u H_d + \text{h.c.})$ via supergravity effects, which are comparable to the gaugino and scalar masses: $\mu \approx F_X/M_{\rm Pl} \approx (g_A^2/16\pi^2) F_X/M_U \approx m_{\lambda,\tilde{q},\tilde{l}}$, where $M_{\rm Pl} \approx 10^{18}$ GeV is the reduced Planck scale, and $m_{\lambda,\tilde{q},\tilde{l}}$ represents the gaugino, squark and slepton masses ($\tilde{\kappa}_b$ must be suppressed for M_* smaller than $M_{\rm Pl}$). The third is a class of theories considered in Ref. [21], where $M_* \approx M_U$, and the gaugino and universal scalar masses arise from low energy gauge mediation.

The right-handed slepton mass-squared, m_E^2, and the bino mass, M_1, at the weak scale are given in terms of their values, $m_{E,H}^2$ and $M_{1,H}$, at some high energy scale M_H by

$$m_E^2 \simeq m_{E,H}^2 + \frac{2}{11}\left(1 - \frac{g_1^4}{g_{1,H}^4}\right)|M_{1,H}|^2, \tag{2.37}$$

$$M_1 \simeq \frac{g_1^2}{g_{1,H}^2}|M_{1,H}|, \tag{2.38}$$

where g_1 and $g_{1,H}$ are the $U(1)_Y$ gauge couplings at the weak scale and M_H, respectively. In the first case described above, we take $M_H \approx M_*$ and $m_{E,H}^2 \approx 0$ for $\tilde{e}_R$ and $\tilde{\mu}_R$. Neglecting model-dependent effects above M_U, we can set $M_H \approx M_U$, and we find that $m_E^2 < M_1^2$ at the weak scale for these particles, i.e. $\tilde{e}_R$ and $\tilde{\mu}_R$ are lighter than $\tilde{B}$. The mass of $\tilde{\tau}_R$ depends on the sign and size of $m_{E,H}^2 \approx \epsilon_{E_3}^2 |M_{\rm SUSY}|^2$, and may be lighter or heavier than $\tilde{e}_R$, $\tilde{\mu}_R$. In the case where the origin of the gaugino and sfermion masses is gauge mediation, as in the second and third cases above, we should take M_H to be the messenger scale, $M_{\rm mess}$. We find that $\tilde{B}$ is lighter than $\tilde{e}_R$ and $\tilde{\mu}_R$ for $M_{\rm mess} \approx M_U$, but the opposite is possible for lower $M_{\rm mess}$, depending on the number of messenger fields. The mass of $\tilde{\tau}_R$, again, depends on $m_{E,H}^2$.

The gravitino mass is given by

$$m_{3/2} \simeq \frac{F_X}{\sqrt{3} M_{\rm Pl}}, \tag{2.39}$$

which should be compared to the gaugino and sfermion masses. In the case that all the operators of Eq. (2.1) exist (except for the superpotential ones) with order one η_A and tilde parameters, the gaugino and sfermion masses are given by

$$m_{\lambda,\tilde{q},\tilde{l}} \approx \frac{F_X}{M_*}. \tag{2.40}$$

We consider that M_* is at least as large as M_U to preserve successful gauge coupling unification and at most of order $M_{\rm Pl}$ to stay in the field theory regime with weakly coupled gravity. This then leads to

$$\frac{M_U}{M_{\rm Pl}} m_{\lambda,\tilde{q},\tilde{l}} \lesssim m_{3/2} \lesssim m_{\lambda,\tilde{q},\tilde{l}}, \tag{2.41}$$

where $M_U/M_{\rm Pl} \approx 10^{-2}$. Note that order one coefficients are omitted in Eq. (2.41), so that the gravitino can be heavier than some (or all) of the superparticles in the supersymmetric standard model sector. Nevertheless, a natural range for the gravitino mass is below the typical superparticle mass by up to two orders of magnitude.

The gravitino mass in the other two cases also falls in the range of Eq. (2.41). In our second example, the superparticle masses are given approximately by $(g_A^2/16\pi^2)F_X/M_U \approx F_X/M_{\rm Pl}$, leading to $m_{3/2} \approx m_{\lambda,\tilde{q},\tilde{l}}$. The third example has superparticle masses of order $(g_A^2/16\pi^2)F_X/(M_U^2/M_{\rm Pl}) \approx F_X/M_U$, leading to $m_{3/2} \approx (M_U/M_{\rm Pl})\, m_{\lambda,\tilde{q},\tilde{l}} \approx 10^{-2} m_{\lambda,\tilde{q},\tilde{l}}$.

We conclude that the mass ordering between the right-handed sleptons, bino, and gravitino is model dependent. We find, however, that a natural range for the gravitino mass is given by Eq. (2.41).[5] Thus, it is plausible that the LSP is the gravitino with mass smaller than the typical superparticle mass by a factor of a few to a few hundred.

2.5 Signatures at the LHC

Signatures of flavorful supersymmetry at the LHC depend strongly on the mass ordering between the right-handed sleptons, $\tilde{l}_R = \tilde{e}_R, \tilde{\mu}_R, \tilde{\tau}_R$, the bino, $\tilde{B}$, and the gravitino, $\tilde{G}$. Based on signatures at the LHC, the six possible orderings can be classified into three cases.

(a) $m_{\tilde{G}} < m_{\tilde{l}_R} < m_{\tilde{B}}$:

One of the right-handed sleptons is the NLSP, which decays into the LSP gravitino. The lifetime is given by

$$\tau_{\tilde{l}_R} \simeq \frac{48\pi\, m_{\tilde{G}}^2 M_{\rm Pl}^2}{m_{\tilde{l}_R}^5} \left(1 - \frac{m_{\tilde{G}}^2}{m_{\tilde{l}_R}^2}\right)^{-4}, \tag{2.42}$$

which is longer than ~ 100 sec for $m_{3/2}$ in the range of Eq. (2.41). Signatures are therefore stable charged tracks inside the main detectors, as well as the late decay of the lightest slepton in a stopper which could be placed outside the main detector.

(b) $m_{\tilde{l}_R} < m_{\tilde{B}}$, $m_{\tilde{G}}$:

One of the right-handed sleptons is the LSP, leaving charged tracks inside the detector. This case, however, has the cosmological problem of charged stable relics.

(c) $m_{\tilde{B}}$, $m_{\tilde{G}} < m_{\tilde{l}_R}$ or $m_{\tilde{B}} < m_{\tilde{l}_R} < m_{\tilde{G}}$:

A slepton decays into a bino and a lepton inside the detector, so that characteristic signatures are conventional missing energy events. Intrinsic flavor violation in the supersymmetry breaking masses, however, may still be measured by looking at various distributions of kinematic variables.

[5] The gravitino mass can be outside this range. A smaller gravitino mass could arise, for example, if the physics of flavor and supersymmetry breaking occurs below M_U consistently with gauge coupling unification. A larger gravitino mass is also possible if the couplings between X and the matter and Higgs fields are somehow suppressed. For example, if the X field carries a suppression factor ϵ_X then the gravitino mass is enhanced by ϵ_X^{-1}.

2.5.1 Long-lived slepton

We begin our discussion with case (a) above, in which (one of) the right-handed sleptons is the NLSP decaying into the LSP gravitino. The lifetime of the decay, however, is longer than ~ 100 sec, so that the NLSP is stable for collider analyses.

In the LHC, a stable charged particle interacts with the detector in much the same way as a muon. Therefore its momentum can be measured in both the inner tracker and the muon system. Because of its large mass, however, it will generally move slower than a muon. If its speed is in the range $0.6 \lesssim \beta \lesssim 0.8$, then its mass will be measured to a precision of order a few percent [22, 23]. While not all NLSP's produced have velocity in this range, it is reasonable to expect that a substantial fraction will. Even though they are produced from decays of much heavier strongly interacting superparticles, there will usually be several decay branches, each of which will divide the energy of the event. This reasoning is confirmed by more detailed study [24]. With a measurement of the NLSP mass, we can do full reconstruction of decay chains which will reduce the uncertainty in the NLSP mass to of order 0.1% [25],[6] and can measure more parameters of the low energy theory.

To determine the relationship between supersymmetry breaking and flavor physics, a critical measurement is the flavor content of the leptonic NLSP. Because flavor mixing is generically suppressed by ϵ factors, the NLSP will be mostly of a single flavor. In addition, the NLSP is right handed, so the coupling to the charginos will be small, except possibly the Higgsino to $\tilde{\tau}_R$. The coupling to the neutralino with mostly $\tilde{B}$ content, however, will be large, so the NLSP will usually be produced with a charged lepton of the same flavor. Therefore, we can look for events with only two isolated leptons and two NLSP's, and a (large) number of jets. Most such events will have leptons of the same flavor as the NLSP. The high effective mass of the event should significantly reduce the standard model backgrounds (mostly coming from fakes in events with heavy flavors plus jets or electroweak gauge bosons plus jets). Further background rejection, including supersymmetric and combinatoric, will be possible by reconstructing the masses of the intermediate particles. This could be complicated if the NLSP is mostly $\tilde{\tau}_R$, because we cannot fully reconstruct τ's, but the invariant mass can still be reconstructed and the flavor of the NLSP can be identified.

We now analyze the possibility of probing the flavor properties of the heavier sleptons. In particular, we focus on the situation where $\tilde{l}_1$ and $\tilde{l}_2$ are mostly $\tilde{e}_R$ and $\tilde{\mu}_R$. We consider, for definitiveness, the case where $\tilde{e}_R$ is the NLSP, although the same analysis applies if $\tilde{\mu}_R$ is the NLSP. As shown in section 2.4.1, it is likely that $\tilde{\mu}_R$ is only $\epsilon_{E_2}^2 M_{\rm SUSY} \approx$ a few GeV heavier than the NLSP, so the decay of $\tilde{B}$ will produce $\tilde{e}_R$ about half the time and $\tilde{\mu}_R$ just as often. When a $\tilde{\mu}_R$ is produced, it will decay into a $\tilde{e}_R$ and two leptons. The leptons produced in this decay will be soft in the $\tilde{\mu}_R$ rest frame, having energy of order only a few GeV, but in general the system will be boosted. This possibly poses a problem: for a fast $\tilde{\mu}_R$ the leptons will be harder but highly collimated with the NLSP track, $\theta \lesssim 0.1$, while for a slow $\tilde{\mu}_R$ the opening angle will be larger but the leptons will have low p_T. One expects

[6] This precision can be achieved if the systematic uncertainties are ~ 100 MeV and the squarks and gluinos are not too heavy.

that in some intermediate kinematic regime a reconstruction may be feasible, but a detailed study of this issue is beyond the scope of this chapter. If this reconstruction turns out to be possible, one can look for events where one $\tilde{\mu}_R$ is produced, decaying to $\tilde{e}_R$. These events will have two hard leptons, two soft leptons, and two NLSP's. This event topology should make it possible to measure the mass difference between the two lightest sleptons, as well as to provide information on the flavor content of the (N)NLSP by looking at the flavor of the four leptons.

In the region of parameter space where $\alpha_\beta/\alpha_l \ll 1$, the flavor non-universal contribution will be very small and the sleptons will be degenerate. In this co-NLSP region the decay of one slepton into another is suppressed because the decay into charged sleptons is not kinematically allowed and the right-handed sleptons do not couple to neutrinos. In this region, all three right-handed sleptons are long lived, and extracting information on intrinsic flavor violation in the supersymmetry breaking parameters requires careful analyses. Since this is a small region of parameter space, we do not focus on it here.

The above analysis was for case (a) where the slepton was the NLSP and the gravitino the LSP, but it also applies to case (b) where the slepton is the LSP. While this scenario is disfavored cosmologically by limits on charged relics, the situation could be ameliorated by, for example, slight R parity violation in the lepton sector, along with a solution to the dark matter problem independent of supersymmetry.[7]

2.5.2 Late decay of the long-lived slepton

In order to determine the lifetime of the NLSP slepton, we would like to observe its decays. The NLSP's produced with $\beta \lesssim 0.4$ will be stopped within the detector. One can then detect NLSP decays by looking for particles which do not point back to the interaction area. Another possibility is that the NLSP will be stopped in the rock just outside the detector, and then some of the decay products will re-enter the detector. Unfortunately, very few NLSP's will be produced with low enough velocity, and one has to deal with cosmic neutrino background. A further possibility is to use the tracker to determine where in the surrounding rock the NLSP is stopped. If the lifetime is longer than a few weeks, we could then extract pieces of the rock where the NLSP is stopped and study the decay in a more quiet environment [23]. This will also not have very many events, but it will allow very precise measurement of the mass and decay properties of the NLSP.

In addition, a large stopper detector can be built outside the main detector to trap the NLSP's and measure their decay products [24, 26]. Conventional scenarios only consider a $\tilde{\tau}_R$ NLSP, but in flavorful supersymmetry the NLSP could be one of the other sleptons, which would decay to a monochromatic electron or muon. This would make it very easy to (i) measure the mass of the gravitino given the mass of the NLSP measured in the collider, (ii) measure the lifetime of the NLSP by counting the number of decays as a function of time,

[7] An alternative possibility is that the slepton decays into the axino, the fermionic superpartner of the axion, with a lifetime (much) longer than the collider time scale. The phenomenology of this scenario is similar to the case with a gravitino LSP.

and (iii) test supergravity relations such as Eq. (2.42) [27], and make sure that the gravitino is indeed the LSP. The stopper detector proposed in Ref. [24] did not include a magnetic field, so it could not measure the energy of muons, only of electrons and taus. Perhaps this design can be modified to include a magnetic field to measure the momentum of the muons.

A stopper detector can very precisely measure the flavor content of the NLSP. If a sufficient number of NLSP's are trapped and there is flavor mixing, then a few of the NLSP's will decay to a lepton with different flavor. This occurs in a very clean environment so there should be almost no fakes once the accelerator is turned off. A stopper detector can very efficiently separate electrons from muons, and it can use the monochromatic spectrum of the first two generation slepton decays to distinguish τ decay products. Mixing angles as small as about 10^{-2} can be measured [28]. The main background comes from cosmic neutrino events, but those should all have much lower energy than the NLSP decays.

2.5.3 Neutralino (N)LSP

Finally we consider case (c) where the neutralino is lighter than the sleptons. With this spectrum, all sleptons will decay promptly, and measuring flavor violation is more difficult. Because the neutralino will escape the detector without interacting, every event has missing energy, making event reconstruction much more difficult. For direct slepton production one is forced to use kinematic variables such as M_{T2} [29], but they require very high statistics. The low Drell-Yan production cross section quickly prevents this strategy as the slepton mass is increased. The $\tilde{\tau}_R$ is expected to be very split from the other two generations, but looking for τ's means even more particles contributing to missing energy.

We are then driven to study lepton flavor violation in cascade decays by looking at multiple edges in flavor-tagged dilepton invariant mass distributions, along the lines of Refs. [30, 31]. This method requires sizable flavor violating couplings and will probe both those and any modifications to the slepton spectrum. However, in order to perform this study with right-handed sleptons, they must be produced by the second lightest neutralino, χ_2^0, which will be mostly wino, so it has a small branching fraction to right-handed sleptons, typically of order 1%. On the other hand, the χ_2^0 and the left-handed sleptons are expected to be in the same mass range. So if the spectrum is such that the left-handed sleptons are lighter than χ_2^0, then the branching ratio of χ_2^0 to $\tilde{l}_L$ will be large. One can then repeat the analysis of section 2.4.1 in the left-handed slepton sector and use the methods of Ref. [30] to probe flavor violation.

2.6 Conclusions

Weak scale supersymmetry provides elegant solutions to many of the problems of the standard model, but it also generically gives rise to excessive flavor and CP violation. While most existing models assume that the mechanism of mediating supersymmetry breaking to the supersymmetric standard model sector is flavor universal, we have shown that this is not

necessary to satisfy all low energy flavor and CP constraints. We have considered a scenario, flavorful supersymmetry, in which the mechanism that suppresses the Yukawa couplings also suppresses flavor changing interactions in the supersymmetry breaking parameters. We find that a broad region of parameter space is allowed, as long as the superpotential couplings generating scalar trilinear interactions are suppressed or the superparticles have masses of at least a TeV.

The flavorful supersymmetry framework can lead to mass splitting among different generations of squarks and sleptons much larger than in conventional scenarios. This has interesting implications on collider physics. In particular, the mass ordering and splitting among the three right-handed sleptons, which are expected to be the lightest sfermion species, can easily differ significantly from the conventional scenarios. Signatures at colliders depend strongly on the species of the LSP and the NLSP, and we have argued that these are likely to be one of the right-handed sleptons, the bino, or the gravitino. The gravitino mass is typically in the range $10^{-2} m_{\lambda,\tilde{q},\tilde{l}} \lesssim m_{3/2} \lesssim m_{\lambda,\tilde{q},\tilde{l}}$, where $m_{\lambda,\tilde{q},\tilde{l}}$ is a characteristic superparticle mass, so that it is plausible to expect that the LSP is the gravitino with mass smaller than the typical superparticle mass by a factor of a few to a few hundred.

In the case that the lightest right-handed slepton is lighter than the bino, we expect to see the dramatic presence of long-lived charged particles at the LHC. This allows us to do full reconstruction of decay chains and reduce the uncertainty in the NLSP mass determination. Moreover, it is natural to expect that the lightest right-handed slepton is, in fact, the NLSP decaying into the gravitino with the lifetime longer than ~ 100 sec. Because of intrinsic flavor violation in the superparticle masses in flavorful supersymmetry, the NLSP is not necessarily $\tilde{\tau}_R$ but can be $\tilde{e}_R$ or $\tilde{\mu}_R$, leading to the spectacular signature of monochromatic electrons or muons in a stopper detector. This provides a simple method to measure the gravitino mass, as well as the lifetime and the flavor content of the NLSP, and will be a smoking gun signature for flavorful supersymmetry. In general, flavorful supersymmetry predicts flavor violation in both production and decay of sleptons. Precision measurements of these processes will also test the flavor content of the sleptons. While these precision measurements are difficult at the LHC, they can be done by using certain event topologies, regardless of the LSP species. Further study of flavor violation can also be done at a future linear collider.

The origin of the flavor structure is a deep mystery both in the context of the standard model and beyond the standard model. The framework of flavorful supersymmetry allows the LHC to probe this physics which may lie at a scale close to the Planck scale. Precise study of processes such as the ones discussed in this chapter will be crucial to uncover the mechanism that leads to the distinct flavor pattern we see in nature.

Note Added:
While completing this chapter, we received Ref. [32] which discusses similar ideas.

Chapter 3

Flavorful Supersymmetry from Higher Dimensions[1]

3.1 Introduction

One of the longstanding puzzles of the standard model is the distinct pattern of masses and mixings of the quarks and leptons. While supersymmetry addresses many of the other mysteries of the standard model, including the instability of the electroweak scale and the lack of a dark matter candidate, it is not clear if and how supersymmetry helps us understand the flavor puzzle of the standard model at a deeper level. Recently, it has been pointed out that the supersymmetry breaking parameters can exhibit nontrivial flavor structure, and that measurement of these parameters at the LHC can give insight into the flavor sector of the standard model [32, 15]. In particular, it has been shown in Ref. [15] that the class of models called flavorful supersymmetry, in which the supersymmetry breaking parameters receive similar suppressions to those of the Yukawa couplings, can evade all the current experimental bounds and have very distinct signatures at the LHC. In this chapter we present explicit models of flavorful supersymmetry.

In this chapter we construct models in higher dimensional spacetime where supersymmetry breaking and the Higgs fields reside in the same location in the extra dimension(s). This provides a simple way to realize the necessary correlation between the structures of the supersymmetry breaking parameters and the Yukawa couplings [16, 15]. To preserve the successful prediction for supersymmetric gauge coupling unification, we take the size of the extra dimension(s) to be of order the unification scale. The hierarchical structure for the Yukawa couplings is generated by wavefunction overlaps of the matter and Higgs fields [34], and the correlation between flavor and supersymmetry breaking is obtained by relating the location of the Higgs and supersymmetry breaking fields in the extra dimension(s). Models along similar lines were considered previously in Ref. [35], where flavor violation in the supersymmetry breaking masses is induced by finite gauge loop corrections across the bulk.

[1] This chapter was co-written with Yasunori Nomura and Michele Papucci and published in [33].

Here we consider models in which matter fields interact directly with the supersymmetry breaking field, giving the simplest scaling for flavorful effects in the supersymmetry breaking parameters.[2]

While not necessary, the extra dimension(s) with size of order the unification scale can also be used to address various issues of supersymmetric grand unified theories. Grand unification in higher dimensions provides an elegant framework for constructing a simple and realistic model of unification [38, 39]. It naturally achieves doublet-triplet splitting in the Higgs sector and suppresses dangerous proton decay operators, while preserving successful gauge coupling unification. Realistic quark and lepton masses and mixings are also accommodated by placing matter fields in the bulk of higher dimensional spacetime [39, 40, 41]. We thus first construct a grand unified model of flavorful supersymmetry which can successfully address these issues. In this model we also adopt the assumption of strong coupling at the cutoff scale motivated by the simplest understanding of gauge coupling unification in higher dimensions [42, 43], although this is not a necessity to realize flavorful supersymmetry.

There are a variety of ways to incorporate supersymmetry breaking in the present setup. An important constraint on the flavorful supersymmetry framework is that superpotential operators leading to the supersymmetry breaking scalar trilinear interactions must be somewhat suppressed, unless the superparticles are relatively heavy. While it is possible that this suppression arises accidentally or from physics above the cutoff scale, we mainly consider the case where the suppression is due to a symmetry under which the supersymmetry breaking field is charged. This symmetry can also be responsible for a complete solution to the μ problem, the problem of the supersymmetric Higgs mass term (the μ term) being of order the weak scale and not some large mass scale. This leads to a scenario similar to the one discussed in Refs. [21, 44], in which the μ term arises from a cutoff suppressed operator [45] while the gaugino and sfermion masses are generated by gauge mediation [8, 9]. The present setup, however, also leads to flavor violating squark and slepton masses that are correlated with the Yukawa couplings, characterizing flavorful supersymmetry.

We stress that only the extra dimension(s) and the field configuration therein are essential for a realization of flavorful supersymmetry. All the other ingredients, including grand unification, strong coupling, and the particular way of mediating supersymmetry breaking, are not important. While the model described above provides an explicit example of flavorful supersymmetry in which many of the issues of supersymmetric unification are addressed in a relatively simple setup, it is straightforward to eliminate some of the ingredients or to extend the model to accommodate more elaborate structures. In particular, we explicitly discuss a construction in which the theory is weakly coupled at the cutoff scale, which can be straightforwardly applied to models with various spacetime dimensions or gauge groups.

The organization of the chapter is as follows. In the next section we present a unified model of flavorful supersymmetry with the assumption that the theory is strongly coupled at the cutoff scale. We explain how the relevant correlation between the Yukawa couplings and

[2]Flavor violation in higher dimensional supersymmetric models was also discussed in different contexts, see [36, 37].

supersymmetry breaking parameters is obtained. Phenomenology of the model is studied in section 3.3, including constraints from low-energy processes, the superparticle spectrum, and experimental signatures. In section 3.4 we construct a model in warped space, which allows us to obtain a picture of realizing flavorful supersymmetry in a 4D setup, through the AdS/CFT correspondence. In section 3.5 we present a weakly coupled, non-unified model, which does not possess a symmetry under which the supersymmetry breaking field is charged. Extensions to larger gauge groups or higher dimensions are also discussed. Finally, conclusions are given in section 3.6.

3.2 Model

In this section we present a unified, strongly coupled model. We adopt the simplest setup, $SU(5)$ in 5D, to illustrate the basic idea. Extensions to other cases such as larger gauge groups and/or higher dimensions are straightforward. It is also easy to reduce the model to a non-unified model in which the gauge group in 5D is the standard model $SU(3)_C \times SU(2)_L \times U(1)_Y$.

3.2.1 $SU(5)$ grand unification in 5D

We consider a supersymmetric $SU(5)$ gauge theory in 5D flat spacetime with the extra dimension compactified on an S^1/Z_2 orbifold: $0 \le y \le \pi R$, where y represents the coordinate of the extra dimension [38, 39]. Under 4D $N = 1$ supersymmetry, the 5D gauge supermultiplet is decomposed into a vector superfield $V(A_\mu, \lambda)$ and a chiral superfield $\Sigma(\sigma + iA_5, \lambda')$, where both V and Σ are in the adjoint representation of $SU(5)$. We impose the following boundary conditions on these fields:

$$V : \left(\begin{array}{ccc|cc} (+,+) & (+,+) & (+,+) & (+,-) & (+,-) \\ (+,+) & (+,+) & (+,+) & (+,-) & (+,-) \\ (+,+) & (+,+) & (+,+) & (+,-) & (+,-) \\ \hline (+,-) & (+,-) & (+,-) & (+,+) & (+,+) \\ (+,-) & (+,-) & (+,-) & (+,+) & (+,+) \end{array}\right), \tag{3.1}$$

$$\Sigma : \left(\begin{array}{ccc|cc} (-,-) & (-,-) & (-,-) & (-,+) & (-,+) \\ (-,-) & (-,-) & (-,-) & (-,+) & (-,+) \\ (-,-) & (-,-) & (-,-) & (-,+) & (-,+) \\ \hline (-,+) & (-,+) & (-,+) & (-,-) & (-,-) \\ (-,+) & (-,+) & (-,+) & (-,-) & (-,-) \end{array}\right), \tag{3.2}$$

where $+$ and $-$ represent Neumann and Dirichlet boundary conditions, and the first and second signs in parentheses represent boundary conditions at $y = 0$ and $y = \pi R$, respectively. This reduces the gauge symmetry at $y = \pi R$ to $SU(3) \times SU(2) \times U(1)$, which we identify with the standard model gauge group $SU(3)_C \times SU(2)_L \times U(1)_Y$ (321). The zero-mode sector

contains only the 321 component of V, V^{321}, which is identified with the gauge multiplet of the minimal supersymmetric standard model (MSSM).

The Higgs fields are introduced in the bulk as two hypermultiplets transforming as the fundamental representation of $SU(5)$. Using notation where a hypermultiplet is represented by two 4D $N = 1$ chiral superfields $\Phi(\phi, \psi)$ and $\Phi^c(\phi^c, \psi^c)$ with opposite gauge transformation properties, our two Higgs hypermultiplets can be written as $\{H, H^c\}$ and $\{\bar{H}, \bar{H}^c\}$, where H and $\bar{H}^c$ transform as $\mathbf{5}$ and $\bar{H}$ and H^c transform as $\mathbf{5}^*$ under $SU(5)$. The boundary conditions are given by

$$H(\mathbf{5}) = H_T(\mathbf{3},\mathbf{1})^{(+,-)}_{-1/3} \oplus H_D(\mathbf{1},\mathbf{2})^{(+,+)}_{1/2}, \tag{3.3}$$

$$H^c(\mathbf{5}^*) = H^c_T(\mathbf{3}^*,\mathbf{1})^{(-,+)}_{1/3} \oplus H^c_D(\mathbf{1},\mathbf{2})^{(-,-)}_{-1/2}, \tag{3.4}$$

for $\{H, H^c\}$, and similarly for $\{\bar{H}, \bar{H}^c\}$. Here, the right-hand-side shows the decomposition of H and H^c into representations of 321 (with $U(1)_Y$ normalized conventionally), together with the boundary conditions imposed on each component. The zero modes consist of the $SU(2)_L$-doublet components of H and $\bar{H}$, H_D and $\bar{H}_D$, which are identified with the two Higgs doublets of the MSSM, H_u and H_d.

Matter fields are also introduced in the bulk. To have a complete generation, we introduce three hypermultiplets transforming as $\mathbf{10}$, $\{T, T^c\}$, $\{T', T'^c\}$ and $\{T'', T''^c\}$, two transforming as $\mathbf{5}^*$, $\{F, F^c\}$ and $\{F', F'^c\}$, and one transforming as $\mathbf{1}$, $\{O, O^c\}$, for each generation. The boundary conditions are given by

$$T(\mathbf{10}) = T_Q(\mathbf{3},\mathbf{2})^{(+,+)}_{1/6} \oplus T_U(\mathbf{3}^*,\mathbf{1})^{(+,-)}_{-2/3} \oplus T_E(\mathbf{1},\mathbf{1})^{(+,-)}_{1}, \tag{3.5}$$

$$T'(\mathbf{10}) = T'_Q(\mathbf{3},\mathbf{2})^{(+,-)}_{1/6} \oplus T'_U(\mathbf{3}^*,\mathbf{1})^{(+,+)}_{-2/3} \oplus T'_E(\mathbf{1},\mathbf{1})^{(+,-)}_{1}, \tag{3.6}$$

$$T''(\mathbf{10}) = T''_Q(\mathbf{3},\mathbf{2})^{(+,-)}_{1/6} \oplus T''_U(\mathbf{3}^*,\mathbf{1})^{(+,-)}_{-2/3} \oplus T''_E(\mathbf{1},\mathbf{1})^{(+,+)}_{1}, \tag{3.7}$$

$$F(\mathbf{5}^*) = F_D(\mathbf{3}^*,\mathbf{1})^{(+,+)}_{1/3} \oplus F_L(\mathbf{1},\mathbf{2})^{(+,-)}_{-1/2}, \tag{3.8}$$

$$F'(\mathbf{5}^*) = F'_D(\mathbf{3}^*,\mathbf{1})^{(+,-)}_{1/3} \oplus F'_L(\mathbf{1},\mathbf{2})^{(+,+)}_{-1/2}, \tag{3.9}$$

$$O(\mathbf{1}) = O_N(\mathbf{1},\mathbf{1})^{(+,+)}_{0}. \tag{3.10}$$

The boundary conditions for the conjugated fields are given by $+ \leftrightarrow -$, as in Eqs. (3.3, 3.4). With these boundary conditions, the zero modes arise only from T_Q, T'_U, T''_E, F_D, F'_L and O_N, which we identify with a single generation of quark and lepton superfields of the MSSM (together with the right-handed neutrino), Q, U, E, D, L and N.[3]

There are two important scales in the theory: the cutoff scale M_* and the compactification scale $1/R$. We take the ratio of these scales to be $\pi R M_* \approx 16\pi^2/g^2 C \approx O(10 - 100)$, where g

[3]It is possible to extract both U and E from a single hypermultiplet $\{T', T'^c\}$ by adopting the boundary conditions $T'(\mathbf{10}) = T'_Q(\mathbf{3},\mathbf{2})^{(+,-)}_{1/6} \oplus T'_U(\mathbf{3}^*,\mathbf{1})^{(+,+)}_{-2/3} \oplus T'_E(\mathbf{1},\mathbf{1})^{(+,+)}_{1}$, in which case we do not introduce the hypermultiplet $\{T'', T''^c\}$. In fact, this is what we obtain if we naively apply the orbifolding procedure to the matter hypermultiplets. The model also works in this case, with the extra constraint of $M_{U_i} = M_{E_i}$ (see section 3.2.2) and $q_Q = q_L$ (see section 3.2.3).

is the 4D gauge coupling at the unification scale, $g = O(1)$, and $C \simeq 5$ is the group theoretical factor for $SU(5)$. This makes the theory strongly coupled at M_*, suppressing incalculable threshold corrections to gauge coupling unification [42, 43].[4] Motivated by successful gauge coupling unification at about 10^{16} GeV in supersymmetric models, we take the cutoff scale and the scale of the extra dimension to be

$$M_* \approx 10^{17} \text{ GeV}, \qquad 1/\pi R \approx 10^{15} \text{ GeV}. \tag{3.11}$$

More detailed discussions on gauge coupling unification will be given in section 3.3.4.

3.2.2 Quark and lepton masses and mixings

With the boundary conditions given in the previous subsection, the matter content of the theory below $1/R$ reduces to that of the MSSM and right-handed neutrinos: V^{321}, H_u, H_d, Q_i, U_i, D_i, L_i, E_i and N_i, where $i = 1, 2, 3$ is the generation index. The Yukawa couplings for the quarks and leptons are introduced on the $y = 0$ and $y = \pi R$ branes. The sizes of the 4D Yukawa couplings are then determined by the wavefunction values of the matter and Higgs fields on these branes. This can be used to generate the observed hierarchy of quark and lepton masses and mixings [34, 35, 41]. Here we consider particular configurations of these fields, relevant to our framework.

A nontrivial wavefunction profile for a zero mode can be generated by a bulk mass term. A bulk hypermultiplet $\{\Phi, \Phi^c\}$ can generally have a mass term in the bulk, which is written as

$$S = \int d^4x \int_0^{\pi R} dy \int d^2\theta \, M_\Phi \Phi \Phi^c + \text{h.c.}, \tag{3.12}$$

in the basis where the kinetic term is given by $S_{\rm kin} = \int d^4x \int dy \, [\int d^4\theta \, (\Phi^\dagger \Phi + \Phi^c \Phi^{c\dagger}) + \{\int d^2\theta \, \Phi^c \partial_y \Phi + \text{h.c.}\}]$ [46]. The wavefunction of a zero mode arising from Φ is proportional to $e^{-M_\Phi y}$, so that it is localized to the $y = 0$ ($y = \pi R$) brane for $M_\Phi > 0$ (< 0), and flat for $M_\Phi = 0$. (The Φ^c case is the same with $M_\Phi \to -M_\Phi$.) In the present model, we have a bulk mass for each of the Higgs and matter hypermultiplets. For clarity of notation, we specify these masses by the subscript representing the corresponding zero mode: M_{H_u}, M_{H_d}, M_{Q_i}, M_{U_i}, M_{D_i}, M_{L_i}, M_{E_i} and M_{N_i}.

We mainly consider the case that the two Higgs doublets H_u and H_d are strongly localized to the $y = \pi R$ brane:

$$M_{H_u}, \, M_{H_d} \ll -\frac{1}{R}. \tag{3.13}$$

The relevant Yukawa couplings are then those on the $y = \pi R$ brane

$$\begin{aligned} S \;=\; & \int d^4x \int_0^{\pi R} dy \; \delta(y - \pi R) \int d^2\theta \Big\{ (\lambda_u)_{ij} T_{Q_i} T'_{U_j} H_D \\ & + (\lambda_d)_{ij} T_{Q_i} F_{Dj} \bar{H}_D + (\lambda_e)_{ij} F'_{Li} T''_{Ej} \bar{H}_D + (\lambda_\nu)_{ij} F'_{Li} O_{Nj} H_D \Big\} + \text{h.c.}, \end{aligned} \tag{3.14}$$

[4] Our estimate on the strong coupling scale is conservative. It is possible that $M_* R$ can be larger by a factor of $\approx \pi$, but it does not affect our results.

where the sizes of the couplings are naturally given by $(\lambda_u)_{ij}, (\lambda_d)_{ij}, (\lambda_e)_{ij}, (\lambda_\nu)_{ij} \approx 4\pi/M_*^{3/2}$ using naive dimensional analysis [47, 42]. This leads to the low-energy 4D Yukawa couplings

$$W = (y_u)_{ij} Q_i U_j H_u + (y_d)_{ij} Q_i D_j H_d + (y_e)_{ij} L_i E_j H_d + (y_\nu)_{ij} L_i N_j H_u, \tag{3.15}$$

with

$$\begin{aligned} (y_u)_{ij} &\approx 4\pi\, \epsilon_{Q_i} \epsilon_{U_j}, \qquad (y_d)_{ij} \approx 4\pi\, \epsilon_{Q_i} \epsilon_{D_j}, \\ (y_e)_{ij} &\approx 4\pi\, \epsilon_{L_i} \epsilon_{E_j}, \qquad (y_\nu)_{ij} \approx 4\pi\, \epsilon_{L_i} \epsilon_{N_j}, \end{aligned} \tag{3.16}$$

where the factors ϵ_Φ ($\Phi = Q_i, U_i, D_i, L_i, E_i, N_i$) are given by

$$\epsilon_\Phi = \sqrt{\frac{2M_\Phi}{(1 - e^{-2\pi R M_\Phi}) M_*}}\, e^{-\pi R M_\Phi} \simeq \begin{cases} \sqrt{\frac{2M_\Phi}{M_*}}\, e^{-\pi R M_\Phi} & \text{for } \pi R M_\Phi \gtrsim 1 \\ \frac{1}{\sqrt{\pi R M_*}} & \text{for } |\pi R M_\Phi| \ll 1 \\ \sqrt{\frac{2|M_\Phi|}{M_*}} & \text{for } \pi R M_\Phi \lesssim -1 \end{cases}. \tag{3.17}$$

Realistic Yukawa couplings are obtained by localizing lighter generations more towards the $y = 0$ brane so that their wavefunction overlaps with the Higgs fields are more suppressed. For example, we can take

$$\begin{array}{lllll} \epsilon_{Q_1} \approx \tilde{y}^{-\frac{1}{2}} \epsilon^2, & \epsilon_{U_1} \approx \tilde{y}^{-\frac{1}{2}} \epsilon^2, & \epsilon_{D_1} \approx \tilde{y}^{-\frac{1}{2}} \epsilon, & \epsilon_{L_1} \approx \tilde{y}^{-\frac{1}{2}} \epsilon, & \epsilon_{E_1} \approx \tilde{y}^{-\frac{1}{2}} \epsilon^2, \\ \epsilon_{Q_2} \approx \tilde{y}^{-\frac{1}{2}} \epsilon, & \epsilon_{U_2} \approx \tilde{y}^{-\frac{1}{2}} \epsilon, & \epsilon_{D_2} \approx \tilde{y}^{-\frac{1}{2}} \epsilon, & \epsilon_{L_2} \approx \tilde{y}^{-\frac{1}{2}} \epsilon, & \epsilon_{E_2} \approx \tilde{y}^{-\frac{1}{2}} \epsilon, \\ \epsilon_{Q_3} \approx \tilde{y}^{-\frac{1}{2}}, & \epsilon_{U_3} \approx \tilde{y}^{-\frac{1}{2}}, & \epsilon_{D_3} \approx \tilde{y}^{-\frac{1}{2}} \epsilon, & \epsilon_{L_3} \approx \tilde{y}^{-\frac{1}{2}} \epsilon, & \epsilon_{E_3} \approx \tilde{y}^{-\frac{1}{2}}, \end{array} \tag{3.18}$$

and

$$\tan\beta \equiv \frac{\langle H_u \rangle}{\langle H_d \rangle} \approx \epsilon^{-1}, \tag{3.19}$$

where $\epsilon \sim O(0.1)$ and $\tilde{y} \simeq 4\pi \approx 1/\epsilon$, to reproduce the gross structure of the observed quark and lepton masses and mixings. The suppression factors of Eq. (3.18) are obtained by taking bulk masses

$$M_{Q_3, U_3, E_3} \approx -\frac{1}{R}, \qquad M_{Q_2, U_2, D_i, L_i, E_2} \approx \frac{0.5 - 1}{R}, \qquad M_{Q_1, U_1, E_1} \approx \frac{1.5}{R}. \tag{3.20}$$

Small neutrino masses are obtained through the seesaw mechanism by introducing Majorana masses for the right-handed neutrinos on the $y = \pi R$ brane

$$S = \int d^4x \int_0^{\pi R} dy\; \delta(y - \pi R) \int d^2\theta\, \frac{(M_N)_{ij}}{2M_*}\, O_{Ni} O_{Nj} + \text{h.c.} \tag{3.21}$$

The values of ϵ_{N_i} are then not relevant to the low-energy masses and mixings (unless N_i's are localized to the $y = 0$ brane extremely strongly), since they cancel out in the expression for the light neutrino masses.

The localization of various fields in the extra dimension with the bulk masses of Eqs. (3.13, 3.20) is depicted schematically in Fig. 3.1. The quark and lepton masses and

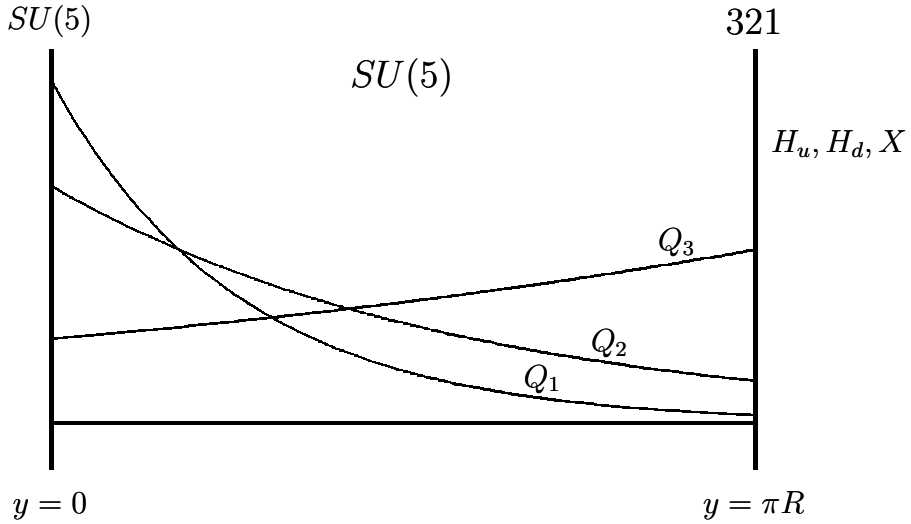

Figure 3.1: A schematic depiction of the localization for various fields. Here, X represents the supersymmetry breaking field (see section 3.2.3).

mixings are given by

$$\begin{array}{lcl} (m_t, m_c, m_u) & \approx & v\,(1, \epsilon^2, \epsilon^4), \\ (m_b, m_s, m_d) & \approx & v\,(\epsilon^2, \epsilon^3, \epsilon^4), \\ (m_\tau, m_\mu, m_e) & \approx & v\,(\epsilon^2, \epsilon^3, \epsilon^4), \\ (m_{\nu_\tau}, m_{\nu_\mu}, m_{\nu_e}) & \approx & \frac{v^2}{M_N}(1, 1, 1), \end{array} \tag{3.22}$$

and

$$V_{\rm CKM} \approx \begin{pmatrix} 1 & \epsilon & \epsilon^2 \\ \epsilon & 1 & \epsilon \\ \epsilon^2 & \epsilon & 1 \end{pmatrix}, \qquad V_{\rm MNS} \approx \begin{pmatrix} 1 & 1 & 1 \\ 1 & 1 & 1 \\ 1 & 1 & 1 \end{pmatrix}, \tag{3.23}$$

where $O(1)$ factors are omitted from each element, and $V_{\rm CKM}$ and $V_{\rm MNS}$ are the quark and lepton mixing matrices, respectively. This reproduces the gross structure of the observed quark and lepton masses and mixings [19].

The matter configuration considered here can be extended easily to account for the more detailed pattern of the observed masses and mixings. For example, we can localize L_1 slightly more towards the $y = 0$ brane to explain the smallness of the $e3$ element of $V_{\rm MNS}$, which is experimentally smaller than about 0.2. The other elements of $V_{\rm CKM}$ and $V_{\rm MNS}$, as well as the mass eigenvalues, can also be better fitted by choosing the bulk masses more carefully. Here we simply adopt Eq. (3.20) (and its variations, discussed in section 3.3.1) for the purpose of illustrating the general idea.

There are also variations on the location of the Higgs fields. For example, we can localize the two Higgs doublets on the $y = 0$ brane, instead of the $y = \pi R$ brane: $M_{H_u}, M_{H_d} \gtrsim 1/\pi R$.

In this case, the localization should not be very strong so that their colored-triplet partners, whose masses are given by $\approx 2M_{H_u}e^{-\pi RM_{H_u}}$ and $2M_{H_d}e^{-\pi RM_{H_d}}$, do not become too light. The location of the matter fields can simply be flipped with respect to $y = \pi R/2$: $M_\Phi \to -M_\Phi$ for $\Phi = Q_i, U_i, D_i, L_i, E_i, N_i$. Another possibility is to (slightly) delocalize H_u and/or H_d from the brane. In this chapter, we focus on the case of Eq. (3.13), where H_u and H_d are strongly localized to the $y = \pi R$ brane.

3.2.3 μ term, $U(1)_H$, and flavorful supersymmetry

In order to have a complete solution to the doublet-triplet splitting problem, a possible large mass term for the Higgs doublets on the $y = \pi R$ brane, $\delta(y - \pi R)\int d^2\theta\, H_D\bar{H}_D$, must be forbidden by some symmetry. Moreover, to understand the weak scale size of the mass term (μ term) for the Higgs doublets, the breaking of this symmetry must be associated with supersymmetry breaking. One possibility to implement this idea is to consider a $U(1)_R$ symmetry under which the two Higgs doublets are neutral [39]. Here we consider the case that the symmetry is a non-R symmetry.

We consider that the bare μ term, $\int d^2\theta\, H_uH_d$, is forbidden, but the effective μ term is generated by the operator $\int d^4\theta\, X^\dagger H_uH_d$ through supersymmetry breaking, where X is a supersymmetry breaking field [45]. We then find that the relevant symmetry is $U(1)$ (a Peccei-Quinn symmetry) whose charge assignment can be taken, without loss of generality, as

$$Q_i(q_Q), \quad U_i(-1-q_Q), \quad D_i(-1-q_Q), \quad L_i(q_L), \quad E_i(-1-q_L), \quad N_i(-1-q_L), \tag{3.24}$$

$$H_u(1), \quad H_d(1), \quad X(2), \tag{3.25}$$

where q_Q and q_L are real numbers, and we have assumed that the Yukawa couplings are invariant under the symmetry. In the context of the 5D theory, this assignment can be implemented by considering $U(1)$ charges for a hypermultiplet $\{\Phi, \Phi^c\}$ ($\Phi = H, \bar{H}, T_i, T_i', T_i'', F_i, F_i', O_i$) such that the charge of Φ follows that of the corresponding zero mode, while the charge of Φ^c is the opposite to that of Φ. This $U(1)$ symmetry commutes with 5D supersymmetry. The X field is introduced on the $y = \pi R$ brane, either as a brane field or a bulk field whose zero mode is strongly localized to the $y = \pi R$ brane by a bulk mass term $M_X \ll -1/R$ (see Fig. 3.1).

The $U(1)$ symmetry of Eqs. (3.24, 3.25), which we call $U(1)_H$, has several immediate virtues. First of all, the most general interactions between the Higgs and X fields, located on the $y = \pi R$ brane, leads (up to the quadratic order in X) to the following interactions in 4D:

$$\mathcal{L} \approx \int d^4\theta \left[\left(\frac{1}{\Lambda}X^\dagger H_uH_d + \text{h.c.}\right) + \frac{1}{\Lambda^2}X^\dagger X H_u^\dagger H_u + \frac{1}{\Lambda^2}X^\dagger X H_d^\dagger H_d\right], \tag{3.26}$$

where we have used naive dimensional analysis to estimate the sizes of various coefficients, and omitted an $O(1)$ factor in each term. The mass scale Λ is defined by

$$\Lambda \equiv \frac{M_*}{4\pi} \approx 10^{16}\ \text{GeV}, \tag{3.27}$$

where we have used Eq. (3.11). After supersymmetry is broken by the F-term vacuum expectation value (VEV), F_X, of the X field (see the next subsection), these interactions lead to the μ term and soft supersymmetry breaking masses for the Higgs fields of order F_X/Λ at the scale M_*:

$$\mu \approx \frac{F_X}{\Lambda}, \qquad m_{H_u}^2 \approx m_{H_d}^2 \approx \left(\frac{F_X}{\Lambda}\right)^2. \tag{3.28}$$

(Note that $O(1)$ coefficients are omitted in these equations, so that the ratio of $m_{H_u}^2$ to $m_{H_d}^2$, for example, can be an arbitrary $O(1)$ number.) An important point here is that the operator $\mathcal{L} \approx \int d^4\theta\, (X^\dagger X H_u H_d/\Lambda^2 + \text{h.c.})$ is prohibited by $U(1)_H$, so that the holomorphic supersymmetry breaking mass-squared for the Higgs doublets ($B\mu$ term) is not generated at order $(F_X/\Lambda)^2$ at tree level.[5] The low-energy value of the $B\mu$ term is then generated by contributions from the gaugino masses through renormalization group evolution. This is crucial to avoid the supersymmetric CP problem, since for weak scale superparticle masses an arbitrary relative phase between the μ and $B\mu$ terms leads to an unacceptably large electric dipole moment for the electron.

Another important implication of $U(1)_H$ is that possible $y = \pi R$ brane operators $\delta(y - \pi R) \int d^2\theta\, (X T_{Q_i} T'_{U_j} H_D + X T_{Q_i} F_{D_j} \bar{H}_D + X F'_{L_i} T''_{E_j} \bar{H}_D + X F'_{L_i} O_{N_j} H_D) + \text{h.c.}$, which reduce in 4D to $\int d^2\theta\, (X Q_i U_j H_u + X Q_i D_j H_d + X L_i E_j H_d + X L_i N_j H_u) + \text{h.c.}$, are forbidden. If these operators were present, they would lead to supersymmetry breaking scalar trilinear interactions (A terms) of order $(a_u)_{ij} \approx 4\pi \epsilon_{Q_i} \epsilon_{U_j} (F_X/\Lambda)$, $(a_d)_{ij} \approx 4\pi \epsilon_{Q_i} \epsilon_{D_j} (F_X/\Lambda)$, $(a_e)_{ij} \approx 4\pi \epsilon_{L_i} \epsilon_{E_j} (F_X/\Lambda)$ and $(a_\nu)_{ij} \approx 4\pi \epsilon_{L_i} \epsilon_{N_j} (F_X/\Lambda)$, which are not necessarily proportional to the corresponding Yukawa matrices in flavor space. Here, $(a_f)_{ij}$ ($f = u, d, e, \nu$) are defined by $\mathcal{L}_{\text{soft}} = -(a_u)_{ij} \tilde{q}_i \tilde{u}_j h_u - (a_d)_{ij} \tilde{q}_i \tilde{d}_j h_d - (a_e)_{ij} \tilde{l}_i \tilde{e}_j h_d - (a_\nu)_{ij} \tilde{l}_i \tilde{n}_j h_u + \text{h.c.}$. While these terms are suppressed by ϵ factors, they still provide sizable contributions to low-energy flavor violating processes, because an A-term insertion flips the chirality of the sfermion and thus eliminates one factor of the Yukawa coupling from an amplitude. We then find that with $O(1)$ coefficients, the rate for $\mu \to e\gamma$ is expected to be larger than the experimental upper bound by a couple of orders of magnitude for weak scale superparticle masses [15, 16]. This problem does not arise in the present model.

The interactions between the matter and X fields relevant to soft supersymmetry breaking parameters take the form $\delta(y - \pi R) \int d^4\theta\, (X^\dagger X T_{Q_i}^\dagger T_{Q_j} + X^\dagger X T'^\dagger_{U_i} T'_{U_j} + X^\dagger X F_{D_i}^\dagger F_{D_j} + X^\dagger X F'^\dagger_{L_i} F'_{L_j} + X^\dagger X T''^\dagger_{E_i} T''_{E_j} + X^\dagger X O_{N_i}^\dagger O_{N_j})$, which reduce in 4D to

$$\mathcal{L} \approx \int d^4\theta \sum_\Phi \sum_{i,j} \frac{\epsilon_{\Phi_i} \epsilon_{\Phi_j}}{\Lambda^2} X^\dagger X \Phi_i^\dagger \Phi_j, \tag{3.29}$$

where $\Phi = Q, U, D, L, E, N$. This leads to the following supersymmetry breaking squared

[5] There are contributions to the $B\mu$ term of order $F_X^2 \langle X \rangle/\Lambda^3$ and $F_X m_{3/2}/\Lambda$, where $m_{3/2}$ is the gravitino mass, coming from operators $\mathcal{L} \approx \int d^4\theta\, (X^{\dagger 2} X H_u H_d/\Lambda^3 + \text{h.c.})$ and the supergravity effects of the first term of Eq. (3.26), respectively. These contributions are, however, negligibly small, since $\langle X \rangle/\Lambda \approx \Lambda/M_{\text{Pl}} \ll 1$ and $m_{3/2} \approx F_X/M_{\text{Pl}} \ll F_X/\Lambda$, where $M_{\text{Pl}} \simeq 2 \times 10^{18}$ GeV is the reduced Planck scale (see section 3.2.4).

masses for the squarks and sleptons at the scale M_*:

$$(m^2_{\tilde{q}})_{ij} \approx \epsilon_{Q_i}\epsilon_{Q_j}\left(\frac{F_X}{\Lambda}\right)^2, \qquad (m^2_{\tilde{u}})_{ij} \approx \epsilon_{U_i}\epsilon_{U_j}\left(\frac{F_X}{\Lambda}\right)^2, \qquad (m^2_{\tilde{d}})_{ij} \approx \epsilon_{D_i}\epsilon_{D_j}\left(\frac{F_X}{\Lambda}\right)^2, \quad (3.30)$$

$$(m^2_{\tilde{l}})_{ij} \approx \epsilon_{L_i}\epsilon_{L_j}\left(\frac{F_X}{\Lambda}\right)^2, \qquad (m^2_{\tilde{e}})_{ij} \approx \epsilon_{E_i}\epsilon_{E_j}\left(\frac{F_X}{\Lambda}\right)^2, \quad (3.31)$$

where we have omitted supersymmetry breaking masses for the right-handed sneutrinos, which are not relevant for low-energy phenomenology. Through Eq. (3.16), these masses are related to the Yukawa couplings — lighter generation scalars receive only small contributions, while heavier generation scalars can receive sizable ones. This is exactly the pattern needed to realize the flavorful supersymmetry scenario, which arises here from the fact that the Higgs and supersymmetry breaking fields reside in the same location in the extra dimension.

As shown in Ref. [15], the existence of flavor non-universal contributions of Eqs. (3.30, 3.31) does not contradict the low-energy data on flavor or CP violating processes for wide parameter regions. Since the masses of Eqs. (3.30, 3.31) are highly flavor non-universal, they cannot be the dominant contribution to the soft masses (except possibly for some of the third generation sfermions), and we need an extra flavor universal contribution as well as the gaugino masses. These are generated in the present model by gauge mediation, as discussed in the next subsection.

Finally, the $U(1)_H$ symmetry forbids any superpotential term involving only the X field. Since breaking supersymmetry requires a linear X term in the superpotential, this implies that supersymmetry is not broken unless $U(1)_H$ is broken, providing a solid relation between breaking of supersymmetry and that of $U(1)_H$.

3.2.4 Supersymmetry breaking and the low-energy spectrum

To induce supersymmetry breaking VEV F_X, we need a linear term of X in the superpotential. This implies that $U(1)_H$ must be broken either explicitly or spontaneously. Here we simply parameterize the effect of $U(1)_H$ breaking in the X potential by a dimensionless chiral spurious parameter η, which we assume to have the $U(1)_H$ charge of -2. The resulting physics does not depend much on the underlying origin of this breaking.

The most general low-energy 4D interactions of X consistent with the (broken) $U(1)_H$ symmetry is given by the following Kähler potential and superpotential:

$$K \approx X^\dagger X - \frac{1}{4\Lambda^2}(X^\dagger X)^2 + \cdots, \quad (3.32)$$

$$W \approx c + \mu_X^2 X + \frac{\mu_X^4}{4\pi\Lambda^3}X^2 + \frac{\mu_X^6}{(4\pi)^2\Lambda^6}X^3 + \cdots, \quad (3.33)$$

where c is a constant term in the superpotential, needed to cancel the cosmological constant, and $\mu_X^2 \equiv 4\pi\eta\Lambda^2$. Here, again, we have used naive dimensional analysis to estimate the sizes

of various coefficients (except for the c term), and omitted an $O(1)$ factor in each term.[6] Note that the terms in Eqs. (3.32, 3.33) arise from operators localized on the $y = \pi R$ brane, except for the c term which can have contributions from other sources as well.

The scalar potential arising from Eqs. (3.32, 3.33) can be minimized in supergravity. Assuming that the coefficient of the $(X^\dagger X)^2/\Lambda^2$ term in the Kähler potential is negative, the minimum of X is given by the competition between the X mass term arising from $V \simeq (\mu_X^4/\Lambda^2)|X|^2 \subset |\partial W/\partial X|^2(\partial^2 K/\partial X^\dagger \partial X)^{-1}$ and the linear term $V \simeq -2\mu_X^2 c(X + X^\dagger)/M_{\rm Pl}^2$ arising in supergravity. The constant c is determined to cancel the vacuum energy $V \simeq |\partial W/\partial X|^2 - 3|W|^2/M_{\rm Pl}^2$ as $c \simeq \mu_X^2 M_{\rm Pl}/\sqrt{3}$. This, therefore, leads to the following supersymmetry breaking minimum

$$\langle X \rangle \simeq \frac{2\Lambda^2}{\sqrt{3} M_{\rm Pl}} \approx 10^{14}\ {\rm GeV}, \qquad F_X \simeq \mu_X^2, \tag{3.34}$$

with the mass-squared for the X excitation given by $m_X^2 \approx \mu_X^4/\Lambda^2$. Note that the X VEV, $\langle X \rangle \approx 10^{14}$ GeV, is smaller than the compactification scale, $1/\pi R \approx 10^{15}$ GeV, so that the 4D analysis of the potential minimization is justified. In fact, with μ_X much smaller than $\langle X \rangle$ to reproduce the weak scale superparticle masses (see Eqs. (3.28, 3.30, 3.31) and below), the only relevant terms in the potential minimization are the first two terms of Eqs. (3.32) and (3.33).

The supersymmetry breaking of Eq. (3.34) can be transmitted to the MSSM gauginos and scalars by gauge mediation by coupling X to the messenger fields f and $\bar{f}$: $W = \lambda X f \bar{f}$ [48]. The minimum of X in Eq. (3.34) is not destabilized as long as the coupling λ is sufficiently small, $\lambda^2 n_f/16\pi^2 \lesssim (\Lambda/M_{\rm Pl})^2$, where n_f is the number of components for the messenger fields. We introduce the messenger fields in the bulk as hypermultiplets: $\{f, f^c\}$ and $\{\bar{f}, \bar{f}^c\}$. The boundary conditions are given by

$$f(\mathbf{5}) = f_D(\mathbf{3},\mathbf{1})^{(+,+)}_{-1/3} \oplus f_L(\mathbf{1},\mathbf{2})^{(+,+)}_{1/2}, \tag{3.35}$$

$$f^c(\mathbf{5}^*) = f^c_D(\mathbf{3}^*,\mathbf{1})^{(-,-)}_{1/3} \oplus f^c_L(\mathbf{1},\mathbf{2})^{(-,-)}_{-1/2}, \tag{3.36}$$

and similarly for $\{\bar{f}, \bar{f}^c\}$, leading to the zero modes from f_D, f_L, $\bar{f}_D$ and $\bar{f}_L$. Here, we have chosen the messenger fields to be a pair of $\mathbf{5} + \mathbf{5}^*$, for simplicity, but they can in general be an arbitrary number of pairs of arbitrary $SU(5)$ representations (as long as they do not make the standard model gauge couplings strong at or below $\sim 1/R$). The messenger fields have interactions to X on the $y = \pi R$ brane:

$$S = \int d^4x \int_0^{\pi R} dy\ \delta(y - \pi R) \int d^2\theta\, (\eta_D\, X f_D \bar{f}_D + \eta_L\, X f_L \bar{f}_L) + {\rm h.c.}, \tag{3.37}$$

where the couplings η_D and η_L are of order $4\pi/M_*$ ($4\pi/M_*^{3/2}$) from naive dimensional analysis if X is a $y = \pi R$ brane (bulk) field. This determines the $U(1)_H$ charges of the $f = f_D + f_L$

[6] The most general insertions of the spurious parameter η allows us to write down the tree-level μ term in the superpotential, with $\mu \approx 4\pi\eta\Lambda \approx \mu_X^2/\Lambda$. This contribution is the same order as the one in Eq. (3.28); see Eq. (3.34).

and $\bar{f} = \bar{f}_D + \bar{f}_L$ fields such that the sum of the f and $\bar{f}$ charges is -2. (The f^c and $\bar{f}^c$ fields have the opposite charges to f and $\bar{f}$, respectively.)

The messenger multiplets in general have the bulk mass terms of the form of Eq. (3.12), M_f and $M_{\bar{f}}$. The interactions of Eq. (3.37) then lead to the 4D superpotential

$$W = \lambda_D X f_D \bar{f}_D + \lambda_L X f_L \bar{f}_L, \tag{3.38}$$

where f_D, f_L, $\bar{f}_D$ and $\bar{f}_L$ represent the zero-mode chiral superfields, and

$$\lambda_D \approx \lambda_L \approx 4\pi\, \epsilon_f \epsilon_{\bar{f}}, \tag{3.39}$$

where $\epsilon_f, \epsilon_{\bar{f}}$ are given by Eq. (3.17) with $\Phi = f, \bar{f}$. The stability condition for the potential is $\lambda_{D,L}^2 n_f / 16\pi^2 \lesssim (\Lambda/M_{\rm Pl})^2 \approx 10^{-4}$, which can be easily satisfied, for example, by taking $M_f, M_{\bar{f}} \gtrsim 1/\pi R$, i.e., f_D, f_L, $\bar{f}_D$ and $\bar{f}_L$ localized towards the $y = 0$ brane. At the scale

$$M_{\rm mess} \approx \lambda_{D,L} \langle X \rangle \approx \frac{\lambda_{D,L} \Lambda^2}{M_{\rm Pl}}, \tag{3.40}$$

the messenger fields are integrated out, generating the gauge-mediated contributions to the MSSM gaugino and scalar masses [8, 9]:

$$M_a = N_{\rm mess} \frac{g_a^2}{16\pi^2} \frac{F_X}{\langle X \rangle}, \qquad m_{\tilde{f}}^2 = 2 N_{\rm mess} \sum_a C_a^{\tilde{f}} \left(\frac{g_a^2}{16\pi^2} \right)^2 \left| \frac{F_X}{\langle X \rangle} \right|^2, \tag{3.41}$$

where $a = 1, 2, 3$ represents the standard model gauge group factors, g_a are the standard model gauge couplings at $M_{\rm mess}$, $\tilde{f} = \tilde{q}, \tilde{u}, \tilde{d}, \tilde{l}, \tilde{e}, H_u, H_d$, and $C_a^{\tilde{f}}$ are the quadratic Casimir coefficients.

The supersymmetry breaking parameters and the μ parameter in our theory receive contributions of Eqs. (3.28, 3.30, 3.31) generated at the scale M_* and those of Eq. (3.41) generated at the scale $M_{\rm mess}$. The low-energy superparticle masses are then obtained by evolving the parameters of Eqs. (3.28, 3.30, 3.31) from M_* to $M_{\rm mess}$, adding the contributions of Eq. (3.41) at $M_{\rm mess}$, and then evolving the resulting parameters from $M_{\rm mess}$ down to the weak scale. Because of the wavefunction suppression factors $\epsilon_{f,\bar{f}}$, which are exponentially sensitive to the bulk masses $M_{f,\bar{f}}$, the value of $M_{\rm mess}$ can in general be anywhere between ≈ 100 TeV and $O(0.1)\langle X \rangle \approx 10^{13}$ GeV. Here, the upper bound comes from the stability condition on $\lambda_{D,L}$, while the lower bound from the messenger stability. Note that since the gauge-mediated contributions of Eq. (3.41) have the size

$$M_a \approx (m_{\tilde{f}}^2)^{1/2} \approx \frac{F_X}{\Lambda} \left(\frac{g^2}{16\pi^2} \frac{M_{\rm Pl}}{\Lambda} \right) \approx \frac{F_X}{\Lambda}, \tag{3.42}$$

where g represents the standard model gauge couplings, they are comparable to the tree-level contributions to the Higgs-sector parameters of Eq. (3.28).[7] On the other hand, the

[7] In contrast with the situation discussed in Ref. [21], there is no reason in the present theory that the μ term must be suppressed compared with the gauge-mediated contributions. In fact, they are naturally expected to be comparable.

flavor non-universal contributions of Eqs. (3.30, 3.31) are suppressed due to the ϵ factors associated with the quark and lepton superfields (except possibly for the third generation). This therefore reproduces precisely the pattern for the low-energy supersymmetry breaking masses in flavorful supersymmetry.

The model also has other flavor violating contributions to the supersymmetry breaking parameters, but they are all small. For example, loops of the higher dimensional gauge and messenger fields produce flavor violating scalar squared masses at $1/R$, but they are of order $N_{\rm mess}(g^2/16\pi^2)^2|F_X/\Lambda|^2 \approx (\langle X\rangle/\Lambda)^2 m_{\tilde{f}}^2$ and thus small. The $y = 0$ brane Kähler potential operators connecting the matter (and messenger) fields, e.g. $\delta(y)\int d^4\theta\, T_i^\dagger T_j T_k^\dagger T_l$ and $\delta(y)\int d^4\theta\, T_i^\dagger T_j f^\dagger f$, also generate flavor violating scalar squared masses through loops of the matter (or messenger) fields. Using naive dimensional analysis to estimate the coefficients of the operators, we find that this contribution is at most of order $|F_X/\Lambda|^2/(\pi R M_*)^5$ and negligible. Possible contributions from bulk higher dimension operators are also expected to be small based on similar dimensional arguments. Finally, $y = 0$ brane localized kinetic terms, e.g. $\delta(y)\int d^4\theta\, T_i^\dagger T_j$, can introduce flavor violation by giving corrections of order $1/M_* R \approx 1/16\pi^2$ to the kinetic terms of the low energy 4D fields. After canonically normalizing the 4D fields, these corrections affect both the Yukawa couplings and the supersymmetry breaking parameters. Interestingly, however, this does not affect the mass insertion parameters used in section 3.3.1 at the order of magnitude level. In other words, we can always take the basis for the low energy 4D fields such that the Yukawa couplings and supersymmetry breaking masses are given by Eqs. (3.16, 3.30, 3.31) at M_* even in the presence of the general brane kinetic terms.[8] Below, we assume that this basis is taken.

Setting the size of the dominant contributions to the supersymmetry breaking and μ parameters to be the weak scale, we obtain $F_X/\Lambda \approx (100\ \text{GeV} - 1\ \text{TeV})$ from Eq. (3.42). The value of F_X is then determined as $\sqrt{F_X} \approx (10^{8.5} - 10^{9.5})$ GeV using Eq. (3.27). This leads to the gravitino mass

$$m_{3/2} \simeq \frac{F_X}{\sqrt{3} M_{\rm Pl}} \approx (0.1 - 10)\ \text{GeV}, \tag{3.43}$$

implying that the gravitino is the lightest supersymmetric particle (LSP). Together with the flavor non-universal contributions of Eqs. (3.30, 3.31), this can lead to spectacular signatures at the LHC [15], some of which will be discussed in section 3.3.5.

3.2.5 Neutrino masses, *R* parity, and dimension five proton decay

The $U(1)_H$ charge assignment of Eqs. (3.24, 3.25) contains two free parameters q_Q and q_L. These parameters can be restricted by imposing various phenomenological requirements [44]. For example, if we require that dangerous dimension-five proton decay operators $W \sim Q_i Q_j Q_k L_l$ and $U_i U_j D_k E_l$ are prohibited by $U(1)_H$, then we obtain the conditions

[8] In fact, this property persists even if the corrections to the 4D kinetic terms are of order unity.

$3q_Q + q_L \neq 0$ and $3q_Q + q_L \neq -4$, respectively. Similarly, if we require that $U(1)_H$ forbids dimension-four R-parity violating operators $W \sim L_i H_u$, $Q_i D_j L_k$, $U_i D_j D_k$, $L_i L_j E_k$ and $K \sim L_i^\dagger H_d$, we obtain $q_L \neq -1$, $q_L \neq 1$, $q_Q \neq -1$, $q_L \neq 1$ and $q_L \neq 1$.

An interesting possibility arises if $q_L = 0$. In this case we can have the following superpotential on the $y = \pi R$ brane:

$$S = \int d^4x \int_0^{\pi R} dy\ \delta(y - \pi R) \int d^2\theta\, \frac{\hat{\kappa}_{ij}}{2} X O_{Ni} O_{Nj} + \text{h.c.}, \tag{3.44}$$

which, together with the last term of Eq. (3.14), leads to

$$W = \frac{\kappa_{ij}}{2} X N_i N_j + (y_\nu)_{ij} L_i N_j H_u, \tag{3.45}$$

in the low-energy 4D theory. Using naive dimensional analysis, the couplings κ_{ij} and $(y_\nu)_{ij}$ are given by $\kappa_{ij} \approx 4\pi\, \epsilon_{N_i} \epsilon_{N_j}$ and $(y_\nu)_{ij} \approx 4\pi\, \epsilon_{L_i} \epsilon_{N_j}$. The vacuum of Eq. (3.34) is not destabilized as long as $\kappa_{ij} \lesssim O(0.1)$, which can be easily satisfied by taking ϵ_{N_i} to be somewhat small, i.e., by taking $M_{N_i} \gtrsim -1/\pi R$. Small neutrino masses are then generated by the seesaw mechanism through the X VEV of Eq. (3.34). Note that the ϵ_{N_i} factors cancel out from the generated neutrino masses:

$$(m_\nu)_{ij} \approx 4\pi \epsilon_{L_i} \epsilon_{L_j} \frac{\langle H_u \rangle^2}{\langle X \rangle}. \tag{3.46}$$

It is interesting that with $\langle X \rangle \approx 10^{14}$ GeV, this is in the right ballpark to explain the experimental data on neutrino oscillations.[9]

It is not necessary to impose all the requirements above for the $U(1)_H$ charge assignment. For example, R-parity violating operators can be forbidden simply by imposing matter parity in addition to $U(1)_H$. Nevertheless, it is interesting that one can consider the $U(1)_H$ assignment that satisfies all these requirements. For example, one can adopt

$$q_Q = \frac{4}{3} + 2n, \qquad q_L = 0, \tag{3.47}$$

where n is an integer. The $U(1)_H$ symmetry is spontaneously broken by the VEV of X, but the charge assignment of Eq. (3.47) leaves a discrete Z_6 symmetry after the breaking. The product of Z_6 and $U(1)_Y$ contains the (anomalous) Z_3 baryon number and (anomaly-free) Z_2 matter parity (R parity) as subgroups. This symmetry, therefore, strictly forbids the R-parity violating operators, and the lightest supersymmetric particle is absolutely stable.

In the rest of the chapter, we assume that the LSP is absolutely stable (although it is not necessarily required by the model). This can be achieved either by choosing the $U(1)_H$ charges so that all the R-parity violating operators are forbidden even after the $U(1)_H$ breaking, as is the case for Eq. (3.47), or simply by imposing matter (or R) parity.

[9] The interactions of Eq. (3.45) also generate supersymmetry breaking masses of order $(y_\nu^2/16\pi^2) F_X/\langle X \rangle$ for L_i and H_u through loops of N_i (A terms at one loop and non-holomorphic supersymmetry breaking masses at two loops [49]). This effect, however, is small for $y_\nu \ll 1$, compared with the contributions of Eqs. (3.28, 3.41).

3.2.6 Origin of $U(1)_H$ breaking

In section 3.2.4, we have simply parameterized the effect of (small) $U(1)_H$ breaking by a spurious parameter $\eta \ll 1$. This breaking controls the size of the coefficient μ_X^2 for the X linear term in the superpotential, and thus the size of supersymmetry breaking. There are a variety of possibilities for the origin of the required small breaking. For example, it may simply arise as a result of string theory dynamics at the cutoff scale M_*. Here, we discuss two explicit examples for the origin of $U(1)_H$ breaking. The validity of the model as well as its basic phenomenological consequences discussed in section 3.3 have little dependence on this physics.

The first possibility is that the $U(1)_H$ breaking effect arises from the mixed $U(1)_H$ anomaly with respect to the hidden sector gauge group. The scale μ_X then arises from dimensional transmutation associated with the hidden sector gauge group. This scenario can be implemented in our higher dimensional framework simply by promoting the model discussed in Refs. [44, 50] to higher dimensions. Specifically, we consider a supersymmetric $SU(5)_{\rm hid} \times SU(5)$ gauge theory on 5D flat spacetime, where the latter $SU(5)$ factor is identified with the unified gauge group, whose gauge multiplet obeys the boundary conditions of Eqs. (3.1, 3.2). The Higgs and matter fields are singlet under $SU(5)_{\rm hid}$, and have the same $SU(5)$ gauge quantum numbers and boundary conditions as in section 3.2.1. The location for the Higgs, matter and X fields, as well as their $U(1)_H$ charges, are also the same as before.

The messenger fields $\{f, f^c\}$ and $\{\bar{f}, \bar{f}^c\}$ are also introduced in the bulk as before, with the interactions to the X field given by Eq. (3.37). Instead of introducing arbitrary explicit $U(1)_H$ breaking, however, here we assign the gauge quantum numbers $(\mathbf{5}^*, \mathbf{5})$ to f and $\bar{f}^c$, and $(\mathbf{5}, \mathbf{5}^*)$ to $\bar{f}$ and f^c, where the numbers in parentheses represent the quantum numbers under $SU(5)_{\rm hid} \times SU(5)$. Below the compactification scale $\approx 1/\pi R$, this reduces to the model discussed in [44, 50]. In particular, the required X linear term in the superpotential is generated:

$$W_{\rm eff} = \lambda \Lambda_{\rm hid}^2 X, \tag{3.48}$$

where $\Lambda_{\rm hid}$ is the dynamical scale of $SU(5)_{\rm hid}$, and we have taken $\lambda_D \approx \lambda_L \approx \lambda$. Note that this superpotential is "exact," i.e., no higher order terms in X are generated.

A virtue of the higher dimensional setup in the context of $SU(5)_{\rm hid} \times SU(5)$ is that the nontrivial wavefunction profiles of f and $\bar{f}$ needed to suppress $\lambda_{D,L}$ (to satisfy the stability condition $\lambda_{D,L}^2 \lesssim 10^{-3}$) also suppress the superpotential coupling $W = \zeta f \bar{f} H_u H_d / \Lambda$ in the low-energy 4D theory, which can arise from the $y = \pi R$ brane localized operator and leads to an unwanted large μ term unless $\zeta \lesssim \lambda_{D,L}$. Using naive dimensional analysis, we find $\lambda_{D,L} \approx \zeta \approx 4\pi \epsilon_f \epsilon_{\bar{f}}$, so that we do not have a large μ term from the superpotential operator.

Another possibility for the $U(1)_H$ breaking is that $U(1)_H$ is spontaneously broken. Since $U(1)_H$ has a mixed anomaly with respect to $SU(3)_C$, this provides a solution to the strong CP problem [51]. We do not attempt here to construct a complete model of this kind. It is, however, straightforward to realize this possibility at the level of a non-linear sigma model, i.e. the axion field being realized nonlinearly.

3.3 Phenomenology

In this section we study phenomenology of the model presented in the previous section. We study constraints from flavor and CP violation and the variation of the superparticle spectrum allowed by these constraints. We find that there are a variety of possibilities for the next-to-lightest supersymmetric particle (NLSP), which decays into the LSP gravitino with the lifetime of $O(10^2 - 10^6$ sec). We also discuss proton decay, precision gauge coupling unification, and possible experimental signatures.

3.3.1 Constraints from flavor violation and the variety of the spectrum

Phenomenology of the model depends on the wavefunction profiles for the quark and lepton zero modes, which are controlled by the bulk masses for these fields. In the low-energy 4D theory, these affect the Yukawa matrices, Eq. (3.16), and the flavor violating contribution to the squark and slepton masses generated at M_*, Eqs. (3.30, 3.31). This effect is parameterized by the factors ϵ_Φ ($\Phi = Q_i, U_i, D_i, L_i, E_i, N_i$) in Eq. (3.17).

The values for the ϵ_Φ factors are restricted by requiring that the gross structure of the observed quark and lepton masses and mixings are reproduced by these factors. This, however, still leaves some freedoms for the choice of the ϵ_Φ factors. For example, scaling $\{\epsilon_{Q_i}, \epsilon_{U_i}, \epsilon_{D_i}\} \to \{\alpha\epsilon_{Q_i}, \alpha^{-1}\epsilon_{U_i}, \alpha^{-1}\epsilon_{D_i}\}$ does not change the quark masses and mixings. Taking these freedoms into account, here we consider

$$\begin{aligned}
&\epsilon_{Q_1} \approx \tilde{y}^{-\frac{1}{2}}\alpha_q\,\epsilon^2, \quad && \epsilon_{U_1} \approx \tilde{y}^{-\frac{1}{2}}\alpha_q^{-1}\epsilon^2, \quad && \epsilon_{D_1} \approx \tilde{y}^{-\frac{1}{2}}\alpha_q^{-1}\alpha_\beta\,\epsilon, \\
&\epsilon_{Q_2} \approx \tilde{y}^{-\frac{1}{2}}\alpha_q\,\epsilon, && \epsilon_{U_2} \approx \tilde{y}^{-\frac{1}{2}}\alpha_q^{-1}\epsilon, && \epsilon_{D_2} \approx \tilde{y}^{-\frac{1}{2}}\alpha_q^{-1}\alpha_\beta\,\epsilon, \\
&\epsilon_{Q_3} \approx \tilde{y}^{-\frac{1}{2}}\alpha_q, && \epsilon_{U_3} \approx \tilde{y}^{-\frac{1}{2}}\alpha_q^{-1}, && \epsilon_{D_3} \approx \tilde{y}^{-\frac{1}{2}}\alpha_q^{-1}\alpha_\beta\,\epsilon,
\end{aligned} \tag{3.49}$$

$$\begin{aligned}
&\epsilon_{L_1} \approx \tilde{y}^{-\frac{1}{2}}\alpha_l\,\epsilon, \quad && \epsilon_{E_1} \approx \tilde{y}^{-\frac{1}{2}}\alpha_l^{-1}\alpha_\beta\,\epsilon^2, \\
&\epsilon_{L_2} \approx \tilde{y}^{-\frac{1}{2}}\alpha_l\,\epsilon, && \epsilon_{E_2} \approx \tilde{y}^{-\frac{1}{2}}\alpha_l^{-1}\alpha_\beta\,\epsilon, \\
&\epsilon_{L_3} \approx \tilde{y}^{-\frac{1}{2}}\alpha_l\,\epsilon, && \epsilon_{E_3} \approx \tilde{y}^{-\frac{1}{2}}\alpha_l^{-1}\alpha_\beta,
\end{aligned} \tag{3.50}$$

with

$$\tan\beta \approx \alpha_\beta\,\epsilon^{-1}, \tag{3.51}$$

where $\epsilon = O(0.1)$ and α_q, α_l and α_β are numbers parameterizing the freedoms unfixed by the data of the quark and lepton masses and mixings. Note that the range of $\alpha_{q,l,\beta}$ is restricted such that the ϵ parameters, $\epsilon_{Q_i,U_i,D_i,L_i,E_i}$, do not exceed ≈ 1; see Eq. (3.17). (The value of α_β is also restricted so that $\tan\beta$ stays within the regime in which none of the Yukawa couplings blow up below the cutoff scale.) The pattern of Eqs. (3.49, 3.50) is a straightforward generalization of Eq. (3.18), and the resulting quark and lepton masses and mixings are still given by Eqs. (3.22, 3.23).

The parameters α_q, α_l and α_β, however, alter the size of the flavor violating contribution to the squark and slepton masses, and are thus constrained by low-energy flavor and CP

violating processes. We use the mass insertion method [18] to derive constraints on these parameters. The experimental bounds on the mass insertion parameters can be found, e.g., in Ref. [20], and are summarized in Ref. [15]. In the quark sector, the most stringent bounds come from K-$\bar{K}$, D-$\bar{D}$ and B-$\bar{B}$ mixings and $\sin 2\beta$, while in the lepton sector the most stringent one comes from the $\mu \to e\gamma$ process, giving

$$\begin{aligned} &\sqrt{|\mathrm{Re}(\delta^d_{12})^2_{LL/RR}|} \lesssim (10^{-2}\text{–}10^{-1}), \qquad \sqrt{|\mathrm{Re}(\delta^d_{12})_{LL}(\delta^d_{12})_{RR}|} \lesssim 10^{-3}, \\ &\sqrt{|\mathrm{Im}(\delta^d_{12})^2_{LL/RR}|} \lesssim (10^{-3}\text{–}10^{-2}), \qquad \sqrt{|\mathrm{Im}(\delta^d_{12})_{LL}(\delta^d_{12})_{RR}|} \lesssim 10^{-4}, \end{aligned} \tag{3.52}$$

$$\begin{aligned} &|(\delta^u_{12})_{LL/RR}| \lesssim (10^{-2}\text{–}10^{-1}), \qquad |(\delta^u_{12})_{LL}| = |(\delta^u_{12})_{RR}| \lesssim (10^{-3}\text{–}10^{-2}), \\ &|(\delta^d_{13})_{LL/RR}| \lesssim (0.1\text{–}1), \qquad\quad |(\delta^d_{13})_{LL}| = |(\delta^d_{13})_{RR}| \lesssim 10^{-2}, \end{aligned} \tag{3.53}$$

$$|(\delta^e_{12})_{LL}| \lesssim (10^{-4}\text{–}10^{-3}), \tag{3.54}$$

where we have kept only the bounds relevant to our model. In deriving the above bounds, we have taken the gluino and squark masses to be the same order of magnitude with $m_{\tilde{q}} \simeq$ 500 GeV, and the same for the weak gaugino and slepton masses with $m_{\tilde{l}} \simeq 200$ GeV. For heavier superparticles, the bounds become weaker linearly with increasing superparticle masses, except for that on $|(\delta^e_{12})_{LL}|$, which scales quadratically with $m_{\tilde{l}}$.

In order to compare our model with the above bounds, we need to obtain the structure of the squark and slepton mass matrices at low energies. We first consider the flavor universal contribution. It comes from two different sources. The first is gauge mediation, generated at the scale $M_{\rm mess}$, while the other is a $U(1)_Y$ Fayet-Iliopoulos D-term piece, $\mathrm{Tr}(Y_{\tilde{f}} m^2_{\tilde{f}}) \neq 0$, of the soft masses generated at M_*, Eqs. (3.28, 3.30, 3.31). The sfermion masses at a low energy, μ_R, can then be written as

$$\begin{aligned} m^2_{\tilde{f}}(\mu_R) \;\simeq\; & 2N_{\rm mess} \sum_{a=1}^{3} C^{\tilde{f}}_a \frac{g^4_a(M_{\rm mess})}{(16\pi^2)^2} \left[1 + \frac{N_{\rm mess}}{b_a}\left(1 - \frac{g^4_a(\mu_R)}{g^4_a(M_{\rm mess})}\right)\right] \frac{F_X^2}{\langle X\rangle^2} \\ & - \frac{6Y_{\tilde{f}}}{5} \frac{g_1^2(\mu_R)}{16\pi^2} \left(x_{H_u} - x_{H_d} + \frac{x_{Q_3}\alpha_q^2}{\tilde{y}} - 2\frac{x_{U_3}}{\tilde{y}\,\alpha_q^2} + \frac{x_{E_3}\alpha_\beta^2}{\tilde{y}\,\alpha_l^2}\right) \frac{F_X^2}{\Lambda^2} \ln\frac{M_*}{\mu_R}, \end{aligned} \tag{3.55}$$

where $(b_1, b_2, b_3) = (33/5, 1, -3)$ are the 321 beta-function coefficients, $Y_{\tilde{f}}$ represents hypercharges in the normalization that Q has $Y_{\tilde{f}} = 1/6$, and x_{H_u,H_d,Q_3,U_3,E_3} are the $O(1)$ factors in front of the corresponding soft masses generated at M_*. (Here, we have kept only the leading terms in ϵ.) As we will see in section 3.3.2, the $U(1)_Y$ D-term piece can considerably affect the superparticle spectrum, leading to interesting phenomenology.

The flavor violating elements of the sfermion mass matrices are renormalized among themselves, and are also generated from the flavor universal piece through the Yukawa couplings.

These effects, however, do not significantly modify the values of these elements in most of the parameter space. We therefore take the approximation that the flavor non-universal part of the sfermion masses is parameterized by Eqs. (3.30, 3.31) with Eqs. (3.49, 3.50) at low energies.[10] The chirality-preserving mass insertion parameters are then obtained by dividing these flavor violating elements by the (average) diagonal elements in the super-CKM basis.

With the low-energy mass parameters described above, one can study the constraints from flavor and CP violation. The scalar trilinear interactions in our model are generated only by renormalization group evolution, so that they are proportional to the corresponding Yukawa couplings with real proportionality constants, in the basis where the gaugino masses are real. They, therefore, do not contribute to flavor or CP violating processes. The constraints on the α parameters are then obtained from Eqs. (3.52 – 3.54). We find that for $\tilde{y} = 4\pi$ and $\epsilon = 0.05$, all constraints from the quark sector are satisfied, while $\mu \to e\gamma$ gives

$$\alpha_l \lesssim 1.8, \tag{3.56}$$

with no further constraints on α_q or α_β. Taking $\epsilon = 0.1$, the constraints become stronger with both $\mu \to e\gamma$ and K-$\bar{K}$ mixing, giving

$$\alpha_l \lesssim 0.9, \qquad \alpha_\beta \lesssim 1.4. \tag{3.57}$$

These bounds are obtained for the superparticle mass scale of $m_{\tilde{l}} \sim 400$ GeV, with $F_X/M_* \sim 1$ TeV. (This corresponds to $m_{\tilde{q}} \sim 1.2$ TeV, which is sufficient to avoid the LEP II bound on the physical Higgs boson mass.) While these bounds are rough ones, they show that there exists a consistent parameter region. For heavier superparticles, the bounds become weaker and the region expands.

3.3.2 The NLSP

As we have seen in section 3.2.4, the LSP is the gravitino with mass $\approx (0.1 - 10)$ GeV. In order to study phenomenology, it is important to determine which particles can be the NLSP. Since the dominant contribution to the masses of most supersymmetric particles comes from gauge mediation, we first consider the spectrum without the corrections from tree-level pieces generated at M_*. Since the masses are determined by the gauge charge, the lightest particles will be those neutral under $SU(3)_C$ and $SU(2)_L$. Therefore, the lightest gaugino is a neutralino, χ_1^0 which is mostly bino, and the lightest sfermions are the right-handed sleptons. The mass of the bino at low energy is given by

$$m_{\tilde{B}}(\mu_R) \simeq N_{\rm mess} \frac{g_1^2(\mu_R)}{16\pi^2} \frac{F_X}{\langle X \rangle}, \tag{3.58}$$

while the mass of the sleptons can be derived from Eq. (3.55). From these two equations we see that with increasing $N_{\rm mess}$ the sleptons become lighter than the bino, while increasing

[10] A possible contribution to $m_{\tilde{l}}^2$ from loops of the right-handed neutrinos is also not important as long as $(y_\nu)_{ij} \lesssim O(1)$, which is the case for the ϵ factor assignment of Eq. (3.50) with $\alpha_l \approx O(1)$.

$M_{\rm mess}$ makes the sleptons heavier because of renormalization group effects. Calculations show that for $N_{\rm mess} = 1$ the bino is always the NLSP, while for larger $N_{\rm mess}$ the sleptons can be lighter. In the case of $N_{\rm mess} = 3$ (5), for example, the sleptons are lighter than the bino for $M_{\rm mess} \lesssim 10^{10}$ (10^{12}) GeV.

The bino mass in the present model is the same as in gauge mediation, but the slepton masses can deviate. As discussed in section 3.3.1, the sleptons receive the contribution from the $U(1)_Y$ D-term, indicated by the second line of Eq. (3.55). This contribution is flavor universal so it does not affect the splitting among sleptons, but it affects the relation between the sleptons and the bino. The other correction to gauge mediation comes from the tree-level masses in Eqs. (3.30, 3.31). From Eqs. (3.49, 3.50), we see that these mass terms are ϵ suppressed for most fields, but the effect can be $O(1)$ for $\tilde{\tau}_R$, and the unknown coefficient could even be negative as long as the sum of the tree-level and gauge mediated pieces bring the physical mass above direct detection bounds. This means that $\tilde{\tau}_R$ could lie anywhere in the spectrum of $\tilde{e}_R$, $\tilde{\mu}_R$ and $\tilde{B}$.

The splitting between $\tilde{e}_R$ and $\tilde{\mu}_R$ is controlled almost entirely by the splitting at M_* because the renormalization group running is universal up to small effects from the muon Yukawa coupling. Phenomenology is governed by the splitting between mass eigenstates which is given by

$$m_{\tilde{\mu}_R} - m_{\tilde{e}_R} \approx \frac{m^2_{\tilde{\mu}_R} - m^2_{\tilde{e}_R}}{2\sqrt{m^2_{\tilde{e}_R,\tilde{\mu}_R}}} \approx \frac{O(0.01)}{N^2_{\rm mess}} \left(\frac{\alpha_\beta}{\alpha_l}\right)^2 \left(\frac{\Lambda/M_{\rm Pl}}{0.01}\right)^2 \frac{m^2_{\tilde{B}}}{\sqrt{m^2_{\tilde{e}_R,\tilde{\mu}_R}}}. \tag{3.59}$$

The splitting between light generation sfermions is much larger than in the usual gauge mediation scenario. It can be large enough that the heavier one can decay to the lighter by emission of an electron and a muon.

There are corners of parameter space where the NLSP is not a right-handed slepton or bino. Since the contribution from the $U(1)_Y$ D-term in Eq. (3.55) has opposite signs for the left-handed and right-handed sleptons, it could invert the usual order between these two species. The lighter stop could also be the NLSP because, like $\tilde{\tau}_R$, it has an $O(1)$ tree-level contribution to its mass. The stops also have a contribution from the large top Yukawa coupling, which decreases the masses through renormalization group evolution. While the tree-level piece is expected to be smaller than the $SU(3)_C$ gauge mediation piece, negative tree-level and Yukawa effects could combine to give a strongly interacting NLSP. We do not consider these exotic NLSPs in the rest of this chapter because they require large cancellation between independent effects.

3.3.3 Proton decay

Dimension four proton decay in the present model can be forbidden by the $U(1)_H$ symmetry or matter parity. Dimension five proton decay caused by colored Higgsino exchange is also absent because of the form of the Higgsino mass matrix determined by higher dimensional spacetime symmetry [39]. Proton decay in the present model can thus arise only from dimension six operators and cutoff suppressed dimension five operators.

As discussed in section 3.2.5, we can take the charge assignment of $U(1)_H$ such that the operators $W \sim Q_i Q_j Q_k L_l$ and $U_i U_j D_k E_l$ are forbidden: $3q_Q + q_L \neq 0, -4$. In this case, dimension five proton decay arises only from operators on the $y = \pi R$ brane which involve the X VEV. The relevant interactions are $W \sim X^m Q_i Q_j Q_k L_l$ and $X^m U_i U_j D_k E_l$, which can be written for $3q_Q + q_L = -2m$ and $3q_Q + q_L = 2m - 4$ ($m \in Z > 0$), respectively. In the low-energy 4D effective theory, these interactions lead to dimension five operators

$$W \approx 4\pi \epsilon_{Q_i} \epsilon_{Q_j} \epsilon_{Q_k} \epsilon_{L_l} \frac{\Lambda^{m-1}}{M_{\rm Pl}^m} Q_i Q_j Q_k L_l \quad \text{and} \quad 4\pi \epsilon_{U_i} \epsilon_{U_j} \epsilon_{D_k} \epsilon_{E_l} \frac{\Lambda^{m-1}}{M_{\rm Pl}^m} U_i U_j D_k E_l, \tag{3.60}$$

where the coefficients are evaluated using naive dimensional analysis, and we have used $\langle X \rangle \approx \Lambda^2 / M_{\rm Pl}$. We find that the approximate sizes of these operators are obtained by replacing the colored Higgsino mass by $4\pi M_{\rm Pl}^m / \Lambda^{m-1}$ in the corresponding expressions in the minimal supersymmetric $SU(5)$ grand unified theory. The resulting proton decay rate is thus much smaller than the current experimental bound for all the values of $3q_Q + q_L \neq 0, -4$.

Dimension six operators are generated in the present model only through brane localized terms, since without them exchange of bulk gauge bosons does not transform a quark into a lepton or vice versa. (Note that different 321 multiplets arise from different $SU(5)$ multiplets, see Eqs. (3.5 – 3.10).) The relevant terms are kinetic mixing operators $K \sim T^\dagger T'$, $T^\dagger T''$, $F^\dagger F'$ and cutoff suppressed dimension six operators $K \sim T^\dagger T' T^\dagger T''$, $T^\dagger T' F'^\dagger F$ on the $y = 0$ brane. Here, we have omitted factors involving the gauge multiplet needed to make operators gauge invariant, and the existence of Hermitian conjugates is implied. The kinetic mixing terms lead, through unified gauge boson exchange, to dimension six operators at low energies, whose coefficients have approximately the size obtained by replacing the unified gauge boson mass by $1/\pi R$ in the corresponding minimal supersymmetric $SU(5)$ expressions. For $1/\pi R \approx 10^{15}$ GeV, this leads to a proton decay rate somewhat larger than the current experimental bound [52]. This implies that the compactification scale should be somewhat larger (by a factor of a few) or the coefficients of the original kinetic mixing operators should be suppressed (by an order of magnitude or so). This potential difficulty does not arise in weakly coupled models, an example of which will be discussed in section 3.5. The coefficients of low-energy dimension six operators arising from the cutoff suppressed operators are similar in size to those in the minimal supersymmetric $SU(5)$ model, so that they do not lead to proton decay at a dangerous level.

In summary, proton decay in the present model is caused by dimension six operators, originating from terms on the $y = 0$ brane. Since the wavefunction values for the first and second generation fields on this brane are typically of the same order, the proton can decay into final states containing μ^+ with a similar rate to those containing e^+. This provides interesting signatures for future proton decay experiments.

3.3.4 Precision gauge coupling unification

Strongly coupled grand unification in higher dimensions allows a precise calculation for gauge coupling unification [42, 43]. Incalculable corrections arising from the cutoff scale

physics are suppressed, and the corrections from higher dimensional fields between the energy interval between M_* and $1/\pi R$ are precisely calculated. Here we study this issue in the model of section 3.2.

We phrase the degree of the success of gauge coupling unification in terms of the prediction of $\alpha_s(M_Z) = g_3^2(M_Z)/4\pi$ obtained from $g_{1,2}(M_Z)$, where $g_{1,2,3}$ represent the standard model gauge couplings. In particular, we consider the deviation of the prediction in the present model, $\alpha_s^{\rm 5D}$, from that obtained by assuming the exact unification in the MSSM, $\alpha_s^{\rm SGUT,0}$:

$$\delta\alpha_s \equiv \alpha_s^{\rm 5D} - \alpha_s^{\rm SGUT,0} \simeq -\frac{1}{2\pi}\alpha_s^2\Delta. \tag{3.61}$$

Here, Δ parameterizes corrections from higher dimensional fields, which can be calculated within higher dimensional effective field theory. Using the result of Ref. [53], we find that in the present model

$$\begin{aligned}\Delta &= -\frac{3}{7}\ln(\pi R M_*) - 3\ln(\epsilon_{Q_1}\epsilon_{Q_2}\epsilon_{Q_3}) + \frac{15}{7}\ln(\epsilon_{U_1}\epsilon_{U_2}\epsilon_{U_3}) \\ &\quad + \frac{9}{7}\ln(\epsilon_{D_1}\epsilon_{D_2}\epsilon_{D_3}) - \frac{9}{7}\ln(\epsilon_{L_1}\epsilon_{L_2}\epsilon_{L_3}) + \frac{6}{7}\ln(\epsilon_{E_1}\epsilon_{E_2}\epsilon_{E_3}),\end{aligned} \tag{3.62}$$

where we have used the approximation that the Higgs doublets are strictly localized to the $y = \pi R$ brane. (The term $-(9/7)\ln(\epsilon_{H_u}\epsilon_{H_d})$ should be added to the right-hand-side if the Higgs fields are delocalized.) Inserting Eqs. (3.49, 3.50) into this equation, we obtain

$$\Delta = -\frac{3}{7}\ln(\pi R M_*) - \frac{135}{7}\ln\alpha_q - \frac{45}{7}\ln\alpha_l + \frac{45}{7}\ln\alpha_\beta. \tag{3.63}$$

Considering that the logarithms are expected to be of order unity, we find that Δ is typically of $O(10)$, with the sign depending on the values of $\alpha_{q,l,\beta}$. For typical superparticle spectra, including the one considered here, a good fit to the experimental values of $g_{1,2,3}(M_Z)$ is obtained for

$$\Delta^{\rm exp} \approx 5 \pm O(1). \tag{3.64}$$

The expression in our model, Eq. (3.63), can easily accommodate this value.

3.3.5 Collider signatures

Phenomenology of the general flavorful supersymmetry scenario has been discussed in Ref. [15]. Here we summarize some of the basic features in the context of the present model. As we saw in section 3.3.2, this model has a large portion of parameter space where there is a charged NLSP which is stable for the purposes of collider studies. Unlike the conventional scenarios, the NLSP in flavorful supersymmetry could be a $\tilde{\tau}_R$ or a right-handed slepton of a different flavor. Heavy stable charged particles are relatively easy to see at colliders. By measuring their velocity and momentum, their mass can be deduced. The mass of the charged NLSP be can measured to better than 1% at the LHC by measuing only a few hundred NLSPs with $0.6 < \beta < 0.91$ [54].

Once the NLSP mass is known, it is possible to fully reconstruct events even in the hadronic environment of the LHC. Therefore we can determine the flavor content of the NLSP by taking its invariant mass with other leptons in the event. If the NLSP is found to be mostly selectron or smuon, this is definitive evidence for nontrivial flavor structure in the supersymmetry breaking sector, and possibly for flavorful supersymmetry. In addition, once we learn the dominant flavor of the NLSP, we can look for NLSP production in association with leptons of other flavors to measure the mixing angles of the NLSP.

Because the lifetime of the NLSP is quite long, it can be studied in a cleaner environment. One proposal involves using the muon tracker to determine where in the surrounding rock an NLSP went, and extracting pieces of rock that likely contain NLSPs to study them elsewhere [23]. Another possibility is to build a large stopper detector outside of one of the main detectors which can stop the NLSPs and then measure the decay products [24]. This would allow precise measurements of the lifetime of the NLSP as well as the masses of the decay products. As pointed out in Ref. [15], a particularly distinct signature of flavorful supersymmetry is monochromatic electrons or muons in the decay of the NLSP, indicating a two body decay of a selectron or smuon. This is not a possibility in the conventional scenarios because the $\tilde{\tau}_R$ is the NLSP, and it decays to a τ which further decays, so the many body decay causes the leptons to have a broad spectrum. Even if the NLSP is a $\tilde{\tau}_R$, a stopper detector will allow us to look for rare decays into other flavors and precisely measure the flavor content of the NLSP. The stopper detector can also check to see if the LSP is the gravitino. From the kinematics, the mass of the LSP can be measured, which can then be tested against the supergravity prediction which relates the lifetime of the NLSP to the mass of the gravitino [27].

While the signatures are much more spectacular if there is a slepton NLSP, evidence for flavorful supersymmetry can still be found with a neutralino NLSP. One possibility is to look for direct slepton production from Drell-Yan processes and measure the spectrum through kinematic variables such as M_{T2} [29]. This is difficult because it requires high statistics and the Drell-Yan cross section falls rapidly with increasing slepton mass. Another possibility is to look for multiple edges in flavor-tagged dilepton invariant mass distributions as in Ref. [30]. This will allow us to find different flavors of sleptons if they are separated by more than a few GeV, which we would expect in flavorful supersymmetry. Finally, we could also study the spectrum of left-handed sleptons or even squarks to look for flavor non-universality. While these measurements are more difficult than those with stable sleptons, they could still provide information on the flavor structure of the supersymmetry breaking sector.

3.4 4D Realization — Model in Warped Space

The model in section 3.2 has been formulated in flat space, but we can also consider a similar model in warped space, along the lines of Ref. [55]. An interesting feature of this model is that it allows for a 4D interpretation through the AdS/CFT correspondence, providing a picture of realizing flavorful supersymmetry in a 4D setup.

Specifically, we take the metric

$$ds^2 = e^{-2ky}\eta_{\mu\nu}dx^\mu dx^\nu + dy^2, \tag{3.65}$$

where k denotes the inverse curvature radius of the warped spacetime. The two branes are located at $y = 0$ (the UV brane) and $y = \pi R$ (the IR brane). The scales of these branes are chosen to be $k \approx 10^{17}$ GeV and $k' \equiv k\, e^{-\pi kR} \approx 10^{16}$ GeV, respectively. The cutoff scale of the 5D theory is taken to be $M_* \approx 10^{18}$ GeV. The gauge symmetry structure is as described in section 3.2; the bulk $SU(5)$ symmetry is broken to 321 on the IR brane at $y = \pi R$. The IR brane thus serves the role of breaking the unified symmetry.

The configuration of the matter and Higgs fields is as described in section 3.2. The locations of these fields are controlled by the bulk masses, and the resulting Yukawa couplings are given by Eq. (3.16), where the ϵ factors are given by Eq. (3.17) with $M_\Phi \to M_\Phi - k/2$. The analysis of $U(1)_H$ and supersymmetry breaking is as in sections 3.2.3 – 3.2.6. (Note that the cutoff scale on the IR brane is warped down to $M'_* \equiv M_* e^{-\pi kR} \approx 10^{17}$ GeV.) This leads to phenomenology discussed in sections 3.3.1, 3.3.2 and 3.3.5. Dimension four and five proton decay is negligible for the reasons described in section 3.3.3. Dimension six proton decay is also not dangerous as the unified gauge boson mass is now of order $\pi k' \approx 10^{16}$ GeV. For gauge coupling unification, we can show, using the results of [56], that the threshold correction is still given by the formula Eq. (3.62). (Note that the contribution from the Higgs doublets to differential running shuts off above M'_*, since these fields are localized on the IR brane.) The experimental values of the low-energy gauge couplings are thus successfully reproduced, as seen in section 3.3.4.

The model described here has the following 4D interpretation through the AdS/CFT correspondence. At very high energies above $k' \approx 10^{16}$ GeV, the theory is a 4D supersymmetric $SU(5) \times G$ gauge theory, where $SU(5)$ is the unified gauge group and G some quasi-conformal gauge group. There are three generations of matter fields, $3 \times (\mathbf{10} + \mathbf{5}^*)$ of $SU(5)$ (and possibly three right-handed neutrinos), but not the Higgs fields. There are also fields charged under G, some of which are charged under $SU(5)$ as well. At the scale $k' \approx 10^{16}$ GeV, the G sector deviates from the conformal fixed point, breaking the unified $SU(5)$ symmetry to 321 by the gauge dynamics. It also produces the MSSM Higgs doublets and the supersymmetry breaking sector containing X as composite states. The effective theory below k' is thus the MSSM (and possibly three right-handed neutrinos) together with the supersymmetry breaking sector.

An important point is that the interaction strengths of the matter fields to the G sector are controlled by the dimensions of operators coupling matter to fields charged under G. In general, these dimensions are generation dependent. Moreover, since G is strongly interacting above k', the anomalous dimensions for these operators can be large. As a result, the interaction strengths of matter to the G sector strongly vary between different generations, and since the Higgs doublets and X arise as composite states of G, the interactions of matter to these states show strong generation dependence. Since the origin of this generation dependence is common for the matter couplings to the Higgs fields (the Yukawa couplings) and to the X field (supersymmetry breaking couplings), the patterns of these two classes

of couplings are correlated. The correlation is exactly the one given in Eqs. (3.16, 3.29), realizing flavorful supersymmetry.

We have considered here a 4D theory in which the G sector is quasi-conformal and has a large 't Hooft coupling above the dynamical scale, motivated by the warped space construction. The dynamics described above, however, are independent of these assumptions. The same dynamics can also be incorporated, in principle, in a purely 4D theory whose 't Hooft coupling is not necessarily large above k'. The quasi-conformal nature of the dynamics is also not essential. It will be interesting to construct an explicit example of purely 4D theory in which the G sector exhibits different renormalization group behavior, e.g. asymptotic freedom, above the dynamical scale $\Lambda_G \approx 10^{16}$ GeV.

3.5 Weakly Coupled (Non-Unified) Models

In this section we present a non-unified model of flavorful supersymmetry in higher dimensions. Here we do not require that the theory is strongly coupled at the cutoff scale, nor that it possesses the $U(1)_H$ symmetry. Rather, we assume that certain operators are small at the cutoff scale due to ultraviolet physics.

We consider a supersymmetric $SU(3)_C \times SU(2)_L \times U(1)_Y$ gauge theory in 5D flat spacetime, compactified on an S^1/Z_2 orbifold: $0 \le y \le \pi R$. As in the model of section 3.2, the two Higgs doublets are localized towards the $y = \pi R$ brane, where supersymmetry is broken by the F-term VEV of a chiral superfield X. The matter fields are introduced in the bulk as hypermultiplets, whose zero modes Q_i, U_i, D_i, L_i, E_i (and N_i) are identified with the MSSM matter fields. The wavefunction profiles of the zero modes are controlled by the bulk masses M_Φ ($\Phi = Q_i, U_i, D_i, L_i, E_i, N_i$), as seen in section 3.2.2.

We do not require that the theory is strongly coupled at the cutoff scale M_*, which is taken to be a factor of a few above $1/R$. We then naturally expect that the operators located on branes have $O(1)$ coefficients in units of M_*. This leads to the 4D Yukawa couplings of Eq. (3.15) with

$$(y_u)_{ij} \approx \epsilon_{Q_i}\epsilon_{U_j}, \qquad (y_d)_{ij} \approx \epsilon_{Q_i}\epsilon_{D_j}, \qquad (y_e)_{ij} \approx \epsilon_{L_i}\epsilon_{E_j}, \qquad (y_\nu)_{ij} \approx \epsilon_{L_i}\epsilon_{N_j}, \tag{3.66}$$

at low energies, where ϵ_Φ are given by Eq. (3.17). By choosing ϵ_Φ and $\tan\beta$ to be as given in Eqs. (3.49 – 3.51) with $\tilde{y} = 1$, this reproduces the gross structure of the observed quark and lepton masses and mixings, Eqs. (3.22, 3.23).[11] The configuration of the matter fields, as well as those of the Higgs and supersymmetry breaking fields, are depicted schematically in Fig. 3.2.

The supersymmetry breaking parameters are generated through the interactions of the MSSM states to the X field on the $y = \pi R$ brane. In the absence of the $U(1)_H$ symmetry, the

[11] Here we have assumed that the Majorana masses for N_i are on the $y = \pi R$ brane, but not on the $y = 0$ brane. This can be realized, for example, by introducing the $U(1)_{B-L}$ symmetry broken on the $y = \pi R$ brane.

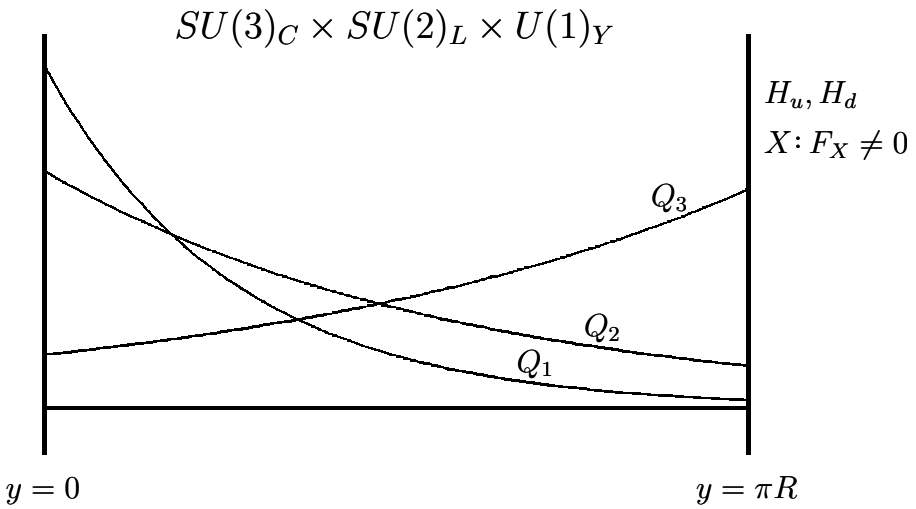

Figure 3.2: A schematic depiction of the configuration for various fields.

superpotential operators $W \sim XQ_iU_jH_u + XQ_iD_jH_d + XL_iE_jH_d + XL_iN_jH_u$ are not forbidden in general. These operators generate flavor non-universal left-right mixing terms for the squarks and sleptons that require relatively heavy superparticles to avoid the constraints from low-energy flavor and CP violating processes. Here we assume that these operators are somehow suppressed. We also assume that the direct μ term, $W \sim H_uH_d$, is absent. Note that these assumptions are technically natural because of the nonrenormalization theorem. The supersymmetry breaking parameters are then generated by the Kähler potential operators and $\mathcal{L} \sim \int d^2\theta\, X\mathcal{W}_a^\alpha \mathcal{W}_{a\alpha} + \text{h.c.}$, where $\mathcal{W}_a^\alpha$ $(a = 1, 2, 3)$ are the 321 gauge field strength superfields, giving

$$M_a \approx \mu \approx \frac{F_X}{M_*}, \qquad m_{H_u}^2 \approx m_{H_d}^2 \approx B\mu \approx \left(\frac{F_X}{M_*}\right)^2, \tag{3.67}$$

$$(m_{\tilde{q}}^2)_{ij} \approx \epsilon_{Q_i}\epsilon_{Q_j}\left(\frac{F_X}{M_*}\right)^2, \qquad (m_{\tilde{u}}^2)_{ij} \approx \epsilon_{U_i}\epsilon_{U_j}\left(\frac{F_X}{M_*}\right)^2, \qquad (m_{\tilde{d}}^2)_{ij} \approx \epsilon_{D_i}\epsilon_{D_j}\left(\frac{F_X}{M_*}\right)^2, \tag{3.68}$$

$$(m_{\tilde{l}}^2)_{ij} \approx \epsilon_{L_i}\epsilon_{L_j}\left(\frac{F_X}{M_*}\right)^2, \qquad (m_{\tilde{e}}^2)_{ij} \approx \epsilon_{E_i}\epsilon_{E_j}\left(\frac{F_X}{M_*}\right)^2, \tag{3.69}$$

$$(a_u)_{ij} \approx \{(y_u)_{kj}(\eta_Q)_{ki} + (y_u)_{ik}(\eta_U)_{kj} + (y_u)_{ij}\}\frac{F_X}{M_*}, \tag{3.70}$$

$$(a_d)_{ij} \approx \{(y_d)_{kj}(\eta_Q)_{ki} + (y_d)_{ik}(\eta_D)_{kj} + (y_d)_{ij}\}\frac{F_X}{M_*}, \tag{3.71}$$

$$(a_e)_{ij} \approx \{(y_e)_{kj}(\eta_L)_{ki} + (y_e)_{ik}(\eta_E)_{kj} + (y_e)_{ij}\} \frac{F_X}{M_*}. \tag{3.72}$$

Here, we have omitted $O(1)$ coefficients in each term, and $(\eta_\Phi)_{ij} \approx \epsilon_{\Phi_i}\epsilon_{\Phi_j}$ ($\Phi = Q, U, D, L, E$) are general complex 3×3 matrices. This gives a correlation between the Yukawa couplings Eq. (3.66), and the supersymmetry breaking parameters Eqs. (3.67 – 3.72), realizing flavorful supersymmetry. Note that because of the absence of a factor 4π in Eq. (3.66), the mass splittings between different generation sfermions in Eqs. (3.68, 3.69) can be larger than those in the strongly coupled case.

The model has other flavor violating contributions to the supersymmetry breaking parameters, but they can be controlled. For example, loops of the higher dimensional gauge fields produce flavor violating supersymmetry breaking masses at $1/R$, but they are not much larger than the tree-level masses in the parameter region considered, as long as the coefficients of the matter brane kinetic operators at $y = 0$ are of order $1/16\pi^2 M_*$ or smaller. Note that this size of the coefficients is technically natural. The matter 4-point Kähler potential operators on the $y = 0$ brane also give flavor violating contributions at loop level. They are, however, suppressed by a factor of $1/(\pi R M_*)^5$ and negligible. Possible contributions from bulk higher dimension operators are also expected to be small.

The compactification scale $1/R$ in the present model is naturally of order the unification scale $M_U \approx 10^{16}$ GeV to preserve the successful supersymmetric prediction for the low-energy gauge couplings. In this case, the gaugino and sfermion masses are of order $\tilde{m} \approx F_X/M_U$ while the gravitino mass is $m_{3/2} \approx F_X/M_{\rm Pl}$, so that $m_{3/2} \approx (M_U/M_{\rm Pl})\tilde{m} \approx (1 - 10)$ GeV, leading to signatures discussed in section 3.3.5 with the NLSP being one of the right-handed sleptons. The compactification scale, however, can in principle take any value larger than of order a few TeV, in which case the gravitino may be (much) lighter. Note that the supersymmetry breaking parameters of Eqs. (3.67 – 3.72) are running parameters evaluated at the scale $1/R$. The low-energy superparticle spectrum is obtained by evolving them down to the weak scale using renormalization group equations.

Here we have presented a non-unified model of flavorful supersymmetry in 5D. It is, however, straightforward to make it a unified model, e.g., based on $SU(5)$. We simply have to adopt the field content and boundary conditions of section 3.2.1 and follow the analysis above. To understand gauge coupling unification, we need to assume that incalculable brane-localized gauge kinetic terms on the $y = \pi R$ brane are somehow suppressed (or universal), but dangerous proton decay can be easily suppressed, possibly by $U(1)_R$ symmetry [39].[12] It is also straightforward to extend the model to higher dimensions. The only requirement is that the Higgs fields and the supersymmetry breaking field X are localized in the same place in the extra dimensions.[13] An advantage of such a setup is that we can suppress cutoff scale dimension-five proton decay operators by localizing the Q, U, E and D, L fields in different

[12] It is interesting to note that the 321 gaugino masses do not have to be unified at the unification scale even if the model is unified because the gaugino mass operators reside on the $y = \pi R$ brane, where the active gauge group is only 321 [39].

[13] To be more precise, it is sufficient to require that the matter interactions to the Higgs and X fields are suppressed by common wavefunction factors, allowing the Higgs and X to propagate in different subspaces.

subspaces in higher dimensions. These extensions allow us to realize flavorful supersymmetry in a wide variety of higher dimensional models, with varying spacetime dimensions, compact space geometries, and gauge groups.

3.6 Conclusions

In this chapter we have presented explicit models of flavorful supersymmetry in higher dimensions. The basic idea is to localize the Higgs fields and the supersymmetry breaking field in the same location in the extra dimension(s). The interactions of matter fields to the Higgs fields (the Yukawa couplings) and to the supersymmetry breaking field (operators generating the supersymmetry breaking parameters) then receive the same suppression factors from the wavefunction profiles of the matter fields. This leads to a specific correlation between these two classes of interactions, realizing flavorful supersymmetry. The resulting phenomenology at future colliders is very rich, while stringent experimental constraints from the low-energy flavor and CP violating processes can all be satisfied.

We have constructed a unified model of flavorful supersymmetry in 5D, in which the theory is strongly coupled at the cutoff scale. Supersymmetry breaking is mediated to the supersymmetric standard model sector by a combination of cutoff suppressed operators and gauge mediation. This model addresses various issues in supersymmetric unification. We have also presented a model in warped space, which allows us to obtain a picture of realizing flavorful supersymmetry in a 4D setup, through the AdS/CFT correspondence. Finally, we have discussed models which do not require that the theory is strongly coupled at the cutoff scale. This construction can be easily extended to a wide variety of higher dimensional theories, with varying spacetime geometries and gauge groups.

It is interesting to note that the present setup is very generic in the context of a single extra dimension. If we want to explain the observed hierarchical structure of the Yukawa couplings by wavefunction overlaps between the matter and Higgs fields, the simplest way is to localize the Higgs fields to one of the branes and lighter generation matter more towards the other brane. Now, if the supersymmetry breaking field X is *not* localized to the same brane as the Higgs fields, interactions of lighter generation matter to X are *not* suppressed, leading to large flavor violating supersymmetry breaking masses. To avoid this problem, we need to localize X to the same brane as the Higgs fields (unless some other flavor universal mediation mechanism dominates). This gives the spectrum of flavorful supersymmetry.

As the LHC will turn on this year, it is important to explore possible theoretical constructions and experimental signatures of supersymmetric theories. The models presented here provide an example in which the supersymmetry breaking spectrum can be a window into the physics of flavor in the standard model. If supersymmetry is discovered at the LHC, it will be interesting to see if the longstanding assumption of flavor universality holds, or if there is a richer flavor structure within the supersymmetry breaking sector. This structure could give us information about the physics of flavor which could lie at energy scales as high as the unification or Planck scale.

Chapter 4

Naturally Flavorful Supersymmetry at the LHC[1]

4.1 Introduction

The origin of the flavor structure is one of the deepest mysteries of the standard model. In the absence of the Yukawa couplings (and neutrino masses), the standard model respects the following flavor symmetry:[2]

$$G_{\rm flavor}^{\rm SM} \equiv U(3)^5 = U(3)_Q \times U(3)_U \times U(3)_D \times U(3)_L \times U(3)_E. \tag{4.1}$$

Is this symmetry a mere artifact of the low-energy Lagrangian, or is it (or its subgroup) physically realized at high energies and spontaneously broken to produce the Yukawa couplings? If the latter, what is the fundamental flavor group $G_{\rm flavor}$ ($\subset G_{\rm flavor}^{\rm SM}$), and how is it broken? In the standard model, these questions can be explored only through the observed pattern of masses and mixings of the quarks and leptons, making it difficult to arrive at conclusive answers.

Theories beyond the standard model may provide additional clues to address the puzzle of flavor, since the new physics sector may contain new information on flavor. In supersymmetric theories, for example, supersymmetry breaking parameters for squarks and sleptons may carry such information. It is, however, not obvious how much new information one can expect. In supersymmetric theories, generic weak scale values for the supersymmetry breaking parameters

$$(m_\Phi^2)_{ij} \sim m_{\rm SUSY}^2, \qquad (a_f)_{ij} \sim m_{\rm SUSY}, \tag{4.2}$$

lead to flavor changing neutral currents far in excess of current experimental bounds. Here, $(m_\Phi^2)_{ij}$ ($\Phi = Q, U, D, L, E$) and $(a_f)_{ij}$ ($f = u, d, e$) represent scalar squared masses and trilin-

[1] This chapter, as well as Appendix A, were co-written with Yasunori Nomura and published in [57].

[2] $G_{\rm flavor}^{\rm SM}$ contains hypercharge, baryon number, and lepton number. Out of the five $U(1)$ factors, only hypercharge and baryon minus lepton number are anomaly free with respect to the standard model gauge group.

ear interactions, respectively, $i, j = 1, 2, 3$ are generation indices, and $m_{\rm SUSY}$ is a parameter of order the weak scale. A common solution to this problem is to assume flavor universality

$$(m_\Phi^2)_{ij} \propto \delta_{ij} \text{ or } \ll m_{\rm SUSY}^2, \qquad (a_f)_{ij} \propto (y_f)_{ij} \text{ or } \ll m_{\rm SUSY}, \tag{4.3}$$

at a scale M where the supersymmetry breaking parameters are generated [58, 10, 59, 60, 8, 61, 62, 63, 9, 64, 65, 66]. Here, $(y_f)_{ij}$ are the Yukawa matrices. This assumption, however, greatly reduces the flavor information encoded in low energy supersymmetry. A nontrivial flavor structure can still be found in the low energy squark and slepton masses due to renormalization group evolution below M. This structure, however, does not carry any information on flavor beyond Yukawa couplings Φ have, although it does allow us to explore some of these couplings that cannot be probed in the standard model [18]. In addition, the size of the relevant flavor nonuniversality is typically so small that most of the interesting parameters can be probed only indirectly through low energy flavor and CP violating processes.

In this chapter we study the question: is there a natural and generic framework for supersymmetry which is sufficiently "flavorful," i.e. which allows us to obtain more detailed information on flavor through measurements of superparticle masses and interactions at the LHC? This is not trivial because such a framework must satisfy stringent constraints from flavor and CP violation while the deviation from universality must be sufficiently large to be experimentally observable. In particular, in order for the flavor information to be extracted at the LHC, superparticles must be light enough to be produced at the LHC, making it more difficult to satisfy the bounds from the low energy flavor and CP violating processes.

While it is not too difficult to consider an ad hoc deviation from universality that is measurable at the LHC and not excluded by the low energy data, an important question is if there is a theoretically well-motivated setup which naturally produces measurable effects that are consistent with the low energy experiments and encode information on the origin of flavor. In a previous chapter, we studied a simple setup in which flavor changing interactions in the supersymmetry breaking parameters are scaled by factors associated with the Yukawa couplings [15]. We showed that such a setup can avoid all the low energy constraints, while giving interesting flavor signatures at the LHC. This clearly illustrates that there is an interesting, natural stage between Eqs. (4.2, 4.3). In fact, there have been many models proposed to address the problem of flavor changing neutral currents, in which flavor violation in the supersymmetry breaking parameters is somehow related to the Yukawa couplings [67, 68, 17, 69, 70, 71, 72, 73, 74, 75, 32, 76, 77, 78, 79, 80, 81, 82, 83, 84, 85, 86, 87, 88, 35, 89, 36, 90, 37, 33, 91]. While many of these models require rather special structures or setups to avoid all the current experimental bounds, the analysis of Ref. [15] suggests that the minimal structure needed to obtain a consistent framework for flavor signatures at the LHC may, in fact, be much simpler.

In this chapter we study the tension between LHC observability and constraints from low energy flavor and CP violation in generic supersymmetric theories in which the structure of the supersymmetry breaking parameters is correlated with that of the Yukawa couplings. An

interesting general point emphasized in Ref. [15] (see also [16]) is that among the operators giving supersymmetry breaking parameters, a class of operators in the superpotential

$$W \sim XQ_iU_jH_u,\ XQ_iD_jH_d,\ XL_iE_jH_d, \tag{4.4}$$

generally leads to a strong tension. Here, X represents a chiral superfield whose F-term vacuum expectation value (VEV) is responsible for supersymmetry breaking. We first elucidate this point, and define what we call the superpotential flavor problem. We emphasize that the problem is general and does not depend on any particular theory of flavor. In fact, this problem is part of a more general problem associated with left-right propagation of sfermions, which is also discussed in detail.

We then discuss how the problems described above can be solved. We present several possibilities that can avoid the stringent constraints from left-right sfermion propagation without suppressing the operators of Eq. (4.4). We also present simple frameworks in which the operators of Eq. (4.4) are naturally absent. These frameworks can be combined with many theories of flavor, including theories with (flat or warped) extra dimensions, strong dynamics, or flavor symmetries. We perform detailed studies of the constraints from low energy flavor and CP violation within these frameworks, and find that they can naturally avoid all the constraints while preserving the observability of superparticles at the LHC. We also find that the intergenerational mass splittings among sfermions can show a variety of patterns depending on the details of the underlying flavor theory, allowing us to gain additional handles on the origin of flavor at the LHC.

The organization of the chapter is as follows. In section 4.2 we discuss constraints from low energy flavor and CP violation arising from left-right propagation of sfermions. We emphasize the model-independent nature of the problem associated with the operators of Eq. (4.4), but also discuss additional stringent model dependent constraints. In section 4.3 we discuss possibilities to avoid these constraints. In particular, we present simple frameworks in which the operators of Eq. (4.4) are naturally absent. In section 4.4 we study constraints from flavor and CP violation, including ones arising from left-left and right-right sfermion propagation, in these frameworks. We also analyze the size of the intergenerational mass splittings among sfermions, and find that they can differ significantly from the flavor universal case. Prospects for observing these features at the LHC are discussed in section 4.5. Finally, discussion and conclusions are given in section 4.6.

4.2 The Supersymmetric Left-Right Flavor Problem

The flavor problem in supersymmetric models is typically phrased such that generic supersymmetry breaking parameters, Eq. (4.2), lead to excessive flavor and CP violation at low energies. This, however, neglects the possibility that the physics responsible for the observed Yukawa couplings also controls the pattern of the supersymmetry breaking parameters. Here we argue that there is a *generic* tension between weak scale supersymmetry and low energy flavor and CP violation even if we take this possibility into account. Throughout

the discussion, we assume that CP violating effects not associated with flavor, e.g. those arising from a nontrivial phase in the Higgs sector, are adequately suppressed. We also assume that the strong CP problem is solved.

4.2.1 Flavor (non)universality in the operator language

We begin our discussion by listing all the operators in the supersymmetric standard model (SSM). In the gauge sector, the relevant operators are

$$\mathcal{O}_{g_A} : \int d^2\theta \, \frac{1}{4g_A^2} \mathcal{W}^{A\alpha} \mathcal{W}^A_\alpha + \text{h.c.}, \qquad \mathcal{O}_{\lambda_A} : \int d^2\theta \, \eta_A \frac{X}{M} \mathcal{W}^{A\alpha} \mathcal{W}^A_\alpha + \text{h.c.}, \tag{4.5}$$

where $A = 1, 2, 3$ represents the standard model gauge group, $U(1)_Y$, $SU(2)_L$ and $SU(3)_C$, and $\mathcal{O}_{g_A}$ and $\mathcal{O}_{\lambda_A}$ give the gauge kinetic terms and the gaugino masses, respectively.[3] Here, X is the supersymmetry breaking superfield, $\langle X \rangle = \theta^2 F_X$, and M characterizes a scale at which supersymmetry breaking effects are mediated to the SSM sector. Since F_X/M sets the scale for superparticle masses, we consider $F_X/M \approx O(\text{TeV})$. In the minimal supersymmetric standard model (MSSM), the Higgs sector operators are given by

$$\mathcal{O}_{Z_H} : \int d^4\theta \, Z_H \, H^\dagger H, \tag{4.6}$$

$$\mathcal{O}_{\kappa_H} : \int d^4\theta \, \kappa_H \frac{X^\dagger X}{M^2} H^\dagger H, \qquad \mathcal{O}_{\eta_H} : \int d^4\theta \, \eta_H \frac{X}{M} H^\dagger H + \text{h.c.}, \tag{4.7}$$

$$\mathcal{O}_\mu : \int d^4\theta \, \eta_\mu \frac{X^\dagger}{M} H_u H_d + \text{h.c.}, \qquad \mathcal{O}_b : \int d^4\theta \, \kappa_b \frac{X^\dagger X}{M^2} H_u H_d + \text{h.c.}, \tag{4.8}$$

$$\mathcal{O}_{\text{SUGRA}} : \int d^4\theta \, \lambda_H \, H_u H_d + \text{h.c.}, \tag{4.9}$$

where $H = H_u, H_d$. The operators $\mathcal{O}_{Z_H}$ give the kinetic terms, while the rest provide the supersymmetric mass, μ, and the holomorphic and non-holomorphic supersymmetry breaking squared masses, b, $m^2_{H_u}$ and $m^2_{H_d}$, for the Higgs doublets.[4] The last operator is relevant only in the context of supergravity. In non-minimal models, e.g. in models with extra gauge groups and/or singlet fields, the set of operators in Eqs. (4.5 – 4.9) is extended.

The operators described above (or their extensions in non-minimal models) do not introduce flavor violation. Flavor violation may arise when we introduce matter fields. With matter fields, we can write operators

$$\mathcal{O}_{Z_\Phi} : \int d^4\theta \, (Z_\Phi)_{ij} \Phi_i^\dagger \Phi_j, \tag{4.10}$$

$$\mathcal{O}_{\kappa_\Phi} : \int d^4\theta \, (\kappa_\Phi)_{ij} \frac{X^\dagger X}{M^2} \Phi_i^\dagger \Phi_j, \qquad \mathcal{O}_{\eta_\Phi} : \int d^4\theta \, (\eta_\Phi)_{ij} \frac{X}{M} \Phi_i^\dagger \Phi_j + \text{h.c.}, \tag{4.11}$$

[3] We define an operator $\mathcal{O}$ to be the entire term that appears in the Lagrangian, including the coefficient.

[4] Here we have neglected the tree-level superpotential operator $\int d^2\theta \, \mu_0 \, H_u H_d + \text{h.c.}$. In order to have weak scale values for μ and b, the coefficient of this operator must be suppressed: $\mu_0 \lesssim O(\text{TeV})$.

$$\mathcal{O}_{\lambda_f} : \int d^2\theta\, (\lambda_f)_{ij} \Phi_{Li} \Phi_{Rj} H + \text{h.c.}, \qquad \mathcal{O}_{\zeta_f} : \int d^2\theta\, (\zeta_f)_{ij} \frac{X}{M} \Phi_{Li} \Phi_{Rj} H + \text{h.c.}, \tag{4.12}$$

where $\Phi = \Phi_L, \Phi_R$ with $\Phi_L = Q, L$ and $\Phi_R = U, D, E$ represents matter fields, $i, j = 1, 2, 3$ are generation indices, and $f = u, d, e$ corresponds to

$$\{\Phi_L, \Phi_R, H\} = \{Q, U, H_u\},\ \{Q, D, H_d\},\ \{L, E, H_d\}.$$

Here, Z_Φ and κ_Φ are 3×3 Hermitian matrices, while η_Φ, λ_f and ζ_f are general complex 3×3 matrices. The operators $\mathcal{O}_{Z_\Phi}$ give the kinetic terms, $\mathcal{O}_{\lambda_f}$ the Yukawa couplings, and $\mathcal{O}_{\kappa_\Phi}$, $\mathcal{O}_{\eta_\Phi}$ and $\mathcal{O}_{\zeta_f}$ the soft supersymmetry breaking parameters.

Flavor universality is the assumption that

$$(\kappa_\Phi)_{ij} \propto (Z_\Phi)_{ij}, \qquad (\eta_\Phi)_{ij} \propto (Z_\Phi)_{ij}, \qquad (\zeta_f)_{ij} \propto (\lambda_f)_{ij}, \tag{4.13}$$

for all $\Phi = Q, U, D, L, E$ and $f = u, d, e$, which leads to supersymmetry breaking parameters of the form

$$(m_\Phi^2)_{ij} \propto \delta_{ij}, \qquad (a_f)_{ij} \propto (y_f)_{ij}, \tag{4.14}$$

where $(m_\Phi^2)_{ij}$, $(a_f)_{ij}$ and $(y_f)_{ij}$ represent the scalar squared masses, scalar trilinear interactions, and the Yukawa couplings in the basis where the fields are canonically normalized. In fact, the three conditions of Eq. (4.13) could each be replaced by

$$|(\kappa_\Phi)_{ij}| \ll |\eta_A|^2, \qquad |(\eta_\Phi)_{ij}| \ll |\eta_A|, \qquad |(\zeta_f)_{ij}| \ll |(\lambda_f)_{ij} \eta_A|, \tag{4.15}$$

since then the low energy supersymmetry breaking parameters, generated by SSM renormalization group evolution, take approximately the form of Eq. (4.14).

Deviations from Eqs. (4.13, 4.15) generically lead to flavor and CP violating effects. If the supersymmetry breaking parameters take the flavor universal form at some scale below the scale of flavor physics M_F, then small deviations from universality are caused only by SSM renormalization group evolution below that scale, which do not provide much insight into the origin of flavor at the LHC. On the other hand, if $M_F \lesssim M$ (or if the mediation mechanism of supersymmetry breaking somehow carries information on physics responsible for the Yukawa structure), then we expect that the supersymmetry breaking parameters have an intrinsic flavor nonuniversality, which contains information on the physics of flavor at M_F. Of course, this deviation from universality cannot be arbitrary. In order to satisfy all the constraints while keeping superparticles within the reach of the LHC, the deviation must somehow be correlated with the Yukawa structure. This is, however, precisely what we expect if the supersymmetry breaking parameters feel the physics responsible for the flavor structure.

4.2.2 Generic scalar trilinear interactions

We consider the case where $M_F \lesssim M$ and flavor nonuniversality in the operators of Eqs. (4.10 – 4.12) at M_F is controlled by the physics responsible for the structure of the

Yukawa couplings. This provides a possibility of avoiding the low energy constraints without imposing flavor universality, allowing us to probe the origin of flavor through the superparticle spectrum. In general, correlations between the structure of the Yukawa couplings and that of the nonuniversality in the operators of Eqs. (4.10 – 4.12) are model dependent. However, one class of operators, $\mathcal{O}_{\zeta_f}$ in Eq. (4.12), is expected to have a structure similar to the Yukawa couplings. This is relatively model independent because the matter and Higgs fields appear in $\mathcal{O}_{\zeta_f}$ in precisely the same way as in $\mathcal{O}_{\lambda_f}$, which produces the Yukawa couplings.

Suppose that the Yukawa couplings

$$(y_f)_{ij} = (\lambda_f)_{kl} \left(Z_{\Phi_L}^{-1/2}\right)_{ki} \left(Z_{\Phi_R}^{-1/2}\right)_{lj} Z_H^{-1/2}, \tag{4.16}$$

have a hierarchical structure as a result of some flavor physics, for example, physics associated with spontaneous breaking of a flavor symmetry or wavefunction profiles of matter fields in extra dimensions. We then expect that the scalar trilinear interactions generated by $\mathcal{O}_{\zeta_f}$,

$$(a_f)_{ij} = -(\zeta_f)_{kl} \left(Z_{\Phi_L}^{-1/2}\right)_{ki} \left(Z_{\Phi_R}^{-1/2}\right)_{lj} Z_H^{-1/2} \frac{F_X}{M}, \tag{4.17}$$

also have a similar structure. Specifically, we can consider that the Yukawa couplings take the form

$$(y_u)_{ij} \approx \mathcal{E}_{ij}^u \, \tilde{y}, \qquad (y_d)_{ij} \approx \mathcal{E}_{ij}^d \, \tilde{y}, \qquad (y_e)_{ij} \approx \mathcal{E}_{ij}^e \, \tilde{y}, \tag{4.18}$$

and that the observed structure for the quark and lepton masses and mixings is generated by the "suppression factors" $\mathcal{E}_{ij}^f$. Here, $\tilde{y}$ represents the "natural" size of the couplings before taking into account the origin of the flavor structure; for example, we expect $\tilde{y} \approx O(1)$ if the relevant physics is weakly coupled, but it could be as large as of $O(4\pi)$ if strongly coupled. The scalar trilinear interactions are then expected to take the form

$$(a_u)_{ij} \approx \mathcal{E}_{ij}^u \frac{\tilde{\zeta} F_X}{M}, \qquad (a_d)_{ij} \approx \mathcal{E}_{ij}^d \frac{\tilde{\zeta} F_X}{M}, \qquad (a_e)_{ij} \approx \mathcal{E}_{ij}^e \frac{\tilde{\zeta} F_X}{M}, \tag{4.19}$$

where $\tilde{\zeta}$ again represents the "natural" size of the coefficients. Note that $O(1)$ coefficients are omitted in the expressions of Eqs. (4.18, 4.19); for example, we expect that $(a_f)_{ij}$ is in general not proportional to $(y_f)_{ij}$ because of an arbitrary $O(1)$ coefficient in each element.

The structure of Eqs. (4.18, 4.19) is expected to appear in most theories of flavor. A special case is when $\mathcal{E}_{ij}^f$ factorize as $\mathcal{E}_{ij}^u = \epsilon_{Q_i} \epsilon_{U_j}$, $\mathcal{E}_{ij}^d = \epsilon_{Q_i} \epsilon_{D_j}$ and $\mathcal{E}_{ij}^e = \epsilon_{L_i} \epsilon_{E_j}$, so that each matter field carries its own suppression factor. This arises in many models of flavor, for example in classes of models with flavor symmetries or strong dynamics. The important point is the similarity between the forms of $(y_f)_{ij}$ and $(a_f)_{ij}$. This comes from the fact that matter and Higgs fields appear identically in the two classes of operators in Eq. (4.12).

The gaugino masses, which arise from $\mathcal{O}_{\lambda_A}$ as $M_A = -2\eta_A g_A^2 F_X / M$, set the scale for the superparticle masses. Assuming that the mediation mechanism produces unsuppressed $\mathcal{O}_{\zeta_f}$, i.e. $\tilde{\zeta} \approx \eta_A$, we then obtain $(a_f)_{ij} \approx \mathcal{E}_{ij}^f M_A / g_A^2$ at the scale M_F.[5] Taking into account

[5]Note that in our notation, the grand unified relations for the gaugino masses correspond to $\eta_1 = \eta_2 = \eta_3$.

Eq. (4.18) and SSM renormalization group evolution below M, we can write the flavor nonuniversal part of the low energy scalar trilinear interactions as

$$(a_u)_{ij} \approx (y_u)_{ij} \frac{a_{\rm C}}{\tilde{y}}, \qquad (a_d)_{ij} \approx (y_d)_{ij} \frac{a_{\rm C}}{\tilde{y}}, \qquad (a_e)_{ij} \approx (y_e)_{ij} \frac{a_{\rm N}}{\tilde{y}}, \tag{4.20}$$

where $a_{\rm C}, a_{\rm N} \approx O(M_A)$ are characteristic mass scales for these interactions associated with colored and non-colored sfermions, and we expect $a_{\rm C} \gtrsim a_{\rm N}$ due to the structure of the SSM renormalization group equations. We note again that $O(1)$ coefficients are omitted for each element of Eq. (4.20), so that $(a_f)_{ij}$ is not proportional to $(y_f)_{ij}$ as a matrix.

4.2.3 The superpotential flavor problem

The flavor nonuniversality at the level of Eq. (4.20) can be problematic. Flavor and CP violation can in general be quantified by mass insertion parameters, which are obtained by dividing the off-diagonal entry of the sfermion mass-squared matrix by the average diagonal entry in the super-CKM basis [92, 20]. The mass insertion parameters obtained from Eq. (4.20) are

$$(\delta^u_{LR})_{ij} \approx \frac{a_{\rm C}}{\tilde{y}\, m^2_{\rm C}} (M_u)_{ij}, \qquad (\delta^d_{LR})_{ij} \approx \frac{a_{\rm C}}{\tilde{y}\, m^2_{\rm C}} (M_d)_{ij}, \qquad (\delta^e_{LR})_{ij} \approx \frac{a_{\rm N}}{\tilde{y}\, m^2_{\rm N}} (M_e)_{ij}, \tag{4.21}$$

for $i \neq j$, where $m_{\rm C}$ and $m_{\rm N}$ are characteristic masses for colored and non-colored superparticles, and we expect $m_{\rm C} \gtrsim m_{\rm N}$. Here, $(M_u)_{ij} = (y_u)_{ij}\langle H_u\rangle$, $(M_d)_{ij} = (y_d)_{ij}\langle H_d\rangle$ and $(M_e)_{ij} = (y_e)_{ij}\langle H_d\rangle$ are the quark and lepton mass matrices in the original (not super-CKM) basis. The diagonal elements, $(\delta^f_{LR})_{ii}$, receive additional terms coming from the flavor universal contribution to $(a_f)_{ij}$ from renormalization group evolution below M and the contribution to the sfermion left-right masses proportional to $|\mu|$. However, assuming there is no intrinsic CP violation associated with supersymmetry breaking, these terms do not contribute to the imaginary parts of $(\delta^f_{LR})_{ii}$, which are relevant in the discussion below. We thus find

$$\begin{aligned} {\rm Im}(\delta^u_{LR})_{ii} \approx \frac{a_{\rm C} \sin\varphi_u}{\tilde{y}\, m^2_{\rm C}} (M_u)_{ii}, \qquad {\rm Im}(\delta^d_{LR})_{ii} \approx \frac{a_{\rm C} \sin\varphi_d}{\tilde{y}\, m^2_{\rm C}} (M_d)_{ii}, \\ {\rm Im}(\delta^e_{LR})_{ii} \approx \frac{a_{\rm N} \sin\varphi_e}{\tilde{y}\, m^2_{\rm N}} (M_e)_{ii}, \end{aligned} \tag{4.22}$$

where φ_f are the phases of the contributions to $(\delta^f_{LR})_{ii}$ from the flavor nonuniversal part of $(a_f)_{ij}$. Note that $\varphi_f \approx O(1)$ is expected even if supersymmetry breaking does not introduce new CP violating phases because these complex phases arise generically from the Yukawa couplings when going into the super-CKM basis.[6]

[6]This may be avoided in certain models, e.g., models with hermitian Yukawa and scalar trilinear interaction matrices [93] and those with spontaneous CP violation [94].

The theoretical estimate of Eqs. (4.21, 4.22) can be compared with experimental constraints from low energy observables. The bound on the $\mu \to e\gamma$ process [95] gives

$$\frac{1}{\sqrt{2}}\sqrt{|(\delta^e_{LR})_{12}|^2 + |(\delta^e_{LR})_{21}|^2} \lesssim 4 \times 10^{-6} \left(\frac{m_{\rm N}}{200\ {\rm GeV}}\right). \tag{4.23}$$

The $\mu \to e$ conversion and $\mu \to eee$ processes also give comparable bounds. The limits on the electric dipole moments (EDMs) of the electron [96], neutron [97] and mercury atom [98] lead to

$$|{\rm Im}(\delta^e_{LR})_{11}| \lesssim 2 \times 10^{-7} \left(\frac{m_{\rm N}}{200\ {\rm GeV}}\right), \tag{4.24}$$

$$|{\rm Im}(\delta^u_{LR})_{11}| \lesssim 2 \times 10^{-6} \left(\frac{m_{\rm C}}{600\ {\rm GeV}}\right), \qquad |{\rm Im}(\delta^d_{LR})_{11}| \lesssim 1 \times 10^{-6} \left(\frac{m_{\rm C}}{600\ {\rm GeV}}\right), \tag{4.25}$$

$$|{\rm Im}(\delta^u_{LR})_{11}| \lesssim 4 \times 10^{-7} \left(\frac{m_{\rm C}}{600\ {\rm GeV}}\right), \qquad |{\rm Im}(\delta^d_{LR})_{11}| \lesssim 4 \times 10^{-7} \left(\frac{m_{\rm C}}{600\ {\rm GeV}}\right), \tag{4.26}$$

respectively. Here, the bounds of Eqs. (4.23 – 4.26) are obtained conservatively by scanning the ratios of the superparticle masses in a reasonable range (see e.g. [20, 99]).[7] The bounds from neutron and mercury EDMs are subject to large theoretical uncertainties [100], and we have used conservative estimates. The constraints from $(\epsilon'/\epsilon)_K$ and $b \to s\gamma$ also lead to bounds on $|{\rm Im}(\delta^d_{LR})_{12,\,21}|$ and $|(\delta^d_{LR})_{23,\,32}|$, but they are not as strong as the bounds above when the left-right mass insertion parameters scale naively with the quark masses.

We can obtain the bounds on the superparticle masses using Eqs. (4.21, 4.22), with the approximation $a_{\rm C} \approx m_{\rm C}$ and $a_{\rm N} \approx m_{\rm N}$, which is sufficient for the level of analysis here. Taking $(M_u)_{11} \simeq m_u \simeq 2$ MeV and $(M_d)_{11} \simeq m_d \simeq 4$ MeV, the neutron EDM bound of Eq. (4.25) leads to the following bound on m_C:

$$m_{\rm C} \gtrsim \max\left\{800\ {\rm GeV} \left(\frac{\sin\varphi_u}{\tilde{y}}\right)^{1/2},\ \ 1.5\ {\rm TeV} \left(\frac{\sin\varphi_d}{\tilde{y}}\right)^{1/2}\right\}, \tag{4.27}$$

whereas the mercury EDM bound, Eq. (4.26), gives

$$m_{\rm C} \gtrsim \max\left\{1.3\ {\rm TeV} \left(\frac{\sin\varphi_u}{\tilde{y}}\right)^{1/2},\ \ 1.9\ {\rm TeV} \left(\frac{\sin\varphi_d}{\tilde{y}}\right)^{1/2}\right\}. \tag{4.28}$$

The bound on m_N depends on the assumption on the charged lepton mass matrix. If we conservatively take $(M_e)_{11} \simeq m_e \simeq 0.5$ MeV and $(M_e)_{12} \simeq (M_e)_{21} \simeq (m_e\, m_\mu)^{1/2} \simeq 7$ MeV, we obtain

$$m_{\rm N} \gtrsim \max\left\{600\ {\rm GeV}\frac{1}{\tilde{y}^{1/2}},\ \ 700\ {\rm GeV} \left(\frac{\sin\varphi_e}{\tilde{y}}\right)^{1/2}\right\}. \tag{4.29}$$

[7] Here we consider the ranges $m^2_{\tilde{g}}/m^2_{\tilde{q}} \lesssim 2$ and $m^2_{\chi}/m^2_{\tilde{l}} \lesssim 3$, where $m_{\tilde{g}}$, $m_{\tilde{q}}$, m_χ, and $m_{\tilde{l}}$ are the gluino, squark, weak gaugino, and slepton average masses. These ranges are motivated by renormalization group considerations with M_F well above the TeV scale, e.g. $M_F \gtrsim 10^{10}$ GeV. The case of smaller M_F will be discussed in section 4.3.1.

On the other hand, if the large neutrino mixing angle θ_{12} receives a significant contribution from the charged lepton Yukawa matrix, we expect $(M_e)_{12} \simeq m_\mu \tan\theta_{12} \simeq 70$ MeV, giving a much stronger bound

$$m_{\rm N} \gtrsim \max\left\{1.9\ {\rm TeV}\frac{1}{\tilde{y}^{1/2}},\ \ 700\ {\rm GeV}\left(\frac{\sin\varphi_e}{\tilde{y}}\right)^{1/2}\right\}. \tag{4.30}$$

In fact, this latter bound is expected to apply in the case where $\mathcal{E}^e_{ij}$ factorizes: $\mathcal{E}^e_{ij} = \epsilon_{L_i}\epsilon_{E_j}$, since then the large 1-2 neutrino mixing angle generically implies $\epsilon_{L_1} \approx \epsilon_{L_2}$, leading to a large 1-2 element of the charged lepton mass matrix of $O(m_\mu)$.

In addition to the uncertainties already described, the bounds on $m_{\rm C,N}$ derived above are subject to uncertainties coming from $O(1)$ coefficients in front of Eq. (4.20). Only the square root of these coefficients, however, appear in the bounds. For example, if we take the magnitude of these coefficients to be between 0.5 and 2, the bounds receive unknown coefficients of $O(0.7-1.4)$, which do not significantly affect the results. These bounds also scale with the square root of the natural size of the scalar trilinear interactions at M, $(\tilde{\zeta}/\eta_A)^{1/2}$, which we have set unity. In addition, the bounds scale with the experimental limits on the $\mu \to e\gamma$ branching ratio, ${\rm Br}(\mu \to e\gamma)$, and the electron, neutron and mercury EDMs, d_e, d_n and $d_{\rm Hg}$, as

$$\left(\frac{{\rm Br}(\mu \to e\gamma)}{1.2\times 10^{-11}}\right)^{-1/4}, \tag{4.31}$$

$$\left(\frac{d_e}{1.6\times 10^{-27}\, e\,{\rm cm}}\right)^{-1/2}, \qquad \left(\frac{d_n}{2.9\times 10^{-26}\, e\,{\rm cm}}\right)^{-1/2}, \qquad \left(\frac{d_{\rm Hg}}{2.1\times 10^{-28}\, e\,{\rm cm}}\right)^{-1/2}. \tag{4.32}$$

Therefore, if future experiments such as ones in [101, 102, 103, 104, 105, 106, 107, 108, 109] improve the upper bounds on these (and other) quantities, the lower bounds on $m_{\rm C,N}$ increase accordingly.

The bounds of Eqs. (4.27 – 4.30) place lower limits on the superparticle masses, yielding a tension with the observability of supersymmetry at the LHC. In fact, the conservative bound of Eq. (4.29) already gives strong constraints on the superparticle spectrum for $\tilde{y} \approx 1$. In particular, in the case that colored and non-colored superparticles do not have a strong mass hierarchy at $M \gg$ TeV, we expect that $m_{\rm C} \approx (2-4)m_{\rm N}$ at low energies. This pushes up the masses of colored superparticles beyond 1 TeV, and, in many cases, beyond the reach of the LHC. The constraints are even stronger if the large neutrino mixing angle θ_{12} receives a sizable contribution from the charged lepton Yukawa matrix, as in Eq. (4.30). We call this generic tension between low energy flavor and CP violation and the observability of supersymmetry at the LHC *the superpotential flavor problem*, since it is caused by the superpotential operators $\mathcal{O}_{\zeta_f}$. An important point, again, is that the problem is relatively model independent because the flavor structure of $\mathcal{O}_{\zeta_f}$ is expected to be correlated with that of $\mathcal{O}_{\lambda_f}$ in wide classes of flavor theories.

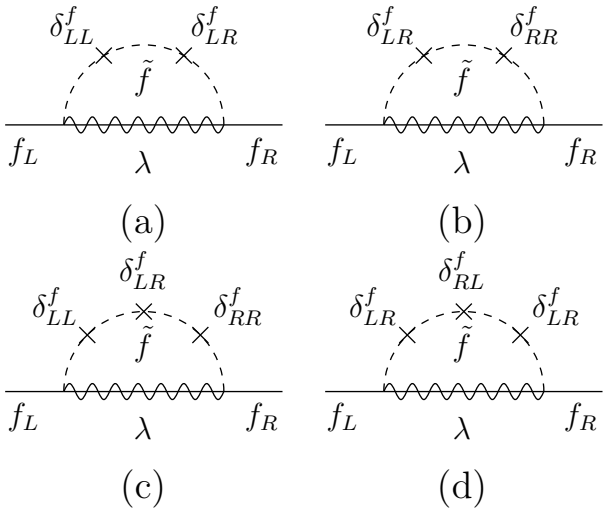

Figure 4.1: Multiple mass insertion diagrams that lead to dangerous flavor and CP violating contributions. Here, $f_{L,R}$, $\tilde{f}$ and λ represent fermions, scalars and gauginos, respectively.

4.2.4 More general problem with left-right sfermion propagation

The superpotential flavor problem provides a strong, model-independent tension between weak scale supersymmetry and low energy flavor and CP violating observables. This is, however, only one aspect of a more general problem associated with left-right propagation of the sfermions in flavor and CP violating amplitudes.

Suppose that the superpotential flavor problem is somehow solved, i.e. the operators $\mathcal{O}_{\zeta_f}$ are strongly suppressed. There will still be the contributions to lepton flavor violation and EDMs associated with left-right propagation of sfermions. First of all, there are flavor nonuniversal scalar trilinear interactions generated by $\mathcal{O}_{Z_\Phi,\eta_\Phi}$, yielding $(\delta^f_{LR})_{ij}$ $(i \neq j)$ and $\mathrm{Im}(\delta^f_{LR})_{ii}$. These contributions must be sufficiently suppressed. Moreover, even if they are small, lepton flavor violation and EDMs are induced by diagrams that use multiple mass insertion parameters $(\delta^f_{LR})_{ij}$, $(\delta^f_{LL})_{ij}$ and $(\delta^f_{RR})_{ij}$ (see Fig. 4.1) [110], instead of a single insertion of $(\delta^f_{LR})_{ij}$. Since the diagrams depend on parameters $(\delta^f_{LL})_{ij}$ and $(\delta^f_{RR})_{ij}$, whose correlations with the Yukawa couplings are model dependent, the tension caused by these diagrams is not as model independent as the superpotential flavor problem. Nevertheless, this provides strong constraints on supersymmetric models in which the structure of the supersymmetry breaking parameters is correlated with that of the Yukawa couplings.

One might naively think that because of the use of multiple mass insertion parameters, the diagrams of Fig. 4.1 are much smaller than those using a single $(\delta^f_{LR})_{ij}$. This is, however, not always the case for the following reasons:

- The left-right mass insertions used can be flavor universal, $\mathrm{Re}(\delta^f_{LR})_{ii}$, since the necessary flavor/CP violation can come from insertions of $(\delta^f_{LL})_{ij}$ and/or $(\delta^f_{RR})_{ij}$. This

may enhance the contributions from multiple mass insertion diagrams relative to single insertion ones, especially for $f = d, e$, since the flavor universal part of $(\delta^{d,e}_{LR})_{ij}$ is enhanced by $\tan\beta \equiv \langle H_u\rangle/\langle H_d\rangle$. (For $f = e$, it is also enhanced by $\mu/m_{\rm N}$, which is typically of $O(m_{\rm C}/m_{\rm N})$.)

- The sfermions propagating between two mass insertions can be from a heavier generation. For diagrams with triple mass insertions, for example, the states propagating between mass insertions can be third generation states, minimizing extra suppressions arising from use of more mass insertion parameters.

In fact, these two ingredients can make the contributions from the diagrams of Fig. 4.1 comparable or even larger than those from the diagrams with a single insertion of $(\delta^f_{LR})_{ij}$ of Eqs. (4.21, 4.22).

To illustrate this point, suppose that $\mathcal{E}^f_{ij}$ in Eq. (4.18) factorize, $\mathcal{E}^u_{ij} = \epsilon_{Q_i}\epsilon_{U_j}$, $\mathcal{E}^d_{ij} = \epsilon_{Q_i}\epsilon_{D_j}$ and $\mathcal{E}^e_{ij} = \epsilon_{L_i}\epsilon_{E_j}$, giving the Yukawa couplings $(y_u)_{ij} \approx \tilde{y}\,\epsilon_{Q_i}\epsilon_{U_j}$, $(y_d)_{ij} \approx \tilde{y}\,\epsilon_{Q_i}\epsilon_{D_j}$ and $(y_e)_{ij} \approx \tilde{y}\,\epsilon_{L_i}\epsilon_{E_j}$. Suppose also that the flavor nonuniversal part of the sfermion squared masses scale naively with the ϵ factors:

$$(m^2_\Phi)_{ij} \approx \epsilon_{\Phi_i}\epsilon_{\Phi_j} m^2_{\rm S}, \tag{4.33}$$

where $m_{\rm S} \approx \eta_A F_X/M$ is the scale of supersymmetry breaking parameters at M, which we assume to be the same for colored and non-colored superparticles. The mass insertion parameters generated by Eq. (4.33) are then

$$(\delta^u_{LL})_{ij} \approx (\delta^d_{LL})_{ij} \approx \epsilon_{Q_i}\epsilon_{Q_j}\frac{m^2_{\rm S}}{m^2_{\rm C}}, \qquad (\delta^u_{RR})_{ij} \approx \epsilon_{U_i}\epsilon_{U_j}\frac{m^2_{\rm S}}{m^2_{\rm C}}, \qquad (\delta^d_{RR})_{ij} \approx \epsilon_{D_i}\epsilon_{D_j}\frac{m^2_{\rm S}}{m^2_{\rm C}}, \tag{4.34}$$

$$(\delta^e_{LL})_{ij} \approx (\delta^\nu_{LL})_{ij} \approx \epsilon_{L_i}\epsilon_{L_j}\frac{m^2_{\rm S}}{m^2_{\rm N}}, \qquad (\delta^e_{RR})_{ij} \approx \epsilon_{E_i}\epsilon_{E_j}\frac{m^2_{\rm S}}{m^2_{\rm N}}, \tag{4.35}$$

where $i \neq j$, and we have included the mass insertion parameters for the sneutrinos. On the other hand, the dominant contribution to the flavor universal part of the left-right mass insertion parameters are given by

$$\begin{aligned} {\rm Re}(\delta^u_{LR})_{ii} &\approx \frac{1}{m_{\rm C}}(M_u)_{ii}, \\ {\rm Re}(\delta^d_{LR})_{ii} &\approx \frac{\mu\tan\beta}{m^2_{\rm C}}(M_d)_{ii}, \\ {\rm Re}(\delta^e_{LR})_{ii} &\approx \frac{\mu\tan\beta}{m^2_{\rm N}}(M_e)_{ii}, \end{aligned} \tag{4.36}$$

where we have taken $\mu \approx m_{\rm C} \gtrsim m_{\rm N}$ and $\tan\beta \gtrsim 1$, and assumed that flavor universal scalar trilinear interactions $(a_{u,d})_{ii} \approx (y_{u,d})_{ii} m_{\rm C}$ and $(a_e)_{ii} \approx (y_e)_{ii} m_{\rm N}$ are generated by renormalization group evolution. (The expression of Eq. (4.36) also applies to the case where $\mathcal{E}^f_{ij}$ do not factorize.)

Consider, for example, the diagram of Fig. 4.1(c) with $f = u$. This leads to the contribution to the up quark EDM that scales with

$$(\delta^u_{LL})_{13}(\delta^u_{LR})_{33}(\delta^u_{RR})_{31} \approx \frac{(M_u)_{11}}{\tilde{y}\, m_{\rm C}} \left(\frac{m_{\rm S}}{m_{\rm C}}\right)^4 \frac{(y_u)^2_{33}}{\tilde{y}}, \tag{4.37}$$

which can be comparable to the dangerous contribution that scales with $(\delta^u_{LR})_{11} \approx (M_u)_{11}/\tilde{y}\, m_{\rm C}$ of Eq. (4.21) with $a_{\rm C} \approx m_{\rm C}$. The diagram of Fig. 4.1(a) with $f = e$ gives a contribution to the $\mu \to e\gamma$ process that scales with

$$(\delta^e_{LL})_{12}(\delta^e_{LR})_{22} \approx \frac{(M_e)_{12}}{\tilde{y}\, m_{\rm N}} \, \frac{m^2_{\rm S}\, \mu}{m^3_{\rm N}}\, \tilde{y}\, \epsilon^2_{L_2} \tan\beta, \tag{4.38}$$

which can also be dangerous because it could be comparable to the contribution from $(\delta^e_{LR})_{12} \approx (M_e)_{12}/\tilde{y}\, m_{\rm N}$ of Eq. (4.21) with $a_{\rm N} \approx m_{\rm N}$, especially for large $\tan\beta$. These examples show that the multiple mass insertion diagrams may lead to flavor and CP violation at a dangerous level even in the absence of flavor and CP violating $(\delta^f_{LR})_{ij}$.

In practice, the constraints from multiple mass insertion diagrams can be taken into account by considering the effective left-right mass insertion parameters

$$\begin{aligned}(\delta^f_{LR,\rm eff})_{ij} \;\equiv\; \max\Big\{ & c_d(\delta^f_{LL})_{ik}(\delta^f_{LR})_{kj},\; c_d(\delta^f_{LR})_{ik}(\delta^f_{RR})_{kj}, \\ & c_t(\delta^f_{LL})_{ik}(\delta^f_{LR})_{kk}(\delta^f_{RR})_{kj},\; c_t(\delta^f_{LR})_{ik}(\delta^f_{RL})_{kk}(\delta^f_{LR})_{kj} \Big\},\end{aligned} \tag{4.39}$$

and requiring that $(\delta^f_{LR,\rm eff})_{ij}$ satisfy the bounds of Eqs. (4.23 – 4.26) with $(\delta^f_{LR})_{ij}$ replaced by $(\delta^f_{LR,\rm eff})_{ij}$. Here, $c_d \simeq (0.5-0.8)$ and $c_t \simeq (0.3-0.6)$ are numerical coefficients arising from the difference of momentum integral functions with various numbers of insertions. Once $(\delta^f_{LL})_{ij}$ and $(\delta^f_{RR})_{ij}$ are given, these constraints can be checked.

4.3 Approaches to the Problem

In order to have a framework for weak scale supersymmetry in which the LHC can provide additional insight into the origin of the observed flavor structure, the supersymmetric left-right flavor problem must somehow be addressed. The bounds associated with left-left and right-right sfermion propagation must also be avoided, although they are, in general, less stringent. To address the issue of whether there are theories that naturally satisfy all these constraints, we start by identifying classes of theories that do not have the superpotential flavor problem, a robust part of the supersymmetric left-right flavor problem. While it is not automatic that these theories will be safe from low energy constraints or even solve the supersymmetric left-right flavor problem, they provide frameworks with which to build more detailed theories that can avoid all low energy constraints. The remaining constraints will be discussed in the next section.

4.3.1 General considerations

There are essentially two different directions to address the superpotential flavor problem. One is to assume that the operators $\mathcal{O}_{\zeta_f}$ exist with their natural size, but the bounds are somehow avoided. Barring accidental cancellations in the amplitudes for low energy flavor and CP violating effects, this includes the following possibilities:

(i) The bounds are given by Eq. (4.29), and the superparticles are not too much heavier. If the superparticle masses satisfy $m_{\rm C} \approx (2-4) m_{\rm N}$, the viable parameter region is somewhat squeezed. The constraints are slightly relaxed if we allow the masses of colored and non-colored superparticles to be of similar size, $m_{\rm C} \sim m_{\rm N}$. Avoiding the bound of Eq. (4.30), however, is still not easy.

(ii) The intrinsic size of the Yukawa couplings is large, $\tilde{y} \gg O(1)$. In this case the bounds on m_C and m_N are not significant, especially in the case where the large neutrino mixing angle θ_{12} arises only from the neutrino mass matrix, Eqs. (4.27 – 4.29). If the bound is given by Eq. (4.30), the lower bound on $m_{\rm N}$ can be relaxed to about 500 GeV by taking the largest possible value of $\tilde{y} \approx 4\pi$. This constraint, however, is still significant.

(iii) The gauginos are significantly heavier than the sfermions. In this case the bounds of Eqs. (4.27, 4.28) and Eqs. (4.29, 4.30) are relaxed approximately by a factor of $(m_{\tilde{g}}/m_{\tilde{q}})/\sqrt{2}$ and $(m_\chi/m_{\tilde{l}})/\sqrt{3}$, respectively, with $m_{\rm C,N}$ now interpreted as the masses of the sfermions. This situation can occur if M_F is close to the TeV scale, and the masses of the sfermions at M_F are suppressed by the dynamics generating the Yukawa hierarchy, as in flavor models of Ref. [85].[8] Note that we only need sfermions to be accessible at the LHC to probe the origin of the flavor structure.

These possibilities are certainly viable, especially given uncertainties in our estimates. The tension between flavor constraints and the LHC observability, however, still exists. If one of these possibilities is realized, and the superparticles are within the LHC reach, we expect that $\mu \to e$ processes and/or atomic and nuclear EDMs will be discovered in the near future, for example in the experiments of [101, 102, 103, 104, 105, 106, 107, 108, 109], which expect to improve present bounds by several orders of magnitude.

The other direction to address the superpotential flavor problem is to consider that the operators $\mathcal{O}_{\zeta_f}$ are somehow suppressed. This includes the following possibilities:

(iv) The coefficients of the operators $\mathcal{O}_{\zeta_f}$ (or at least those of the 1-2 and 2-1 elements of $\mathcal{O}_{\zeta_e}$) are accidentally suppressed. The required amount of suppression is not strong if we adopt Eq. (4.29). However, if we instead use Eq. (4.30), we need to have $\tilde{\zeta}/\eta_A \lesssim 0.07\, \tilde{y}\, (m_{\rm N}/500\ {\rm GeV})^2$, which provides a strong bound on $\tilde{\zeta}/\eta_A$ for $\tilde{y} \approx 1$.

[8] M_F needs to be low to prevent the scalar masses from becoming comparable to the gaugino masses through SSM renormalization group evolution.

(v) The scalar trilinear interactions are exactly proportional to the Yukawa matrices, $(a_f)_{ij} \propto (y_f)_{ij}$, leading to vanishing flavor and CP violating mass insertion parameters. This may be achieved, for example, if $(a_f)_{ij}$ and $(y_f)_{ij}$ arise from a single operator through the lowest and highest components VEVs of X, $\langle X \rangle = X_0 + \theta^2 F_X$, with $\arg(F_X/X_0) \approx \arg(M_A)$. The large top quark mass, however, requires that X_0 is close to the cutoff scale M_*, and the problem may be regenerated by higher order terms in X_0/M_*.

(vi) The operators $\mathcal{O}_{\zeta_f}$ are suppressed by some mechanism, $\tilde{\zeta} \ll \eta_A$. This mechanism may or may not operate in the regime where effective field theory is valid.

Note that (iv), (v) and (vi) above can also be combined with (i), (ii) and (iii) described before. For example, we can consider a setup where $\mathcal{O}_{\zeta_f}$ are suppressed by some mechanism, (vi), *and* the natural size of the Yukawa couplings, $\tilde{y}$, is large, (ii).

In the rest of this chapter, we focus on the last possibility, (vi), and see how much the situation will be improved. As we discussed, we still need to address the more general left-right flavor problem and the constraints from left-left and right-right sfermion propagation, which we defer to the next section. Here we present simple classes of theories in which $\mathcal{O}_{\zeta_f}$ are naturally suppressed. In fact, this provides a platform for the analysis of the more model dependent part of the flavor problem.

There are several possible ways that the operators $\mathcal{O}_{\zeta_f}$ can be suppressed. In fact, they may simply be absent at a scale where the SSM arises as an effective field theory, as a result of the dynamics of some more fundamental theory. This is not unreasonable because $\mathcal{O}_{\zeta_f}$ are the only superpotential operators associated with supersymmetry breaking, so if supersymmetry breaking is mediated to the SSM sector by loop processes then these operators may be absent. In the remainder of this section we discuss three simple classes of theories for suppressing $\mathcal{O}_{\zeta_f}$. We classify them according to the pattern of the supersymmetry breaking parameters obtained at M_F. The simple suppression of $\mathcal{O}_{\zeta_f}$ described above can effectively be classified into the first class, because it leads to the same pattern of the supersymmetry breaking masses at M_F. There are clearly many models within each class, and we explicitly discuss some of them.

4.3.2 Framework I — Higgsphobic supersymmetry breaking

We here present the first class of theories in which $\mathcal{O}_{\zeta_f}$ are naturally suppressed. A unique feature of the operators $\mathcal{O}_{\zeta_f}$ is that among the operators relevant to flavor violation, Eqs. (4.10 – 4.12), these are the only operators that contain both Higgs fields, H, and the supersymmetry breaking field, X. Therefore, if the theory does not allow direct coupling between H and X, a framework which we call *Higgsphobic supersymmetry breaking*, then $\mathcal{O}_{\zeta_f}$ are forbidden. The other operators $\mathcal{O}_{Z_\Phi, \kappa_\Phi, \eta_\Phi, \lambda_f}$ can exist as long as couplings between Φ and X and between Φ and H are allowed. A simple way of realizing this is to assume that H and X are localized in different points in extra dimensions, while Φ have broad wavefunctions

overlapping with both H and X.[9]

Let us now focus on the extra dimensional way of suppressing $\mathcal{O}_{\zeta_f}$ described above. In theories with extra dimensions, wavefunction overlaps between Φ and H control the size of the 4D Yukawa couplings [111, 34, 35]. This motivates a configuration where heavier generation matter fields have larger wavefunction overlaps with the Higgs fields. For example, if the widths of all the matter wavefunctions are the same, then heavier generation fields have wavefunctions peaked closer to the Higgs fields. On the other hand, if all the matter wavefunctions are peaked at the same point (separated from where the Higgs fields reside), then heavier generation fields have wider wavefunctions. A schematic depiction of these possibilities is shown in Fig. 4.2.

The location of X cannot be arbitrary. If the X field is localized to a generic point in the region where matter wavefunctions are significant, the generated soft supersymmetry breaking parameters have a random structure, e.g. Eq. (4.2), leading to large flavor and CP violation. One way of avoiding this is to localize X far away from wavefunction peaks for all the matter fields, in which case flavor violation in the low energy supersymmetry breaking masses arises only from loop effects across the bulk [35]. Another way is to localize X at a point close to where the Higgs fields are localized [33]. In this case the tree-level structure of the operators $\mathcal{O}_{\kappa_\Phi,\eta_\Phi}$ is correlated with that of the Yukawa couplings $\mathcal{O}_{\lambda_f}$, since they are both controlled by the wavefunction values of the matter fields in the region where the X and the Higgs fields reside. In the case where all the matter wavefunctions are spherically symmetric and peaked at the same point o, a similar correlation can be obtained by localizing X to a point (approximately) the same distance away from o as the Higgs fields. In all these cases, flavor violation also arises from loop effects across the bulk.

Some of the field configurations discussed above are depicted schematically in Fig. 4.2. Note that while the figures describe only three matter wavefunctions for illustrative purposes, all Q_i, U_i, D_i, L_i and E_i fields can have distinct wavefunctions. The geometry of the extra dimensions can also be more general: the number of extra dimensions is arbitrary, and the spacetime need not be flat. While the scale of the extra dimensions, i.e. the scale of Kaluza-Klein resonances, is, in principle, arbitrary, it is simplest to consider it to be of order the unification scale, $1/R \approx M_{\rm unif} \approx 10^{16}$ GeV, to preserve the success of supersymmetric gauge coupling unification in the most straightforward manner. In the case where H and X are localized in the infrared region of warped spacetime, the scale can be lower, 10 TeV $\lesssim 1/R \lesssim M_{\rm unif}$ (in which case gauge coupling unification can occur through modified gauge coupling running above $1/R$, as in Ref. [112].) It is also possible to consider the framework in the context of grand unification in higher dimensions [38, 55]. In the theories considered here, a natural scale for flavor physics is of order $1/R$, while a natural scale for supersymmetry breaking mediation is of order the (local) cutoff scale M_*, which we take to be somewhat above $1/R$.

One consequence of Higgsphobic supersymmetry breaking is that the Higgs sector oper-

[9] Precisely speaking, in extra dimensional theories it is sufficient to assume that the Yukawa couplings are allowed only in places separated from the X field. The Higgs fields can be delocalized in that case.

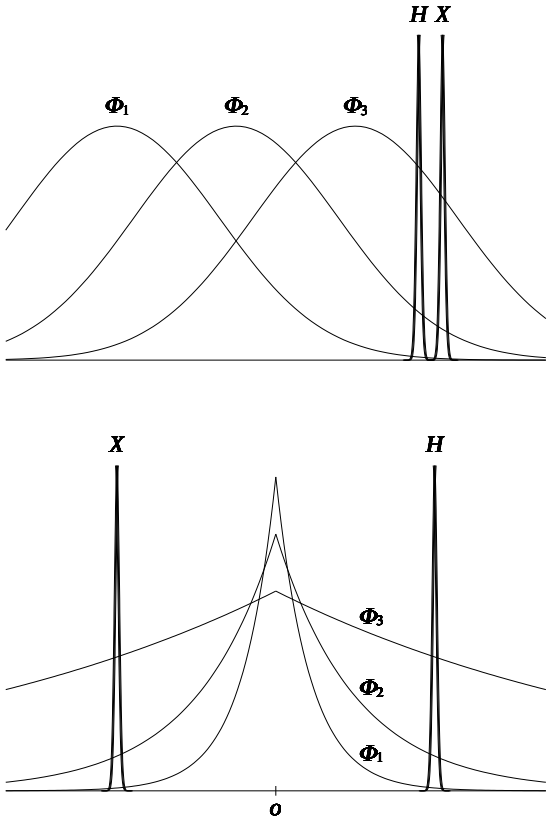

Figure 4.2: A schematic depiction of possible configurations of the matter, Higgs and supersymmetry breaking fields. The Higgs and supersymmetry breaking fields are localized to separate but nearby points (left). In the case where all the matter wavefunctions are spherically symmetric and centered around the same point o, the Higgs and supersymmetry breaking fields can be localized (approximately) the same distance away from o (right). The gauge fields are assumed to propagate in the bulk.

operators	$\mathcal{O}_{Z_\Phi}$	$\mathcal{O}_{\kappa_\Phi}$	$\mathcal{O}_{\eta_\Phi}$	$\mathcal{O}_{\lambda_f}$	$\mathcal{O}_{\zeta_f}$
$G_{\rm flavor}$ breaking				$\surd$	$\surd$
supersymmetry breaking		$\surd$	$\surd$		$\surd$

Table 4.1: Required symmetry breaking to write down operators in Eqs. (4.10 – 4.12). The operators $\mathcal{O}_{\lambda_f,\zeta_f}$ require $G_{\rm flavor}$ breaking, while $\mathcal{O}_{\kappa_\Phi,\eta_\Phi,\zeta_f}$ require supersymmetry breaking.

ators $\mathcal{O}_{\kappa_H,\eta_H,\mu,b}$ in Eqs. (4.7, 4.8) are forbidden in the minimal setup. There are, however, several ways to generate the desired μ and b parameters, which are discussed in Appendix A.1.

4.3.3 Framework II — Remote flavor-supersymmetry breaking

We now consider the second framework. An essential ingredient of this framework is a "separation" between supersymmetry breaking and flavor symmetry breaking. Consider a flavor symmetry $G_{\rm flavor}$ that prohibits the Yukawa operators $\mathcal{O}_{\lambda_f}$ in the unbroken limit. The SSM Yukawa couplings are then generated through breaking of $G_{\rm flavor}$, which we assume to be the origin of the observed Yukawa structure [113]. An important point is that among the operators relevant to flavor violation, $\mathcal{O}_{Z_\Phi,\kappa_\Phi,\eta_\Phi,\lambda_f,\zeta_f}$ in Eqs. (4.10 – 4.12), $\mathcal{O}_{\zeta_f}$ are the only operators that *require* both $G_{\rm flavor}$ breaking and supersymmetry breaking (see Table 4.1). Therefore, if we assume that the theory possesses $G_{\rm flavor}$, and that $G_{\rm flavor}$ and supersymmetry are broken in different sectors of the theory that do not directly communicate with each other, a framework which we call *remote flavor-supersymmetry breaking*, then the operators $\mathcal{O}_{\zeta_f}$ are absent.

In the present framework, the Yukawa couplings are generated through breaking of $G_{\rm flavor}$. Assuming that the breaking is caused by the VEV of a chiral superfield ϕ, the relevant operators are written schematically as

$$\mathcal{L} \approx \int d^2\theta \sum_{i,j} \left(\frac{\phi}{M_*}\right)^{(n_f)_{ij}} \Phi_{Li}\Phi_{Rj}H + \text{h.c.}, \tag{4.40}$$

where M_* is the (effective) cutoff scale and $(n_f)_{ij}$ are integers. In general, these operators could generate dangerous scalar trilinear interactions through supersymmetry breaking. Here we assume that they do not generate significant scalar trilinear interactions. The conditions under which this is indeed the case are discussed in Appendix A.2 for the general case that $G_{\rm flavor}$ is broken by the VEVs of several fields ϕ_m $(m = 1, 2, \cdots)$.

A symmetry group $G_{\rm flavor}$ needs to be chosen to avoid all the low energy flavor and CP violating constraints. Suppose that $G_{\rm flavor}$ were a simple $U(1)$ symmetry, whose breaking controls the size of the Yukawa couplings. In this case the Cabibbo angle, θ_C, would be reproduced by the difference of the $U(1)$ charges of Q_1 and Q_2, q_{Q_1} and q_{Q_2}, as $\sin\theta_C \approx \epsilon^{q_{Q_1}-q_{Q_2}}$, where ϵ is the dimensionless $U(1)$ breaking parameter normalized to have a charge of -1, and $q_{Q_1} > q_{Q_2}$. This, however, would lead to too large flavor violation in $\mathcal{O}_{\kappa_Q}$,

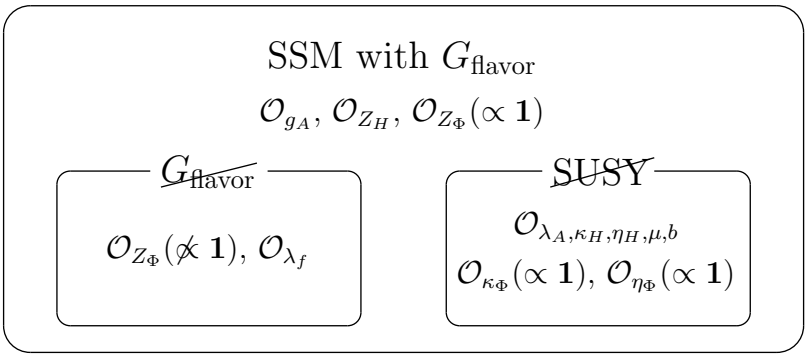

Figure 4.3: The schematic picture of a remote flavor-supersymmetry breaking theory with $G_{\rm flavor}$ being a sufficiently large subgroup of $SU(3)^5$. Here, we have depicted only operators relevant for the analysis.

giving $(\delta^d_{LL})_{12} \approx (\delta^d_{LL})_{21} \approx O(\epsilon^{q_{Q_1}-q_{Q_2}}) \approx O(\sin\theta_C)$, which needs to be smaller than of order $10^{-2}(m_C/600\ \text{GeV})$ to avoid the bound from ϵ_K. (Here we have assumed $\eta_A^2 \approx \kappa_\Phi$ and a generic Yukawa structure.) Similar conflicts between the Yukawa structure and flavor violating processes also arise in other places. One possibility of avoiding these bounds is to consider more elaborate Abelian charge assignments, for example, under $G_{\rm flavor} = U(1)\times U(1)$ (see e.g. [32]). Another, perhaps simpler, approach is to consider a non-Abelian $G_{\rm flavor}$ symmetry under which (at least) the first two generations of quarks and leptons having the same standard model gauge quantum numbers are in a single $G_{\rm flavor}$ multiplet. This makes the relevant coefficients of $\mathcal{O}_{\kappa_\Phi}$ proportional to the unit matrix, significantly reducing the problem.

Note that flavor violation in this framework can come mainly from the operators $\mathcal{O}_{Z_\Phi}$ (in the $G_{\rm flavor}$ symmetric field basis). Consider that $G_{\rm flavor}$ is a sufficiently large subgroup of $SU(3)^5 = SU(3)_Q \times SU(3)_U \times SU(3)_D \times SU(3)_L \times SU(3)_E$ so that all the three generations are treated equally under $G_{\rm flavor}$. In this case the sector breaking supersymmetry generates the operators $\mathcal{O}_{\kappa_\Phi}$ and $\mathcal{O}_{\eta_\Phi}$, but they are completely flavor universal:

$$(\kappa_\Phi)_{ij} \propto \delta_{ij}, \qquad (\eta_\Phi)_{ij} \propto \delta_{ij}. \tag{4.41}$$

Flavor violation, however, still arises at M_F because the operators $\mathcal{O}_{Z_\Phi}$ receive flavor nonuniversal contributions from the sector breaking $G_{\rm flavor}$:

$$(Z_\Phi)_{ij} \not\propto \delta_{ij}. \tag{4.42}$$

This situation is depicted schematically in Fig. 4.3. The scalar squared masses and trilinear interactions in the basis where the fields are canonically normalized are, therefore, flavor nonuniversal at M_F.

A simple way of realizing the present framework is to consider higher dimensional theories in which the bulk flavor symmetry $G_{\rm flavor}$ and supersymmetry are broken on separate branes.

Note that $G_{\rm flavor}$ can be broken on multiple branes, which could help address the issue of vacuum alignment, depending on $G_{\rm flavor}$ and its breaking pattern. If the relevant extra dimension is warped [114], $G_{\rm flavor}$ and supersymmetry can be broken at the ultraviolet and infrared branes, respectively. Through the AdS/CFT correspondence, these theories have a 4D interpretation that supersymmetry is dynamically broken by strong gauge dynamics that have an approximate flavor symmetry. Exchanging the locations of supersymmetry and flavor breaking is also an interesting possibility, which corresponds to 4D theories in which nontrivial flavor structures arise dynamically at low energies.

4.3.4 Framework III — Charged supersymmetry breaking

The final framework we consider is one in which X carries a nontrivial charge of some symmetry, so that the operators $\mathcal{O}_{\zeta_f}$ are forbidden. (We assume that the Yukawa couplings, $\mathcal{O}_{\lambda_f}$, are allowed.) This symmetry should have anomalies with respect to the standard model gauge group so that the gaugino mass operators $\mathcal{O}_{\lambda_A}$ can be written. (For an example of this class of models, see [33].) An immediate consequence of this framework, which we call *charged supersymmetry breaking*, is that the operators $\mathcal{O}_{\eta_H}$ and $\mathcal{O}_{\eta_\Phi}$ are also forbidden. This class of theories, therefore, has vanishing scalar trilinear interactions at the scale M.[10]

The operator $\mathcal{O}_\mu$, which leads to the μ parameter, may or may not be forbidden, depending on the charge assignments of X and H. An interesting point is that once we choose the charge assignment such that $\mathcal{O}_\mu$ is allowed, $\mathcal{O}_b$ is always forbidden. Assuming that the gravitino mass is small, $m_{3/2} \ll m_{\rm C,N}$, this implies that $|b| \ll |\mu|^2$, solving the supersymmetric CP problem associated with the Higgs sector. In the case where $\mathcal{O}_\mu$ is not allowed, the μ and b parameters can be generated from $\mathcal{O}_{\rm SUGRA}$, as long as $m_{3/2}$ is of order the weak scale.

The framework of charged supersymmetry breaking is compatible with many theories of flavor, including theories with extra dimensions or flavor symmetries. For example, it can be combined with the framework described in the previous subsection. This will prohibit the operators $\mathcal{O}_{\eta_H,\eta_\Phi}$, which would otherwise be there. Another interesting way of obtaining the Yukawa hierarchy in this framework is to generate it at lower energies by some strong gauge dynamics [85]. This generates large anomalous dimensions for Φ, and, after canonically normalizing fields, the Yukawa and supersymmetry breaking parameters develop a hierarchy. Note that unlike Higgsphobic or remote flavor-supersymmetry breaking, charged supersymmetry breaking guarantees that the scalar trilinear interactions vanish at M, which is necessary to prevent reintroducing the superpotential flavor problem in models of the type given in Ref. [85] (although the problem may be avoided by making the gauginos much heavier than the scalars, as discussed in (iii) in section 4.3.1). In these theories, the scale for supersymmetry breaking mediation can be high to naturally preserve gauge coupling

[10] It is possible that the mechanism generating $\mathcal{O}_{\lambda_A}$, $\approx \int d^2\theta\, (\ln X) \mathcal{W}^{A\alpha}\mathcal{W}^A_\alpha + \text{h.c.}$, also generates other operators, e.g. $\mathcal{O}_{\eta_H}$ and $\mathcal{O}_{\eta_\Phi}$ of the form $\int d^4\theta\, \ln(X^\dagger X) H^\dagger H$ and $\int d^4\theta\, \ln(X^\dagger X)\Phi_i^\dagger \Phi_j + \text{h.c.}$, with the similar size. In the minimal case such as one in Ref. [33], $\mathcal{O}_{\lambda_A}$ are generated by gauge mediation and the other operators are suppressed (except for $\mathcal{O}_{\kappa_\Phi}$ with $(\kappa_\Phi)_{ij} \propto (Z_\Phi)_{ij}$). The scales of M_A and other supersymmetry breaking masses are of the same order for $\langle X\rangle \approx g_A^2 M/16\pi^2$. We here assume that these are the case.

unification, e.g. $M \gtrsim M_{\rm unif}$, while the scale of flavor physics, M_F, can be much lower as long as the mechanism generating the Yukawa structure does not introduce large relative running between the standard model gauge couplings. In these models, the scale of flavor physics can be as low as 10 – 100 TeV.

4.4 Superparticle Spectra and Low Energy Constraints

In the previous section we have presented three classes of theories in which $\mathcal{O}_{\zeta_f}$ are naturally suppressed. This, however, is not sufficient to avoid all the flavor and CP constraints while keeping superparticles light. The constraints from general left-right sfermion propagation discussed in section 4.2.4, as well as those from left-left and right-right sfermion propagation, must still be addressed. The strongest constraints on left-left and right-right sfermion propagation arise from ϵ_K and the $\mu \to e\gamma$ process, giving

$$\begin{aligned}
\sqrt{|{\rm Im}(\delta^d_{LL/RR})^2_{12}|} &\lesssim 1 \times 10^{-2} \left(\frac{m_{\rm C}}{600\ {\rm GeV}}\right), \\
\sqrt{|{\rm Im}(\delta^d_{LL})_{12}(\delta^d_{RR})_{12}|} &\lesssim 2 \times 10^{-4} \left(\frac{m_{\rm C}}{600\ {\rm GeV}}\right),
\end{aligned} \tag{4.43}$$

$$\begin{aligned}
|(\delta^e_{LL})_{12}| &\lesssim 6 \times 10^{-4} \frac{10}{\tan\beta} \left(\frac{m_{\rm N}}{200\ {\rm GeV}}\right)^2, \\
|(\delta^e_{RR})_{12}| &\lesssim 3 \times 10^{-3} \frac{10}{\tan\beta} \left(\frac{m_{\rm N}}{200\ {\rm GeV}}\right)^2.
\end{aligned} \tag{4.44}$$

Here, the bounds are obtained conservatively by scanning the ratios of the superparticle masses in the same range as that leading to Eqs. (4.23 – 4.26) (see e.g. [20]).[11] The bounds from ϵ_K are obtained from the conservative requirement that the supersymmetric contribution does not exceed the experimental value of $|\epsilon_{K,{\rm exp}}| \simeq 2.23 \times 10^{-3}$ [115]. The $\mu \to e\gamma$ process also leads to the bounds on $|(\delta^\nu_{LL})_{ij}|$, which provide similar constraints on the parameters as the bound on $|(\delta^e_{LL})_{12}|$ in factorized flavor theories considered below.

In this section we perform general analyses on flavor and CP constraints in the classes of theories discussed in section 4.3, assuming that the Yukawa structure coefficients $\mathcal{E}^f_{ij}$ factorize. This is possible because the supersymmetry breaking parameters follow a definite pattern in each class of theories, which, up to $O(1)$ coefficients, is described by a few free parameters.

4.4.1 Factorized flavor structure

In many of the theories discussed in section 4.3, the Yukawa structure coefficients $\mathcal{E}^f_{ij}$ take a factorized form: $\mathcal{E}^u_{ij} = \epsilon_{Q_i}\epsilon_{U_j}$, $\mathcal{E}^d_{ij} = \epsilon_{Q_i}\epsilon_{D_j}$ and $\mathcal{E}^e_{ij} = \epsilon_{L_i}\epsilon_{E_j}$, where $\epsilon_{\Phi_1} \le \epsilon_{\Phi_2} \le \epsilon_{\Phi_3}$

[11] Here, we have also scanned the region $0.3\,\alpha_1/\alpha_2 \lesssim M_1^2/M_2^2 \lesssim 3\,\alpha_1/\alpha_2$ and $1 \lesssim \mu^2/m_{\rm N}^2 \lesssim 16$, and required that 10% of the region evades the experimental constraints. If we change these conditions, the bounds would change by a factor of a few, but our conclusions would be unaffected.

without loss of generality. The Yukawa couplings, Eq. (4.18), are then given by

$$(y_u)_{ij} \approx \tilde{y}\,\epsilon_{Q_i}\epsilon_{U_j}, \qquad (y_d)_{ij} \approx \tilde{y}\,\epsilon_{Q_i}\epsilon_{D_j}, \qquad (y_e)_{ij} \approx \tilde{y}\,\epsilon_{L_i}\epsilon_{E_j}. \tag{4.45}$$

In fact, this factorization generically appears in models with Abelian flavor symmetries and those with extra dimensions. Models with non-Abelian symmetries may also obey this, for example, if the $SU(3)_\Phi$ symmetry is broken by three spurions, $\approx (0, 0, \epsilon_{\Phi_3})$, $(0, \epsilon_{\Phi_2}, \epsilon_{\Phi_2})$, and $(\epsilon_{\Phi_1}, \epsilon_{\Phi_1}, \epsilon_{\Phi_1})$ for each $\Phi = Q, U, D, L, E$. The Yukawa couplings of Eq. (4.45) lead to the following quark and lepton masses and mixings

$$\begin{array}{lcl} (m_t, m_c, m_u) & \approx & \tilde{y}\,\langle H_u\rangle\,(\epsilon_{Q_3}\epsilon_{U_3},\ \epsilon_{Q_2}\epsilon_{U_2},\ \epsilon_{Q_1}\epsilon_{U_1}), \\ (m_b, m_s, m_d) & \approx & \tilde{y}\,\langle H_d\rangle\,(\epsilon_{Q_3}\epsilon_{D_3},\ \epsilon_{Q_2}\epsilon_{D_2},\ \epsilon_{Q_1}\epsilon_{D_1}), \\ (m_\tau, m_\mu, m_e) & \approx & \tilde{y}\,\langle H_d\rangle\,(\epsilon_{L_3}\epsilon_{E_3},\ \epsilon_{L_2}\epsilon_{E_2},\ \epsilon_{L_1}\epsilon_{E_1}), \\ (m_{\nu_\tau}, m_{\nu_\mu}, m_{\nu_e}) & \approx & \frac{\tilde{y}^2\langle H_u\rangle^2}{M_N}\,(\epsilon_{L_3}^2,\ \epsilon_{L_2}^2,\ \epsilon_{L_1}^2), \end{array} \tag{4.46}$$

and

$$V_{\rm CKM} \approx \begin{pmatrix} 1 & \epsilon_{Q_1}/\epsilon_{Q_2} & \epsilon_{Q_1}/\epsilon_{Q_3} \\ \epsilon_{Q_1}/\epsilon_{Q_2} & 1 & \epsilon_{Q_2}/\epsilon_{Q_3} \\ \epsilon_{Q_1}/\epsilon_{Q_3} & \epsilon_{Q_2}/\epsilon_{Q_3} & 1 \end{pmatrix},$$
$$V_{\rm MNS} \approx \begin{pmatrix} 1 & \epsilon_{L_1}/\epsilon_{L_2} & \epsilon_{L_1}/\epsilon_{L_3} \\ \epsilon_{L_1}/\epsilon_{L_2} & 1 & \epsilon_{L_2}/\epsilon_{L_3} \\ \epsilon_{L_1}/\epsilon_{L_3} & \epsilon_{L_2}/\epsilon_{L_3} & 1 \end{pmatrix}, \tag{4.47}$$

where we have included the neutrino masses through the seesaw mechanism with the right-handed neutrino Majorana masses $W \approx M_N \epsilon_{N_i}\epsilon_{N_j} N_i N_j$, and $V_{\rm CKM}$ and $V_{\rm MNS}$ are the quark and lepton mixing matrices, respectively.

The values of the ϵ parameters are constrained by the observed quark and lepton masses and mixings through Eqs. (4.46, 4.47). They may also be constrained by possible grand unification. In the analysis of this section we use the following values for ϵ_{Φ_i}, inferred from the quark and lepton masses and mixing run up to the unification scale [116]:

$$\begin{array}{lll} \epsilon_{Q_1} \approx 0.003\,\tilde{y}^{-\frac{1}{2}}\alpha_q, & \epsilon_{U_1} \approx 0.001\,\tilde{y}^{-\frac{1}{2}}\alpha_q^{-1}, & \epsilon_{D_1} \approx 0.002\,\tilde{y}^{-\frac{1}{2}}\alpha_q^{-1}\tan\beta, \\ \epsilon_{Q_2} \approx 0.03\,\tilde{y}^{-\frac{1}{2}}\alpha_q, & \epsilon_{U_2} \approx 0.04\,\tilde{y}^{-\frac{1}{2}}\alpha_q^{-1}, & \epsilon_{D_2} \approx 0.004\,\tilde{y}^{-\frac{1}{2}}\alpha_q^{-1}\tan\beta, \\ \epsilon_{Q_3} \approx 0.7\,\tilde{y}^{-\frac{1}{2}}\alpha_q, & \epsilon_{U_3} \approx 0.7\,\tilde{y}^{-\frac{1}{2}}\alpha_q^{-1}, & \epsilon_{D_3} \approx 0.01\,\tilde{y}^{-\frac{1}{2}}\alpha_q^{-1}\tan\beta, \end{array} \tag{4.48}$$

$$\begin{array}{ll} \epsilon_{L_1} \approx 0.002\,\tilde{y}^{-\frac{1}{2}}\alpha_l\,\tan\beta, & \epsilon_{E_1} \approx 0.001\,\tilde{y}^{-\frac{1}{2}}\alpha_l^{-1}, \\ \epsilon_{L_2} \approx 0.008\,\tilde{y}^{-\frac{1}{2}}\alpha_l\,\tan\beta, & \epsilon_{E_2} \approx 0.04\,\tilde{y}^{-\frac{1}{2}}\alpha_l^{-1}, \\ \epsilon_{L_3} \approx 0.01\,\tilde{y}^{-\frac{1}{2}}\alpha_l\,\tan\beta, & \epsilon_{E_3} \approx 0.7\,\tilde{y}^{-\frac{1}{2}}\alpha_l^{-1}, \end{array} \tag{4.49}$$

where $\alpha_{q,l}$ are numbers parameterizing the freedoms unfixed by the data. We have chosen $\alpha_{q,l}$ so that $SU(5)$ grand unified relations, $\epsilon_{Q_i} = \epsilon_{U_i} = \epsilon_{E_i}$ and $\epsilon_{D_i} = \epsilon_{L_i}$, are almost satisfied with $\alpha_q = \alpha_l = 1$. Note that the precise numbers in Eqs. (4.48, 4.49) are not very important because of unknown $O(1)$ coefficients in the expressions of the quark and lepton masses and

mixings as well as the bounds from low energy flavor and CP violation. In addition, while we have used the data at $M_F \simeq M_{\rm unif}$, using a lower value of M_F would not qualitatively change the results, as it would only change the numbers in Eqs. (4.48, 4.49) by additional $O(1)$ factors.

4.4.2 Higgsphobic supersymmetry breaking

Higgsphobic supersymmetry breaking theories discussed in section 4.3.2 give the following pattern for the flavor supersymmetry breaking parameters at M_F:

$$(m_\Phi^2)_{ij} \approx \{\epsilon_{\Phi_i}\epsilon_{\Phi_j} + (\eta_\Phi^\dagger \eta_\Phi)_{ij} + \Delta_{ij}^\Phi\}\, m_{\rm S}^2, \tag{4.50}$$

$$(a_f)_{ij} \approx \{(y_f)_{kj}(\eta_{\Phi_L})_{ki} + (y_f)_{ik}(\eta_{\Phi_R})_{kj}\}\, m_{\rm S}, \tag{4.51}$$

where we have suppressed flavor universal contributions as well as a possible difference between the colored and non-colored superparticle mass scales. Here, $m_{\rm S}$ is the characteristic scale for supersymmetry breaking parameters, $(\eta_\Phi)_{ij} \approx \epsilon_{\Phi_i}\epsilon_{\Phi_j}$ are complex 3×3 matrices, and Δ_{ij}^Φ parameterize flavor violating effects arising from bulk loops in higher dimensional theories discussed in section 4.3.2. In flat space models, we typically find $\Delta_{ii}^\Phi \lesssim g^2/16\pi^2 \approx O(10^{-2})$ because they arise from bulk gauge loops, where g represents the standard model gauge couplings. The off-diagonal components are smaller, $\Delta_{ij}^\Phi (i \neq j) \ll \Delta_{ii}^\Phi$, since they arise through brane-localized terms which are volume suppressed. On the other hand, in warped space models where H and X are in the infrared region, we expect $\Delta_{ij}^\Phi \lesssim \epsilon_{\Phi_i}\epsilon_{\Phi_j}$, since in the dual 4D picture any couplings of a matter field to H and X, including flavor violating loops in higher dimensions, are controlled by the anomalous dimension of the corresponding strong dynamics operator, which provides a factor ϵ_{Φ_i} for each Φ_i.[12]

The pattern of Eqs. (4.50, 4.51) is essentially the one discussed in Ref. [15] (for $\Delta_{ij}^\Phi \lesssim \epsilon_{\Phi_i}\epsilon_{\Phi_j}$). The left-left and right-right mass insertion parameters generated by Eq. (4.50) are

$$(\delta_{LL}^u)_{ij} \approx \left\{(1+\epsilon_{Q_3}^2)\epsilon_{Q_i}\epsilon_{Q_j} + (\Delta_i^Q - \Delta_j^Q)\frac{\epsilon_{Q_i}}{\epsilon_{Q_j}}\right\}\frac{m_{\rm S}^2}{m_{\rm C}^2}, \quad (\delta_{RR}^u)_{ij} \approx (\delta_{LL}^u)_{ij}\Big|_{Q\to U}, \tag{4.52}$$

$$(\delta_{LL}^d)_{ij} \approx \left\{(1+\epsilon_{Q_3}^2)\epsilon_{Q_i}\epsilon_{Q_j} + (\Delta_i^Q - \Delta_j^Q)\frac{\epsilon_{Q_i}}{\epsilon_{Q_j}}\right\}\frac{m_{\rm S}^2}{m_{\rm C}^2}, \quad (\delta_{RR}^d)_{ij} \approx (\delta_{LL}^d)_{ij}\Big|_{Q\to D}, \tag{4.53}$$

$$(\delta_{LL}^e)_{ij} \approx \left\{(1+\epsilon_{L_3}^2)\epsilon_{L_i}\epsilon_{L_j} + (\Delta_i^L - \Delta_j^L)\frac{\epsilon_{L_i}}{\epsilon_{L_j}}\right\}\frac{m_{\rm S}^2}{m_{\rm N}^2}, \quad (\delta_{RR}^e)_{ij} \approx (\delta_{LL}^e)_{ij}\Big|_{L\to E}, \tag{4.54}$$

for $i < j$, and $(\delta_{LL}^f)_{ij} \approx (\delta_{LL}^f)_{ji}$ and $(\delta_{RR}^f)_{ij} \approx (\delta_{RR}^f)_{ji}$. Here, we have retained only the diagonal components of Δ_{ij}^Φ, $\Delta_i^\Phi \equiv \Delta_{ii}^\Phi$, which is justified in most models, as discussed

[12] In these warped space models, the gaugino masses M_A are likely to be somewhat suppressed compared with $m_{\rm S}$, and a flavor universal contribution to the scalar squared masses at M_F, $\delta m_\Phi^2|_{\rm univ} \lesssim M_A^2$, is also expected. Using naive dimensional analysis in the dual 4D picture, we find $M_A \approx g_A^2 (N/16\pi^2)^{3/4} m_{\rm S}/\tilde{y}^{1/2}$, where N is the size of the strongly coupled sector yielding H and X. This does not significantly affect the analysis below in some parameter region, although the top squarks may be somewhat heavy in these theories.

above. The left-right mass insertion parameters given by Eq. (4.51) are

$$(\delta^u_{LR})_{ij} = (\delta^u_{RL})^*_{ji} \approx \epsilon_{Q_i}\epsilon_{U_j}(\epsilon^2_{Q_j} + \epsilon^2_{U_i})\frac{v\sin\beta}{m_{\rm C}}, \tag{4.55}$$

$$(\delta^d_{LR})_{ij} = (\delta^d_{RL})^*_{ji} \approx \epsilon_{Q_i}\epsilon_{D_j}(\epsilon^2_{Q_j} + \epsilon^2_{D_i})\frac{v\cos\beta}{m_{\rm C}}, \tag{4.56}$$

$$(\delta^e_{LR})_{ij} = (\delta^e_{RL})^*_{ji} \approx \epsilon_{L_i}\epsilon_{E_j}(\epsilon^2_{L_j} + \epsilon^2_{E_i})\frac{v\cos\beta}{m_{\rm N}}, \tag{4.57}$$

where we have assumed that the renormalization group effect makes $m_{\rm S} \to m_{\rm C}$ and $m_{\rm N}$ in the scalar trilinear interactions for colored and non-colored superparticles, respectively. Note that we have suppressed all the subleading terms as well as $O(1)$ coefficients in Eqs. (4.52 – 4.57).

One finds that $(\delta^f_{LR})_{ij}$ in Eqs. (4.55 – 4.57) are typically much smaller than those in Eq. (4.21) with $a_{\rm C,N} \approx m_{\rm C,N}$ for $i,j = 1,2$, so that the left-right flavor violation caused by this source is small. For the multiple mass insertion diagrams discussed in section 4.2.4, we find that the effective mass insertion parameters of Eq. (4.39) for $i,j = 1,2$ are given in terms of

$$\begin{aligned} d^f_{ij} \;\approx\; \max\Bigg\{ & (\epsilon^2_{\Phi_{Lj}} + \epsilon^2_{\Phi_{R3}})\hat\Delta^{\Phi_L}_{i3}\frac{c_d m_{\rm S}^2}{m^2_{\rm C,N}},\;\; (\epsilon^2_{\Phi_{L3}} + \epsilon^2_{\Phi_{Ri}})\hat\Delta^{\Phi_R}_{3j}\frac{c_d m_{\rm S}^2}{m^2_{\rm C,N}}, \\ & \hat\Delta^{\Phi_L}_{i3}\hat\Delta^{\Phi_R}_{3j}\frac{c_t\tilde y\, m_{\rm C} m_{\rm S}^4\, t}{m^5_{\rm C,N}},\;\; (\epsilon^2_{\Phi_{L3}} + \epsilon^2_{\Phi_{Ri}})(\epsilon^2_{\Phi_{Lj}} + \epsilon^2_{\Phi_{R3}})\epsilon^2_{\Phi_{L3}}\epsilon^2_{\Phi_{R3}}\frac{c_t\tilde y\, v^2 m_{\rm C}}{m^3_{\rm C,N}\, t}\Bigg\}, \end{aligned} \tag{4.58}$$

as

$$(\delta^f_{LR,\rm eff})_{ij} \approx \epsilon_{\Phi_{Li}}\epsilon_{\Phi_{Rj}}\frac{v}{m_{\rm C,N}\, t}\max\left\{ d^f_{ij},\;\; \hat\Delta^{\Phi_L}_{ij}\frac{c_d\tilde y\, m_{\rm C} m_{\rm S}^2\, t}{m^3_{\rm C,N}},\;\; \hat\Delta^{\Phi_R}_{ij}\frac{c_d\tilde y\, m_{\rm C} m_{\rm S}^2\, t}{m^3_{\rm C,N}}\right\}, \quad (i \neq j), \tag{4.59}$$

and

$$(\delta^f_{LR,\rm eff})_{ii} \approx \epsilon_{\Phi_{Li}}\epsilon_{\Phi_{Ri}}\frac{v}{m_{\rm C,N}\, t}\, d^f_{ii}. \tag{4.60}$$

Here,

$$\hat\Delta^{\Phi_L}_{ij} \;\equiv\; (\Delta^{\Phi_L}_i - \Delta^{\Phi_L}_j)\,\theta_L + \epsilon^2_{\Phi_{Lj}}, \qquad \theta_L = \begin{cases} 1 & \text{for } i<j \\ \epsilon^2_{\Phi_{Lj}}/\epsilon^2_{\Phi_{Li}} & \text{for } i>j \end{cases}, \tag{4.61}$$

$$\hat\Delta^{\Phi_R}_{ij} \;\equiv\; (\Delta^{\Phi_R}_i - \Delta^{\Phi_R}_j)\,\theta_R + \epsilon^2_{\Phi_{Ri}}, \qquad \theta_R = \begin{cases} \epsilon^2_{\Phi_{Ri}}/\epsilon^2_{\Phi_{Rj}} & \text{for } i<j \\ 1 & \text{for } i>j \end{cases}, \tag{4.62}$$

$(\Phi_L, \Phi_R, m_{\rm C,N}, t) = (Q, U, m_{\rm C}, 1), (Q, D, m_{\rm C}, \tan\beta), (L, E, m_{\rm N}, \tan\beta)$ for $f = u, d, e$, and we have assumed $\epsilon_{\Phi_1} \lesssim \epsilon_{\Phi_2} \lesssim \epsilon_{\Phi_3} \lesssim O(1)$, $\tan\beta \gtrsim O(1)$, and $\mu \approx m_{\rm C}$. The values of $(\delta^f_{LR,\rm eff})_{ij}$ above should be compared with the "naive" $(\delta^f_{LR})_{ij}$ in Eq. (4.21) with $a_{\rm C,N} \approx m_{\rm C,N}$:

$$(\delta^f_{LR,\rm naive})_{ij} \approx \epsilon_{\Phi_{Li}}\epsilon_{\Phi_{Ri}}\frac{v}{m_{\rm C,N}\, t}. \tag{4.63}$$

Using Eqs. (4.48, 4.49) and $\Delta_i^\Phi \lesssim \max\{g^2/16\pi^2, \epsilon_{\Phi_i}^2\}$, and neglecting contributions sufficiently smaller than $(\delta^f_{LR,\mathrm{naive}})_{ij}$, the expressions of Eqs. (4.59, 4.60) for moderate $\tan\beta \approx O(10)$ and $\tilde{y} \approx O(1)$ become

$$(\delta^f_{LR,\mathrm{eff}})_{ij} \approx (\delta^f_{LR,\mathrm{naive}})_{ij} \max\left\{(y_f)^2_{33}\frac{c_d m_{\mathrm{S}}^2}{\tilde{y}^2 m^2_{\mathrm{C,N}}},\ \ (y_f)^2_{33}\frac{c_t m_{\mathrm{C}} m_{\mathrm{S}}^4\, t}{\tilde{y}\, m^5_{\mathrm{C,N}}},\ \ (y_f)^4_{33}\frac{c_t v^2 m_{\mathrm{C}}}{\tilde{y}^3 m^3_{\mathrm{C,N}}\, t}\right\}. \tag{4.64}$$

(For larger $\tilde{y}$, we have additional potentially relevant contributions of order $\Delta^\Phi_{ij} c_d \tilde{y}\, m_{\mathrm{C}} m_{\mathrm{S}}^2 t/m^3_{\mathrm{C,N}}$ inside the curly brackets.) From this, we find that $(\delta^f_{LR,\mathrm{eff}})_{ij}$ can in fact be smaller than $(\delta^f_{LR,\mathrm{naive}})_{ij}$, so that the supersymmetric left-right flavor problem can be solved. Natural values of $(\delta^f_{LR,\mathrm{eff}})_{ij}$ inferred from Eq. (4.64), however, are not very much smaller than $(\delta^f_{LR,\mathrm{naive}})_{ij}$ (typically no more than an order of magnitude for $f = e$), so we can still expect positive signatures in future search on flavor and CP violation, e.g. in EDM experiments, in this class of theories. For larger $\tan\beta$, it becomes increasingly difficult to obtain $(\delta^f_{LR,\mathrm{eff}})_{ij} \ll (\delta^f_{LR,\mathrm{naive}})_{ij}$, so that very large $\tan\beta$, e.g. $\tan\beta \gtrsim 30$, is disfavored.

We now consider constraints from left-left and right-right sfermion propagation. Using Eqs. (4.48, 4.49) in Eqs. (4.53, 4.54), the bounds of Eqs. (4.43, 4.44) give

$$(\Delta_1^Q - \Delta_2^Q) + 9\times 10^{-4}\,\frac{\alpha_q^2}{\tilde{y}} \ \lesssim\ 0.1\left(\frac{m_{\mathrm{C}}}{600\ \mathrm{GeV}}\right)\frac{m_{\mathrm{C}}^2}{m_{\mathrm{S}}^2}, \tag{4.65}$$

$$(\Delta_1^D - \Delta_2^D) + 2\times 10^{-5}\,\frac{\tan^2\beta}{\tilde{y}\,\alpha_q^2} \ \lesssim\ 2\times 10^{-2}\left(\frac{m_{\mathrm{C}}}{600\ \mathrm{GeV}}\right)\frac{m_{\mathrm{C}}^2}{m_{\mathrm{S}}^2}, \tag{4.66}$$

$$\left\{(\Delta_1^Q - \Delta_2^Q) + 9\times 10^{-4}\,\frac{\alpha_q^2}{\tilde{y}}\right\}^{1/2}\left\{(\Delta_1^D - \Delta_2^D) + 2\times 10^{-5}\,\frac{\tan^2\beta}{\tilde{y}\,\alpha_q^2}\right\}^{1/2} \lesssim 9\times 10^{-4}\left(\frac{m_{\mathrm{C}}}{600\ \mathrm{GeV}}\right)\frac{m_{\mathrm{C}}^2}{m_{\mathrm{S}}^2}, \tag{4.67}$$

$$(\Delta_1^L - \Delta_2^L) + 6\times 10^{-5}\,\frac{\alpha_l^2\tan^2\beta}{\tilde{y}} \ \lesssim\ 2\times 10^{-3}\frac{10}{\tan\beta}\left(\frac{m_{\mathrm{N}}}{200\ \mathrm{GeV}}\right)^2\frac{m_{\mathrm{N}}^2}{m_{\mathrm{S}}^2}, \tag{4.68}$$

$$(\Delta_1^E - \Delta_2^E) + 2\times 10^{-3}\,\frac{1}{\tilde{y}\,\alpha_l^2} \ \lesssim\ 0.1\,\frac{10}{\tan\beta}\left(\frac{m_{\mathrm{N}}}{200\ \mathrm{GeV}}\right)^2\frac{m_{\mathrm{N}}^2}{m_{\mathrm{S}}^2}, \tag{4.69}$$

where we have assumed $\epsilon_{\Phi_3} \lesssim O(1)$. While there is an $O(1)$ coefficient omitted in front of each term, we still find some tension in Eqs. (4.66, 4.67, 4.68). For $m_{\mathrm{S}} \approx m_{\mathrm{N}} \approx m_{\mathrm{C}}/(2-4)$, for example, these bounds require

$$\frac{1}{\tilde{y}\,\alpha_q^2} \ \lesssim\ 10^2\left(\frac{10}{\tan\beta}\right)^2\left(\frac{m_{\mathrm{C}}}{600\ \mathrm{GeV}}\right), \tag{4.70}$$

$$(\Delta_1^Q - \Delta_2^Q)^{1/2} \left\{ (\Delta_1^D - \Delta_2^D) + 2 \times 10^{-5} \frac{\tan^2\beta}{\tilde{y}\, \alpha_q^2} \right\}^{1/2} \lesssim 10^{-2} \left(\frac{m_{\rm C}}{600\ {\rm GeV}} \right), \tag{4.71}$$

$$(\Delta_1^L - \Delta_2^L) + 6 \times 10^{-5} \frac{\alpha_l^2 \tan^2\beta}{\tilde{y}} \lesssim 10^{-3} \frac{10}{\tan\beta} \left(\frac{m_{\rm N}}{200\ {\rm GeV}} \right)^2, \tag{4.72}$$

at the order of magnitude level. The conditions of Eqs. (4.70, 4.71) are satisfied in a wide parameter region, while the condition of Eq. (4.72) requires

$$(\Delta_1^L - \Delta_2^L) \lesssim 10^{-3} \frac{10}{\tan\beta} \left(\frac{m_{\rm N}}{200\ {\rm GeV}} \right)^2, \qquad \frac{\alpha_l^2}{\tilde{y}} \lesssim 0.1 \left(\frac{10}{\tan\beta} \right)^3 \left(\frac{m_{\rm N}}{200\ {\rm GeV}} \right)^2, \tag{4.73}$$

unless there is a strong cancellation. The first inequality leads to a tension in theories with $\Delta_i^\Phi \approx g^2/16\pi^2 \approx O(10^{-2})$, although it can be ameliorated by taking somewhat large $m_{\rm N}$, e.g. $m_{\rm N} \gtrsim 600\ {\rm GeV} (\tan\beta/10)^{1/2}$ or smaller $\tan\beta$. On the other hand, theories with $\Delta_i^\Phi \approx \epsilon_{\Phi_i}^2$ have little tension, and taking somewhat small α_l is enough to avoid the bounds. Note that very large $\tan\beta$ is, again, disfavored.

Finally, we discuss implications on the superparticle spectrum. The intergenerational mass splittings between the sfermions are controlled by Eq. (4.50), leading to

$$|m_{\Phi_i}^2 - m_{\Phi_j}^2| \approx m_{\rm S}^2\ \max\{\Delta_{i,j}^\Phi, \epsilon_{\Phi_{i,j}}^2\}. \tag{4.74}$$

In particular, this gives

$$|m_{\tilde{\tau}_R}^2 - m_{\tilde{\mu}_R}^2| \approx m_{\rm S}^2\ \max\{\Delta_2^E, \Delta_3^E, \epsilon_{E_3}^2\}, \tag{4.75}$$

$$|m_{\tilde{\tau}_R}^2 - m_{\tilde{e}_R}^2| \approx m_{\rm S}^2\ \max\{\Delta_1^E, \Delta_3^E, \epsilon_{E_3}^2\}, \tag{4.76}$$

$$|m_{\tilde{\mu}_R}^2 - m_{\tilde{e}_R}^2| \approx m_{\rm S}^2\ \max\{\Delta_1^E, \Delta_2^E, \epsilon_{E_2}^2\}, \tag{4.77}$$

which can lead to $O(1)$ fractional mass splittings between $\tilde{\tau}_R$ and $\tilde{e}_R, \tilde{\mu}_R$, and $O(10^{-3}$–$10^{-2})$ fractional mass splitting between $\tilde{\mu}_R$ and $\tilde{e}_R$. The signs of the splittings are arbitrary, so that, for example, $\tilde{\tau}_R$ can be heavier than $\tilde{e}_R, \tilde{\mu}_R$. Similar levels of intergenerational mass splittings are also possible for other sfermions, although for squarks, splittings will be somewhat diluted by large flavor universal renormalization effects by a factor of order $m_{\rm S}^2/m_{\rm C}^2$.

4.4.3 Remote flavor-supersymmetry breaking

The remote flavor-supersymmetry breaking scenario discussed in section 4.3.3 can give a variety of patterns for the supersymmetry breaking parameters, depending on $G_{\rm flavor}$ and its breaking. In general, $G_{\rm flavor}$ can be a product of a "3 generation," "2 generation," or "single generation" symmetry acting on each $\Phi = Q, U, D, L, E$. The first class corresponds to (a sufficiently large subgroup of) $SU(3)$ acting on three generations (Φ_1, Φ_2, Φ_3), the second to (a sufficiently large subgroup of) $SU(2)$ acting on the first two generations (Φ_1, Φ_2), and the third to products of $U(1)$ symmetries.

In the limit of unbroken $G_{\rm flavor}$, the coefficients of the matter supersymmetry breaking operators are given by

$$(\kappa_\Phi)_{ij} \approx \delta_{ij}\kappa_i^\Phi, \qquad (\eta_\Phi)_{ij} \approx \delta_{ij}\eta_i^\Phi, \tag{4.78}$$

in the field basis where $(Z_\Phi)_{ij} = \delta_{ij}$. Here, depending on the component of $G_{\rm flavor}$ acting on Φ_i, the parameters κ_i^Φ and η_i^Φ exhibit the following pattern:

$$\kappa_1^\Phi = \kappa_2^\Phi = \kappa_3^\Phi, \qquad \eta_1^\Phi = \eta_2^\Phi = \eta_3^\Phi, \qquad \text{for "3 generation" symmetry,} \tag{4.79}$$

$$\kappa_1^\Phi = \kappa_2^\Phi \neq \kappa_3^\Phi, \qquad \eta_1^\Phi = \eta_2^\Phi \neq \eta_3^\Phi, \qquad \text{for "2 generation" symmetry,} \tag{4.80}$$

$$\kappa_1^\Phi \neq \kappa_2^\Phi \neq \kappa_3^\Phi, \qquad \eta_1^\Phi \neq \eta_2^\Phi \neq \eta_3^\Phi, \qquad \text{for "single generation" symmetry.} \tag{4.81}$$

In any of these theories, our framework provides a solution to the superpotential problem. To see if all the constraints are avoided, we also need to study effects coming from $G_{\rm flavor}$ violation.

We now focus on the case where $G_{\rm flavor}$ contains a "3 generation" symmetry for each $\Phi = Q, U, D, L, E$, e.g. $G_{\rm flavor} = SU(3)^5$. We also assume that $G_{\rm flavor}$ is broken by three spurions, $\approx (0, 0, \epsilon_{\Phi_3})$, $(0, \epsilon_{\Phi_2}, \epsilon_{\Phi_2})$, and $(\epsilon_{\Phi_1}, \epsilon_{\Phi_1}, \epsilon_{\Phi_1})$ for each $\Phi = Q, U, D, L, E$, which guarantees that $\mathcal{E}_{ij}^f$ take a factorized form. The operator coefficients at M_F in the field basis that naturally realizes $G_{\rm flavor}$ are then given by

$$(Z_\Phi)_{ij} \approx \delta_{ij} + \gamma\, \epsilon_{\Phi_i}\epsilon_{\Phi_j}, \qquad (\kappa_\Phi)_{ij} \approx \delta_{ij} + (D\text{-term}), \qquad (\eta_\Phi)_{ij} \approx \delta_{ij}, \tag{4.82}$$

where we have omitted $O(1)$ coefficients that appear in each (i, j)-element of the second term of $(Z_\Phi)_{ij}$, in front of the first term of $(\kappa_\Phi)_{ij}$, and in front of the expression for $(\eta_\Phi)_{ij}$. Here, γ parameterizes the strength of the $G_{\rm flavor}$ breaking effect, which is suppressed by the volume of the extra dimensions in a higher dimensional realization of the scenario. (If the matter fields have nontrivial wavefunctions and/or $G_{\rm flavor}$ is broken on several different branes, γ can depend on Φ, i, j.) The second term of $(\kappa_\Phi)_{ij}$, denoted as D-term, arises if $G_{\rm flavor}$ contains a continuous gauge symmetry component (for $M_F \lesssim M$), but it is absent if $G_{\rm flavor}$ is a global or discrete symmetry.

After canonically normalizing fields, $(Z_\Phi)_{ij} = \delta_{ij}$, Eq. (4.82) leads to the following operator coefficients:

$$(\kappa_\Phi)_{ij} \approx \delta_{ij}(1 + \gamma\epsilon_{\Phi_i}^2 + \Delta_i^\Phi), \qquad (\eta_\Phi)_{ij} \approx \delta_{ij}(1 + \gamma\epsilon_{\Phi_i}^2), \tag{4.83}$$

where we have diagonalized $(Z_\Phi)_{ij}$ of Eq. (4.82) and then rescaled fields so that the $(Z_\Phi)_{ij}$ become δ_{ij}. Here, the third term of $(\kappa_\Phi)_{ij}$ parameterizes the possible D-term contribution (which is always flavor diagonal in this basis). This contribution arises when a continuous gauged $G_{\rm flavor}$ symmetry is broken by the VEVs of fields ϕ_m ($m = 1, 2, \cdots$) which have supersymmetry breaking masses [117]. For example, if $G_{\rm flavor}$ is broken by ϕ_1 and ϕ_2 whose transformation properties under $G_{\rm flavor}$ is opposite, a D-term contribution of order $m_{\phi_1}^2 - m_{\phi_2}^2$ generically arises, where $m_{\phi_m}^2$ represents the supersymmetry breaking mass squared of ϕ_m. While the D-term contribution is generically dangerous in theories with a gauged

flavor symmetry, in the present framework the supersymmetry breaking masses of ϕ_m are suppressed because of the separation between $G_{\rm flavor}$ and supersymmetry breaking, so that the resulting D-term contribution Δ_i^Φ is also suppressed. (This was observed in Ref. [118] in theories with $G_{\rm flavor} = U(1)$.) The contribution is typically suppressed by a loop factor, as well as by powers of the ratio of the compactification scale, M_c, to the (effective) cutoff scale, M_*, in theories with extra dimensions. We therefore expect $\Delta_i^\Phi \approx (M_c/M_*)^n/16\pi^2 \lesssim O(10^{-2})$, where n is a model-dependent integer which can in general depend on Φ and i.[13]

Note that in the field basis leading to Eq. (4.83) the Yukawa couplings are still given by Eq. (4.45). The left-left and right-right mass insertion parameters are then given by

$$(\delta^u_{LL})_{ij} \approx \left\{\gamma(1+\gamma\epsilon^2_{Q_3})\epsilon_{Q_i}\epsilon_{Q_j} + (\Delta^Q_i - \Delta^Q_j)\frac{\epsilon_{Q_i}}{\epsilon_{Q_j}}\right\}\frac{m_{\rm S}^2}{m_{\rm C}^2}, \quad (\delta^u_{RR})_{ij} \approx (\delta^u_{LL})_{ij}\Big|_{Q\to U}, \tag{4.84}$$

$$(\delta^d_{LL})_{ij} \approx \left\{\gamma(1+\gamma\epsilon^2_{Q_3})\epsilon_{Q_i}\epsilon_{Q_j} + (\Delta^Q_i - \Delta^Q_j)\frac{\epsilon_{Q_i}}{\epsilon_{Q_j}}\right\}\frac{m_{\rm S}^2}{m_{\rm C}^2}, \quad (\delta^d_{RR})_{ij} \approx (\delta^d_{LL})_{ij}\Big|_{Q\to D}, \tag{4.85}$$

$$(\delta^e_{LL})_{ij} \approx \left\{\gamma(1+\gamma\epsilon^2_{L_3})\epsilon_{L_i}\epsilon_{L_j} + (\Delta^L_i - \Delta^L_j)\frac{\epsilon_{L_i}}{\epsilon_{L_j}}\right\}\frac{m_{\rm S}^2}{m_{\rm N}^2}, \quad (\delta^e_{RR})_{ij} \approx (\delta^e_{LL})_{ij}\Big|_{L\to E}, \tag{4.86}$$

for $i<j$, and $(\delta^f_{LL})_{ij} \approx (\delta^f_{LL})_{ji}$ and $(\delta^f_{RR})_{ij} \approx (\delta^f_{RR})_{ji}$. The flavor and CP violating left-right mass insertion parameters are given by

$$(\delta^u_{LR})_{ij} = (\delta^u_{RL})^*_{ji} \approx \gamma\epsilon_{Q_i}\epsilon_{U_j}(\epsilon^2_{Q_j} + \epsilon^2_{U_i})\frac{v\sin\beta}{m_{\rm C}}, \tag{4.87}$$

$$(\delta^d_{LR})_{ij} = (\delta^d_{RL})^*_{ji} \approx \gamma\epsilon_{Q_i}\epsilon_{D_j}(\epsilon^2_{Q_j} + \epsilon^2_{D_i})\frac{v\cos\beta}{m_{\rm C}}, \tag{4.88}$$

$$(\delta^e_{LR})_{ij} = (\delta^e_{RL})^*_{ji} \approx \gamma\epsilon_{L_i}\epsilon_{E_j}(\epsilon^2_{L_j} + \epsilon^2_{E_i})\frac{v\cos\beta}{m_{\rm N}}. \tag{4.89}$$

We find that the mass insertion parameters of Eqs. (4.84 – 4.89) take the same form as those of Eqs. (4.52 – 4.57) for $\gamma = 1$, although the origins of Δ_i^Φ are different. Since γ is expected to be smaller than 1, the present class of theories is at least as safe as Higgsphobic theories with $\Delta_i^\Phi \approx O(10^{-2})$ from the flavor and CP violation point of view. Moreover, since we expect $\Delta_i^\Phi < O(10^{-2})$ in most cases due to power suppressions of $(M_c/M_*)^n$, the low energy constraints from flavor and CP violation generically give little tension with the LHC observability in the present class of theories.

The intergenerational mass splittings between sfermions have a similar formula to the Higgsphobic case:

$$|m^2_{\Phi_i} - m^2_{\Phi_j}| \approx m_{\rm S}^2 \ \max\{\Delta^\Phi_{i,j}, \gamma\epsilon^2_{\Phi_{i,j}}\}. \tag{4.90}$$

In particular, the right-handed sleptons have the splittings

$$|m^2_{\tilde\tau_R} - m^2_{\tilde\mu_R}| \ \approx \ m_{\rm S}^2 \ \max\{\Delta^E_2, \Delta^E_3, \gamma\epsilon^2_{E_3}\}, \tag{4.91}$$

[13] If different ϕ_m have different renormalizable interactions of order λ, $\Delta_i^\Phi \approx (\lambda^2/16\pi^2)^2(m_{3/2}/m_{\rm S})^2$ can be generated through anomaly mediation. This contribution is typically of order 10^{-4} or smaller.

$$|m^2_{\tilde{\tau}_R} - m^2_{\tilde{e}_R}| \approx m^2_{\rm S} \max\{\Delta^E_1, \Delta^E_3, \gamma\epsilon^2_{E_3}\}, \quad (4.92)$$

$$|m^2_{\tilde{\mu}_R} - m^2_{\tilde{e}_R}| \approx m^2_{\rm S} \max\{\Delta^E_1, \Delta^E_2, \gamma\epsilon^2_{E_2}\}. \quad (4.93)$$

The size of the splittings depends on the details of the theory, specifically the size of Δ^E_i and γ. We expect that the fractional mass splittings between $\tilde{\tau}_R$ and $\tilde{e}_R, \tilde{\mu}_R$ and between $\tilde{\mu}_R$ and $\tilde{e}_R$ are at most of $O(1)$ and $O(10^{-2})$, respectively, and typically smaller by at least a factor of a few because of the suppression by γ and $(M_c/M_*)^n$.

In the above analysis, we have focused on the case that $G_{\rm flavor}$ is the product of five "3 generation" symmetries acting on Q, U, D, L, E. Similar analyses, however, can also be performed in the case where (some of) Q, U, D, L, E have only "2 generation" or "single generation" symmetries. In particular, in the case of a "2 generation" symmetry, we expect that the conclusion on flavor and CP violation does not change because the constraints from the processes involving the third generation particles are weak. The fractional mass splittings between the third and first two generation sfermions in this case are expected to be of $O(1)$, without a suppression from γ or $(M_c/M_*)^n$. In the case of a "single generation" symmetry, model by model analyses are needed. We expect, however, that the model can avoid the constraints if it involves "single generation" symmetries only for some Φ. For example, we can consider only E has a "single generation" symmetry while the rest have "3 generation" symmetries, e.g. $G_{\rm flavor} = SU(3)_Q \times SU(3)_U \times SU(3)_D \times SU(3)_L \times U(1)_E$. In this case the fractional mass splittings between $\tilde{\tau}_R$ and $\tilde{\mu}_R$ and between $\tilde{\mu}_R$ and $\tilde{e}_R$ are of the same order, and presumably of $O(1)$.

4.4.4 Charged supersymmetry breaking

If the supersymmetry breaking field is charged under some symmetry, the operators $\mathcal{O}_{\eta_\Phi}$ are forbidden. In fact, this charged supersymmetry breaking framework can be combined with many flavor theories. To parameterize these wide classes of theories, we somewhat arbitrarily take

$$(\kappa_\Phi)_{ij} \approx \delta_{ij} + \gamma\epsilon_{\Phi_i}\epsilon_{\Phi_j} + \delta_{ij}\Delta^\Phi_i, \qquad (\eta_\Phi)_{ij} = 0, \quad (4.94)$$

at the scale M_F. This parameterization accommodates many theories of flavor, including ones based on extra dimensions, strong dynamics, and "3 generation" flavor symmetries. (In some of these theories, the flavor universal part, i.e. the first term, of $(\kappa_\Phi)_{ij}$ is absent, but this does not affect the analysis of flavor and CP violation.) This parameterization needs to be modified appropriately for other types of theories, for example those based on "2 generation" or "single generation" flavor symmetries.

The left-left and right-right mass insertion parameters generated by Eq. (4.94) are

$$(\delta^u_{LL})_{ij} \approx \left\{\gamma\epsilon_{Q_i}\epsilon_{Q_j} + (\Delta^Q_i - \Delta^Q_j)\frac{\epsilon_{Q_i}}{\epsilon_{Q_j}}\right\}\frac{m^2_{\rm S}}{m^2_{\rm C}}, \qquad (\delta^u_{RR})_{ij} \approx (\delta^u_{LL})_{ij}\Big|_{Q\to U}, \quad (4.95)$$

$$(\delta^d_{LL})_{ij} \approx \left\{\gamma\epsilon_{Q_i}\epsilon_{Q_j} + (\Delta^Q_i - \Delta^Q_j)\frac{\epsilon_{Q_i}}{\epsilon_{Q_j}}\right\}\frac{m^2_{\rm S}}{m^2_{\rm C}}, \qquad (\delta^d_{RR})_{ij} \approx (\delta^d_{LL})_{ij}\Big|_{Q\to D}, \quad (4.96)$$

$$(\delta^e_{LL})_{ij} \approx \left\{ \gamma \epsilon_{L_i} \epsilon_{L_j} + (\Delta^L_i - \Delta^L_j) \frac{\epsilon_{L_i}}{\epsilon_{L_j}} \right\} \frac{m^2_{\rm S}}{m^2_{\rm N}}, \qquad (\delta^e_{RR})_{ij} \approx (\delta^e_{LL})_{ij}\Big|_{L \to E}, \quad (4.97)$$

for $i < j$, and $(\delta^f_{LL})_{ij} \approx (\delta^f_{LL})_{ji}$ and $(\delta^f_{RR})_{ij} \approx (\delta^f_{RR})_{ji}$, while the flavor and CP violating left-right mass insertion parameters are

$$(\delta^f_{LR})_{ij} = (\delta^f_{RL})^*_{ji} \approx 0. \quad (4.98)$$

The constraints from low energy flavor and CP violation are obviously not stronger than in the classes of theories discussed in the previous two subsections for the same values of γ and Δ^Φ_i. Note that while the flavor and CP violating left-right mass insertion parameters are vanishing (up to the higher order effects from the Yukawa couplings), we still have flavor and CP violating effects generated by multiple mass insertion diagrams through the flavor universal part of $(\delta^f_{LR})_{ij}$ and through flavor and CP violating $(\delta^f_{LL,RR})_{ij}$. Nontrivial flavor and CP violation, therefore, can still be discovered in future experiments such as ones in [101, 102, 103, 104, 105, 106, 107, 108, 109].

The intergenerational mass splittings between sfermions are given by the formula in Eq. (4.90). The size of the splittings is controlled by the parameters γ and Δ^Φ_i, which are model dependent. In many models, $\gamma \lesssim O(1)$ and $\Delta^\Phi_i \lesssim O(10^{-2})$. We can, however, still expect that a variety of patterns for the intergenerational mass splittings can be obtained in this framework.

4.5 Probing the Origin of Flavor at the LHC

We have seen that supersymmetry with a flavorful spectrum is consistent with bounds from low energy flavor and CP violating processes in a wide variety of models where the superpotential flavor problem is solved. Furthermore, the spectrum in these models can easily be light enough that it will have a substantial production cross section at the LHC. While it appears that the deviation from flavor universality is small, especially in the first two generations, the splittings are large enough that they can be significant at the LHC. Consider the right-handed sleptons, which from the structure of the SSM renormalization group equations are expected to be the lightest sfermions. If flavor nonuniversality comes only from renormalization group evolution, then the fractional mass splitting between $\tilde{e}_R$ and $\tilde{\mu}_R$ is controlled by the muon Yukawa coupling, and is expected to be of $O(10^{-4})$ for $\tan\beta \approx O(10)$. On the other hand, the analysis in section 4.4 shows that the fractional mass splitting from the contribution at M_F can be easily of $O(10^{-2})$. The splittings between $\tilde{\tau}_R$ and $\tilde{e}_R, \tilde{\mu}_R$ will also be larger than the renormalization group prediction in the moderate $\tan\beta$ regime. Furthermore, the contribution from renormalization group flow has a definite sign, with the mass ordering of the superparticles being anticorrelated with that of the standard model particles, i.e. $m_{\tilde{\tau}_R} < m_{\tilde{\mu}_R} < m_{\tilde{e}_R}$. On the other hand, the contributions considered in section 4.4 could be positive or negative, and could thus produce a spectrum which is unambiguously different from flavor universality.

An interesting possibility considered in Refs. [15, 32] is the case where the lightest supersymmetric particle (LSP) is the gravitino, and the next-to-lightest supersymmetric particle (NLSP) is one of the right-handed sleptons. In the case where the supersymmetry breaking scale is large, i.e. M is large, the lifetime of the NLSP is long enough that it escapes the detector. A slepton NLSP will then appear as a heavy charged stable particle, something quite spectacular at the LHC. (Here we consider the case where R parity is conserved so that decay of the NLSP into only standard model particles is forbidden.) Furthermore, the LHC will usually produce squarks or gluinos, so NLSPs will generally be produced after a chain of decays. This cascade decay must produce a slepton in conjunction with a lepton, and because the NLSP is right-handed, the coupling to neutrinos is strongly suppressed. Therefore, NLSPs will be produced mostly with charged leptons that can be used to measure the flavor content of the NLSP.

If we could observe the decay of the NLSP, we could measure the flavor content of the NLSP more easily. In particular, we could precisely determine, by observation of flavor violating decays, if the flavor eigenbasis differs from the mass eigenbasis for the sleptons. Flavorful models including those discussed in section 4.3 generically have this property, so this is an interesting test of intrinsic flavor nonuniversality. One way to measure decays of long-lived NLSP sleptons is to build a stopper detector outside one of the main LHC detectors, which would stop some of the NLSPs and measure their decays [26]. If the NLSP has a sufficiently long lifetime and a large number of decays are observed in a stopper detector, then the flavor composition of the NLSP can be measured very accurately.

While the scenario with a weak scale gravitino LSP has an NLSP with lifetime much longer than the flight time in the detector, the scenario can be extended to a much lighter gravitino LSP or another extremely weakly interacting particle, such as the axino. In fact, if the NLSP has a lifetime of order $c\tau \approx O(100\ \mu\text{m} - 10\ \text{m})$, then there is a clean signal of a non-minimum ionizing track with a kink that turns into a minimum ionizing track [119]. Furthermore, an ATLAS study with the NLSP decaying to photons showed that a substantial number of decays can be measured if $c\tau \lesssim 100$ km [22], so it is conceivable that the decay of an NLSP can be observed in the detector for a large range of NLSP lifetimes. This kind of measurement would allow us to study the decays of the NLSP and gain knowledge on its flavor content.

We now focus on the case where the lightest neutralino is lighter than all of the right-handed sleptons, although the analysis also applies if all the superparticles promptly decay to a different particle which escapes the detector. In this case, the events are similar to well studied supersymmetric missing energy events, but many interesting studies of flavor violation can still be done. For example, if $m_{\tilde{\tau}_R} > m_{\chi_2^0} > m_{\tilde{e}_R, \tilde{\mu}_R}$, a natural spectrum in the models of section 4.3 given the $O(1)$ mass splitting of the $\tilde{\tau}_R$ from the other sleptons, then the detectors can measure a fractional mass splitting between $\tilde{e}_R$ and $\tilde{\mu}_R$ as small as $O(10^{-4})$ [120]. This may help discriminate different classes of theories discussed in section 4.3. These and other studies could be performed not only in the right-handed slepton sector, but also with squarks and left-handed sleptons, which may determine whether the different SSM fields transform under different classes of flavor symmetries, as discussed in section 4.4.3.

With a little luck, the LHC could discover a smoking gun for intrinsic flavor nonuniversal effects in the supersymmetry breaking sector, which may hint at the high energy theory that gives rise to the standard model flavor structure.

4.6 Discussion and Conclusions

The problem of excessive flavor and CP violation arising from generic weak scale supersymmetry breaking parameters has been a guiding principle in searching for viable supersymmetric theories. In particular, this has been a strong motivation behind the search for flavor universal mediation mechanisms of supersymmetry breaking. On the other hand, the puzzle of flavor already exists in the standard model, and it is possible that the mechanism producing the observed Yukawa structure is also responsible for the suppression of possibly large flavor and CP violation in supersymmetric theories. How natural is this possibility? Is there any generic tension between the constraints from low energy flavor and CP violation and the observability of superparticles at the LHC, even if we take into account the possibility of a correlation between the structures of the Yukawa couplings and supersymmetry breaking parameters?

In this chapter we have studied, in a model independent way, the question of compatibility between the low energy flavor and CP constraints and the observability of a nontrivial flavor structure in superparticle spectra at the LHC. We have seen that there is a model independent tension arising from the superpotential operators $\mathcal{O}_{\zeta_f}$ leading to scalar trilinear interactions. In particular, the constraint from the $\mu \to e\gamma$ process pushes the mass scale for non-colored superparticles $m_{\rm N}$ relatively high. Under the assumption of a factorized flavor structure, $m_{\rm N}$ should be of order a TeV or larger for a natural size of $\mathcal{O}_{\zeta_f}$. Assuming the usual hierarchy between colored and non-colored superparticle masses, this pushes up the masses of colored superparticles beyond several TeV, making supersymmetry unobservable at the LHC. Similar, though somewhat weaker constraints also arise from the bounds on the electron, neutron and mercury EDMs. In fact, these observables also constrain flavor violation arising from other operators through multiple mass insertion diagrams.

We have discussed several ways in which these stringent constraints are naturally avoided. They include relaxing the mass hierarchy between colored and non-colored superparticles, making the fundamental strength of the Yukawa couplings strong, and making the gaugino masses larger than the scalar masses. We have also presented simple frameworks in which the dangerous operators $\mathcal{O}_{\zeta_f}$ are naturally absent. Since these operators are special, they can be absent in the low energy effective theory. We have considered separating the Higgs and supersymmetry breaking fields (Higgsphobic), separating supersymmetry and flavor symmetry breaking (remote flavor-supersymmetry breaking), and assigning a nontrivial charge to the supersymmetry breaking field (charged supersymmetry breaking). These frameworks can be combined with a variety of flavor theories, including ones with (flat or warped) extra dimensions, strong dynamics, or flavor symmetries. In fact, we can consider many variations of flavor models using the basic setups discussed in this chapter. The mediation scale of

supersymmetry breaking, M, and the scale for flavor physics, M_F, can vary by many orders of magnitude in these theories.

We have performed detailed analyses on the constraints from low energy flavor and CP violation in the frameworks described above. We have shown that the constraints, including ones arising from multiple mass insertion diagrams and left-left and right-right sfermion propagation, can be avoided in natural parameter regions while keeping the superparticles light. Expected sizes of flavor and CP violation, however, are not too much smaller than the current bounds, so signatures in future search on flavor and CP violation are not eliminated. The intergenerational mass splittings among sfermions in these theories can show a variety of patterns depending on the underlying mechanism responsible for the structure of the Yukawa couplings. For example, if SSM multiplets belonging to different representations of the standard model gauge group have different flavor symmetry structures, then it will show up in the spectrum of superparticles. In general, it is significant that the spectrum of superparticles contains information on left-handed and right-handed fields separately, while the Yukawa couplings contain only "products" of them.

While the size of the fractional mass splittings directly generated by the physics of flavor at M_F is not necessarily very large, e.g. of $O(10^{-2})$ or smaller for the first two generations, they are large enough to significantly affect the phenomenology at the LHC. This is because the intergenerational mass splittings generated by the standard SSM renormalization group evolution are typically very small, so that additional mass splittings can give large effects on the structure of the intergenerational superparticle spectrum. Moreover, because the signs of the intergenerational mass splittings caused by effects at M_F are arbitrary (at least from the low energy effective field theory point of view), these additional splittings can change the mass ordering among different generation sfermions. In particular, this can make a third generation sfermion heavier than the corresponding first two generation sfermions, which can drastically affect the signatures at the LHC. We find it very possible that the intergenerational mass splittings of the size implied by the classes of theories discussed in this chapter will be measured at the LHC.

The LHC will start running this year, and it is expected to give us meaningful data on TeV scale physics as early as next year. If supersymmetry is found, it will not only provide an explanation for the stability of the gauge hierarchy and a potential dark matter candidate, but it will also allow for a substantial number of new flavor measurements. While there are many viable supersymmetric models which are flavor universal, we have shown that there are also many nonuniversal models which avoid the stringent low energy constraints. If supersymmetry is in fact flavorful, then its discovery at the LHC could shed new light on the longstanding mystery of the flavor pattern in the standard model.

Chapter 5

Dark Matter Signals From Cascade Annihilations[1]

5.1 Introduction

Recent observations by PAMELA [13] and ATIC [14] strongly suggest a new primary source of galactic electrons and positrons. Three leading interpretations of the PAMELA/ATIC excesses are astrophysical sources [122], decay of dark matter [123], and annihilation of dark matter [124, 125, 126, 127, 128]. While the current PAMELA/ATIC data cannot distinguish between these possibilities, one expects that the correct scenario will ultimately be determined with the help of complementary data from synchrotron, gamma ray, and neutrino telescopes, as well as collider and direct detection experiments.

One piece of data that points toward an annihilation interpretation is the WMAP Haze [129], an apparent excess of synchrotron radiation coming from the galactic center. Dark matter annihilation into charged particles is uniquely positioned to explain the Haze [130, 131]. If n is the dark matter number density near the galactic center, then the synchrotron signal for dark matter annihilation scales like n^2, while the signal for dark matter decay scales only as n. (Astrophysical signals also roughly scale like n.) Given the normalization of the PAMELA/ATIC excess, the n^2 scaling is favored to explain the size of the Haze anomaly [132].

On the other hand, the same n^2 versus n logic implies that the dark matter annihilation interpretation is more strongly constrained by the *absence* of gamma ray or neutrino excesses from the galactic center. While these constraints are dependent on the Milky Way dark matter halo profile, there are already strong bounds on the annihilation interpretation for strongly peaked halos [133, 134, 135, 136, 137]. Therefore, it is worth exploring dark matter annihilation scenarios in detail to understand how robust the tension is between explaining PAMELA/ATIC/Haze and satisfying other bounds.

[1] This chapter, as well as Appendix B, were co-written with Jeremy Mardon, Yasunori Nomura, and Jesse Thaler and published in [121].

Given the absence of anti-proton [138] or gamma ray [139, 140, 141] excesses, the dark matter annihilation scenarios favored to explain PAMELA/ATIC involve annihilation into electrons and muons. However, dark matter need not annihilate into leptons directly. There are a variety of "cascade annihilation" models where dark matter annihilates into light resonances which in turn decay into electrons or muons. These light resonances can lead to nonperturbative enhancements [142, 143] of the dark matter annihilation rate in the galactic halo, providing the large boost factors necessary to explain PAMELA/ATIC [124, 125, 126]. Also, annihilation into light fields gives a kinematic explanation for why dark matter annihilation preferentially yields light leptons [131, 125, 126]. Previous studies of cascade annihilation models appear in Refs. [127, 135].

In the present context, these cascade annihilation scenarios are interesting because they have the potential to explain PAMELA/ATIC while weakening constraints from gamma rays, as measured by atmospheric Cerenkov telescopes like H.E.S.S. [139, 140, 141]. The reason is that gamma ray experiments are directly sensitive to the primary injection spectra, and cascade annihilations yield softer and smaller injection spectra of gamma rays from final state radiation (FSR). PAMELA/ATIC sees electrons and positrons through the filter of charged cosmic ray transport, a process which introduces large uncertainties. Considering also the uncertainties in the highest energy ATIC data, we find that softer spectra of primary leptons can still explain the PAMELA/ATIC excesses.

For cascade annihilations that terminate in muons, there is also an irreducible source of galactic neutrinos, which can be observed as an upward-going muon flux on earth, for example, by water Cerenkov detectors like Super-Kamiokande (Super-K) [144]. While cascades soften the neutrino spectrum, we will see that the final constraints from neutrinos are rather insensitive to the number of cascade steps, and may provide the most robust bound on muon cascade scenarios.

The organization of this chapter is as follows. In the next section, we define our framework for analyzing signals of dark matter through cascade annihilations, with details of the cascade energy spectra given in Appendix B.1. In Section 5.3, we find the best fit dark matter masses and annihilation cross sections for various cascade scenarios given the PAMELA/ATIC data. We consider H.E.S.S. gamma ray bounds from FSR in Section 5.4 and Super-K neutrino bounds in Section 5.5. In Section 5.6, we study a particular cascade annihilation scenario called the axion portal [126], and present a less constrained "leptonic" version in Appendix B.2. Conclusions are given in Section 5.7.

5.2 Cascade Annihilations

If dark matter is a thermal relic, then it will have at least one annihilation mode into standard model fields, since in the early universe, the dark matter annihilation channels keep dark matter in thermal equilibrium with the standard model until freezeout. However, dark matter need not annihilate into standard model particles directly; it can annihilate into new (unstable) resonances which in turn decay into standard model fields. As long as the new

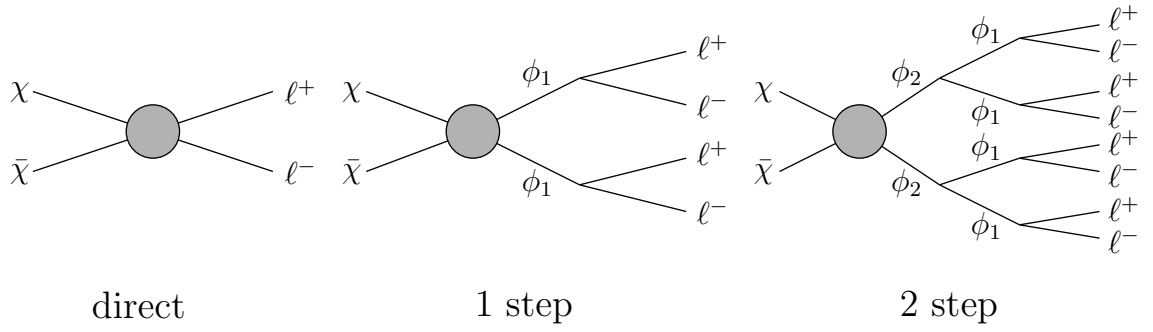

Figure 5.1: For an n-step cascade annihilation, dark matter χ annihilates into $\phi_n\phi_n$. The cascade annihilation then occurs through $\phi_{i+1} \to \phi_i\phi_i$ ($i = 1, \cdots, n-1$), and in the last stage, ϕ_1 decays into standard model particles. The figure represents the cases where $\phi_1 \to \ell^+\ell^-$.

resonances are sufficiently broad, then dark matter will be in close enough thermal contact with the standard model for a freezeout calculation to be valid.

These "cascade annihilations" can occur in one or more steps, as shown in Figure 5.1, and there are a variety of motivations for such cascade scenarios. Since the direct coupling between dark matter and the standard model can be small while still achieving the desired thermal relic abundance, such models can have reduced direct detection cross sections compared to generic weakly interacting massive particles (WIMPs) [145]. Cascade annihilations can arise whenever new light resonances have large couplings to dark matter, such as in exciting dark matter [146]. In the context of PAMELA/ATIC, there has been interest in using light resonances to provide large enhancement to the galactic annihilation rate through the Sommerfeld effect or bound state (WIMPonium) formation [124, 125, 126]. These light resonances can also explain the lepton-richness of dark matter annihilation through kinematic thresholds [125, 126].

Cascade annihilations give softer primary spectra for the annihilation products than direct annihilation. As reviewed in Appendix B.1, for (scalar) cascade annihilations involving well-separated kinematic scales, the approximate primary spectra can be calculated using a simple convolution formula. The energy spectra are conveniently parametrized in terms of the energy fraction $x_n \equiv E_n/m_{\rm DM}$, where E_n is the final state energy after the n-th step of the cascade, and $m_{\rm DM}$ is the dark matter mass. If $d\tilde{N}/dx_0$ is the normalized primary spectrum from direct annihilation, then the normalized primary spectrum from a 1-step annihilation $d\tilde{N}/dx_1$ is

$$\frac{d\tilde{N}}{dx_1} \approx \int_{x_1}^1 \frac{dx_0}{x_0} \frac{d\tilde{N}}{dx_0}. \tag{5.1}$$

This convolution formula can be iterated to obtain the normalized primary spectrum for an n-step cascade scenario. Eq. (5.1) is also reasonably representative of non-scalar cascades, since indirect detection measurements are unpolarized.

While cascade annihilations give softer spectra, they typically yield a higher multiplicity of annihilation products. The final primary spectrum dN/dx_n must take into account the multiplicity of annihilation products per dark matter annihilation, and in a typical n-step cascade, the final state multiplicity scales like 2^n.

An important exception, however, is in cases involving singularities, where cascade annihilations yield both a softer spectrum *and* a lower multiplicity. For example, FSR from charged leptons has a collinear singularity that is regulated by the lepton mass. Integrating over the singularity gives a photon spectrum dN_γ/dx that is proportional to $\ln Q/m_\ell$, where Q is the total energy available for radiation. For direct annihilation $Q \simeq 2m_{\rm DM}$, while for cascade annihilations $Q \simeq m_1$, where m_1 is the mass of the resonance in the last stage of the annihilation $\phi_1 \to \ell^+\ell^-$. Light enough ϕ_1 fields can give a dramatic reduction in the $\ln Q/m_\ell$ factor and thus the FSR photon yield.

In this chapter, we only consider cascade annihilations that terminate in electrons or muons. The same analysis, however, could be repeated for charged pions or taus by changing the direct annihilation spectra. We expect the results for an n-step charged pion cascade to be similar to an $(n+1)$-step muon cascade. Cascades involving taus will face stronger gamma ray bounds because of the $O(1)$ fraction of π^0s in tau decays. For simplicity, we only show plots for direct, 1-step, and 2-step cascades.

5.3 PAMELA/ATIC Spectra

The PAMELA satellite experiment [11] observed an anomalous source of galactic positrons in the energy range 10–100 GeV through a measurement of the positron fraction $\Phi_{e^+}/(\Phi_{e^+} + \Phi_{e^-})$ [13]. The ATIC balloon experiment [12] is not capable of charge separation, but observed a peak in the total electron plus positron flux between 100–1000 GeV in a $(\Phi_{e^+} + \Phi_{e^-})$ measurement [14]. Intriguingly, both excesses can be described by a single new source of galactic electrons and positrons, and here we study the goodness of fit for dark matter cascade annihilations. The primary electron/positron spectra for n-step electron and muon cascade annihilations are given in Appendices B.1.1 and B.1.2. Once the primary spectrum is known and a dark matter halo profile assumed, we can propagate the electrons and positrons through the Milky Way and compare with the PAMELA/ATIC data.

We follow the analysis of Ref. [147], which assumes that galactic electrons and positrons can be described by a diffusion-loss process. In the turbulent galactic magnetic fields, electrons/positrons diffuse within a fiducial region around the galactic disk and escape the galaxy outside that region. An energy loss term incorporates the physics of inverse Compton scattering (ICS) and synchrotron radiation. Dark matter annihilation is represented by a source term proportional to the square of the dark matter halo density. Since the energy loss time is much shorter than the age of the galaxy, the electron/positron system is assumed to be in steady state.

Taking $\psi_{e^-}(\vec{x}, E)$ to be the galactic electron number density per unit energy, the diffusion-

	R (kpc)	L (kpc)	K_0 (kpc^2/Myr)	δ	τ_E (sec)
MED	20	4	0.0112	0.70	10^{16}
M1	20	15	0.0765	0.46	10^{16}
M2	20	1	0.00595	0.55	10^{16}

Table 5.1: Diffusion-loss parameters for the three benchmark models (MED, M1, and M2) for electron/positron propagation.

loss equation is

$$K_0\,\varepsilon^\delta\,\nabla^2\psi_{e^-}(\vec{x},E)+\frac{\partial}{\partial\varepsilon}\left(\frac{\varepsilon^2}{\tau_E}\,\psi_{e^-}(\vec{x},E)\right)+q(\vec{x},E)=0, \tag{5.2}$$

where $\varepsilon = E/\mathrm{GeV}$, K_0 and δ parametrize the (energy dependent) diffusion, τ_E is a characteristic energy loss time, and $q(\vec{x},E)$ is the electron source term for dark matter annihilations. The same equation also holds for the positron number density per unit energy $\psi_{e^+}(\vec{x},E)$. The electron/positron densities $\psi_{e^-/e^+}(\vec{x},E)$ are assumed to have vanishing boundary conditions on the surface of a cylinder of height $2L$ and radius R. We consider the three benchmark models from Ref. [147], which are summarized in Table 5.1.

The electron/positron source term is given by

$$q(\vec{x},E)=\frac{1}{2\eta}\langle\sigma v\rangle\left(\frac{\rho(\vec{x})}{m_{\rm DM}}\right)^2\frac{dN_e}{dE}, \tag{5.3}$$

where $\rho(\vec{x})$ is an assumed dark matter halo profile, $m_{\rm DM}$ is the dark matter mass, $\langle\sigma v\rangle$ is the average dark matter annihilation cross section in the galactic halo, and dN_e/dE is the electron energy spectrum per dark matter annihilation. $\eta = 1$ if dark matter is self-conjugate (e.g. a Majorana fermion), while $\eta = 2$ if not (e.g. a Dirac fermion). We consider three spherically symmetric benchmark halo profiles (cored isothermal [148], NFW [149], and Einasto [150]) with $r_\odot = 8.5$ kpc and $\rho_\odot = 0.3\ \mathrm{GeV\,cm^{-3}}$:

$$\rho(r)_{\rm Isothermal}=\rho_\odot\frac{1+(r_\odot/r_c)^2}{1+(r/r_c)^2},\qquad r_c=5\ \mathrm{kpc}, \tag{5.4}$$

$$\rho(r)_{\rm NFW}=\rho_\odot\frac{r_\odot}{r}\left(\frac{1+r_\odot/r_c}{1+r/r_c}\right)^2,\qquad r_c=20\ \mathrm{kpc}, \tag{5.5}$$

$$\rho(r)_{\rm Einasto}=\rho_\odot\exp\left\{-\frac{2}{\alpha}\left[\left(\frac{r}{r_c}\right)^\alpha-\left(\frac{r_\odot}{r_c}\right)^\alpha\right]\right\},\qquad \alpha=0.17,\quad r_c=20\ \mathrm{kpc}. \tag{5.6}$$

N-body simulations suggest that Einasto and NFW are more realistic profiles for $r \gtrsim 1$ kpc. Within the inner region, however, there is considerable uncertainty, and we include the cored isothermal profile to explore the possibility of a less peaked distribution.

Once the source term is specified, Eq. (5.2) can be solved using the methods of [147, 151], and the electron/positron intensities (fluxes per energy per solid angle) at the earth due to dark matter annihilations are given by

$$\frac{d\Phi^{(\mathrm{DM})}_{e^-/e^+}}{dE\,d\Omega}(E) = \frac{B_{e,\mathrm{astro}}}{4\pi}\psi_{e^-/e^+}(\vec{x}_\odot, E), \tag{5.7}$$

where $\vec{x}_\odot$ is the location of the solar system and $B_{e,\mathrm{astro}}$ is an astrophysical boost factor. Since the annihilation rate is proportional to the squared density of dark matter ρ^2_{DM}, clumping of dark matter tends to increase the local electron/positron flux, and the $B_{e,\mathrm{astro}}$ factor accounts for differences from the assumed smooth halo profile, as well as uncertainties in $\rho_\odot$. Of course, in the presence of clumpiness, the true electron/positron spectrum is also modified [152].

Galactic cosmic rays are a known source of background primary electrons. Background secondary electrons and positrons arise, e.g., from collisions of cosmic ray protons with interstellar gas. In principle, the spectra of background electrons/positrons are correlated with the diffusion-loss parameters for electrons/positrons, but for simplicity we will use the parameterization of background primaries and secondaries from Ref. [153]:

$$\frac{d\Phi^{(\mathrm{prim})}_{e^-}}{dE\,d\Omega} = \frac{0.16\,\varepsilon^{-1.1}}{1 + 11\,\varepsilon^{0.9} + 3.2\,\varepsilon^{2.15}}\ \mathrm{GeV}^{-1}\,\mathrm{cm}^{-2}\,\mathrm{s}^{-1}\,\mathrm{sr}^{-1}, \tag{5.8}$$

$$\frac{d\Phi^{(\mathrm{sec})}_{e^-}}{dE\,d\Omega} = \frac{0.70\,\varepsilon^{0.7}}{1 + 110\,\varepsilon^{1.5} + 600\,\varepsilon^{2.9} + 580\,\varepsilon^{4.2}}\ \mathrm{GeV}^{-1}\,\mathrm{cm}^{-2}\,\mathrm{s}^{-1}\,\mathrm{sr}^{-1}, \tag{5.9}$$

$$\frac{\Phi^{(\mathrm{sec})}_{e^+}}{dE\,d\Omega} = \frac{4.5\,\varepsilon^{0.7}}{1 + 650\,\varepsilon^{2.3} + 1500\,\varepsilon^{4.2}}\ \mathrm{GeV}^{-1}\,\mathrm{cm}^{-2}\,\mathrm{s}^{-1}\,\mathrm{sr}^{-1}, \tag{5.10}$$

where again $\varepsilon = E/\mathrm{GeV}$. To treat background uncertainties, we will marginalize over the normalization and overall slope of the background in our analysis:

$$\Phi^{(\mathrm{back.\ fit})}_{e^-} = A_-\varepsilon^{P_-}\left(\Phi^{(\mathrm{prim})}_{e^-} + \Phi^{(\mathrm{sec})}_{e^-}\right), \qquad \Phi^{(\mathrm{back.\ fit})}_{e^+} = A_+\varepsilon^{P_+}\left(\Phi^{(\mathrm{sec})}_{e^+}\right), \tag{5.11}$$

where we allow $0 < A_\pm < \infty$, $-0.05 < P_\pm < 0.05$, as in [124].

In the limit that Eq. (5.1) holds, any given dark matter cascade topology has just two free parameters: the dark matter mass m_{DM} and the annihilation cross section $\langle\sigma v\rangle$. Following the literature, we normalize the cross section to the value that leads to the right relic thermal abundance $\langle\sigma v\rangle_0 \simeq 3\times10^{-26}\,\eta\,\mathrm{cm}^3\,\mathrm{s}^{-1}$ and express our results in terms of an effective boost factor

$$B = B_{e,\mathrm{astro}}\frac{\langle\sigma v\rangle}{\langle\sigma v\rangle_0}, \tag{5.12}$$

which includes both the deviation from the naive thermal freezeout cross section and dark matter clumping. Using only the statistical error bars, we perform a chi-squared fit of the derived electron/positron intensities to the PAMELA $e^+/(e^+ + e^-)$ and ATIC $e^+ + e^-$ data, treating m_{DM} and B as free parameters. We use only $E \gtrsim 10$ GeV bins for the PAMELA

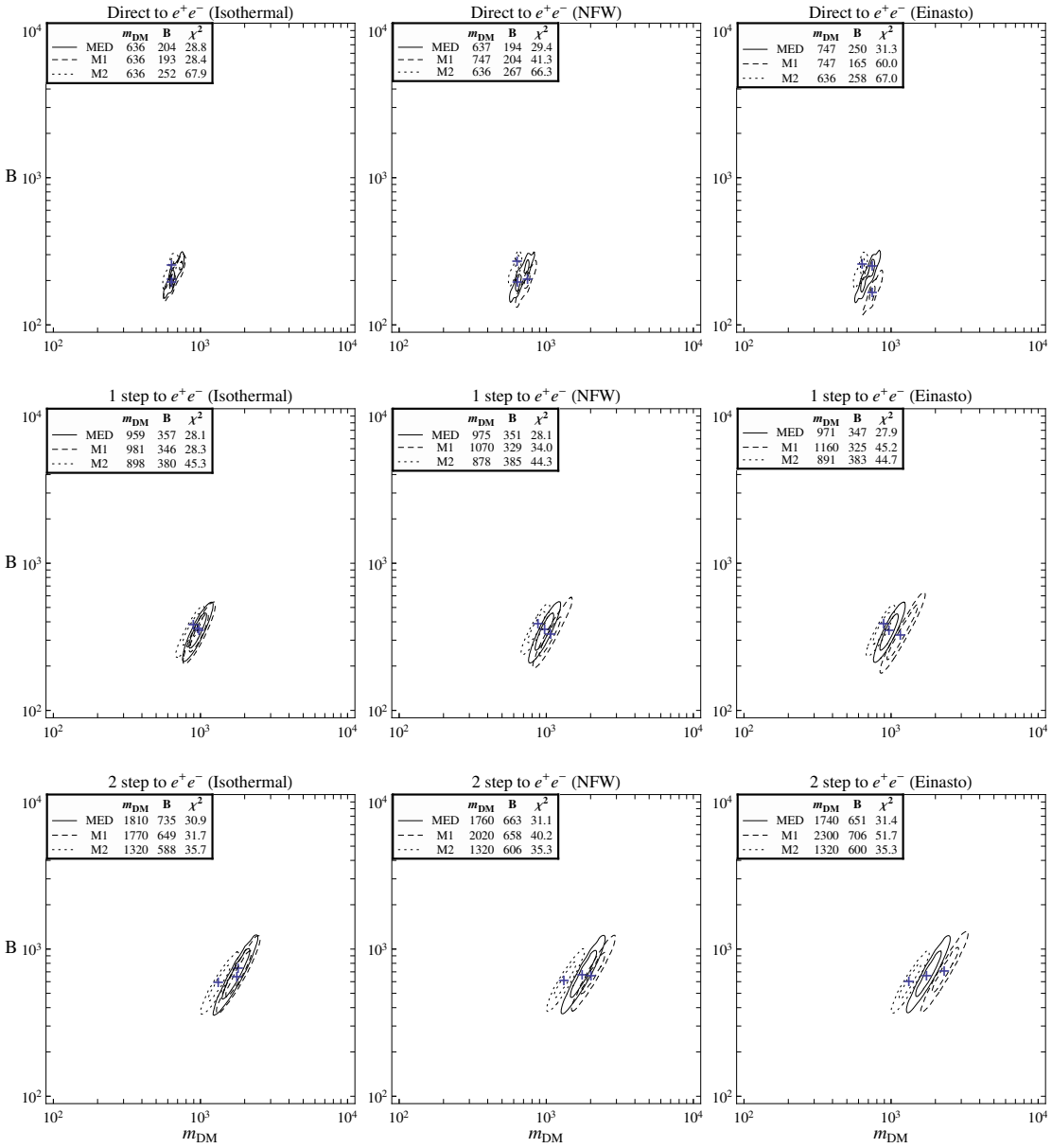

Figure 5.2: The best fit regions for the dark matter mass $m_{\rm DM}$ and boost factor B in the cases of direct, 1-step, and 2-step annihilations into e^+e^- for different halo profiles and propagation models. The best fit values are indicated by the crosses, and the contours are for 1σ and 2σ.

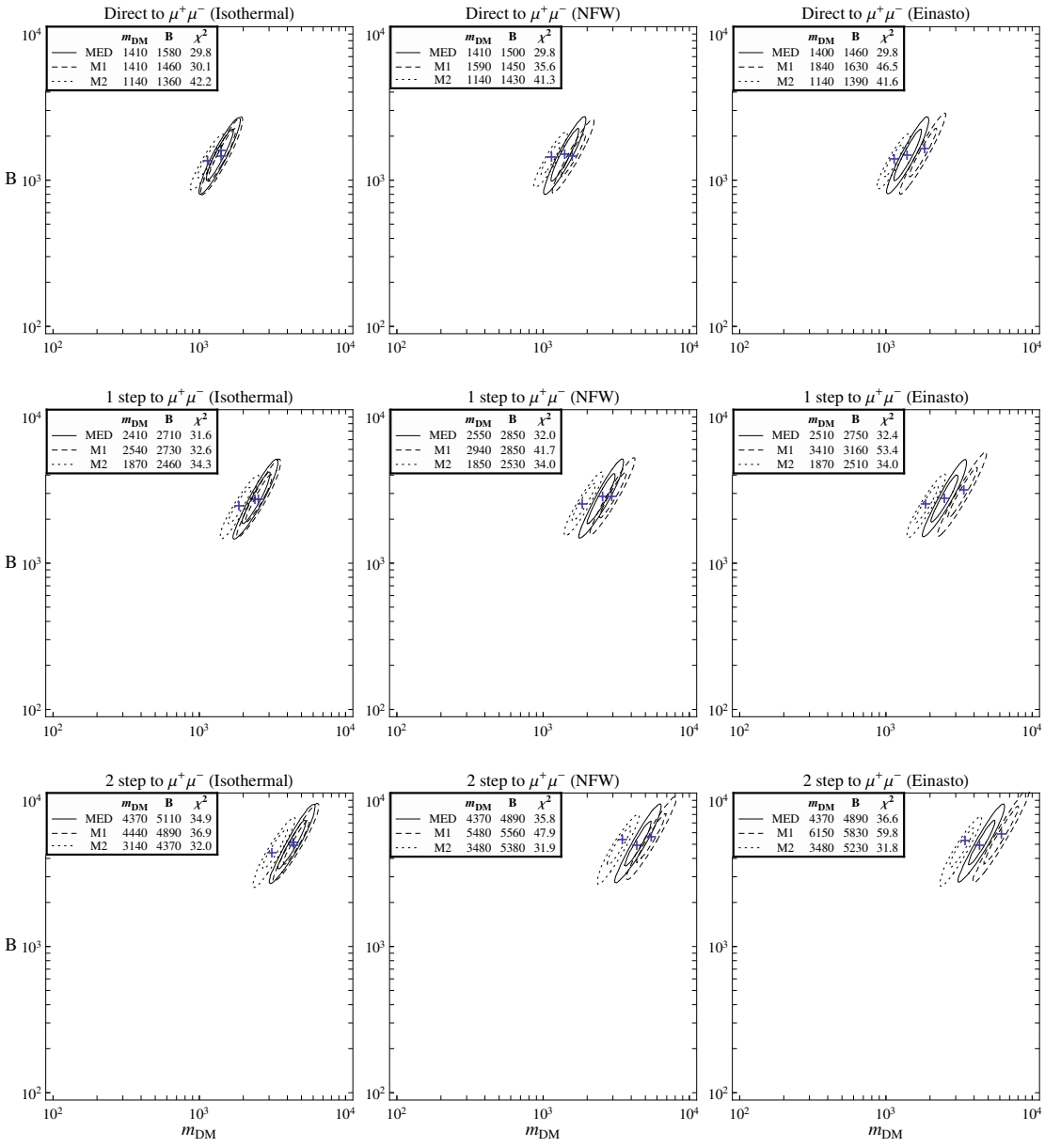

Figure 5.3: The same as Figure 5.2 but for annihilations into $\mu^+\mu^-$.

	Direct e	1 step e	2 step e	Direct μ	1 step μ	2 step μ
Isothermal	16%	17%	9.8%	12%	8.5%	7.7%
NFW	13%	17%	9.4%	12%	7.7%	7.9%
Einasto	9.0%	18%	8.8%	12%	7.1%	8.1%

Table 5.2: The p-value for the best propagation model for each plot in Figures 5.2 and 5.3.

data, as the lower energy bins are strongly affected by solar modulation effects (see the discussion in [13]).

The results of the fit for direct, 1-step, and 2-step annihilations are shown in the case of electron final states in Figure 5.2 and muon final states in Figure 5.3. (The results do not depend on whether the dark matter particle is self-conjugate or not.) Each plot corresponds to a definite cascade annihilation pattern with a definite halo profile, and shows 1σ and 2σ contours for three propagation models in the $m_{\rm DM}$-B plane. The best fit values for $m_{\rm DM}$ and B, as well as the χ^2 values, are also given, where χ^2 follows the chi-squared distribution with 22 degrees of freedom (7 PAMELA $+ 21$ ATIC $- 6$ fitting parameters: $m_{\rm DM}, B, A_\pm, P_\pm$). To evaluate goodness of fit, we also give p-values in Table 5.2, where we have chosen the propagation model giving smallest χ^2 for each plot of Figures 5.2 and 5.3. As we can see, the fits are reasonable for all the cases presented.

In Figures 5.4 and 5.5, we show the comparisons of the $e^\pm$ intensities with the PAMELA and ATIC data in the cases of electron and muon final states. Solid, dashed, and dotted lines represent direct, 1-step, and 2-step annihilations, and we have chosen the NFW halo profile and the MED propagation model for illustrative purposes. We clearly see the trend that more steps in cascades lead to flatter $e^\pm$ spectra, but that the fits are good for all cases shown. Note that we have not optimized the propagation model here. Adjusting the propagation model can lead to a better fit in certain cases, especially the 2-step annihilation into $\mu^+\mu^-$.

Summarizing the analysis of the $e^\pm$ data, we find:

- The PAMELA and ATIC data require the dark matter mass and boost factor in the region $m_{\rm DM} = O(\text{TeV})$ and $B = O(1000)$, which is consistent with earlier analyses on the direct [124] and 1-step [127] cases. More steps in the cascade lead to larger values of $m_{\rm DM}$ and B, and roughly speaking, both B and $m_{\rm DM}$ scale as 2^n. The reason is that the peak location in the ATIC data sets the scale for the final state $e^\pm$ energy, and since the average $e^\pm$ energy over $m_{\rm DM}$ in an n-step cascade scales like $1/2^n$, $m_{\rm DM}$ must increase by 2^n to keep the peak location fixed. Similarly, the annihilation signal scales like $BN_e/m_{\rm DM}^2$ (assuming fixed $\rho_{\rm DM}$), where $N_e = 2^{n+1}$ is the final state $e^\pm$ multiplicity. Thus, to keep the PAMELA/ATIC rate fixed, B must scale like 2^n.

- The fits do not become much worse by going to multiple steps, due to uncertainties in the highest energy ATIC data and uncertainties in the $e^\pm$ propagation model. In

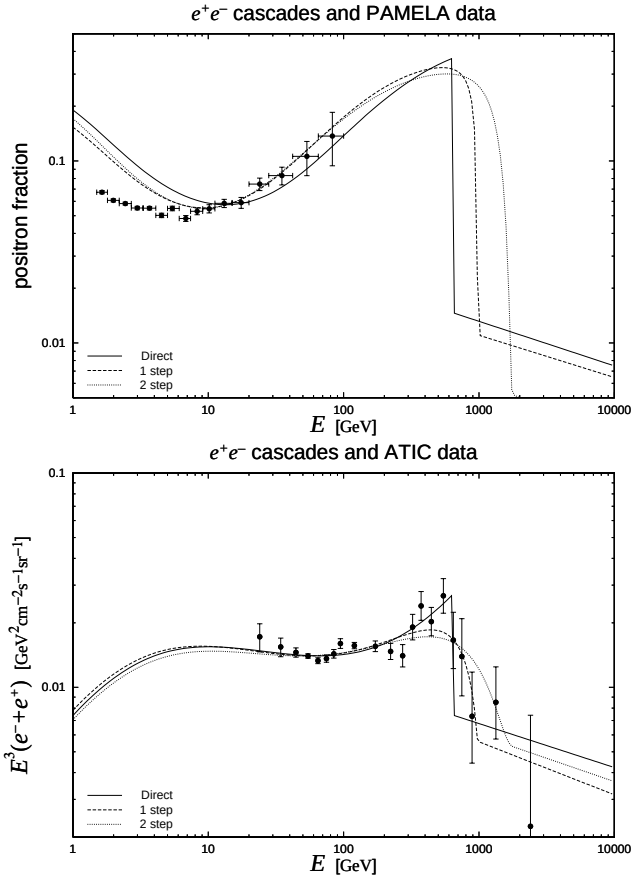

Figure 5.4: The predicted $e^{\pm}$ intensities compared to the PAMELA (left) and ATIC (right) data for direct (solid), 1-step (dashed), and 2-step (dotted) annihilations into electron final states. The NFW halo profile and the MED propagation model are chosen, and the $e^{\pm}$ backgrounds are marginalized as described in Eq. (5.11). Note that we fit the PAMELA data only for $E \gtrsim 10$ GeV because solar modulation effects are important at lower energies.

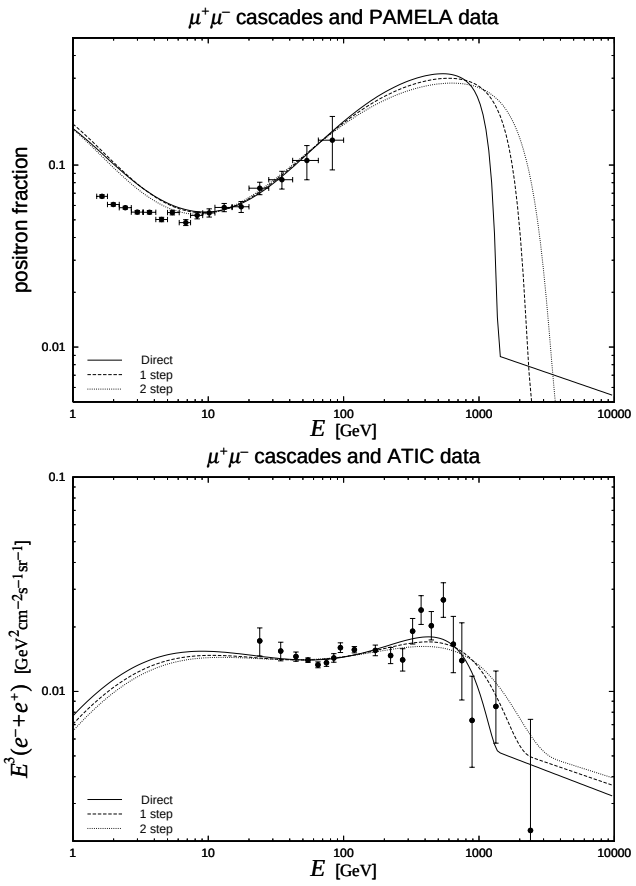

Figure 5.5: The same as Figure 5.4 but for annihilations into muon final states.

particular, 2-step annihilations still fit the data reasonably well for both electron and muon final states. The required boost factors are rather large in the case of muon final states: B of a few thousand. Such large boost factors may come from both astrophysics, e.g. uncertainties in $\rho_\odot$ and nearby clumps of dark matter, and particle physics.

- Uncertainties in halo profiles and propagation models do not significantly affect the dark matter mass and the boost factor. Errors from these uncertainties are mostly of $O(10\%)$ and at most a factor of 2. The 2σ ranges of the fits then determine $m_{\rm DM}$ and B up to a factor of a few.

Recent measurements at H.E.S.S. [154] of the electron plus positron flux above 600 GeV [155] are qualitatively consistent with the ATIC spectrum. Given the large systematic energy uncertainties and hadronic background, we do not use the H.E.S.S. data in our fits, although we remark that the observed steepening of the spectrum places some bounds on very long cascade decays and may disfavor spectra with a hard cutoff such as direct $e^\pm$ annihilation.

5.4 Gamma Ray Constraints

When dark matter annihilates into charged leptons, there is a primary source of gamma rays coming from FSR. Various gamma ray telescopes have looked for excess gamma rays coming from the galactic center, and the null result of such searches puts bounds on dark matter annihilation into charged leptons. An additional effect that is beyond the scope of this chapter is ICS, where electrons/positrons from dark matter annihilation lose energy by upscattering starlight photons into gamma rays. The rate of ICS photon production depends on the modeling of galactic starlight, and we here focus only on the bounds from FSR. For an early analysis of FSR in dark matter annihilation, see [156].

There is negligible energy loss as gamma rays propagate from the galactic center to the earth. The total power (flux per energy) on earth depends on the dark matter halo profile through

$$\frac{d\Phi_\gamma}{dE} = \frac{B_{\gamma,\rm astro}}{8\pi\eta\, m_{\rm DM}^2}\langle\sigma v\rangle \bar{J}\Delta\Omega\,\frac{dN_\gamma}{dE}, \tag{5.13}$$

where $B_{\gamma,\rm astro}$ is an astrophysical boost factor for photons that may differ from $B_{e,\rm astro}$, and dN_γ/dE is the photon energy spectrum per dark matter annihilation. The energy spectrum from FSR is reviewed in Appendix B.1.3, and we also include the effect of radiative muon decays as described in Appendix B.1.4. $\Delta\Omega$ is the solid angle integration region, and $\bar{J}$ is the average line-of-sight-integrated squared dark matter density for a given halo model

$$\bar{J} = \frac{1}{\Delta\Omega}\int_{\Delta\Omega} d\Omega \int_{\rm line-of-sight} ds\, \rho(\vec{x})^2. \tag{5.14}$$

The strongest bounds on FSR gamma rays come from atmospheric Cerenkov telescopes, but the way these experiments extract gamma ray signals affects the final dark matter

	GC (on)	GC (off)	GC (eff)	GR (on)	GR (off)	GR (eff)
Isothermal	10	10	0.028	10	10	0.019
NFW	$1.1 \cdot 10^4$	$3.6 \cdot 10^2$	$1.1 \cdot 10^4$	$1.8 \cdot 10^3$	$4.3 \cdot 10^2$	$1.4 \cdot 10^3$
Einasto	$5.8 \cdot 10^3$	$7.3 \cdot 10^2$	$5.1 \cdot 10^3$	$2.3 \cdot 10^3$	$8.7 \cdot 10^2$	$1.5 \cdot 10^3$

Table 5.3: $\bar{J}$ values for GC and GR gamma ray observations (on-source, off-source, and effective) in units of $\mathrm{GeV}^2\,\mathrm{cm}^{-6}\,\mathrm{kpc}$.

annihilation bounds. To enable background subtraction, these telescopes operate either in on-off mode or wobble mode, meaning the effective $\bar{J}$ exposure is [157]

$$\bar{J}_{\rm eff} = \bar{J}_{\rm on-source} - \bar{J}_{\rm off-source}. \tag{5.15}$$

By definition, $\bar{J}_{\rm eff}$ is smaller than $\bar{J}_{\rm on-source}$, and neglecting the $\bar{J}_{\rm off-source}$ contribution gives bounds that are too aggressive. This means that one must know both the on- and off-source integration regions to derive a bound on the cross section. For shallow dark matter halo profiles, there can be large cancellations in the value of $\bar{J}_{\rm eff}$, and in principle a stronger bound could be obtained using the raw unsubtracted data.

We set bounds on FSR using three H.E.S.S. gamma ray data sets. The first two are observations of the Galactic Center (GC) [139] and the Galactic Ridge (GR) [140]. Neither is ideal for dark matter observations because of the large contamination from gamma ray point sources and molecular gas, and in principle one should put bounds on a dark matter signal after subtracting both these foregrounds. Since such subtractions are not available, we derive conservative bounds by insisting that the dark matter signal does not exceed any of the H.E.S.S. data points by more than 2σ. For the GC and GR samples, values of $\bar{J}$ for the three dark matter halos in Eqs. (5.4, 5.5, 5.6) are shown in Table 5.3 for both the on-source and off-source regions.

The GC data set comes from the inner 0.1° of the galaxy with a solid angle integration of $\Delta\Omega = 1 \times 10^{-5}$, corresponding to the gamma ray source HESS J1745-290. This sample was taken in wobble mode, and the off-source region corresponds to a ring at a distance of 1.4° from the GC. Apart from the off-source subtraction, no other corrections were made to the data, so the data points include both the HESS J1745-290 point source as well as any putative dark matter signal.

The GR data set comes from the region $|\ell| < 0.8^\circ$, $|b| < 0.3^\circ$ in galactic coordinates, with foreground point sources HESS J1745-290 and G0.9 + 0.1 subtracted. The GR sample was taken in on-off mode, and the region $|\ell| < 0.8^\circ$, $0.8^\circ < |b| < 1.5^\circ$ was used for background subtraction. In the GR data, H.E.S.S. finds that the gamma ray emissions are spatially correlated with molecular gas traced by CS emission lines, but a molecular gas foreground component is not subtracted from the data. The GR bounds are expected to strengthen if one were to subtract a molecular gas component.

H.E.S.S. looked more directly for dark matter annihilation in the Sagittarius dwarf spheroidal galaxy (Sgr dSph) [141]. Sgr dSph has negligible foregrounds and is thought

to be dark matter dominated. A 95% C.L. model-independent bound on the gamma ray flux was obtained for $E_\gamma > 250$ GeV:

$$\Phi_\gamma(E_\gamma > 250 \text{ GeV}) < 3.6 \times 10^{-12} \text{ cm}^{-2}\,\text{s}^{-1}, \tag{5.16}$$

with a solid angle integration of $\Delta\Omega = 2 \times 10^{-5}$. Since the Sgr dSph data was taken in wobble mode and the contribution from the Sgr dSph halo is negligible in a 1.4° ring, we use $\bar{J}_{\text{eff}} = \bar{J}_{\text{on-source}}$. The value of $\bar{J}_{\text{eff}}$ strongly depends on the halo profile of Sgr dSph. For example, an NFW profile, a large core profile, and a small core profile quoted in [134] lead to

$$\bar{J}^{\text{Sgr dSph}}_{\text{NFW}} = 7.8 \times 10^2, \qquad \bar{J}^{\text{Sgr dSph}}_{\text{Large Core}} = 1.1 \times 10^2, \qquad \bar{J}^{\text{Sgr dSph}}_{\text{Small Core}} = 2.4 \times 10^4, \tag{5.17}$$

in units of $\text{GeV}^2\,\text{cm}^{-6}\,\text{kpc}$. To derive bounds, we consider NFW and large core profiles.

In Figures 5.6 and 5.7, we show the resulting constraints from the GC, GR, and Sgr dSph gamma ray observations in the m_{DM}-B plane. We also superimpose the 1σ and 2σ contours reproducing the PAMELA/ATIC data for the MED propagation model; see Figures 5.2 and 5.3. In order to plot the Sgr dSph and Milky Way bounds on the same plane, we associate the Sgr dSph small core profile with the Milky Way cored isothermal profile, and the Sgr dSph NFW profile with the Milky Way NFW and Einasto profiles. The ragged lines in the GC and GR constraints come from the binning of the H.E.S.S. data.

We note that here we have drawn the gamma ray constraints and $e^\pm$ contours assuming a common $B_{\gamma,\text{astro}}$ and $B_{e,\text{astro}}$. This is most likely not the case. For example, if dark matter clumping decreases toward the galactic center, then the gamma ray flux will decrease compared to the local positron flux. If the astrophysical boost factor for $e^\pm$ is larger than that for γ, then the gamma ray constraints become weaker by a factor of $B_{e,\text{astro}}/B_{\gamma,\text{astro}}$ compared to those shown in Figures 5.6 and 5.7.

The bounds from Sgr dSph can be modified if there are nonperturbative enhancements to the dark matter annihilation cross section. Since the velocity dispersion of dark matter in Sgr dSph is $v_{\text{Sgr}} \sim 10$ km/s [158], as opposed to $v_{\text{MW}} \sim 200$ km/s in the Milky Way, the boost factor relevant for Sgr dSph may be larger than that for electrons/positrons if part of the boost factor arises from the Sommerfeld or bound state enhancement. This would make the Sgr dSph constraint stronger than what is naively read from Figures 5.6 and 5.7.

Summarizing the analysis of the gamma ray constraints, we find:

- For FSR gamma rays from the galactic center region, the GR data gives somewhat stronger constraints than the GC data. For direct annihilation, this disfavors the NFW and Einasto profiles, as also seen in Refs. [133, 134]. The Sgr dSph data is not constraining unless we were to take a highly peaked halo such as the small core profile.

- The constraints from FSR photons are weaker in the cascade annihilation case than in the direct annihilation case. This is because cascade annihilations give smaller photon yield at high energies, as discussed in Appendix B.1.3. The smaller the ϕ_1 mass is, the

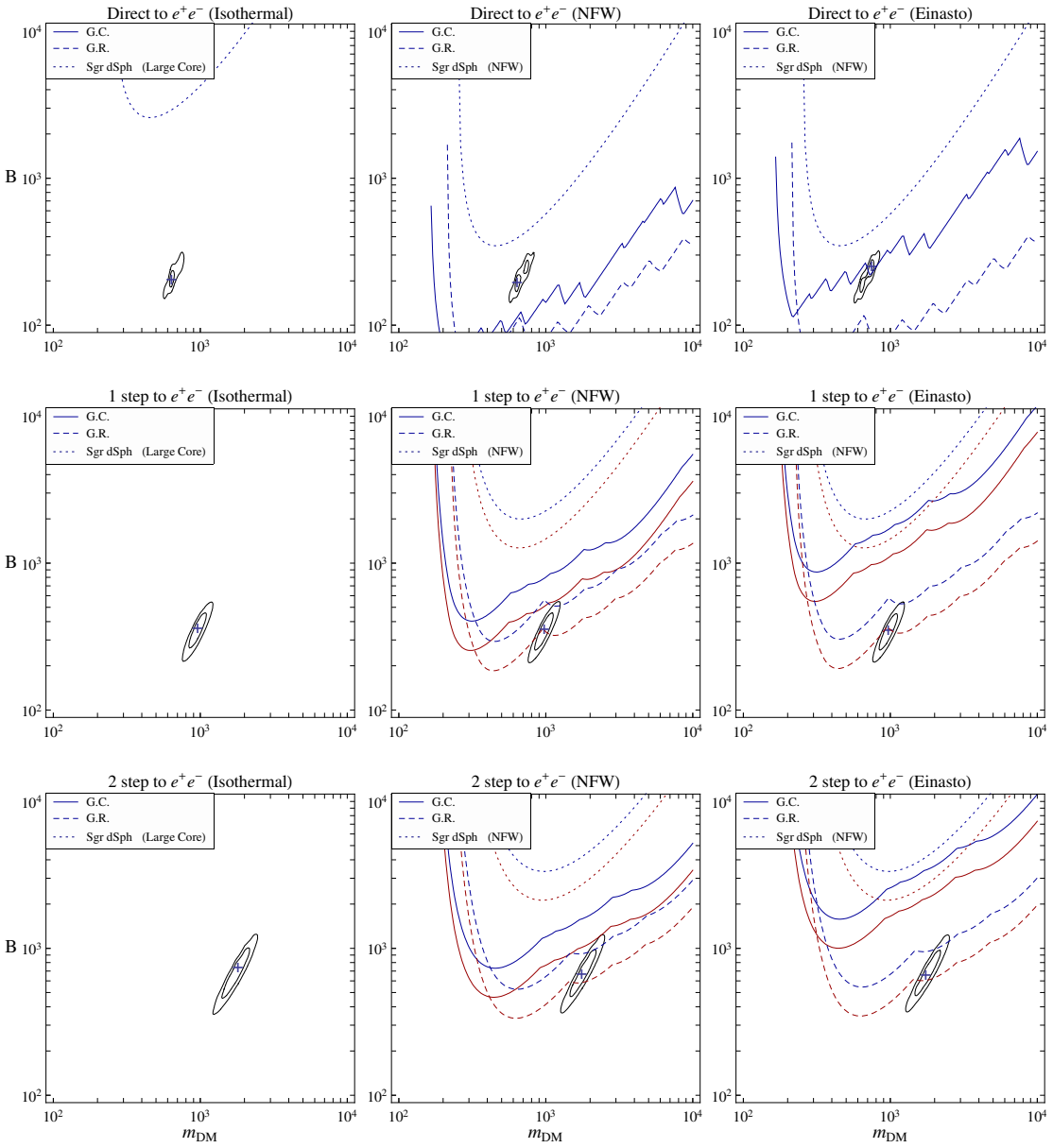

Figure 5.6: Constraints from gamma ray observations, GC (solid), GR (dashed), and Sgr dSph (dotted), in the $m_{\rm DM}$-B plane for direct, 1-step, and 2-step annihilations into electron final states. All the constraints, as well as the best fit region for PAMELA/ATIC (MED propagation), are plotted assuming $B_{e,\rm astro} = B_{\gamma,\rm astro}$. For cascade annihilations, each of the GC, GR, and Sgr dSph constraints consist of two curves, with the upper (blue) and lower (red) curves corresponding to $m_1 = 100$ MeV and 1 GeV, respectively. Note that the constraint lines in the cored isothermal case are above the plot region, and that the halo profiles for Sgr dSph are given in the legends.

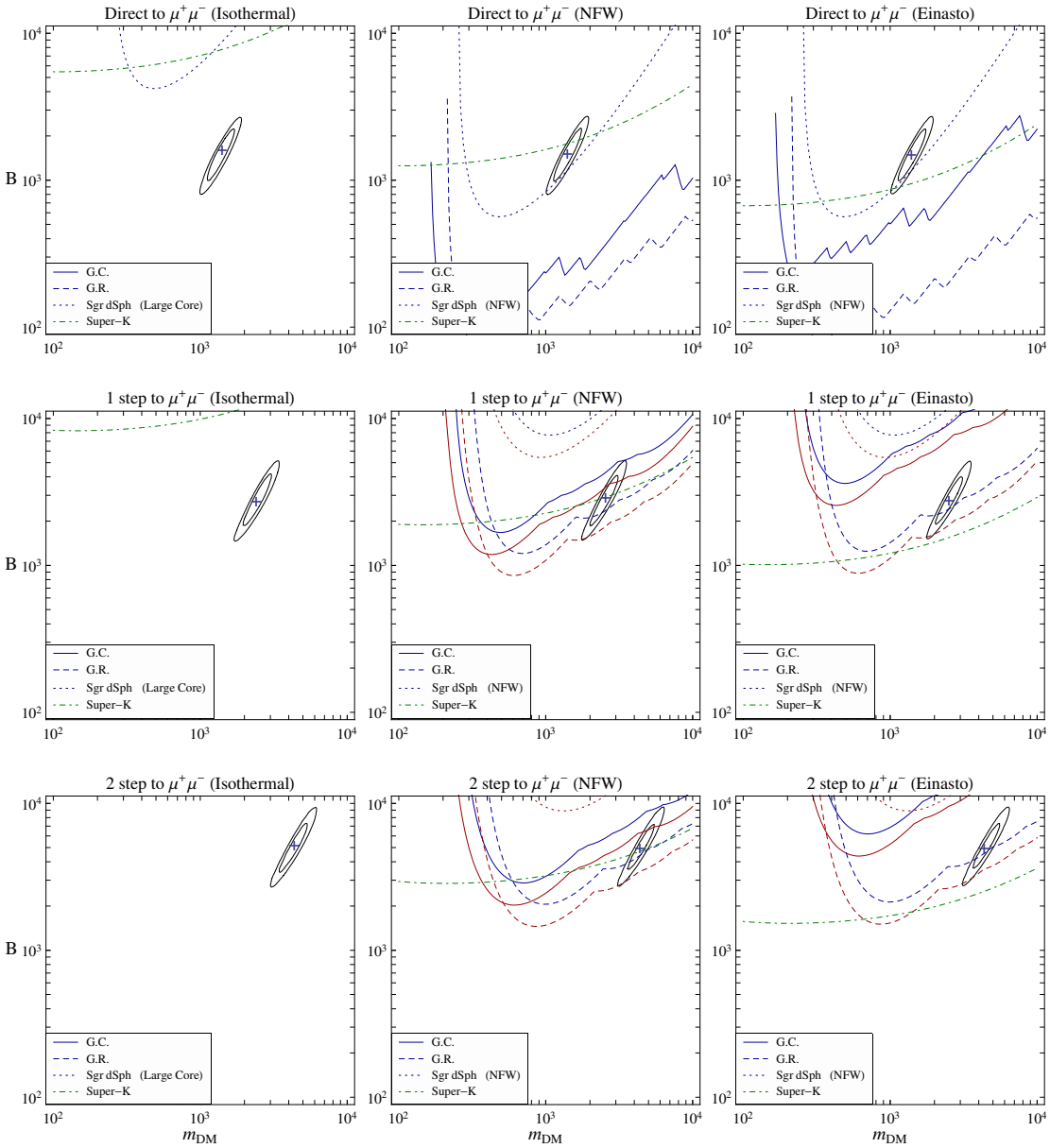

Figure 5.7: The same as Figure 5.6 but for muon final states. Also included are constraints from neutrino observations (dot-dashed) assuming $B_{\nu,\mathrm{astro}} = B_{e,\mathrm{astro}}$. For cascade annihilations, the upper (blue) and lower (red) curves now correspond to $m_1 = 600$ MeV and 1 GeV, respectively.

weaker the constraints become. The constraints, however, do not become weaker by increasing the number of steps, as can be seen by comparing the best fit region for the $e^{\pm}$ data with the gamma ray constraints. This is because the reduction in the photon yield depends only on the ϕ_1 mass and not on the number of cascade steps, and the softening of the gamma ray spectra is compensated by the increase in the best fit dark matter mass and boost factor.

- The constraints are very weak for shallow halo profiles such as the cored isothermal profile for the Milky Way in Eq. (5.4). This is particularly true for the GC and GR data because the background subtraction due to on-off or wobble mode operation also subtracts (most of) the signals from dark matter annihilations. The constraints from these data, therefore, are rather weak as long as the halo profile is relatively flat within about 100 pc of the galactic center. A better bound may be obtained if we could use the unsubtracted data.

While we have focused only on FSR photons in our analysis, we wish to make a few comments about ICS, the WMAP Haze, and radio bounds. In the context of dark matter, the WMAP Haze arises because electrons from dark matter annihilation emit synchrotron radiation in the galactic magnetic fields. The total synchrotron power—and hence the size of the predicted WMAP Haze signal—depends on whether these electrons can lose energy via non-synchrotron channels. Ref. [127] found that in order to be consistent with the large boost factors necessary to explain PAMELA/ATIC, one had to assume a larger rate for ICS compared to earlier Haze analyses [130]. Given the uncertainty in galactic starlight and the dark matter halo profile, it is consistent to conservatively ignore potential bounds from ICS, but since the WMAP Haze is one of the motivations for considering dark matter annihilation, strictly speaking one should verify that the assumed electron energy loss mechanisms can yield the WMAP Haze while satisfying ICS photon bounds.

That said, we do not expect much variation in the ICS bounds between direct and cascade annihilation scenarios. ICS is calculated from a steady state configuration of charged particles, so to the extent that the PAMELA/ATIC data already normalizes the steady state electron/positron densities, the ICS yield should be similar regardless of the annihilation scenario. Therefore, the recent analysis of Ref. [127] should be representative of generic multi-step cascade annihilation scenarios. This is similar in spirit to the WMAP Haze, in that the Haze requires a source of charged particles to generate the synchrotron signal, but the precise particle energy distribution has only a secondary effect.

Finally, there has also been recent suggestions [134, 135] of a possible tension between a dark matter annihilation interpretation of the WMAP Haze and bounds from 408 MHz radio observations in the inner $4''$ of the Milky Way [159]. Such bounds assume that the steep halo profiles necessary to generate the Haze at a latitudinal distance between 5° and 30° can be extrapolated to sub-parsec distances away from the galactic center. There are a number of reasons to distrust such an extreme extrapolation of the dark matter halo, including possible effects of baryons [160] and hierarchical mergers [161] to soften cuspy behavior. At minimum, N-body simulations [162] do not have resolution to such small scales. Therefore, we find no

reason to disfavor a dark matter annihilation scenario on the basis of the 408 MHz radio bound. Note that the analysis of Ref. [163] using an all-sky radio model [164] finds only relatively mild synchrotron constraints on TeV-scale dark matter after masking the inner $15^\circ \times 15^\circ$ of the galaxy.

5.5 Neutrino Constraints

When dark matter annihilates into muons, there is an irreducible source of neutrinos. Neutrinos produced in the galactic center oscillate as they travel towards earth, and if they are muon-type neutrinos when they collide with rock in the earth's crust, they can create an upward-going flux of muons. These muons could be observed by water Cerenkov detectors, and the absence of such observations puts bounds on the dark matter annihilation rate into muons. For muon cascades, there is no high energy neutrino source from dark matter that accretes in the sun and earth, because the muons from dark matter annihilation are stopped before they decay [165].

Since neutrinos have negligible energy losses as they traverse the galaxy, the muon-neutrino flux incident on earth is

$$\frac{d\Phi_{\nu_\mu}}{dE_\nu} = \sum_i P_{\nu_i\nu_\mu} \frac{B_{\nu,\text{astro}}}{8\pi\eta\, m_{\text{DM}}^2} \langle\sigma v\rangle \bar{J}\Delta\Omega \, \frac{dN_{\nu_i}}{dE}, \tag{5.18}$$

where i runs over the neutrino flavors, $B_{\nu,\text{astro}}$ is the astrophysical boost factor for the neutrino signal which could differ from $B_{e,\text{astro}}$, and $P_{\nu_i\nu_\mu}$ is the probability that ν_i has oscillated into ν_μ [115]:

$$P_{\nu_\mu\nu_\mu} = 0.39, \qquad P_{\nu_e\nu_\mu} = 0.21. \tag{5.19}$$

There is an analogous formula for $\bar{\nu}_\mu$, but in dark matter annihilations the ν_μ and $\bar{\nu}_\mu$ fluxes are equal. The primary neutrino spectra are given in Appendix B.1.2.

We now calculate the resulting upward-going muon flux following the analysis of Ref. [166]. An incident neutrino of energy E_ν creates muons of energy E_μ according to the neutrino-nucleon scattering cross sections $\sigma_{\nu N\to\mu X}$. For the propagation of created muons, we use an approximate energy loss parameterization

$$\frac{dE}{dL} = \rho_{\text{mat}}(-\alpha - \beta E), \tag{5.20}$$

with "standard rock" values $\alpha = 2\times10^{-6}$ TeV cm^2/g and $\beta = 4\times10^{-6}$ cm^2/g; ρ_{mat} will cancel in the final muon flux expression. In this approximation, a muon of starting energy E_μ can travel a distance

$$L(E_\mu, E_{\text{thres.}}) = \frac{1}{\rho_{\text{mat}}\beta} \ln\left(\frac{\alpha+\beta E_\mu}{\alpha+\beta E_{\text{thres.}}}\right) \tag{5.21}$$

before its energy drops below the muon detection threshold $E_{\text{thres.}}$.

	3°	5°	10°	15°	20°	25°	30°
Isothermal	10	10	9.7	9.0	8.2	7.4	6.6
NFW	340	190	84	51	35	26	20
Einasto	640	370	160	91	60	43	32
Super-K (95% C.L.)	2.70	4.82	6.43	10.6	11.2	17.6	19.5

Table 5.4: $\bar{J}$ values for neutrino observations in units of $\mathrm{GeV}^2\,\mathrm{cm}^{-6}\,\mathrm{kpc}$, and Super-K 95% C.L. flux limits in units of $10^{-15}\ \mathrm{cm}^{-2}\,\mathrm{s}^{-1}$.

For a given $d\Phi_{\nu_\mu}/dE_\nu$, the observed muon flux is

$$\Phi_\mu = \int_{E_{\rm thres.}}^{m_{\rm DM}} dE_\mu \int_{E_\mu}^{m_{\rm DM}} dE_\nu\, n_N \left(\frac{d\Phi_{\nu_\mu}}{dE_\nu} \frac{d\sigma_{\nu_\mu N\to\mu^- X}}{dE_\mu} + \frac{d\Phi_{\bar\nu_\mu}}{dE_\nu} \frac{d\sigma_{\bar\nu_\mu N\to\mu^+ X}}{dE_\mu} \right) L(E_\mu, E_{\rm thres.}), \tag{5.22}$$

where $n_N = \rho_{\rm mat}/m_N$ is the nucleon number density in the earth's crust, and N refers to an average nucleon. We calculate the neutrino-nucleon scattering cross sections assuming an equal fraction of protons and neutrons in rock, using CTEQ5M parton distribution functions [167] to include the effect of sea quarks, and retaining the full W boson propagator in the cross section.

Super-K [168] placed 90% confidence bounds on the upward-going muon flux [144] in various cone sizes ranging from 3° to 30° around the galactic center, with $E_{\rm thres.} = 1.6$ GeV. To be more conservative, we consider 95% confidence bounds [169], as shown in Table 5.4. The relevant values of $\bar{J}$ for the three dark matter halos in Eqs. (5.4, 5.5, 5.6) are also shown in Table 5.4. To derive a bound on the annihilation rate, we insist that the predicted flux does not exceed the 95% confidence bound for any of the Super-K cone sizes. The neutrino constraints for muon cascade scenarios appear in Figure 5.7, assuming a common boost factor for the electron, gamma ray, and neutrino signals.

As observed in Ref. [165], for sufficiently small dark matter masses, the observed muon flux is nearly independent of the dark matter mass. The reason is that both the neutrino-nucleon scattering cross section and the muon range scale like energy, but the dark matter number density squared (and hence the annihilation signal) scales like $1/m_{\rm DM}^2$, so the final observed flux is simply related to the normalized second-moment of the neutrino energy spectrum. Hence the exclusion limit for the neutrino boost factor is approximately flat in $m_{\rm DM}$ for small enough dark matter masses. As the dark matter mass increases, the average neutrino gets harder, and the neutrino-nucleon cross section grows less steeply because of the W boson propagator. In addition, the energy-dependent term in dE/dL begins to take effect, relaxing the neutrino bounds for high dark matter masses.

Summarizing the analysis of the neutrino constraints, we find:

- Since the neutrinos are softer in cascade annihilations, the bounds on the boost factor are weaker than for direct annihilation. However, the electrons are also softer in cascade

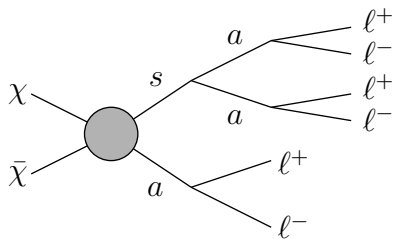

Figure 5.8: In the axion portal, fermionic dark matter annihilates dominantly into a scalar s and a pseudoscalar "axion" a. The scalar then decays as $s \to aa$, and the axion decays as $a \to \ell^+\ell^-$. In the minimal axion portal, the axion dominantly decays into muons, but in the leptonic axion portal it can dominantly decay into electrons. These models are partway between a 1-step and a 2-step cascade annihilation scenario.

annihilations, so the PAMELA/ATIC best fit mass and boost factor rise. Put together, the neutrino tension increases marginally as the number of cascade steps increase. For direct annihilation, our results agree qualitatively with [136, 137].

- Super-K considered solid angles as large as 30°, so a large fraction ($\simeq 30\%$ to $\simeq 70\%$) of the total dark matter annihilation signal is contained within the observed region. While the Einasto profile is less peaked than NFW toward the galactic center, the Einasto bound happens to be stronger because of the large integration region. For the NFW and Einasto profiles, the dominant bounds come from the 10° cone, while for the cored isothermal profile they come from the 30° cone.

- Since the gross structure of the dark matter halo is better understood than the halo density at the galactic center, the Super-K neutrino constraints are in some sense more robust than the H.E.S.S. gamma ray constraints. As in the case of gamma rays, the bounds are rather weak for the cored isothermal profile. They are, however, significantly stronger in the more realistic NFW and Einasto profiles. For cascade decays, the neutrino constraints are comparable to or stronger than the FSR gamma ray constraints, and highlight the tension in muon cascade scenarios. As with the gamma ray bounds, however, differences between the astrophysical boost factors $B_{e,\text{astro}}$ and $B_{\nu,\text{astro}}$ could alleviate the tension.

5.6 The Axion Portal

One well-motivated example of a cascade annihilation scenario is the axion portal [126]. In this scenario, dark matter is a TeV-scale particle that obtains a mass from spontaneous symmetry breaking. The spontaneous breaking of $U(1)_X$ yields a pseudoscalar "axion" a

	Minimal Axion Portal	Leptonic Axion Portal
Isothermal	7.9%	9.2%
NFW	7.9%	9.2%
Einasto	8.3%	8.8%

Table 5.5: The p-values for the best propagation model for each plot in Figure 5.9.

and a scalar "Higgs" s, and for fermionic dark matter the dominant annihilation channel is

$$\chi\bar{\chi} \to sa \tag{5.23}$$

($\chi\chi \to sa$ if χ is a Majorana fermion). The scalar s dominantly decays as $s \to aa$, and if standard model leptons carry axial $U(1)_X$ charges, then $a \to \ell^+\ell^-$. Since a is a pseudoscalar, helicity suppression implies a will decay into the heaviest kinematically allowed lepton, which we assume is either an electron or muon. An exchange of s can also provide the necessary enhancement of the annihilation cross section through the Sommerfeld and/or bound state effect. As shown in Figure 5.8, the axion portal effectively gives a one-and-a-half step cascade annihilation in the language used here.

The simplest model for the axion portal—the minimal axion portal—is obtained if we identify $U(1)_X$ with a Peccei-Quinn symmetry rotating two Higgs doublets. In this case, a has large hadronic couplings, and there are strong constraints on the axion mass from beam dump experiments and rare meson decays. Ref. [126] found that the preferred axion mass range was 360 MeV $\lesssim m_a \lesssim$ 800 MeV, in which case a preferentially decays into muons. In the analysis here, we also consider a variant of the axion portal—the leptonic axion portal—where only leptons are charged under $U(1)_X$. This possibility was mentioned in [126], and is described in more detail in Appendix B.2. Dark matter in this model annihilates through the axion a_ℓ associated with the leptonic symmetry, which does not have a coupling to hadrons. The absence of hadronic couplings allows the parameter range $2m_e < m_{a_\ell} < 2m_\mu$, so a_ℓ can preferentially decay into electrons. Note that the nonperturbative enhancement of the halo cross section is caused by the exchange of another scalar s_ℓ and not by the axion a_ℓ, so the bound of Ref. [170] does not exclude a_ℓ masses smaller than ≈ 100 MeV.

In Figure 5.9, we show the best fit values for $m_{\rm DM}$ and B for the PAMELA/ATIC data for the three different diffusion models and three different halo profiles. In Figure 5.10, we compare the best fit regions to FSR and neutrino constraints. Here we assume that B is common for electron, gamma ray, and neutrino signals, so that the same qualifications as Figures 5.6 and 5.7 apply. To account for the fact that smaller masses for a_ℓ are allowed, we are considering smaller values of m_{a_ℓ} in Figure 5.10 than those of m_1 in Figure 5.6. For completeness, we also show the best fit spectra to the PAMELA and ATIC data in Figure 5.11, and the p-values of the fit in Table 5.5. As expected, the best fit values and qualitative features of the plots are partway between a 1-step and a 2-step cascade scenario.

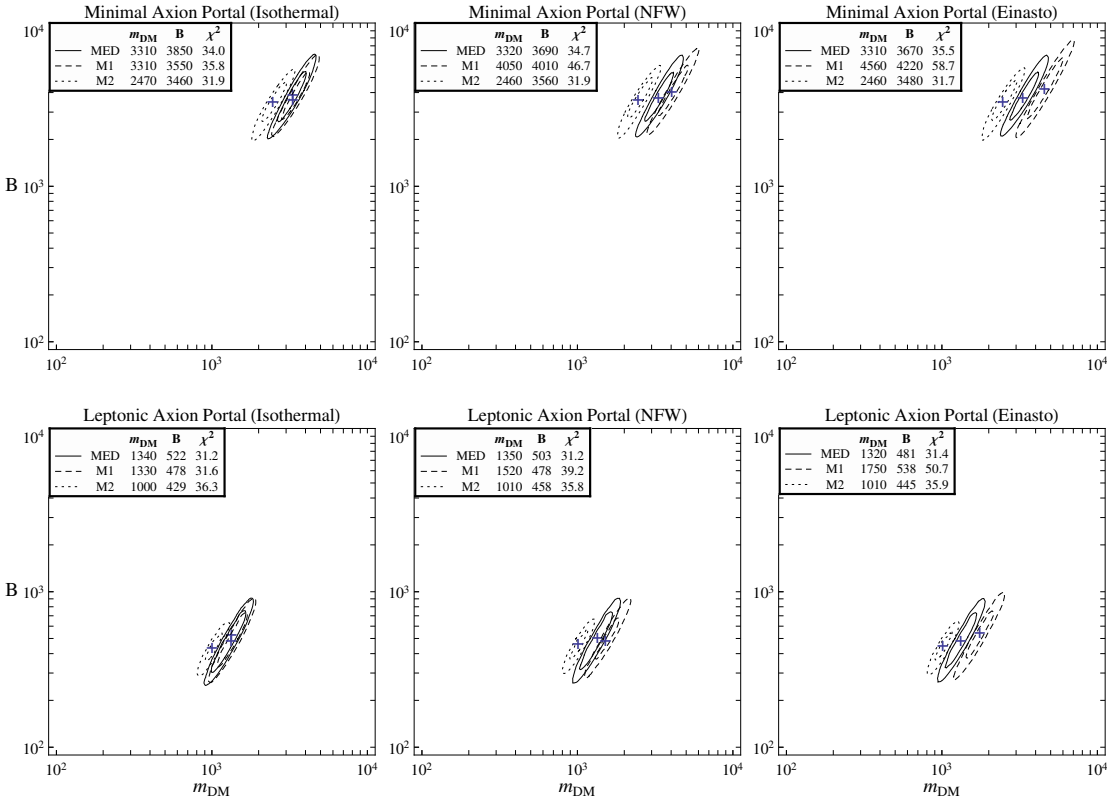

Figure 5.9: The best fit regions for the dark matter mass $m_{\rm DM}$ and boost factor B in the minimal axion portal (top row, $a \to \mu^+\mu^-$) and leptonic axion portal (bottom row, $a_\ell \to e^+e^-$) for different halo profiles and propagation models. The best fit values are indicated by the crosses, and the contours are for 1σ and 2σ.

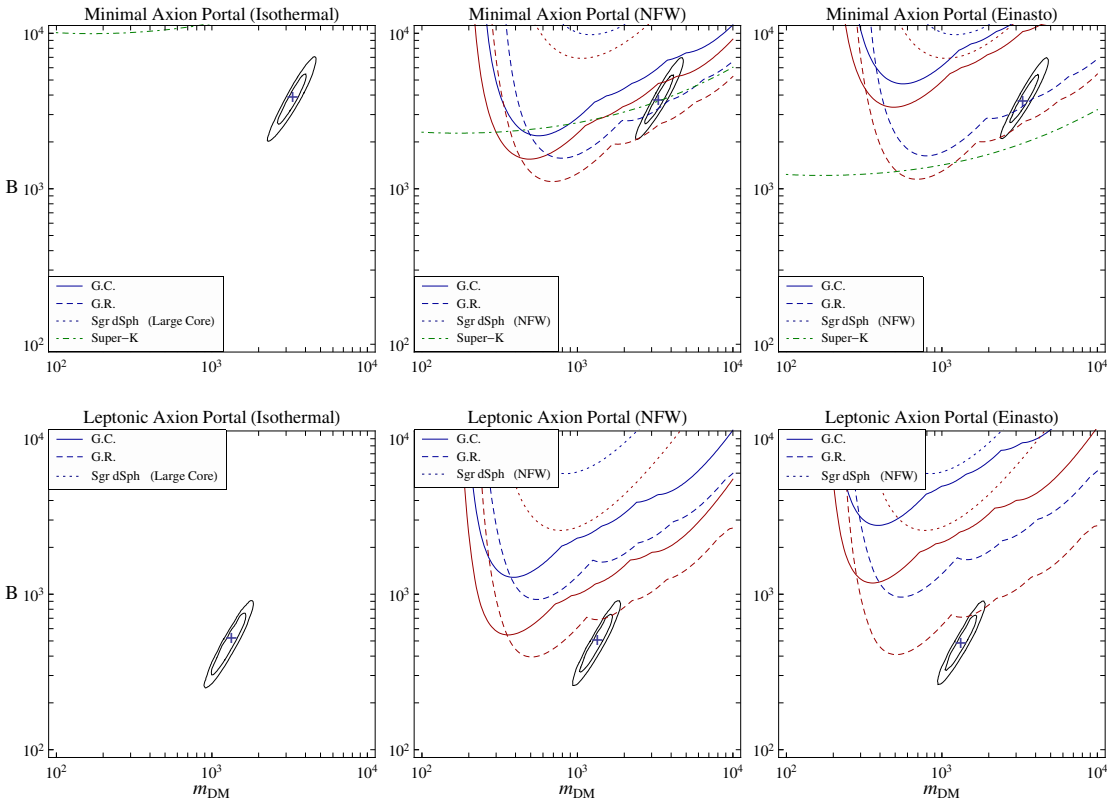

Figure 5.10: Constraints from gamma ray, GC (solid), GR (dashed), and Sgr dSph (dotted), and neutrino (dot-dashed) observations in the $m_{\rm DM}$-B plane in the minimal axion portal (top row, $a \to \mu^+\mu^-$) and leptonic axion portal (bottom row, $a_\ell \to e^+e^-$). All the constraints, as well as the best fit region for PAMELA/ATIC (MED propagation), are plotted assuming that B is common. Each of the GC, GR, and Sgr dSph constraints consist of two curves. For the minimal axion portal, the upper (blue) curve is $m_a = 600$ MeV and the lower (red) curve is $m_a = 1$ GeV. For the leptonic axion portal, the upper (blue) curve is $m_{a_\ell} = 10$ MeV and the lower (red) curve is $m_{a_\ell} = 100$ MeV, which differs from the choice in Figure 5.6. Note that the constraint lines in the cored isothermal case are above the plot region, and that the halo profiles for Sgr dSph are given in the legends.

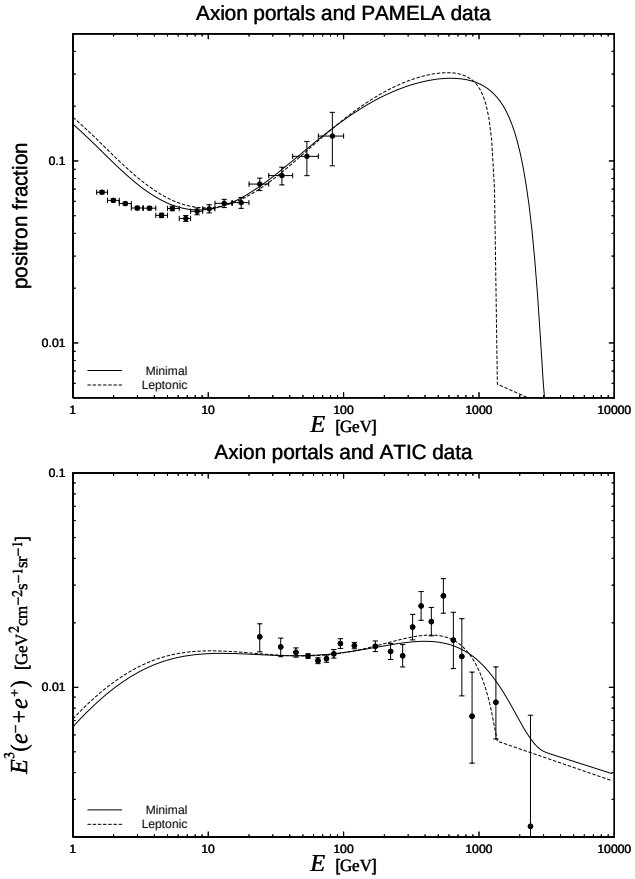

Figure 5.11: The predicted $e^{\pm}$ intensities compared to the PAMELA (left) and ATIC (right) data for the minimal axion portal (solid, $a \to \mu^+\mu^-$) and leptonic axion portal (dashed, $a_\ell \to e^+e^-$). The NFW halo profile and the MED propagation model are chosen, and the $e^{\pm}$ backgrounds are marginalized as described in Eq. (5.11). Note that we fit the PAMELA data only for $E \gtrsim 10$ GeV because solar modulation effects are important at lower energies.

$\mathrm{Br}(a \to \gamma\gamma)$	GC	GR	Sgr dSph
NFW Best	$2.2 \cdot 10^{-3}$	$1.1 \cdot 10^{-3}$	$2.5 \cdot 10^{-2}$
Einasto Best	$4.8 \cdot 10^{-3}$	$1.2 \cdot 10^{-3}$	—
$\mathrm{Br}(a \to \pi^+\pi^-\pi^0)$	GC	GR	Sgr dSph
NFW Best	$1.3 \cdot 10^{-2}$	$7.5 \cdot 10^{-3}$	$5.2 \cdot 10^{-2}$
Einasto Best	$3.0 \cdot 10^{-2}$	$7.9 \cdot 10^{-3}$	—

Table 5.6: Bounds from gamma rays on the branching fractions of $a \to \gamma\gamma$ and $a \to \pi^+\pi^-\pi^0$ in the minimal axion portal ($a \to \mu^+\mu^-$). These are obtained neglecting all other sources of gamma rays and correspond to the best fit values for m_{DM} and B and the propagation model giving smallest χ^2. The bounds assume an equal boost factor for $e^\pm$ and gamma rays, and should be multiplied by $B_{e,\mathrm{astro}}/B_{\gamma,\mathrm{astro}}$ if the boost factors differ.

$\mathrm{Br}(a_\ell \to \gamma\gamma)$	GC	GR	Sgr dSph
NFW Best	$8.2 \cdot 10^{-3}$	$4.6 \cdot 10^{-3}$	$6.5 \cdot 10^{-2}$
Einasto Best	$1.8 \cdot 10^{-2}$	$4.9 \cdot 10^{-3}$	—

Table 5.7: The same as Table 5.6, but for the leptonic axion portal ($a_\ell \to e^+e^-$). The $a \to \pi^+\pi^-\pi^0$ mode is irrelevant in this case.

Depending on the axion mass, there are also potential gamma ray constraints from rare $a \to \gamma\gamma$ and $a \to \pi^+\pi^-\pi^0$ decay modes, and we can place bounds on the branching fractions to these modes. The $a \to \gamma\gamma$ mode is potentially dangerous for the entire axion mass range, but the $a \to \pi^+\pi^-\pi^0$ mode only when $m_a > 3m_\pi$. The gamma ray spectra for these rare decays are given in Appendix B.1.5. For each halo profile and for the three H.E.S.S. data sets, we turn off FSR and find the values of the branching ratios where the H.E.S.S. bound is saturated for the best fit values of m_{DM} and B and the best propagation model (assuming B is common for $e^\pm$ and gamma rays).

The branching ratio bounds are shown in Tables 5.6 and 5.7. The constraints from Sgr dSph match the estimates in [126], but the GC and GR data imply a factor of 5–10 stronger bound. In the minimal axion portal, $\mathrm{Br}(a \to \gamma\gamma) \sim 10^{-5}$–$10^{-4}$, which is safe from the bounds. There is somewhat more tension for $a \to \pi^+\pi^-\pi^0$ where the estimated branching fraction was $\sim 10^{-2}$. Note, however, that the constraints from the GC and GR data are weak for any halo profile relatively flat within about 100 pc of the galactic center. In particular, there is no meaningful branching ratio constraint for the cored isothermal profile in Eq. (5.4).

Gamma ray and radio bounds on the axion portal were also considered in Ref. [135], where potential $s \to b\bar{b}$ and $s \to \tau^+\tau^-$ decay modes were included. Since these additional s decay modes depend on details of the model, we do not consider them here. For FSR gamma rays, our results and conclusions agree qualitatively with [135]. As mentioned already, we do not consider 408 MHz radio observations to place any meaningful constraint on the axion

portal.

5.7 Conclusions

The possibility of indirect detection of dark matter has been considered for over 25 years [171], but the annihilation rates expected from WIMP thermal relics are typically too small to give appreciable gamma ray or neutrino fluxes from the galactic center unless a very peaked dark matter halo profile is assumed. If the PAMELA/ATIC data is indicative of dark matter annihilation, however, then the galactic annihilation rate must be boosted by $O(1000)$. This large boost factor considerably enhances the potential for galactic gamma ray and neutrino signals from the dark sector. In this context, hints from the WMAP Haze may also point towards an annihilation explanation of PAMELA/ATIC.

In this chapter, we have explored the robustness of dark matter annihilation predictions by considering cascade scenarios where dark matter annihilates into new resonances that in turn decay in one or more steps into standard model leptons. These cascade annihilation scenarios are directly motivated by the PAMELA/ATIC data, since light resonances can enhance the galactic annihilation rate through nonperturbative effects and explain the lepton-richness of the annihilation through kinematic thresholds.

We have shown that electron and muon cascades give reasonable fits to the PAMELA/ATIC data. As a rule of thumb, the best fit dark matter mass and boost factor both scale as 2^n for n-step cascade decays. We then compared these best fit values to constraints from gamma rays and neutrinos. The gamma ray bounds from FSR can be weakened by an order of magnitude through cascade decays, although increasing the length of cascades does not further weaken the bounds. Neutrino bounds for dark matter annihilating into muons are robust to changing the length of the cascade, which is particularly relevant for models with large branching fractions to muons such as the minimal axion portal.

Assuming standard NFW or Einasto halo profiles, there is tension between a dark matter annihilation interpretation of PAMELA/ATIC and the non-observation of galactic gamma rays or neutrinos. Such tension does not invalidate a dark matter annihilation hypothesis since there is considerable uncertainty in the dark matter halo distribution and velocity profile, and the constraints are uniformly weaker for shallower halo profiles. For gamma rays in particular, the galactic center and galactic ridge constraints assume an understanding of the dark matter halo profile in the inner 100 pc of the galaxy, where there is considerable uncertainty. The dark matter halo profile in the inner $4''$ of the galaxy is even more uncertain, so we do not consider radio measurements of synchrotron to be constraining. Also, for both gamma rays and neutrinos, the bounds can be weakened if the astrophysical boost factor for electrons/positrons is larger than those for gamma rays and neutrinos.

If a dark matter annihilation scenario is realized in nature with the boost factor suggested by PAMELA/ATIC, then one would expect future experiments to see a gamma ray or neutrino flux given standard halo assumptions. ANTARES [172], IceCube [173], and KM3NeT [174] will greatly increase current sensitivity to upward-going muons resulting

from galactic neutrinos. Future atmospheric Cerenkov telescopes as envisioned in Ref. [175] will also improve the prospects of finding gamma rays from dark matter annihilation. While we did not include the effect of ICS in our gamma ray analysis, ICS is expected to be a dominant dark matter annihilation signal in the energy range available to the Fermi Gamma-ray Space Telescope [176]. Ultimately, one hopes that future experiments could probe the detailed energy spectra of dark matter annihilation products to distinguish between direct annihilation and the cascade scenarios considered here.

Note added: When this chapter was first written, we became aware of Ref. [177] which considers similar issues.

Bibliography

[1] S. Glashow, "Towards a unied theory - threads in a tapestry.". Nobel Lecture, December 8, 1979.

[2] A. Salam, "Gauge unication of fundamental forces.". Nobel Lecture, December 8, 1979.

[3] S. Weinberg, "Conceptual foundations of the unied theory of weak and electromagnetic interactions.". Nobel Lecture, December 8, 1979.

[4] P. W. Higgs, "Broken symmetries, massless particles and gauge fields," *Phys. Lett.* **12** (1964) 132–133.

[5] E. Komatsu *et al.*, "Seven-Year Wilkinson Microwave Anisotropy Probe (WMAP) Observations: Cosmological Interpretation," `arXiv:1001.4538 [astro-ph.CO]`.

[6] H. Murayama, "Physics Beyond the Standard Model and Dark Matter," `arXiv:0704.2276 [hep-ph]`. And references therein.

[7] S. P. Martin, "A Supersymmetry Primer," `arXiv:hep-ph/9709356`.

[8] M. Dine and W. Fischler, "A Phenomenological Model of Particle Physics Based on Supersymmetry," *Phys. Lett.* **B110** (1982) 227.

[9] M. Dine, A. E. Nelson, and Y. Shirman, "Low-energy dynamical supersymmetry breaking simplified," *Phys. Rev.* **D51** (1995) 1362–1370, `arXiv:hep-ph/9408384`.

[10] A. H. Chamseddine, R. L. Arnowitt, and P. Nath, "Locally Supersymmetric Grand Unification," *Phys. Rev. Lett.* **49** (1982) 970.

[11] P. Picozza *et al.*, "PAMELA - A Payload for Antimatter Matter Exploration and Light-nuclei Astrophysics," *Astropart. Phys.* **27** (2007) 296–315, `arXiv:astro-ph/0608697`.

[12] T. G. Guzik *et al.*, "The ATIC long duration balloon project," *Adv. Space Res.* **33** (2004) 1763–1770.

[13] **PAMELA** Collaboration, O. Adriani *et al.*, "An anomalous positron abundance in cosmic rays with energies 1.5.100 GeV," *Nature* **458** (2009) 607–609, arXiv:0810.4995 [astro-ph].

[14] J. Chang *et al.*, "An excess of cosmic ray electrons at energies of 300.800 GeV," *Nature* **456** (2008) 362–365.

[15] Y. Nomura, M. Papucci, and D. Stolarski, "Flavorful Supersymmetry," *Phys. Rev.* **D77** (2008) 075006, arXiv:0712.2074 [hep-ph].

[16] R. Kitano and Y. Nomura, "Supersymmetry with small mu: Connections between naturalness, dark matter, and (possibly) flavor," arXiv:hep-ph/0606134.

[17] A. Pomarol and D. Tommasini, "Horizontal symmetries for the supersymmetric flavor problem," *Nucl. Phys.* **B466** (1996) 3–24, arXiv:hep-ph/9507462.

[18] L. J. Hall, V. A. Kostelecky, and S. Raby, "New Flavor Violations in Supergravity Models," *Nucl. Phys.* **B267** (1986) 415.

[19] L. J. Hall, H. Murayama, and N. Weiner, "Neutrino mass anarchy," *Phys. Rev. Lett.* **84** (2000) 2572–2575, arXiv:hep-ph/9911341.

[20] F. Gabbiani, E. Gabrielli, A. Masiero, and L. Silvestrini, "A complete analysis of FCNC and CP constraints in general SUSY extensions of the standard model," *Nucl. Phys.* **B477** (1996) 321–352, arXiv:hep-ph/9604387.

[21] M. Ibe and R. Kitano, "Sweet Spot Supersymmetry," *JHEP* **08** (2007) 016, arXiv:0705.3686 [hep-ph].

[22] A. Collaboration, "ATLAS: Detector and physics performance technical design report. Volume 1,". CERN-LHCC-99-14.

[23] A. De Roeck *et al.*, "Supersymmetric benchmarks with non-universal scalar masses or gravitino dark matter," *Eur. Phys. J.* **C49** (2007) 1041–1066, arXiv:hep-ph/0508198.

[24] K. Hamaguchi, M. M. Nojiri, and A. de Roeck, "Prospects to study a long-lived charged next lightest supersymmetric particle at the LHC," *JHEP* **03** (2007) 046, arXiv:hep-ph/0612060.

[25] I. Hinchliffe and F. E. Paige, "Measurements in gauge mediated SUSY breaking models at LHC," *Phys. Rev.* **D60** (1999) 095002, arXiv:hep-ph/9812233.

[26] K. Hamaguchi, Y. Kuno, T. Nakaya, and M. M. Nojiri, "A study of late decaying charged particles at future colliders," *Phys. Rev.* **D70** (2004) 115007, arXiv:hep-ph/0409248.

[27] W. Buchmuller, K. Hamaguchi, M. Ratz, and T. Yanagida, "Supergravity at colliders," *Phys. Lett.* **B588** (2004) 90–98, arXiv:hep-ph/0402179.

[28] K. Hamaguchi and A. Ibarra, "Probing lepton flavour violation in slepton NLSP scenarios," *JHEP* **02** (2005) 028, arXiv:hep-ph/0412229.

[29] C. G. Lester and D. J. Summers, "Measuring masses of semiinvisibly decaying particles pair produced at hadron colliders," *Phys. Lett.* **B463** (1999) 99–103, arXiv:hep-ph/9906349.

[30] A. Bartl *et al.*, "Test of lepton flavour violation at LHC," *Eur. Phys. J.* **C46** (2006) 783–789, arXiv:hep-ph/0510074.

[31] **CMS** Collaboration, G. L. Bayatian *et al.*, "CMS technical design report, volume II: Physics performance," *J. Phys.* **G34** (2007) 995–1579.

[32] J. L. Feng, C. G. Lester, Y. Nir, and Y. Shadmi, "The Standard Model and Supersymmetric Flavor Puzzles at the Large Hadron Collider," *Phys. Rev.* **D77** (2008) 076002, arXiv:0712.0674 [hep-ph].

[33] Y. Nomura, M. Papucci, and D. Stolarski, "Flavorful Supersymmetry from Higher Dimensions," *JHEP* **07** (2008) 055, arXiv:0802.2582 [hep-ph].

[34] N. Arkani-Hamed and M. Schmaltz, "Hierarchies without symmetries from extra dimensions," *Phys. Rev.* **D61** (2000) 033005, arXiv:hep-ph/9903417.

[35] D. E. Kaplan and T. M. P. Tait, "Supersymmetry breaking, fermion masses and a small extra dimension," *JHEP* **06** (2000) 020, arXiv:hep-ph/0004200.

[36] L. J. Hall and Y. Nomura, "A complete theory of grand unification in five dimensions," *Phys. Rev.* **D66** (2002) 075004, arXiv:hep-ph/0205067.

[37] H. Abe, K. Choi, K.-S. Jeong, and K.-i. Okumura, "Scherk-Schwarz supersymmetry breaking for quasi-localized matter fields and supersymmetry flavor violation," *JHEP* **09** (2004) 015, arXiv:hep-ph/0407005.

[38] Y. Kawamura, "Triplet-doublet splitting, proton stability and extra dimension," *Prog. Theor. Phys.* **105** (2001) 999–1006, arXiv:hep-ph/0012125.

[39] L. J. Hall and Y. Nomura, "Gauge unification in higher dimensions," *Phys. Rev.* **D64** (2001) 055003, arXiv:hep-ph/0103125.

[40] L. J. Hall, Y. Nomura, and D. Tucker-Smith, "Gauge-Higgs unification in higher dimensions," *Nucl. Phys.* **B639** (2002) 307–330, arXiv:hep-ph/0107331.

[41] A. Hebecker and J. March-Russell, "The flavour hierarchy and see-saw neutrinos from bulk masses in 5d orbifold GUTs," *Phys. Lett.* **B541** (2002) 338–345, arXiv:hep-ph/0205143.

[42] Y. Nomura, "Strongly coupled grand unification in higher dimensions," *Phys. Rev.* **D65** (2002) 085036, arXiv:hep-ph/0108170.

[43] L. J. Hall and Y. Nomura, "Gauge coupling unification from unified theories in higher dimensions," *Phys. Rev.* **D65** (2002) 125012, arXiv:hep-ph/0111068.

[44] Y. Nomura and M. Papucci, "A Simple and Realistic Model of Supersymmetry Breaking," *Phys. Lett.* **B661** (2008) 145–153, arXiv:0709.4060 [hep-ph].

[45] G. F. Giudice and A. Masiero, "A Natural Solution to the mu Problem in Supergravity Theories," *Phys. Lett.* **B206** (1988) 480–484.

[46] N. Arkani-Hamed, T. Gregoire, and J. G. Wacker, "Higher dimensional supersymmetry in 4D superspace," *JHEP* **03** (2002) 055, arXiv:hep-th/0101233.

[47] A. Manohar and H. Georgi, "Chiral Quarks and the Nonrelativistic Quark Model," *Nucl. Phys.* **B234** (1984) 189.

[48] R. Kitano, "Gravitational gauge mediation," *Phys. Lett.* **B641** (2006) 203–207, arXiv:hep-ph/0607090.

[49] G. F. Giudice and R. Rattazzi, "Extracting Supersymmetry-Breaking Effects from Wave- Function Renormalization," *Nucl. Phys.* **B511** (1998) 25–44, arXiv:hep-ph/9706540.

[50] M. Ibe and R. Kitano, "Sweet Spot Supersymmetry and Composite Messengers," *Phys. Lett.* **B663** (2008) 242–246, arXiv:0710.3796 [hep-ph].

[51] R. D. Peccei and H. R. Quinn, "CP Conservation in the Presence of Instantons," *Phys. Rev. Lett.* **38** (1977) 1440–1443.

[52] **Super-Kamiokande** Collaboration, M. Shiozawa *et al.*, "Search for Proton Decay via p -¿ e+ pi0 in a Large Water Cherenkov Detector," *Phys. Rev. Lett.* **81** (1998) 3319–3323, arXiv:hep-ex/9806014.

[53] K.-w. Choi, I.-W. Kim, and W. Y. Song, "Flavor hierarchy from extra dimension and gauge threshold correction," *Nucl. Phys.* **B687** (2004) 101–123, arXiv:hep-ph/0307365.

[54] S. Ambrosanio, B. Mele, S. Petrarca, G. Polesello, and A. Rimoldi, "Measuring the SUSY breaking scale at the LHC in the slepton NLSP scenario of GMSB models," *JHEP* **01** (2001) 014, arXiv:hep-ph/0010081.

[55] Y. Nomura, D. Poland, and B. Tweedie, "Holographic Grand Unification," *JHEP* **12** (2006) 002, arXiv:hep-ph/0605014.

[56] K.-w. Choi and I.-W. Kim, "One loop gauge couplings in AdS(5)," *Phys. Rev.* **D67** (2003) 045005, arXiv:hep-th/0208071.

[57] Y. Nomura and D. Stolarski, "Naturally Flavorful Supersymmetry at the LHC," *Phys. Rev.* **D78** (2008) 095011, arXiv:0808.1380 [hep-ph].

[58] S. Dimopoulos and H. Georgi, "Softly Broken Supersymmetry and SU(5)," *Nucl. Phys.* **B193** (1981) 150.

[59] R. Barbieri, S. Ferrara, and C. A. Savoy, "Gauge Models with Spontaneously Broken Local Supersymmetry," *Phys. Lett.* **B119** (1982) 343.

[60] L. J. Hall, J. D. Lykken, and S. Weinberg, "Supergravity as the Messenger of Supersymmetry Breaking," *Phys. Rev.* **D27** (1983) 2359–2378.

[61] M. Dine and W. Fischler, "A Supersymmetric GUT," *Nucl. Phys.* **B204** (1982) 346.

[62] L. Alvarez-Gaume, M. Claudson, and M. B. Wise, "Low-Energy Supersymmetry," *Nucl. Phys.* **B207** (1982) 96.

[63] S. Dimopoulos and S. Raby, "Geometric Hierarchy," *Nucl. Phys.* **B219** (1983) 479.

[64] M. Dine, A. E. Nelson, Y. Nir, and Y. Shirman, "New tools for low-energy dynamical supersymmetry breaking," *Phys. Rev.* **D53** (1996) 2658–2669, arXiv:hep-ph/9507378.

[65] D. E. Kaplan, G. D. Kribs, and M. Schmaltz, "Supersymmetry breaking through transparent extra dimensions," *Phys. Rev.* **D62** (2000) 035010, arXiv:hep-ph/9911293.

[66] Z. Chacko, M. A. Luty, A. E. Nelson, and E. Ponton, "Gaugino mediated supersymmetry breaking," *JHEP* **01** (2000) 003, arXiv:hep-ph/9911323.

[67] M. Dine, R. G. Leigh, and A. Kagan, "Flavor symmetries and the problem of squark degeneracy," *Phys. Rev.* **D48** (1993) 4269–4274, arXiv:hep-ph/9304299.

[68] P. Pouliot and N. Seiberg, "(S)quark masses and nonAbelian horizontal symmetries," *Phys. Lett.* **B318** (1993) 169–173, arXiv:hep-ph/9308363.

[69] R. Barbieri, G. R. Dvali, and L. J. Hall, "Predictions From A U(2) Flavour Symmetry In Supersymmetric Theories," *Phys. Lett.* **B377** (1996) 76–82, arXiv:hep-ph/9512388.

[70] R. Barbieri, L. J. Hall, S. Raby, and A. Romanino, "Unified theories with U(2) flavor symmetry," *Nucl. Phys.* **B493** (1997) 3–26, arXiv:hep-ph/9610449.

[71] R. Barbieri, L. J. Hall, and A. Romanino, "Consequences of a U(2) flavour symmetry," *Phys. Lett.* **B401** (1997) 47–53, arXiv:hep-ph/9702315.

[72] Y. Nir and N. Seiberg, "Should squarks be degenerate?," *Phys. Lett.* **B309** (1993) 337–343, arXiv:hep-ph/9304307.

[73] M. Leurer, Y. Nir, and N. Seiberg, "Mass matrix models: The Sequel," *Nucl. Phys.* **B420** (1994) 468–504, arXiv:hep-ph/9310320.

[74] Y. Grossman and Y. Nir, "Lepton mass matrix models," *Nucl. Phys.* **B448** (1995) 30–50, arXiv:hep-ph/9502418.

[75] J. L. Feng, Y. Nir, and Y. Shadmi, "Neutrino parameters, Abelian flavor symmetries, and charged lepton flavor violation," *Phys. Rev.* **D61** (2000) 113005, arXiv:hep-ph/9911370.

[76] Z. Berezhiani, "Unified picture of the particle and sparticle masses in SUSY GUT," *Phys. Lett.* **B417** (1998) 287–296, arXiv:hep-ph/9609342.

[77] S. F. King and G. G. Ross, "Fermion masses and mixing angles from SU(3) family symmetry," *Phys. Lett.* **B520** (2001) 243–253, arXiv:hep-ph/0108112.

[78] S. F. King and G. G. Ross, "Fermion masses and mixing angles from SU(3) family symmetry and unification," *Phys. Lett.* **B574** (2003) 239–252, arXiv:hep-ph/0307190.

[79] G. G. Ross, L. Velasco-Sevilla, and O. Vives, "Spontaneous CP violation and non-Abelian family symmetry in SUSY," *Nucl. Phys.* **B692** (2004) 50–82, arXiv:hep-ph/0401064.

[80] S. Antusch, S. F. King, and M. Malinsky, "Solving the SUSY Flavour and CP Problems with SU(3) Family Symmetry," *JHEP* **06** (2008) 068, arXiv:0708.1282 [hep-ph].

[81] L. Calibbi, J. Jones-Perez, and O. Vives, "Electric dipole moments from flavoured CP violation in SUSY," *Phys. Rev.* **D78** (2008) 075007, arXiv:0804.4620 [hep-ph].

[82] D. B. Kaplan and M. Schmaltz, "Flavor unification and discrete nonAbelian symmetries," *Phys. Rev.* **D49** (1994) 3741–3750, arXiv:hep-ph/9311281.

[83] L. J. Hall and H. Murayama, "A Geometry of the generations," *Phys. Rev. Lett.* **75** (1995) 3985–3988, arXiv:hep-ph/9508296.

[84] K. Hamaguchi, M. Kakizaki, and M. Yamaguchi, "Democratic (s)fermions and lepton flavor violation," *Phys. Rev.* **D68** (2003) 056007, arXiv:hep-ph/0212172.

[85] A. E. Nelson and M. J. Strassler, "Suppressing flavor anarchy," *JHEP* **09** (2000) 030, arXiv:hep-ph/0006251.

[86] A. E. Nelson and M. J. Strassler, "Exact results for supersymmetric renormalization and the supersymmetric flavor problem," *JHEP* **07** (2002) 021, arXiv:hep-ph/0104051.

[87] T. Kobayashi and H. Terao, "Sfermion masses in Nelson-Strassler type of models: SUSY standard models coupled with SCFTs," *Phys. Rev.* **D64** (2001) 075003, arXiv:hep-ph/0103028.

[88] T. Kobayashi, H. Nakano, T. Noguchi, and H. Terao, "Sfermion mass degeneracy, superconformal dynamics and supersymmetric grand unified theories," *Phys. Rev.* **D66** (2002) 095011, arXiv:hep-ph/0202023.

[89] D. E. Kaplan and T. M. P. Tait, "New tools for fermion masses from extra dimensions," *JHEP* **11** (2001) 051, arXiv:hep-ph/0110126.

[90] K.-w. Choi, D. Y. Kim, I.-W. Kim, and T. Kobayashi, "Supersymmetry breaking in warped geometry," *Eur. Phys. J.* **C35** (2004) 267–275, arXiv:hep-ph/0305024.

[91] K. Choi, K. S. Jeong, and K.-I. Okumura, "Flavor and CP conserving moduli mediated SUSY breaking in flux compactification," *JHEP* **07** (2008) 047, arXiv:0804.4283 [hep-ph].

[92] M. Dugan, B. Grinstein, and L. J. Hall, "CP Violation in the Minimal N=1 Supergravity Theory," *Nucl. Phys.* **B255** (1985) 413.

[93] R. Kuchimanchi, "Solution to the Strong CP Problem: Supersymmetry with Partiy," *Phys. Rev. Lett.* **76** (1996) 3486–3489, arXiv:hep-ph/9511376.

[94] Y. Nir and R. Rattazzi, "Solving the Supersymmetric CP Problem with Abelian Horizontal Symmetries," *Phys. Lett.* **B382** (1996) 363–368, arXiv:hep-ph/9603233.

[95] **MEGA** Collaboration, M. L. Brooks *et al.*, "New Limit for the Family-Number Non-conserving Decay mu+ to e+ gamma," *Phys. Rev. Lett.* **83** (1999) 1521–1524, arXiv:hep-ex/9905013.

[96] B. C. Regan, E. D. Commins, C. J. Schmidt, and D. DeMille, "New limit on the electron electric dipole moment," *Phys. Rev. Lett.* **88** (2002) 071805.

[97] C. A. Baker *et al.*, "An improved experimental limit on the electric dipole moment of the neutron," *Phys. Rev. Lett.* **97** (2006) 131801, arXiv:hep-ex/0602020.

[98] M. V. Romalis, W. C. Griffith, and E. N. Fortson, "A new limit on the permanent electric dipole moment of Hg- 199," *Phys. Rev. Lett.* **86** (2001) 2505–2508, arXiv:hep-ex/0012001.

[99] S. Abel, S. Khalil, and O. Lebedev, "EDM constraints in supersymmetric theories," *Nucl. Phys.* **B606** (2001) 151–182, arXiv:hep-ph/0103320.

[100] T. Falk, K. A. Olive, M. Pospelov, and R. Roiban, "MSSM predictions for the electric dipole moment of the Hg- 199 atom," *Nucl. Phys.* **B560** (1999) 3–22, arXiv:hep-ph/9904393.

[101] T. Moroi *et al.*, "Research proposal to psi,". R-99-5.

[102] Y. Kuno, "Lepton flavor violation in muon coherent scattering on nuclei: Muon to electron conversion," *Nucl. Phys. Proc. Suppl.* **168** (2007) 353–355.

[103] Y. Kuno, "PRISM/PRIME," *Nucl. Phys. Proc. Suppl.* **149** (2005) 376–378.

[104] B. Bernstein *et al.*, "mu2e collaboration.". http://mu2e.fnal.gov

[105] D. Kawall, F. Bay, S. Bickman, Y. Jiang, and D. DeMille, "Progress towards measuring the electric dipole moment of the electron in metastable PbO," *AIP Conf. Proc.* **698** (2004) 192–195.

[106] J. J. Hudson, B. E. Sauer, M. R. Tarbutt, and E. A. Hinds, "Measurement of the electron electric dipole moment using YbF molecules," *Phys. Rev. Lett.* **89** (2002) 023003, arXiv:hep-ex/0202014.

[107] S. K. Lamoreaux, "Solid state systems for electron electric dipole moment and other fundamental measurements," *Phys. Rev.* **A66** (2002) 022109, arXiv:nucl-ex/0109014.

[108] T. M. Ito, "Plans for a neutron EDM experiment at SNS," *J. Phys. Conf. Ser.* **69** (2007) 012037, arXiv:nucl-ex/0702024.

[109] **EDM** Collaboration, Y. K. Semertzidis *et al.*, "A new method for a sensitive deuteron EDM experiment," *AIP Conf. Proc.* **698** (2004) 200–204, arXiv:hep-ex/0308063.

[110] J. L. Feng, K. T. Matchev, and Y. Shadmi, "Theoretical Expectations for the Muon's Electric Dipole Moment," *Nucl. Phys.* **B613** (2001) 366–381, arXiv:hep-ph/0107182.

[111] S. Hamidi and C. Vafa, "Interactions on Orbifolds," *Nucl. Phys.* **B279** (1987) 465.

[112] T. Gherghetta, "Partly supersymmetric grand unification," *Phys. Rev.* **D71** (2005) 065001, arXiv:hep-ph/0411090.

[113] C. D. Froggatt and H. B. Nielsen, "Hierarchy of Quark Masses, Cabibbo Angles and CP Violation," *Nucl. Phys.* **B147** (1979) 277.

[114] L. Randall and R. Sundrum, "A large mass hierarchy from a small extra dimension," *Phys. Rev. Lett.* **83** (1999) 3370–3373, arXiv:hep-ph/9905221.

[115] **Particle Data Group** Collaboration, C. Amsler *et al.*, "Review of particle physics," *Phys. Lett.* **B667** (2008) 1.

[116] H. Fusaoka and Y. Koide, "Updated estimate of running quark masses," *Phys. Rev.* **D57** (1998) 3986–4001, arXiv:hep-ph/9712201.

[117] M. Drees, "Intermediate Scale Symmetry Breaking and the Spectrum of Super Partners in Superstring Inspired Supergravity Models," *Phys. Lett.* **B181** (1986) 279.

[118] T. Kobayashi, H. Nakano, H. Terao, and K. Yoshioka, "Flavor violation in supersymmetric theories with gauged flavor symmetries," *Prog. Theor. Phys.* **110** (2003) 247–267, arXiv:hep-ph/0211347.

[119] S. Dimopoulos, M. Dine, S. Raby, and S. D. Thomas, "Experimental Signatures of Low Energy Gauge Mediated Supersymmetry Breaking," *Phys. Rev. Lett.* **76** (1996) 3494–3497, arXiv:hep-ph/9601367.

[120] B. C. Allanach, J. P. Conlon, and C. G. Lester, "Measuring Smuon-Selectron Mass Splitting at the CERN LHC and Patterns of Supersymmetry Breaking," *Phys. Rev.* **D77** (2008) 076006, arXiv:0801.3666 [hep-ph].

[121] J. Mardon, Y. Nomura, D. Stolarski, and J. Thaler, "Dark Matter Signals from Cascade Annihilations," *JCAP* **0905** (2009) 016, arXiv:0901.2926 [hep-ph].

[122] D. Hooper, P. Blasi, and P. D. Serpico, "Pulsars as the Sources of High Energy Cosmic Ray Positrons," *JCAP* **0901** (2009) 025, arXiv:0810.1527 [astro-ph].

[123] P.-f. Yin *et al.*, "PAMELA data and leptonically decaying dark matter," *Phys. Rev.* **D79** (2009) 023512, arXiv:0811.0176 [hep-ph].

[124] M. Cirelli, M. Kadastik, M. Raidal, and A. Strumia, "Model-independent implications of the e+, e-, anti-proton cosmic ray spectra on properties of Dark Matter," *Nucl. Phys.* **B813** (2009) 1–21, arXiv:0809.2409 [hep-ph].

[125] N. Arkani-Hamed, D. P. Finkbeiner, T. R. Slatyer, and N. Weiner, "A Theory of Dark Matter," *Phys. Rev.* **D79** (2009) 015014, arXiv:0810.0713 [hep-ph].

[126] Y. Nomura and J. Thaler, "Dark Matter through the Axion Portal," *Phys. Rev.* **D79** (2009) 075008, arXiv:0810.5397 [hep-ph].

[127] I. Cholis, G. Dobler, D. P. Finkbeiner, L. Goodenough, and N. Weiner, "The Case for a 700+ GeV WIMP: Cosmic Ray Spectra from ATIC and PAMELA," *Phys. Rev.* **D80** (2009) 123518, arXiv:0811.3641 [astro-ph].

[128] M. Fairbairn and J. Zupan, "Two component dark matter," *JCAP* **0907** (2009) 001, arXiv:0810.4147 [hep-ph].

[129] D. P. Finkbeiner, "Microwave ISM Emission Observed by WMAP," *Astrophys. J.* **614** (2004) 186–193, arXiv:astro-ph/0311547.

[130] D. P. Finkbeiner, "WMAP microwave emission interpreted as dark matter annihilation in the inner Galaxy," arXiv:astro-ph/0409027.

[131] I. Cholis, L. Goodenough, and N. Weiner, "High Energy Positrons and the WMAP Haze from Exciting Dark Matter," *Phys. Rev.* **D79** (2009) 123505, arXiv:0802.2922 [astro-ph].

[132] J. Zhang *et al.*, "Discriminating different scenarios to account for the cosmic e + /- excess by synchrotron and inverse Compton radiation," *Phys. Rev.* **D80** (2009) 023007, arXiv:0812.0522 [astro-ph].

[133] N. F. Bell and T. D. Jacques, "Gamma-ray Constraints on Dark Matter Annihilation into Charged Particles," *Phys. Rev.* **D79** (2009) 043507, arXiv:0811.0821 [astro-ph].

[134] G. Bertone, M. Cirelli, A. Strumia, and M. Taoso, "Gamma-ray and radio tests of the e+e- excess from DM annihilations," *JCAP* **0903** (2009) 009, arXiv:0811.3744 [astro-ph].

[135] L. Bergstrom, G. Bertone, T. Bringmann, J. Edsjo, and M. Taoso, "Gamma-ray and Radio Constraints of High Positron Rate Dark Matter Models Annihilating into New Light Particles," *Phys. Rev.* **D79** (2009) 081303, arXiv:0812.3895 [astro-ph].

[136] J. Hisano, M. Kawasaki, K. Kohri, and K. Nakayama, "Neutrino Signals from Annihilating/Decaying Dark Matter in the Light of Recent Measurements of Cosmic Ray Electron/Positron Fluxes," *Phys. Rev.* **D79** (2009) 043516, arXiv:0812.0219 [hep-ph].

[137] J. Liu, P.-f. Yin, and S.-h. Zhu, "Prospects for Detecting Neutrino Signals from Annihilating/Decaying Dark Matter to Account for the PAMELA and ATIC results," *Phys. Rev.* **D79** (2009) 063522, arXiv:0812.0964 [astro-ph].

[138] O. Adriani *et al.*, "A new measurement of the antiproton-to-proton flux ratio up to 100 GeV in the cosmic radiation," *Phys. Rev. Lett.* **102** (2009) 051101, arXiv:0810.4994 [astro-ph].

[139] **H.E.S.S.** Collaboration, F. Aharonian *et al.*, "HESS observations of the galactic center region and their possible dark matter interpretation," *Phys. Rev. Lett.* **97** (2006) 221102, arXiv:astro-ph/0610509.

[140] **H.E.S.S.** Collaboration, F. Aharonian *et al.*, "Discovery of Very-High-Energy Gamma-Rays from the Galactic Centre Ridge," *Nature* **439** (2006) 695–698, arXiv:astro-ph/0603021.

[141] **HESS** Collaboration, . F. Aharonian, "Observations of the Sagittarius Dwarf galaxy by the H.E.S.S. experiment and search for a Dark Matter signal," *Astropart. Phys.* **29** (2008) 55–62, arXiv:0711.2369 [astro-ph].

[142] J. Hisano, S. Matsumoto, and M. M. Nojiri, "Explosive dark matter annihilation," *Phys. Rev. Lett.* **92** (2004) 031303, arXiv:hep-ph/0307216.

[143] M. Pospelov and A. Ritz, "Astrophysical Signatures of Secluded Dark Matter," *Phys. Lett.* **B671** (2009) 391–397, arXiv:0810.1502 [hep-ph].

[144] **Super-Kamiokande** Collaboration, S. Desai *et al.*, "Search for dark matter WIMPs using upward through-going muons in Super-Kamiokande," *Phys. Rev.* **D70** (2004) 083523, arXiv:hep-ex/0404025.

[145] M. Pospelov, A. Ritz, and M. B. Voloshin, "Secluded WIMP Dark Matter," *Phys. Lett.* **B662** (2008) 53–61, arXiv:0711.4866 [hep-ph].

[146] D. P. Finkbeiner and N. Weiner, "Exciting Dark Matter and the INTEGRAL/SPI 511 keV signal," *Phys. Rev.* **D76** (2007) 083519, arXiv:astro-ph/0702587.

[147] T. Delahaye, R. Lineros, F. Donato, N. Fornengo, and P. Salati, "Positrons from dark matter annihilation in the galactic halo: theoretical uncertainties," *Phys. Rev.* **D77** (2008) 063527, arXiv:0712.2312 [astro-ph].

[148] J. N. Bahcall and R. M. Soneira, "The Universe at faint magnetidues. 2. Models for the predicted star counts," *Astrophys. J. Suppl.* **44** (1980) 73–110.

[149] J. F. Navarro, C. S. Frenk, and S. D. M. White, "A Universal Density Profile from Hierarchical Clustering," *Astrophys. J.* **490** (1997) 493–508, arXiv:astro-ph/9611107.

[150] J. F. Navarro *et al.*, "The Inner Structure of LambdaCDM Halos III: Universality and Asymptotic Slopes," *Mon. Not. Roy. Astron. Soc.* **349** (2004) 1039, arXiv:astro-ph/0311231.

[151] J. Hisano, S. Matsumoto, O. Saito, and M. Senami, "Heavy Wino-like neutralino dark matter annihilation into antiparticles," *Phys. Rev.* **D73** (2006) 055004, arXiv:hep-ph/0511118.

[152] J. Lavalle, J. Pochon, P. Salati, and R. Taillet, "Clumpiness of dark matter and positron annihilation signal: Computing the odds of the galactic lottery," arXiv:astro-ph/0603796.

[153] I. V. Moskalenko and A. W. Strong, "Production and propagation of cosmic-ray positrons and electrons," *Astrophys. J.* **493** (1998) 694–707, arXiv:astro-ph/9710124.

[154] F. Aharonian *et al.*, "High Energy Spectroscopic System (H.E.S.S.).". http://www.mpi-hd.mpg.de/hfm/HESS/

[155] **H.E.S.S.** Collaboration, F. Aharonian *et al.*, "The energy spectrum of cosmic-ray electrons at TeV energies," *Phys. Rev. Lett.* **101** (2008) 261104, arXiv:0811.3894 [astro-ph].

[156] A. Birkedal, K. T. Matchev, M. Perelstein, and A. Spray, "Robust gamma ray signature of WIMP dark matter," arXiv:hep-ph/0507194.

[157] G. D. Mack, T. D. Jacques, J. F. Beacom, N. F. Bell, and H. Yuksel, "Conservative Constraints on Dark Matter Annihilation into Gamma Rays," *Phys. Rev.* **D78** (2008) 063542, arXiv:0803.0157 [astro-ph].

[158] N. W. Evans, F. Ferrer, and S. Sarkar, "A 'Baedecker' for the dark matter annihilation signal," *Phys. Rev.* **D69** (2004) 123501, arXiv:astro-ph/0311145.

[159] R. D. Davies, D. Walsh, and R. S. Booth, "The Radio Source at the Galactic Nucleus," *Mon. Not. R. Astr. Soc.* **177** (1976) 319–333.

[160] A. A. Dutton, F. C. van den Bosch, A. Dekel, and S. Courteau, "A Revised Model for the Formation of Disk Galaxies: Quiet History, Low Spin, and Dark-Halo Expansion," *Astrophys. J.* **654** (2006) 27–52, arXiv:astro-ph/0604553.

[161] D. Merritt, M. Milosavljevic, L. Verde, and R. Jimenez, "Dark matter spikes and annihilation radiation from the galactic center," *Phys. Rev. Lett.* **88** (2002) 191301, arXiv:astro-ph/0201376.

[162] J. Diemand *et al.*, "Clumps and streams in the local dark matter distribution," *Nature* **454** (2008) 735–738, arXiv:0805.1244 [astro-ph].

[163] E. Borriello, A. Cuoco, and G. Miele, "Radio constraints on dark matter annihilation in the galactic halo and its substructures," *Phys. Rev.* **D79** (2009) 023518, arXiv:0809.2990 [astro-ph].

[164] A. de Oliveira-Costa *et al.*, "A model of diffuse Galactic Radio Emission from 10 MHz to 100 GHz," arXiv:0802.1525 [astro-ph].

[165] S. Ritz and D. Seckel, "DETAILED NEUTRINO SPECTRA FROM COLD DARK MATTER ANNIHILATIONS IN THE SUN," *Nucl. Phys.* **B304** (1988) 877.

[166] V. Barger, W.-Y. Keung, G. Shaughnessy, and A. Tregre, "High energy neutrinos from neutralino annihilations in the Sun," *Phys. Rev.* **D76** (2007) 095008, arXiv:0708.1325 [hep-ph].

[167] **CTEQ** Collaboration, H. L. Lai *et al.*, "Global QCD analysis of parton structure of the nucleon: CTEQ5 parton distributions," *Eur. Phys. J.* **C12** (2000) 375–392, arXiv:hep-ph/9903282.

[168] Y. Fukuda *et al.*, "The Super-Kamiokande detector," *Nucl. Instrum. Meth.* **A501** (2003) 418–462.

[169] S. Desai. private communication.

[170] M. Kamionkowski and S. Profumo, "Early Annihilation and Diffuse Backgrounds in Models of Weakly Interacting Massive Particles in Which the Cross Section for Pair Annihilation Is Enhanced by 1/v," *Phys. Rev. Lett.* **101** (2008) 261301, arXiv:0810.3233 [astro-ph].

[171] Y. B. Zeldovich, A. A. Klypin, M. Y. Khlopov, and V. M. Chechetkin, "Astrophysical constraints on the mass of heavy stable neutral leptons," *Sov. J. Nucl. Phys.* **31** (1980) 664–669.

[172] **ANTARES** Collaboration, E. Aslanides *et al.*, "A deep sea telescope for high energy neutrinos," arXiv:astro-ph/9907432.

[173] **IceCube** Collaboration, J. Ahrens *et al.*, "Sensitivity of the IceCube detector to astrophysical sources of high energy muon neutrinos," *Astropart. Phys.* **20** (2004) 507–532, arXiv:astro-ph/0305196.

[174] A. Kappes and f. t. K. Consortium, "KM3NeT: A Next Generation Neutrino Telescope in the Mediterranean Sea," arXiv:0711.0563 [astro-ph].

[175] J. Buckley *et al.*, "The Status and future of ground-based TeV gamma-ray astronomy. A White Paper prepared for the Division of Astrophysics of the American Physical Society," arXiv:0810.0444 [astro-ph].

[176] F. Collaboration, "Fermi Gamma-ray Space Telescope (formerly GLAST).". http://fermi.gsfc.nasa.gov/

[177] P. Meade, M. Papucci, and T. Volansky, "Dark Matter Sees The Light," *JHEP* **12** (2009) 052, arXiv:0901.2925 [hep-ph].

[178] T. Yanagida and J. Sato, "Large lepton mixing in seesaw models: Coset-space family unification," *Nucl. Phys. Proc. Suppl.* **77** (1999) 293–298, arXiv:hep-ph/9809307.

[179] P. Ramond, "Neutrinos: A glimpse beyond the standard model," *Nucl. Phys. Proc. Suppl.* **77** (1999) 3–9, arXiv:hep-ph/9809401.

[180] A. Masiero, S. K. Vempati, and O. Vives, "Flavour physics and grand unification," arXiv:0711.2903 [hep-ph].

[181] A. Collaboration, "ATLAS detector and physics performance. Technical design report. Vol. 2,". CERN-LHCC-99-15.

[182] J. L. Feng and B. T. Smith, "Slepton trapping at the Large Hadron and International Linear Colliders," *Phys. Rev.* **D71** (2005) 015004, arXiv:hep-ph/0409278.

[183] L. J. Hall, J. March-Russell, T. Okui, and D. Tucker-Smith, "Towards a theory of flavor from orbifold GUTs," *JHEP* **09** (2004) 026, arXiv:hep-ph/0108161.

[184] U. Ellwanger, "Nonrenormalizable Interactions From Supergravity, Quantum Corrections and Effective Low-Energy Theories," *Phys. Lett.* **B133** (1983) 187–191.

[185] Z. Chacko, M. A. Luty, and E. Ponton, "Massive higher-dimensional gauge fields as messengers of supersymmetry breaking," *JHEP* **07** (2000) 036, arXiv:hep-ph/9909248.

[186] W. D. Goldberger, Y. Nomura, and D. Tucker-Smith, "Warped supersymmetric grand unification," *Phys. Rev.* **D67** (2003) 075021, arXiv:hep-ph/0209158.

[187] F. Borzumati and A. Masiero, "Large Muon and electron Number Violations in Supergravity Theories," *Phys. Rev. Lett.* **57** (1986) 961.

[188] R. Barbieri and L. J. Hall, "Signals for supersymmetric unification," *Phys. Lett.* **B338** (1994) 212–218, arXiv:hep-ph/9408406.

[189] G. D. Kribs, E. Poppitz, and N. Weiner, "Flavor in supersymmetry with an extended R-symmetry," *Phys. Rev.* **D78** (2008) 055010, arXiv:0712.2039 [hep-ph].

[190] A. Masiero and H. Murayama, "Can epsilon'/epsilon be supersymmetric?," *Phys. Rev. Lett.* **83** (1999) 907–910, arXiv:hep-ph/9903363.

[191] R. N. Mohapatra and A. Rasin, "A Supersymmetric Solution to CP Problems," *Phys. Rev.* **D54** (1996) 5835–5844, arXiv:hep-ph/9604445.

[192] S. Abel, D. Bailin, S. Khalil, and O. Lebedev, "Flavour-dependent CP violation and natural suppression of the electric dipole moments," *Phys. Lett.* **B504** (2001) 241–246, arXiv:hep-ph/0012145.

[193] J. Hisano and Y. Shimizu, "Hadronic EDMs induced by the strangeness and constraints on supersymmetric CP phases," *Phys. Rev.* **D70** (2004) 093001, arXiv:hep-ph/0406091.

[194] M. Pospelov and A. Ritz, "Electric dipole moments as probes of new physics," *Annals Phys.* **318** (2005) 119–169, arXiv:hep-ph/0504231.

[195] D. DeMille *et al.*, "Investigation of PbO as a system for measuring the electric dipole moment of the electron," *Phys. Rev.* **A61** (2000) 052507.

[196] I. Masina and C. A. Savoy, "Sleptonarium (constraints on the CP and flavour pattern of scalar lepton masses)," *Nucl. Phys.* **B661** (2003) 365–393, arXiv:hep-ph/0211283.

[197] L. E. Ibanez, "HIERARCHY OF QUARK - LEPTON MASSES IN ORBIFOLD SUPERSTRING COMPACTIFICATION," *Phys. Lett.* **B181** (1986) 269.

[198] T. Gherghetta and A. Pomarol, "Bulk fields and supersymmetry in a slice of AdS," *Nucl. Phys.* **B586** (2000) 141–162, arXiv:hep-ph/0003129.

[199] K. Agashe, R. Contino, and R. Sundrum, "Top compositeness and precision unification," *Phys. Rev. Lett.* **95** (2005) 171804, arXiv:hep-ph/0502222.

[200] L. J. Hall and Y. Nomura, "Grand unification in higher dimensions," *Annals Phys.* **306** (2003) 132–156, arXiv:hep-ph/0212134.

[201] G. Ross and M. Serna, "Unification and Fermion Mass Structure," *Phys. Lett.* **B664** (2008) 97–102, arXiv:0704.1248 [hep-ph].

[202] J. S. Hagelin and S. Kelley, "SPARTICLE MASSES AS A PROBE OF GUT PHYSICS," *Nucl. Phys.* **B342** (1990) 95–107.

[203] Y. Kawamura, H. Murayama, and M. Yamaguchi, "Low-energy effective Lagrangian in unified theories with nonuniversal supersymmetry breaking terms," *Phys. Rev.* **D51** (1995) 1337–1352, arXiv:hep-ph/9406245.

[204] J. A. Casas and C. Munoz, "A Natural Solution to the MU Problem," *Phys. Lett.* **B306** (1993) 288–294, arXiv:hep-ph/9302227.

[205] E. Cremmer *et al.*, "Spontaneous Symmetry Breaking and Higgs Effect in Supergravity Without Cosmological Constant," *Nucl. Phys.* **B147** (1979) 105.

[206] E. Cremmer, S. Ferrara, L. Girardello, and A. Van Proeyen, "Yang-Mills Theories with Local Supersymmetry: Lagrangian, Transformation Laws and SuperHiggs Effect," *Nucl. Phys.* **B212** (1983) 413.

[207] G. G. Ross and O. Vives, "Yukawa structure, flavour and CP violation in supergravity," *Phys. Rev.* **D67** (2003) 095013, arXiv:hep-ph/0211279.

[208] S. Abel, S. Khalil, and O. Lebedev, "Additional stringy sources for electric dipole moments," *Phys. Rev. Lett.* **89** (2002) 121601, arXiv:hep-ph/0112260.

[209] L. Randall and R. Sundrum, "Out of this world supersymmetry breaking," *Nucl. Phys.* **B557** (1999) 79–118, arXiv:hep-th/9810155.

[210] G. F. Giudice, M. A. Luty, H. Murayama, and R. Rattazzi, "Gaugino Mass without Singlets," *JHEP* **12** (1998) 027, arXiv:hep-ph/9810442.

[211] S. Antusch, S. F. King, M. Malinsky, and G. G. Ross, "Solving the SUSY Flavour and CP Problems with Non-Abelian Family Symmetry and Supergravity," *Phys. Lett.* **B670** (2009) 383–389, arXiv:0807.5047 [hep-ph].

[212] H. Yuksel, M. D. Kistler, and T. Stanev, "TeV Gamma Rays from Geminga and the Origin of the GeV Positron Excess," *Phys. Rev. Lett.* **103** (2009) 051101, arXiv:0810.2784 [astro-ph].

[213] S. Profumo, "Dissecting Pamela (and ATIC) with Occam's Razor: existing, well-known Pulsars naturally account for the 'anomalous' Cosmic-Ray Electron and Positron Data," arXiv:0812.4457 [astro-ph].

[214] K. Ioka, "A Gamma-Ray Burst for Cosmic-Ray Positrons with a Spectral Cutoff and Line," arXiv:0812.4851 [astro-ph].

[215] H.-B. Hu *et al.*, "On the cosmic electron/positron excesses and the knee of the cosmic rays – a key to the 50 years' puzzle?," arXiv:0901.1520 [astro-ph].

[216] C.-R. Chen, M. M. Nojiri, F. Takahashi, and T. T. Yanagida, "Decaying Hidden Gauge Boson and the PAMELA and ATIC/PPB- BETS Anomalies," *Prog. Theor. Phys.* **122** (2009) 553–559, arXiv:0811.3357 [astro-ph].

[217] E. Nardi, F. Sannino, and A. Strumia, "Decaying Dark Matter can explain the electron/positron excesses," *JCAP* **0901** (2009) 043, arXiv:0811.4153 [hep-ph].

[218] K. Ishiwata, S. Matsumoto, and T. Moroi, "Synchrotron Radiation from the Galactic Center in Decaying Dark Matter Scenario," *Phys. Rev.* **D79** (2009) 043527, arXiv:0811.4492 [astro-ph].

[219] A. Arvanitaki *et al.*, "Astrophysical Probes of Unification," *Phys. Rev.* **D79** (2009) 105022, arXiv:0812.2075 [hep-ph].

[220] K. Hamaguchi, S. Shirai, and T. T. Yanagida, "Cosmic Ray Positron and Electron Excess from Hidden- Fermion Dark Matter Decays," *Phys. Lett.* **B673** (2009) 247–250, arXiv:0812.2374 [hep-ph].

[221] F. Takahashi and E. Komatsu, "Gravitational Dark Matter Decay and the ATIC/PPB-BETS Excess," arXiv:0901.1915 [astro-ph].

[222] A. E. Nelson and C. Spitzer, "Slightly Non-Minimal Dark Matter in PAMELA and ATIC," arXiv:0810.5167 [hep-ph].

[223] R. Harnik and G. D. Kribs, "An Effective Theory of Dirac Dark Matter," *Phys. Rev.* **D79** (2009) 095007, arXiv:0810.5557 [hep-ph].

[224] Y. Bai and Z. Han, "A Unified Dark Matter Model in sUED," *Phys. Rev.* **D79** (2009) 095023, arXiv:0811.0387 [hep-ph].

[225] P. J. Fox and E. Poppitz, "Leptophilic Dark Matter," *Phys. Rev.* **D79** (2009) 083528, arXiv:0811.0399 [hep-ph].

[226] K. M. Zurek, "Multi-Component Dark Matter," *Phys. Rev.* **D79** (2009) 115002, arXiv:0811.4429 [hep-ph].

[227] E. J. Chun and J.-C. Park, "Dark matter and sub-GeV hidden U(1) in GMSB models," *JCAP* **0902** (2009) 026, arXiv:0812.0308 [hep-ph].

[228] R. Allahverdi, B. Dutta, K. Richardson-McDaniel, and Y. Santoso, "A Supersymmetric B^- L Dark Matter Model and the Observed Anomalies in the Cosmic Rays," *Phys. Rev.* **D79** (2009) 075005, arXiv:0812.2196 [hep-ph].

[229] D. Hooper, A. Stebbins, and K. M. Zurek, "Excesses in cosmic ray positron and electron spectra from a nearby clump of neutralino dark matter," *Phys. Rev.* **D79** (2009) 103513, arXiv:0812.3202 [hep-ph].

[230] C.-R. Chen, K. Hamaguchi, M. M. Nojiri, F. Takahashi, and S. Torii, "Dark Matter Model Selection and the ATIC/PPB-BETS anomaly," *JCAP* **0905** (2009) 015, arXiv:0812.4200 [astro-ph].

[231] I. Gogoladze, R. Khalid, Q. Shafi, and H. Yuksel, "CMSSM Spectroscopy in light of PAMELA and ATIC," *Phys. Rev.* **D79** (2009) 055019, arXiv:0901.0923 [hep-ph].

[232] G. Dobler and D. P. Finkbeiner, "Extended Anomalous Foreground Emission in the WMAP 3-Year Data," *Astrophys. J.* **680** (2008) 1222–1234, arXiv:0712.1038 [astro-ph].

[233] D. Hooper, D. P. Finkbeiner, and G. Dobler, "Evidence Of Dark Matter Annihilations In The WMAP Haze," *Phys. Rev.* **D76** (2007) 083012, arXiv:0705.3655 [astro-ph].

[234] J. Hisano, S. Matsumoto, M. M. Nojiri, and O. Saito, "Non-perturbative effect on dark matter annihilation and gamma ray signature from galactic center," *Phys. Rev.* **D71** (2005) 063528, arXiv:hep-ph/0412403.

[235] M. Cirelli, A. Strumia, and M. Tamburini, "Cosmology and Astrophysics of Minimal Dark Matter," *Nucl. Phys.* **B787** (2007) 152–175, arXiv:0706.4071 [hep-ph].

[236] J. March-Russell, S. M. West, D. Cumberbatch, and D. Hooper, "Heavy Dark Matter Through the Higgs Portal," *JHEP* **07** (2008) 058, arXiv:0801.3440 [hep-ph].

[237] M. Lattanzi and J. I. Silk, "Can the WIMP annihilation boost factor be boosted by the Sommerfeld enhancement?," *Phys. Rev.* **D79** (2009) 083523, arXiv:0812.0360 [astro-ph].

[238] J. D. March-Russell and S. M. West, "WIMPonium and Boost Factors for Indirect Dark Matter Detection," *Phys. Lett.* **B676** (2009) 133–139, arXiv:0812.0559 [astro-ph].

[239] W. Shepherd, T. M. P. Tait, and G. Zaharijas, "WIMPonium," *Phys. Rev.* **D79** (2009) 055022, arXiv:0901.2125 [hep-ph].

[240] E. A. Baltz and J. Edsjo, "Positron Propagation and Fluxes from Neutralino Annihilation in the Halo," *Phys. Rev.* **D59** (1998) 023511, arXiv:astro-ph/9808243.

[241] J. F. Navarro *et al.*, "The Diversity and Similarity of Cold Dark Matter Halos," arXiv:0810.1522 [astro-ph].

[242] E. Borriello, A. Cuoco, and G. Miele, "Radio Signal by Galactic Dark Matter," *Nucl. Phys. Proc. Suppl.* **190** (2009) 185–190, arXiv:0812.2932 [astro-ph].

[243] Y. Kuno and Y. Okada, "Muon decay and physics beyond the standard model," *Rev. Mod. Phys.* **73** (2001) 151–202, arXiv:hep-ph/9909265.

[244] G. G. Raffelt, "Astrophysical methods to constrain axions and other novel particle phenomena," *Phys. Rept.* **198** (1990) 1–113.

Appendix A

Subtleties of Flavorful Supersymmetry

A.1 μ and b in Higgsphobic SUSY Breaking

In minimal Higgsphobic supersymmetry breaking, the operators $\mathcal{O}_{\kappa_H,\eta_H,\mu,b}$ in Eqs. (4.7, 4.8) are forbidden. The μ and b parameters are then generated only by the operator $\mathcal{O}_{\rm SUGRA}$ through supergravity effects [45], giving

$$\mu = \frac{\lambda_H m_{3/2}^*}{(Z_{H_u} Z_{H_d})^{1/2}}, \qquad b = \frac{\lambda_H |m_{3/2}|^2}{(Z_{H_u} Z_{H_d})^{1/2}}, \tag{A.1}$$

where $m_{3/2}$ is the gravitino mass. The non-holomorphic supersymmetry breaking masses are vanishing, $m_{H_u}^2 = m_{H_d}^2 = 0$, at the scale M. The expressions of Eq. (A.1) imply that the gravitino mass should be of order the weak scale to use this contribution. The μ and b parameters of Eq. (A.1) also lead to dangerous CP violation at low energies unless $\arg(m_{3/2}) \simeq \arg(M_A)$, providing an additional constraint on the setup. In the context of the higher dimensional models of section 4.3.2, a weak scale gravitino mass is obtained if $M_* \approx M_{\rm Pl}$ or if there is an additional supersymmetry breaking field X' that does not couple to the SSM field and has $F_{X'} \approx F_X (M_{\rm Pl}/M_*)$.

It is possible to extend the minimal Higgsphobic setup by introducing fields B which directly couple with both H and X. In higher dimensional models, these B fields propagate in the bulk, and integrating them out can generate the operators $\mathcal{O}_{\kappa_H,\eta_H,\mu,b}$ in the low energy effective field theory below $1/R$. The operators $\mathcal{O}_{\zeta_f}$ can still be absent by arranging the interactions of B appropriately, for example by suppressing the couplings of B with matter fields. With these extensions, the generated Higgs sector parameters need not take the form in the minimal setup. In particular, the gravitino mass need not be of order the weak scale, and its phase need not be aligned with that of M_A. The requirement from suppressing CP violation, instead, constrains the representations and interactions of the B fields. For example, if the exchange of B generates μ but not b, and the contribution from Eq. (A.1) is negligible, then the problem of CP violation disappears.

A.2 $(a_f)_{ij}$ in Remote Flavor-SUSY Breaking

In remote flavor-supersymmetry breaking, the Yukawa couplings are generated through breaking of $G_{\rm flavor}$. Suppose that the breaking is caused by the VEVs of several chiral superfields ϕ_m ($m = 1, 2, \cdots$). The Yukawa couplings are then generated from operators of the form

$$\mathcal{L} = \int d^2\theta \sum_{i,j} \sum_{\{(n_f)^m_{ij}\}} c_{\{(n_f)^m_{ij}\}} \frac{\prod_m \phi_m^{(n_f)^m_{ij}}}{(M_* C)^{(n_f)_{ij}}} \Phi_{Li} \Phi_{Rj} H + \text{h.c.}, \tag{A.2}$$

as

$$(y_f)_{ij} = \sum_{\{(n_f)^m_{ij}\}} c_{\{(n_f)^m_{ij}\}} \frac{\prod_m \phi_{m,0}^{(n_f)^m_{ij}}}{M_*^{(n_f)_{ij}}}, \tag{A.3}$$

where Φ_{Li}, Φ_{Rj}, H and ϕ_m are canonically normalized, M_* is the (effective) cutoff scale, $(n_f)^m_{ij}$ are integers with $(n_f)_{ij} \equiv \sum_m (n_f)^m_{ij}$, and $\phi_{m,0}$ is the lowest component VEV of ϕ_m. The sum $\sum_{\{(n_f)^m_{ij}\}}$ runs over all possible choices of integers $(n_f)^m_{ij}$ consistent with $G_{\rm flavor}$ invariance, and $c_{\{(n_f)^m_{ij}\}}$ are $O(1)$ coefficients in front of each term. Here, we have included the chiral compensator field $C = 1 + \theta^2 m_{3/2}$ which encodes supergravity effects [205].

The operators of Eq. (A.2) may generate dangerous scalar trilinear interactions. These are given by

$$(a_f)_{ij} = \sum_{\{(n_f)^m_{ij}\}} c_{\{(n_f)^m_{ij}\}} \frac{\prod_m \phi_{m,0}^{(n_f)^m_{ij}}}{M_*^{(n_f)_{ij}}} \left\{ (n_f)_{ij} m_{3/2} - \sum_{m'} (n_f)^{m'}_{ij} \frac{F_{\phi_{m'}}}{\phi_{m',0}} \right\}, \tag{A.4}$$

where F_{ϕ_m} is the F-term VEV of ϕ_m. This shows that even with $F_{\phi_m} = 0$, the scalar trilinear interactions are generated, which for $m_{3/2} \approx O(m_{\rm C}, m_{\rm N})$ lead to $(a_f)_{ij} \approx (y_f)_{ij} m_{\rm C,N}$, and are thus dangerous [207].[1] More generally, if some of the ϕ_m are stabilized using supersymmetry breaking effects (e.g. if these fields are flat directions lifted by higher dimension operators), we obtain $F_{\phi_m}/\phi_{m,0} \approx O(\max\{m_{3/2}, m_\phi\})$ with m_ϕ being the scale for the supersymmetry breaking masses of ϕ_m, and we obtain a contribution of order $(a_f)_{ij} \approx (y_f)_{ij} \max\{m_{3/2}, m_\phi\}$.

The contribution to $(a_f)_{ij}$ described above, however, is suppressed if one of the following conditions is satisfied:[2]

(a) The gravitino mass and the F-term VEVs for ϕ_m are all small, $m_a \equiv \max\{m_{3/2}, F_{\phi_m}/\phi_{m,0}\} \ll m_{\rm C,N}$. In this case, the effect of Eq. (A.4) is suppressed by a factor of $m_a/m_{\rm C,N}$, giving $(\delta^{u,d}_{LR})_{ij} \approx (M_{u,d})_{ij} m_a/m_{\rm C}^2$ and $(\delta^{e}_{LR})_{ij} \approx (M_e)_{ij} m_a/m_{\rm N}^2$.

[1] Our language here is different from that used in Ref. [207], in which the F-term VEV of a field is defined including a supergravity contribution so that the effect described here is viewed as arising from the F-term VEVs of the fields ϕ_m.

[2] While completing this chapter, Ref. [211] appeared, which discusses the issue considered in this Appendix. Their main solution corresponds to our (c) below. They also discuss the case (b).

(b) The dimensions of the operators in Eq. (A.2) are the same for all $i, j = 1, 2, 3$, i.e. $(n_f)_{ij} = n_f$, for $f = u, d, e$, and $F_{\phi_m}/\phi_{m,0} \ll m_{\rm C,N}$ with $\arg(m_{3/2}) = \arg(M_A)$ (or $(n_f)_{ij} = n_f$ and $F_{\phi_m}/\phi_{m,0}$ are nearly equal with their phases aligned with those of $m_{3/2}, M_A$). In this case, $(a_f)_{ij}$ is almost proportional to $(y_f)_{ij}$ as a matrix, giving a negligible contribution to $(\delta^f_{LR})_{ij}$.

(c) The VEVs of ϕ_m are stabilized in the supersymmetric limit. In this case, we obtain $\langle\phi_m\rangle = \phi_{m,0}C$, since any supersymmetric mass must be accompanied with C, leading to $F_{\phi_m}/\phi_{m,0} = m_{3/2}$. Equation (A.4) then gives $(a_f)_{ij} = 0$, and the effect disappears.[3]

We find it simplest to stabilize ϕ_m supersymmetrically, (c), although we also leave the possibility open to (a) or (b). (In fact, the experimental bounds may be avoided with one of the above conditions satisfied only for $i, j = 1, 2$.) Note that the consideration here applies to any field that appears in front of $\Phi_{Li}\Phi_{Rj}H$ in the superpotential, and whose lowest component VEV gives a significant contribution to the Yukawa couplings.

The issue of scalar trilinear interactions generated by the F-term VEVs of C and the fields appearing in front of $\Phi_{Li}\Phi_{Rj}H$, in fact, exists in wider classes of theories. For example, in theories where the hierarchical Yukawa couplings are generated by wavefunction profiles of the matter and Higgs fields in extra dimensions, including ones discussed in section 4.3.2, there are generally moduli fields appearing in front of $\Phi_{Li}\Phi_{Rj}H$. These moduli fields must satisfy condition (a) or (c) (option (b) is typically not available). We assume that one of these conditions is satisfied when discussing the classes of theories in section 4.3.

[3]There is still an effect from the chiral compensator field at a loop level (anomaly mediation) [209]. This effect, however, does not lead to flavor or CP violation at a dangerous level. There could also be higher order corrections suppressed by powers of $m_\phi/\phi_{m,0}$, where m_ϕ represents generic supersymmetry breaking masses in the $G_{\rm flavor}$ breaking sector. These corrections are also negligible unless the scale of flavor physics is close to the TeV scale.

Appendix B

Formulas for Cascade Annihilation

B.1 Cascade Energy Spectra

In this appendix, we present formulae for the energy spectra used in the text. In general, the energy spectra of final state particles in cascade annihilations are functions of all the intermediate masses and helicities. In the limit of large mass hierarchies and scalar decays, however, the energy spectra greatly simplify, and we use these simplified formulae in our analysis.

Consider cascading fields ϕ_i of mass m_i ($m_{i+1} > 2m_i$) and a final state ψ with mass m_ψ. Cascade annihilation occurs through $\phi_{i+1} \to \phi_i\phi_i$ ($i = 1, 2, \cdots$), and in the last stage, ϕ_1 decays into $\psi + X$. Let the energy of ψ in the ϕ_1 rest frame be E_0. Defining

$$x_0 = \frac{2E_0}{m_1}, \qquad \epsilon_0 = \frac{2m_\psi}{m_1}, \tag{B.1}$$

the ψ energy spectrum is a function of x_0 and ϵ_0

$$\frac{d\tilde{N}_\psi}{dx_0} = \frac{d\tilde{N}_\psi}{dx_0}(x_0, \epsilon_0), \tag{B.2}$$

where $\epsilon_0 \leq x_0 \leq 1$. In the case where dark matter χ annihilates directly into $\psi + X$, we can regard ϕ_1 as the initial state of dark matter annihilation, $\chi\chi$. In this case $d\tilde{N}_\psi/dx_0$ is the primary injection spectrum with $m_1 = 2m_{\rm DM}$.

Now consider the previous step in the cascade annihilation, $\phi_2 \to \phi_1\phi_1$, with *one of the* ϕ_1 decaying into $\psi + X$. Let the energy of ψ in the ϕ_2 rest frame be E_1 and define

$$x_1 = \frac{2E_1}{m_2}, \qquad \epsilon_1 = \frac{2m_1}{m_2}. \tag{B.3}$$

Assuming isotropic scalar decays, the ψ energy spectrum in the ϕ_2 rest frame is

$$\frac{d\tilde{N}_\psi}{dx_1} = \int_{-1}^{1} d\cos\theta \int_{\epsilon_0}^{1} dx_0 \, \frac{d\tilde{N}_\psi}{dx_0} \, \delta\left(2x_1 - x_0 - \cos\theta\sqrt{x_0^2 - \epsilon_0^2}\sqrt{1 - \epsilon_1^2}\right), \tag{B.4}$$

where θ is the angle between the ψ momentum and the ϕ_1 boost axis as measured in the ϕ_1 rest frame.

Equation (B.4) is complicated to solve in general, but in the limit $\epsilon_i \to 0$ $(i = 0, 1, \cdots)$, it reduces to a simple convolution:

$$\frac{d\tilde{N}_\psi}{dx_1} = \int_{x_1}^1 \frac{dx_0}{x_0} \frac{d\tilde{N}_\psi}{dx_0} + O(\epsilon_i^2), \tag{B.5}$$

where $0 \leq x_1 \leq 1$ up to $O(\epsilon_i^2)$ effects. This convolution can be iterated as many times as necessary to build up the desired energy spectrum for an n-step cascade decay:

$$\frac{d\tilde{N}_\psi}{dx_n} = \int_{x_n}^1 \frac{dx_{n-1}}{x_{n-1}} \frac{d\tilde{N}_\psi}{dx_{n-1}} + O(\epsilon_i^2), \tag{B.6}$$

where $x_{n-1} = 2E_{n-1}/m_n$ with E_{n-1} being the energy of ψ in the ϕ_n rest frame, and $0 \leq x_n \leq 1$ up to $O(\epsilon_i^2)$ effects. Note that we here adopt the normalization convention of

$$\int_0^1 dx_n \frac{d\tilde{N}_\psi}{dx_n} = 1, \tag{B.7}$$

regardless of the value of n, so that the injection spectra per dark matter annihilation must be multiplied by the multiplicity of ψ in the final state.

B.1.1 Direct electron spectra

Here we derive the spectra of electrons/positrons arising directly from ϕ_1 decay, $\phi_1 \to e^+e^-$ (or dark matter annihilation, $\chi\chi \to e^+e^-$). Ignoring the effect of final state radiation to smooth the spectrum, the electron energy spectrum is given by

$$\frac{d\tilde{N}_e}{dx_0} = \delta(1 - x_0), \tag{B.8}$$

where we have adopted the convention $\int_0^1 dx_0\, \delta(1 - x_0) = 1$. The positron energy spectrum is identical.

Applying the simplified convolution formula in Eq. (B.6) for an n-step cascade annihilation, we then find

$$\frac{d\tilde{N}_e}{dx_1} = 1, \tag{B.9}$$

$$\frac{d\tilde{N}_e}{dx_2} = \ln \frac{1}{x_2}, \tag{B.10}$$

$$\frac{d\tilde{N}_e}{dx_n} = Q_n(x_n), \tag{B.11}$$

where we have defined

$$Q_n(x) \equiv \frac{1}{(n-1)!}\left(\ln\frac{1}{x}\right)^{n-1}. \tag{B.12}$$

Note that these are energy spectra for *one* of the electrons (or positrons), so that the electron (or positron) injection spectra per dark matter annihilation $\chi\chi \to 2\phi_n \to \cdots \to 2^n(e^+e^-)$ are

$$\frac{dN_e}{dx_n} = 2^n \frac{d\tilde{N}_e}{dx_n}, \tag{B.13}$$

where $x_n = E_e/m_{\rm DM}$ with E_e being the electron (positron) energy in the center-of-mass frame for dark matter annihilation. The direct annihilation case, $\chi\chi \to e^+e^-$, corresponds to $n = 0$.

B.1.2 Electron and neutrino spectra from muon decay

Here we discuss the spectra of electrons, positrons and neutrinos arising from muon decay. Consider $\phi_1 \to \mu^+\mu^-$ (or $\chi\chi \to \mu^+\mu^-$) followed by $\mu \to e\nu_e\nu_\mu$. (One of the neutrinos here should be an anti-neutrino. We omit the particle-antiparticle identification here and below.) Assuming a massless electron, the (unpolarized) spectra of electrons and neutrinos in the rest frame of the muon are

$$\frac{d\tilde{N}_{\mu\to e}}{dx_{-1}} = \frac{d\tilde{N}_{\mu\to\nu_\mu}}{dx_{-1}} = 6(x_{-1})^2 - 4(x_{-1})^3, \tag{B.14}$$

$$\frac{d\tilde{N}_{\mu\to\nu_e}}{dx_{-1}} = 12(x_{-1})^2 - 12(x_{-1})^3, \tag{B.15}$$

where we are using the notation $x_{-1} = 2E_{-1}/m_\mu$, with E_{-1} being the energy in the muon rest frame.

Applying the cascade convolution for electrons and muon neutrinos

$$\frac{d\tilde{N}_{\mu\to e}}{dx_0} = \frac{d\tilde{N}_{\mu\to\nu_\mu}}{dx_0} = \frac{5}{3} - 3x_0^2 + \frac{4}{3}x_0^3, \tag{B.16}$$

$$\frac{d\tilde{N}_{\mu\to e}}{dx_1} = \frac{d\tilde{N}_{\mu\to\nu_\mu}}{dx_1} = -\frac{19}{18} + \frac{3}{2}x_1^2 - \frac{4}{9}x_1^3 + \frac{5}{3}Q_2(x_1), \tag{B.17}$$

$$\frac{d\tilde{N}_{\mu\to e}}{dx_2} = \frac{d\tilde{N}_{\mu\to\nu_\mu}}{dx_2} = \frac{65}{108} - \frac{3}{4}x_2^2 + \frac{4}{27}x_2^3 - \frac{19}{18}Q_2(x_2) + \frac{5}{3}Q_3(x_2), \tag{B.18}$$

and for electron neutrinos

$$\frac{d\tilde{N}_{\mu\to\nu_e}}{dx_0} = 2 - 6x_0^2 + 4x_0^3, \tag{B.19}$$

$$\frac{d\tilde{N}_{\mu\to\nu_e}}{dx_1} = -\frac{5}{3} + 3x_1^2 - \frac{4}{3}x_1^3 + 2Q_2(x_1), \tag{B.20}$$

$$\frac{d\tilde{N}_{\mu\to\nu_e}}{dx_2} = \frac{19}{18} - \frac{3}{2}x_2^2 + \frac{4}{9}x_2^3 - \frac{5}{3}Q_2(x_2) + 2Q_3(x_2). \tag{B.21}$$

Again, these are energy spectra for *one* of the electrons, positrons or (anti-)neutrinos. To obtain the injection spectra per dark matter annihilation, we must multiply the multiplicity factor, 2^n for n-step, and set $x_n = E/m_{\rm DM}$. Here, E is the energy of a particle in the center-of-mass frame for dark matter annihilation.

For comparison, the corresponding formulae in the approximation of isotropic three-body decays are

$$\frac{d\tilde{N}_{\mu\to e}}{dx_{-1}} \simeq 2x_{-1}, \tag{B.22}$$

$$\frac{d\tilde{N}_{\mu\to e}}{dx_n} \simeq (-1)^{n+1}\left(2x_n + 2\sum_{i=1}^{n+1}(-1)^i Q_i(x_n)\right) \equiv \overline{Q}_{n+1}(x_n). \tag{B.23}$$

As a rough rule of thumb, the electron spectrum for an n-step muon cascade has a shape between $(n+1)$- and $(n+2)$-step electron cascades.

B.1.3 Gamma ray spectra from final state radiation

Primary gamma rays come from final state radiation in the decay $\phi_1 \to \ell^+\ell^-\gamma$. In principle, one could do an exact calculation to $O(\alpha_{\rm EM})$ of the gamma ray spectrum, which would have the full $\epsilon_0 \equiv 2m_\ell/m_1$ dependence. Since we are using the simplified convolution formula in Eq. (B.6), it is not consistent to keep $O(\epsilon_0^2)$ corrections in the exact gamma ray calculation, and it suffices to use twice the Altarelli-Parisi splitting formula

$$\frac{d\tilde{N}_\gamma}{dx_0} = \frac{\alpha_{\rm EM}}{\pi}\frac{1+(1-x_0)^2}{x_0}\left\{-1+\ln\left(\frac{4(1-x_0)}{\epsilon_0^2}\right)\right\}, \tag{B.24}$$

where the normalization of $\tilde{N}_\gamma$ is such that $\int dx_n\, d\tilde{N}_\gamma/dx_n$ gives the (average) number of photons per ϕ_1 decay. Note that the expression of Eq. (B.24) becomes negative at $x_0 > 1 - e\,\epsilon_0^2/4$, which does not correspond to the kinematic threshold. The error from this, however, is formally an $O(\epsilon_0^2)$ effect.

Applying the simplified convolution formula, we obtain

$$\frac{d\tilde{N}_\gamma}{dx_1} = \frac{\alpha_{\rm EM}}{\pi}\frac{1}{x_1}\left\{\left(-1+\ln\frac{4}{\epsilon_0^2}\right)R_1(x_1) + S_1(x_1)\right\}, \tag{B.25}$$

$$\frac{d\tilde{N}_\gamma}{dx_2} = \frac{\alpha_{\rm EM}}{\pi}\frac{1}{x_2}\left\{\left(-1+\ln\frac{4}{\epsilon_0^2}\right)R_2(x_2) + S_2(x_2)\right\}, \tag{B.26}$$

where

$$R_1(x) = 2 - x - x^2 + 2x\ln x, \tag{B.27}$$

$$R_2(x) = 2 - 3x + x^2 + x\ln x - x(\ln x)^2, \tag{B.28}$$

$$S_1(x) = \left(\frac{\pi^2}{3} - 1\right)x + x^2 + 2x\ln x + (2 - x - x^2)\ln(1-x) - 2x\,{\rm Li}_2(x), \tag{B.29}$$

$$S_2(x) = \left(\frac{\pi^2}{6} + 2 - 2\zeta(3)\right)x - 2x^2 - \left(\frac{\pi^2}{3} - 3\right)x\ln x + (2 - 3x + x^2)\ln(1-x) \\ -x(\ln x)^2 - x\,\mathrm{Li}_2(x) + 2x\,\mathrm{Li}_3(x). \quad \text{(B.30)}$$

The photon injection spectra *per dark matter annihilation* are then given by

$$\frac{dN_\gamma}{dx_n} = 2^n \frac{d\tilde{N}_\gamma}{dx_n}, \quad \text{(B.31)}$$

where $x_n = E_\gamma/m_{\rm DM}$, with E_γ being the photon energy in the center-of-mass frame for dark matter annihilation. Here, $\epsilon_0 = m_\ell/m_{\rm DM}$ for direct annihilation and $\epsilon_0 = 2m_\ell/m_1$ otherwise.

For the hardest gamma rays near $x_n \to 1$, the behavior of $d\tilde{N}_\gamma/dx_n$ is

$$\frac{d\tilde{N}_\gamma}{dx_0} \simeq \frac{\alpha_{\rm EM}}{\pi}\frac{1}{x_0}\ln\left(\frac{4(1-x_0)}{\epsilon_0^2}\right), \quad \text{(B.32)}$$

$$\frac{d\tilde{N}_\gamma}{dx_1} \simeq \frac{\alpha_{\rm EM}}{\pi}\frac{1-x_1}{x_1}\ln\left(\frac{4(1-x_1)}{\epsilon_0^2}\right), \quad \text{(B.33)}$$

$$\frac{d\tilde{N}_\gamma}{dx_2} \simeq \frac{\alpha_{\rm EM}}{\pi}\frac{(1-x_2)^2}{2x_2}\ln\left(\frac{4(1-x_2)}{\epsilon_0^2}\right). \quad \text{(B.34)}$$

Compared to direct annihilation into leptons, a 1-step cascade annihilation gives a gamma ray spectrum that is suppressed not only by $\ln(2m_\ell/m_1)/\ln(m_\ell/m_{\rm DM})$ but also by an additional suppression factor of $(1-x)$ for the highest energy gamma rays.

B.1.4 Gamma ray subtlety for muons

There are actually two contributions to the gamma ray spectrum for $\phi_1 \to \mu^+\mu^-\gamma$. In addition to final state radiation from muons, there is the radiative decay of the muon $\mu \to e\nu_e\nu_\mu\gamma$. Formally, this contribution is suppressed by a factor of $1/\ln(m_\mu/m_1)$ or $(1-x_n)^2$, but for $m_1 \approx m_\mu$, it is an important effect.

The gamma ray spectrum in the muon rest frame is known in the limit that $r = m_e^2/m_\mu^2$ is small [243]. Assuming unpolarized muons, we can derive the 0-step cascade annihilation spectrum from the muon rest frame spectrum

$$\frac{d\tilde{N}_{\mu\to\gamma}}{dx_{-1}} = \frac{\alpha_{\rm EM}}{3\pi}\frac{1}{x_{-1}}\left(T_{-1}(x_{-1})\ln\frac{1}{r} + U_{-1}(x_{-1})\right), \quad \text{(B.35)}$$

$$\frac{d\tilde{N}_{\mu\to\gamma}}{dx_0} = \frac{\alpha_{\rm EM}}{3\pi}\frac{1}{x_0}\left(T_0(x_0)\ln\frac{1}{r} + U_0(x_0)\right), \quad \text{(B.36)}$$

where

$$T_{-1}(x) = (1-x)(3 - 2x + 4x^2 - 2x^3), \quad \text{(B.37)}$$

$$T_0(x) = 3 + \frac{2}{3}x - 6x^2 + 3x^3 - \frac{2}{3}x^4 + 5x\ln x, \tag{B.38}$$

$$U_{-1}(x) = (1-x)\Big(-\frac{17}{2} + \frac{23}{6}x - \frac{101}{12}x^2 + \frac{55}{12}x^3 + (3 - 2x + 4x^2 - 2x^3)\ln(1-x)\Big), \tag{B.39}$$

$$U_0(x) = -\frac{17}{2} - \frac{3}{2}x + \frac{191}{12}x^2 - \frac{23}{3}x^3 + \frac{7}{4}x^4 + \left(3 + \frac{2}{3}x - 6x^2 + 3x^3 - \frac{2}{3}x^4\right)\ln(1-x) - \frac{28}{3}x\ln x + 5x\ln(1-x)\ln x + 5x\,\mathrm{Li}_2(1-x). \tag{B.40}$$

The convolutions for 1- and 2-step decays are straightforward to derive.

Note again that $\int dx_n\, d\tilde{N}_{\mu\to\gamma}/dx_n$ give the (average) number of photons per muon decay. The photon spectra from radiative muon decay *per dark matter annihilation* are then given by $2^n d\tilde{N}_{\mu\to\gamma}/dx_n$. The total photon injection spectra per dark matter annihilation are given by

$$\frac{dN_\gamma}{dx_n} = 2^n\left(\frac{d\tilde{N}_\gamma}{dx_n} + 2\frac{d\tilde{N}_{\mu\to\gamma}}{dx_n}\right), \tag{B.41}$$

where $x_n = E_\gamma/m_{\rm DM}$, with E_γ being the photon energy in the center-of-mass frame for dark matter annihilation.

B.1.5 Rare modes in the axion portal

In Section 5.6, we consider bounds on rare $a \to \gamma\gamma$ and $a \to \pi^+\pi^-\pi^0$ decay modes in axion portal models. The axion portal has both a 1-step and a 2-step component, and the gamma ray spectrum for each can be calculated straightforwardly. The $a \to \gamma\gamma$ spectra are identical (up to normalization) to the $\phi_1 \to e^+e^-$ spectra already calculated:

$$\frac{d\tilde{N}_{a\to\gamma}}{dx_1} = 2, \tag{B.42}$$

$$\frac{d\tilde{N}_{a\to\gamma}}{dx_2} = 2\ln\frac{1}{x_2}, \tag{B.43}$$

where the normalization of $\tilde{N}_{a\to\gamma}$ is such that $\int dx_n\, d\tilde{N}_{a\to\gamma}/dx_n$ gives the number of photons per a decay.

For $a \to \pi^+\pi^-\pi^0$ followed by $\pi^0 \to \gamma\gamma$, we can use the $\overline{Q}_n$ function from Eq. (B.23) if we assume that $m_a \gg m_\pi$ and that the $a \to 3\pi$ decay is isotropic:

$$\frac{d\tilde{N}_{a\to\pi^0\to\gamma}}{dx_1} \simeq 2\overline{Q}_2(x_1), \tag{B.44}$$

$$\frac{d\tilde{N}_{a\to\pi^0\to\gamma}}{dx_2} \simeq 2\overline{Q}_3(x_2), \tag{B.45}$$

where again the normalization of $\tilde{N}_{a\to\pi^0\to\gamma}$ is such that $\int dx_n \, d\tilde{N}_{a\to\pi^0\to\gamma}/dx_n$ gives the number of photons per a decay. One should keep in mind that $m_a \simeq 3m_\pi$ in the region of interest, but the hierarchical cascade approximation is still reasonably representative of the true energy spectrum.

B.2 Leptonic Axion Portal

In the minimal axion portal construction, the axion has large hadronic couplings, and is therefore strongly constrained by beam dump and rare meson decay experiments. In particular, the axion is forced to decay primarily into muons, and, as we saw in Section 5.5, there is some degree of tension between a muon annihilation scenario and the absence of galactic neutrinos. Also, we saw in Section 5.6 that there are strong gamma ray bounds on the $a \to \pi^+\pi^-\pi^0$ decay mode, which in the minimal axion portal arises from axion-pion mixing.

Since the decay properties of the axion are irrelevant for dark matter freezeout, we can easily modify the couplings of the axion to standard model fields without losing the good features of this scenario. In particular, we can construct a leptonic axion portal model where the axion has no hadronic couplings. While such a leptonic axion could decay into muons as in the minimal axion portal, in the text we consider the less constrained case where the leptonic axion decays primarily into electrons.

The simplest example for the leptonic axion portal can be constructed as follows. Vector-like fermion dark matter ψ/ψ^c obtains a mass from spontaneous symmetry breaking through the vacuum expectation value of a complex scalar S_ℓ:

$$\mathcal{L} = -\xi S_\ell \psi \psi^c + \text{h.c.}, \qquad S_\ell = \left(f_a + \frac{s_\ell}{\sqrt{2}}\right) e^{i a_\ell/\sqrt{2} f_a}, \tag{B.46}$$

where a_ℓ is the pseudoscalar axion, s_ℓ is a light scalar, and f_a is the axion decay constant, which is assumed to be of order TeV. As in the minimal axion portal, the masses of s_ℓ and a_ℓ can be considered as free parameters. In order for a_ℓ to decay into leptons, S_ℓ must be charged under a leptonic symmetry (which is softly broken to give a mass to a_ℓ). This requires introducing separate electron-type and neutrino-type Higgses:

$$\mathcal{L} = -\lambda_e \ell h_e e^c - \lambda_\nu \ell h_\nu \nu^c - A_\ell S_\ell h_e h_\nu + \text{h.c.} \tag{B.47}$$

These interactions force the standard model leptons to carry axial leptonic charges. (Small neutrino masses can be obtained through the standard see-saw mechanism, and it is straightforward to extend the model to incorporate supersymmetry.)

In order to eliminate the hadronic couplings of a_ℓ, the standard model quarks are assumed not to carry charges under the leptonic symmetry. This requires introducing one or more new Higgses for the quark sector, which must also be singlets under the leptonic symmetry. As long as the potential for these Higgses preserves the leptonic symmetry, then a_ℓ will have

no hadronic couplings and cannot mix with the neutral mesons after the leptonic symmetry is spontaneously broken.

The absence of hadronic couplings allows m_{a_ℓ} to be lighter than $2m_\mu$, and thus a_ℓ to decay dominantly into electrons while satisfying beam dump and rare meson decay constraints. Also, the leptonic axion a_ℓ has no $a_\ell \to \pi^+\pi^-\pi^0$ decay mode, reducing the gamma ray constraints in the case that $m_{a_\ell} > 3m_\pi$ (where a_ℓ dominantly decays into muons). Since the strongest astrophysical bounds on light degrees of freedom come from hadronic couplings [244], m_{a_ℓ} might even be as light as $2m_e$, although a detailed study of the constraints on the leptonic axion is beyond the scope of this chapter.

As an example of the quark sector interactions, there could be separate up-type and down-type Higgses. In this case, it is natural to assume a hadronic symmetry under which the quarks carry axial charges:

$$\mathcal{L} = -\lambda_u q h_u u^c - \lambda_d q h_d d^c - A_q S_q h_u h_d + \text{h.c.} \tag{B.48}$$

The axion contained in the field S_q could then be the QCD axion and solve the strong CP problem. To avoid astrophysical constraints, however, the vacuum expectation value of S_q must be $\gtrsim 10^{10}$ GeV, much larger than $\langle S_\ell \rangle = O(\text{TeV})$. Explicit breaking of the hadronic symmetry must also be much smaller than that of the leptonic symmetry.